Clinical pharmacology of anti-hormonal drugs and gemcitabine in oncology

Bioanalysis - Therapeutic drug monitoring Microdosing

Merel van Nuland

Clinical pharmacology of anti-hormonal drugs and gemcitabine in oncology

Bioanalysis - Therapeutic drug monitoring
Microdosing

Merel van Nuland

Clinical pharmacology of anti-hormonal drugs and gemcitabine in oncology

Bioanalysis - Therapeutic drug monitoring - Microdosing

Klinische farmacologie van
antihormonale geneesmiddelen en gemcitabine in de oncologie
- Bioanalyse – 'Therapeutic drug monitoring' – Microdoseren -
(met een Nederlandse samenvatting)

Proefschrift

Ter verkrijging van de graad van doctor aan de Universiteit Utrecht
op gezag van de rector magnificus, prof. dr. H.R.B.M. Kummeling, ingevolge
het besluit van het college voor promoties in het openbaar te verdedigen op
woensdag 22 januari 2020 des middags te 2.30 uur

door

Merel van Nuland

geboren op 25 oktober 1989 te Oss

Promotoren: Prof. dr. J.H. Beijnen

Copromotor: Dr. H. Rosing
Dr. A.M. Bergman

Content

Preface

Cancer is the leading cause of death worldwide, with prostate- and breast cancer being the most common among men and women in the Western population, respectively (1). Initial strategies to treat cancer were based on unspecific cytotoxicity, thereby preventing tumor growth and inducing apoptosis. These classical chemotherapeutics are still an important pillar for cancer arrest treatment, however, in recent times drug development has shifted towards targeted therapies resulting in tumor specific cell cycle arrest and/or cell death. Many of these new targeted drugs are administered orally, causing an increased variability in drug levels and exposure compared to intravenously administered drugs, due to fluctuating bioavailability. Variability in drug exposure may have consequences for treatment efficacy and toxicity. Therefore, a better understanding of the pharmacokinetics and pharmacodynamics may further optimize treatment and improve drug safety.

Drug pharmacokinetics are investigated in an early stage of drug development and further characterization of the pharmacokinetic profile may be conducted post-registration. The starting point for studying drug pharmacokinetics is the development and validation of an analytical method to quantitate the drug and metabolites of interest in biological matrix (e.g. plasma, serum, urine, tissue). This thesis describes the clinical pharmacology of anti-cancer drugs, with a focus on bioanalysis, therapeutic drug monitoring (TDM) and microdosing. The first chapter describes the development and validation of liquid chromatography-mass spectrometry (LC-MS/MS) assays of several anti-hormonal drugs and gemcitabine. The second and third chapters deal with several aspects of TDM and microdosing studies.

Outline of this thesis
Chapter 1 introduces the development and validation of several LC-MS/MS methods for the quantification of anti-cancer drugs and hormones. The validation of these assays follows the current United States Food and Drug Administration (FDA) and European Medicines Agency (EMA) guidelines for bioanalytical method validation. However, a limited validation approach is recommended for the validation of TDM assays based on the intended use of these methods, as described in **chapter 1.1**. These recommendations have been applied in **chapters 1.2**, **1.3** and **1.4**, to validate LC-MS/MS assays for the quantification of anti-hormonal drugs used in the treatment of prostate cancer and breast cancer. **Chapter 1.5** describes the quantification of testosterone, dihydrotestosterone, androstenedione, dihydrotestosterone, cortisol and prednisone. These hormones play an important role in the pathophysiology and prognosis of prostate cancer. In **chapter 1.6**, we report a full method validation according to FDA and EMA for the quantification of gemcitabine and its metabolite in a microdose study.

Chapter 2 describes the use of TDM for anti-hormonal drugs in oncology. TDM is the clinical practice of individualized drug dosing by monitoring drug concentrations in patient blood, plasma or serum. In current practice, oral anti-hormonal drugs are administered at fixed doses, which could lead to suboptimal exposure or toxic concentrations. Use of TDM in oncology has been strongly recommended for other targeted therapies, such as imatinib and pazopanib (2). **Chapter 2.1** provides recommendations for TDM of anti-hormonal drugs used to treat breast cancer and prostate cancer and evaluates potential targets. **Chapters 2.2** and **2.3** describe the exposure-response relationship of enzalutamide and abiraterone in "real-world" cohorts of patients with metastatic castration-resistant prostate cancer, respectively. The results of a food-intervention to increase plasma concentrations of abiraterone in patients with trough concentrations below the proposed target are given in **chapter 2.4**. TDM may also be valuable to monitor plasma concentrations in patients with organ dysfunction, such as a patient undergoing hemodialysis (**chapter 2.5**) and a patient with a hepatic transplant (**chapter 2.6**). As abiraterone acetate and enzalutamide are primarily administered to elderly patients, **chapter 2.7** specifically describes the impact of age on exposure to these drugs. By implementation of TDM we aim to improve treatment outcome and increase patient safety. Nevertheless, cost aspects of this intervention need to be evaluated. In **Chapters 2.8 and 2.9** the cost-effectiveness of TDM in the Netherlands is assessed, exemplified for Z-endoxifen and abiraterone acetate, respectively.

Phase 0 microdose trials are exploratory studies to early assess human pharmacokinetics with very low drug dosages (≤100 μg) (3). **Chapter 3.1** discusses the predictive value of microdose pharmacokinetics and in **chapter 3.2** a phase 0 trial is described in which we examined whether the pharmacokinetics of gemcitabine in a therapeutic dose could be predicted from the pharmacokinetics of a microdose.

This thesis represents the application of bioanalysis and clinical pharmacology to optimize treatment and to support drug development in oncology. An overall conclusion, including perspectives, is given in the last chapter of this thesis to place gathered information in a broader perspective.

References

1. Bray F, Ferlay J, Soerjomataram I, Siegel RL, Torre LA, Jemal A. Global cancer statistics 2018: GLOBOCAN estimates of incidence and mortality worldwide for 36 cancers in 185 countries. CA Cancer J Clin. 2018;68:394–424.

2. Verheijen RB, Yu H, Schellens JHM, Beijnen JH, Steeghs N, Huitema ADR. Practical Recommendations for Therapeutic Drug Monitoring of Kinase Inhibitors in Oncology. Clin Pharmacol Ther. 2017;102:765–76.

3. Lappin G, Noveck R, Burt T. Microdosing and drug development: Past, present and future. Expert Opin Drug Metab Toxicol. 2013;9:817–34.

Development and validation of bioanalytical methods

Bioanalytical LC-MS/MS validation of therapeutic drug monitoring assays in oncology

Merel van Nuland
Hilde Rosing
Jan H.M. Schellens
Jos H. Beijnen

Abstract

Therapeutic drug monitoring (TDM) has shown to benefit patients treated with drugs of many drug classes, among which oncology. With an increasing demand for drug monitoring, new assays have to be developed and validated. Guidelines for bioanalytical validation issued by the European Medicines Agency (EMA) and US Food and Drug Administration (FDA), are applicable for clinical trials and toxicokinetic studies and demand fully validated bioanalytical methods to yield reliable results. However, for TDM assays a limited validation approach is suggested based on the intended use of these methods. This review presents an overview of publications that describe method validation of assays specifically designed for TDM. In addition to evaluating current practice, we provide recommendations that could serve as a guide for future validations of TDM assays.

Introduction

Therapeutic drug monitoring (TDM) is the clinical practice of measuring drug concentrations in biological fluids to individualize drug dosing. The goal of this intervention is to prevent drug failure by achieving adequate drug levels while also reducing toxicity by preventing overexposure. Some important requirements for drugs to be considered for TDM are long-term therapy, availability of a sensitive bioanalytical method, high inter-patient variability and low intra-patient variability, a narrow therapeutic window, an established dose-response and/or dose-toxicity relationship and a feasible strategy for individualized dosing (1). Many anticancer drugs fit the above described prerequisites, and therefore, TDM of anticancer drugs is becoming an important tool in treatment of patients with cancer, especially with increased use of oral anticancer drugs with highly variable bioavailability (2–7). Consequently, TDM has been shown to be a valuable intervention to optimize dosing of anticancer drugs and resulting in effective treatment (4,5,7–9).

A fundamental requirement for the implementation of TDM is the availability of bioanalytical assays to reliably measure drug concentrations, and concentrations of relevant metabolites. Different analytical techniques can be used, such as immunoassays and liquid-chromatography methods with UV (LC-UV), fluorescence or mass detection (LC-MS/MS) (10,11). Although all four are used in clinical practice, implementation of LC-coupled techniques gained popularity for routine measurements as immunoassays show lack of specificity and precision and show high variability between manufacturers (12). Furthermore, immunoassays could be plagued by cross-reactivity of structural analogous and generally have a shorter linear calibration range (13). LC-MS/MS methods, on the other hand, can be applied for simultaneous quantification of drugs and their metabolites with high sensitivity and selectivity and is therefore superior to LC-UV (10,14). Bioanalytical assays for TDM are used for routine clinical care and should therefore be fast and easy to implement, with high accuracy, precision and selectivity (10). LC-MS/MS assays can offer this by short run times and fast pretreatment procedures.

The focus of TDM assays should be on developing and validating a robust and high-throughput method for routine measurements, while the focus of assays for pharmacokinetic and toxicokinetic studies (PK-TK studies) should be on generating quantitative concentration data in a wider concentration range. Guidelines for bioanalytical method validation, issued by the European Medicines Agency (EMA) and US Food and Drug Administration (FDA), provide valuable assistance for the purpose of assay validation in clinical PK-TK studies (15,16). These guidelines are, however, comprehensive for TDM assays because drug concentrations determined for TDM purpose are generally reported as being below or above a target concentration and, therefore, not the exact concentration but target attainment is of interest. Together with the increasing demand for TDM in oncology, due to the use of oral anticancer drugs with highly variable bioavailability, assay validation ought to be simple and

straightforward, while still offering confidence in the data quality obtained with the validated method. There is a need for more concise guidelines specifically designed for the validation of TDM assays. In addition to more consice validation procedures, the analysis of study samples should have a rapid turnaround by implementation of a short analytical run. This review aims to present an overview of publications that describe LC-MS/MS assays which have been validated specifically for application in TDM. In addition to evaluating current practices, we provide recommendations that could serve as a guide for future validations and analysis of study samples for TDM purposes.

Literature search

PubMed was searched on February 12th 2019 using the following terms: 'Therapeutic drug monitoring AND validation'. We chose not to specify oncology in the search, to evaluate the number of bioanalytical validation papers for therapeutic drug monitoring in other fields. In addition, citation snow-balling was used. Inclusion was limited to bioanalysis in humans and full-text articles available in the English language.
The search identified 941 papers, of which 36 were found to be eligible for inclusion. Figure 1 shows a flow-chart of the inclusion process. Validation papers for therapeutic drug monitoring were identified by studying full-length articles for the aim of the study: assays that were developed specifically for implementation in therapeutic drug monitoring were included, while assays developed for the bioanalytical support of clinical studies and a potential application to TDM were excluded. Furthermore, only full validation articles were included in this review. This review focuses on the 36 published validation papers in the field of oncology, however, recommendations may be applicable to other fields. Results of the literature survey are summarized in Table 1.

Bioanalytical method validation guidelines

Guidelines on bioanalytical method validation are provided by the FDA and EMA (15,16). Although there is an overlap in experiments and acceptance criteria for all validation parameters, some differences are apparent when these guidelines are compared. Table 2 gives a brief overview of the validation experiments and acceptance criteria as described by the FDA and EMA guidelines. Of the 36 included papers, 27 articles refer to EMA and FDA guidelines for validation procedures. Other guidelines are occasionally used for recommendations on specific validation parameters, such as the Clinical & Laboratory Standards Institute (CLSI) guidelines (17,18). Furthermore, matrix effect and recovery were investigated by a variety of methods described in literature (19–23). In this review we will discuss the following aspects of method validation: calibration model, accuracy & precision, lower limit of quantification (LLOQ), carry-over, selectivity (endogenous and exogenous), dilution integrity, matrix effect, recovery and stability. Furthermore, aspects on the analysis of study samples will be evaluated. For each parameter, recommendations from relevant guidelines for assays supporting PK-TK
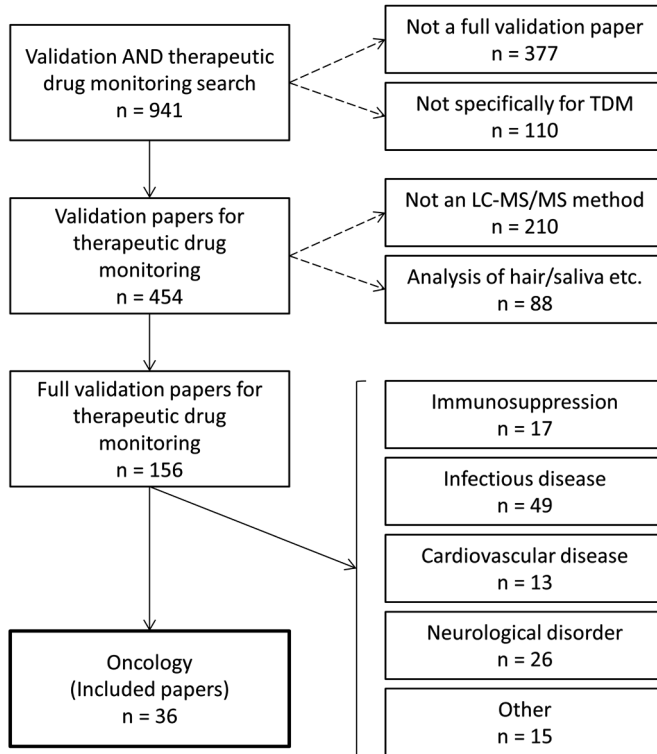
Figure 1. Flowchart that shows the step-by-step process of inclusion to generate a final number of studies for analysis in the review.

studies will be summarized, followed by results from the literature search and recommendations specifically for TDM assays. We aim to provide guidance and criteria for TDM method validation and on the application of these validated methods in the routine analysis of study samples.

Calibration model

The calibration model shows the relationship between instrument response and nominal analyte concentrations. For assays in clinical PK-TK studies, FDA and EMA guidelines have reached consensus on the experiments and acceptance criteria for the calibration model. The matrix of the calibration standards should, if possible, represent the matrix in study samples and fresh calibration standards should be prepared prior to each validation run. The number of calibration standards should be anticipated on the validation range with a minimum of six standards, including an LLOQ sample. Additionally, each set of calibration standards should include a blank sample (processed matrix sample without analyte and without internal standard) and a zero

Table 1. Overview of bioanalytical LC-MS/MS assays for therapeutic drug monitoring in oncology.

Analyte(s)	Calibration		Accuracy & Precision		LLOQ	Selectivity		Carry-over
	Levels	Range (-fold)	Levels	Replic.	S/N	Endo-genous	Exo-genous	n samples
Osimertinib	7	1000	4	Intra: 6 Inter: 18		6 blanks 6 LLOQ 6 zeros		3 blanks
Afatinib Axitinib Dabrafenib Dasatinib Erlotinib Gefitinib Ibrutinib Imatinib Lapatinib Nilotinib Pazopanib Regorafenib Ruxolitinib Sorafenib Sunitinib Trametinib Vandetanib Vemurafenib	6	100	3	Intra: 8 Inter:15	5	6 blanks		
Busulfan	5	300	3	Intra:20 Inter: 20			OTC DOA	5 blanks
Vincristine	8	1000	3	Intra: 5 Inter:4		1 blank (pooled)	OTC ACD	
Pemetrexed	7	64	3	Intra: 10 Inter: 30				
Sorafenib	6	1000	4	Intra:4 inter:6		6 blanks	ACD	
Everolimus	7	80	5	Intra: 10 Inter: 10			IMS	
5-Fluorouracil	8	1000	4	Intra:6 inter:18	5	6 blanks	ACD	
Methotrexate	7	500	3	Intra: 5 Inter:15	5	6 blanks 6 LLOQ		
Busulfan	5	333	3	Intra:10 inter: 28			Hemo Lipi Icte	3 Low
Docetaxel Paclitaxel Vinblastine Vinorelbine	7	100	4	Intra: 5 Inter: 5	10	6 blank 6 LLOQ		
Everolimus Sirolimus	6	19	8	Intra: 15 Inter: 15			IMS	
Octreotide	9	50	4	Intra: 6 Inter: 15				
Imatinib	8	20	3		10	1 blank 1 LLOQ	Cross-IS	1 solvent
Lapatinib	8	50	4	Intra: 5 Inter: 5	10	6 blanks	Cross- IS	

Dilution integrity	Matrix effect	Recovery	Internal standards	Short-term stability		Ref
Levels Replic.	Levels Blanks Replic.	Levels Blanks Replic.		Levels	Conditions	
	2	3 levels 4 replic.	Pazopanib	3	RT 4h F/T 3 FE 24h	(51)
4 replic	1 level 6 blanks 1 replic	6 levels 6 replic.	[^{2}H$_3$]-Erlotinib [^{2}H$_3$]-Gefitinib [^{2}H$_7$]-Lapatinib [^{2}H$_3$]-Sorafenib		FE 96°C	(52)
2 levels	3 levels 3 replic (45)		[^{2}H$_4$]-Busulfan		RT 28d F/T 6 4°C 28d -70°C 28d	(53)
		3 levels 3 replic	Vinblastine	3	RT 15h F/T 3 FE 10h	(50)
			Methotrexate	3	F/T 3 4°C 24h -20°C 20d	(54)
2 levels 5 replic	5 levels 9 blanks 1 replic	5 levels 3 replic	[^{13}C,^{2}H$_4$]-Sorafenib	4	RT 5h FE 24h -30°C 1w	(55)
1 level 10 replic	2 levels 10 blanks 1 replic (22)	5 levels 3 replic	40-O-(3-hydroxy) propyl-rapamycin	3	FE 24h	(56)
1 level 3 replic		3 levels 3 replic	[^{15}N$_2$]-5-Fluorouracil	3	RT 4h F/T 3 FE 96h	(57)
1 level 5 replic	3 levels 1 blank 5 replic	3 levels 5 replic	p-Aminoacetophenone	2	RT 7h F/T 3 FE 48h	(58)
3 levels 1 replic	1 level 3 blanks 3 replic (19)	3 levels. 3 replic.	[^{2}H$_3$]-Busulfan		4°C 1w F/T 8	(40)
	3 levels 1 blank 5 replic (19)	3 levels, 5 replic.	Vindoline		RT 12h F/T/ 3 -20°C 1m	(59)
Patient samples 1 replic	Post-column infusion (23)		[^{13}C,^{2}H$_4$] Everolimus	3	RT 12h	(60)
	3 levels 6 batches 3 replic (21)	3 levels 6 replic	Triptorelin	4	RT 12h F/T 3 FE 3d	(61)
		3 levels 3 blanks	[^{2}H$_8$]-Imatinib			(42)
		3 levels 5 replic	Sorafenib	3	RT 8h F/T 3 FE 10h -70°C 21d	(48)

Table 1. Continued

Analyte(s)	Calibration		Accuracy & Precision		LLOQ	Selectivity		Carry-over
	Levels	Range (-fold)	Levels	Replic.	S/N	Endo-genous	Exo-genous	n samples
Letrozole	6	60	4	Intra: 6 Inter: 18	10	6 blanks		>1 blank
Methotrexate	6	5000	3	Inta:10 Intrer:20		6 spiked samples		1 blank
6-Methylmer-captopurine 6-Thioguanine	6	100	3	Imprecision: 3 Inaccuracy: 12		10 blanks		
Everolimus	5	54	3	Intra: 3 Inter: 30				1 Low
Cobimetinib Dabrafenib Pazopanib Regorafenib Trametinib Vemurafenib	8	500	3	Intra: 6 Inter:6		8 blanks	Metabolites and other	>1 blank
Dasatinib Erlotinib Gefitinib Imatinib Lapatinib Nilotinib Sorafenib Sunitinib	8	500	4	Intra: 15 Inter: 15		6 blanks 6 LLOQ	Cross-analyte/IS	2 blanks
Olaparib Pazopanib Ruxolitinib Vismodegib		250-1000	3	Intra: 25 Inter: 24		6 blanks	TKIs ART AFT other	
Dabrafenib Trametinib	8	100	4	Intra: 15 Inter:15	5	6 blanks 6 LLOQ	Cross-analyte/IS	2 blanks
Dasatinib Erlotinib Gefitinib Imatinib Lapatinib Nilotinib Sorafenib Sunitinib	7	50-100	3	Intra:5 Inter:5	5			
Abiraterone Enzalutamide	4	100	3	Intra: 15 Inter: 15	5	6 blanks 6 LLOQ	Cross-analyte/IS	2 blanks
Dasatinib Imatinib Nilotinib	8	533-2000	4	Inter:6 Intra: 18	5	6 blanks 6 zeros	Cross-analyte/IS	>1 blanks
Pazopanib	8	50	4	Intra: 15 Inter: 15	5	6 blanks 6 LLOQ	Cross-IS	2 blanks
Dasatinib Erlotinib Gefitinib Imatinib Lapatinib Nilotinib Pazopanib Sorafenib Sunitinib Vermurafenib	4	20	3	*Intra: 15 Inter:15*	5	6 blanks 6 LLOQ		2 blanks

Dilution integrity	Matrix effect	Recovery	Internal standards	Short-term stability		Ref
Levels Replic.	**Levels Blanks Replic.**	**Levels Blanks Replic.**		**Levels**	**Conditions**	
	2 levels 6 blanks 1 replic	3 levels 6 replic	Anastrozole	3	RT 4h F/T 3 FE 24h	(62)
3 levels 3 replic	Post-column infusion (23)		[^{2}H$_3$]-Methotrexate	2	RT 4h F/T 3 FE 24h -80°C 30d 4°C 24h	(63)
	1 level 1 blank 5 replic (19)	1 level 5 replic	[^{13}C$_2$,^{15}N]-6-Thioguanine [^{2}H$_3$]-6-Methylmer-captopurine		FE 24h	(64)
	5 blanks 1 replic		[^{2}H$_4$]-Everolimus			(41) (45)
	3 levels 7 blanks 1 replic	3 levels 7 replic	[^{13}C$_6$]-Cobimetinib [^{2}H$_9$]-Dabrafenib [^{13}C,^{2}H$_3$]-Pazopanib [^{13}C,^{2}H$_3$]-Regorafenib [^{13}C$_6$]- Trametinib [^{13}C$_6$]- Vemurafenib	3	RT 48h F/T 3 FE 24h 4°C 48h	(28)
1 level 5 replic	2 levels 1 blank 3 replic	2 levels 3 replic	[^{2}H$_8$]-Dasatinib [^{13}C$_6$]-Erlotinib [^{2}H$_8$]-Gefitinib [^{13}C, ^{2}H$_3$]-Imatinib [^{13}C, ^{2}H$_7$]-Lapatinib [^{2}H$_3$]-Nilotinib [^{13}C, ^{2}H$_3$]-Sorafenib [^{2}H$_{10}$]-Sunitinib	2	RT 48h F/T 3 FE 8d	(65)
	3 levels 1 blank (19)	3 levels	[^{2}H$_8$]-Olaparib [^{2}H$_6$]-Pazopanib [^{2}H$_8$]-Ruxolitinib [^{13}C$_7$,^{2}H$_3$]-Vismodegib	3	RT 4d F/T 4 FE 24h 4°C 4d	(66)
1 level 5 replic	2 levels 6 blanks 1 replic		[^{2}H$_9$]-Dabrafenib [^{13}C$_6$]-Trametinib	2	RT 24h F/T 3 2-8°C 68 -20°C 20d	(25)
	1 level 6 blanks 1 replic	1 level 6 replic	[^{2}H$_8$]-Gefitinib [^{2}H$_8$]-Imatinib [^{13}C$_2$,^{15}N$_2$]-Nilotinib [^{2}H$_{10}$]-Sunitinib	3	RT 1d F/T 3 4°C 1w	(67)
1 level 5 replic	2 levels 6 blanks 1 replic	2 levels 3 replic	[^{2}H$_4$]-Abiraterone [^{2}H$_6$]-Enzalutamide	2	RT 5d F/T 3 FE 5d -20°C 1m	(35)
	3 levels 6 blanks 1 replic	3 levels 6 replic	[^{2}H$_8$]-Dasatinib [^{2}H$_8$]-Imatinib [^{13}C,^{2}H$_3$]-Nilotinib	2	RT 48h F/T 3 FE 24h 4°C 24h	(68)
1 level 5 replic	2 levels 6 blanks 1 replic	2 levels 5 replic	[^{13}C,^{2}H$_3$]-Pazopanib	2	RT 5d F/T 3 FE 70d	(26)
1 level 5 replic			[^{2}H$_3$]-Dasatinib [^{13}C$_6$]-Erlotinib [^{2}H$_3$]-Gefitinib [^{13}C]-Imatinib [^{13}C]-Lapatinib [^{2}H$_3$]-Nilotinib [^{13}C]-Pazopanib [^{13}C]-Sorafenib [^{2}H$_{10}$]-Sunitinib [^{13}C$_6$]-Vermurafenib	2	RT 48h F/T/ 3 FE 8d -20°C 1m	(69)

23

Table 1. Continued

Analyte(s)	Calibration		Accuracy & Precision		LLOQ	Selectivity		Carry-over
	Levels	Range (-fold)	Levels	Replic.	S/N	Endo-genous	Exo-genous	n samples
Bosutinib Cobimetinib Dabrafenib Dasatinib Erlotinib Ibrutinib Imatinib Lapatinib Nilotinib Ponatinib Sorafenib Sunitinib Trametinib Vemurafenib	6-8	100-500	4		Intra: 25 Inter: 24		6 blanks	ART, AFT, other
Z-Endoxifen	4	25	3		Intra: 15 Inter: 15	5	6 blanks 6 LLOQ	Cross-IS	
Binimetinib Cobimetinib Dabrafenib Trametinib Vemurafenib	7-9	250-1000	3		Intra: 5 Inter:15		6 blanks 6 zeros	Cross-analyte/IS	
Afatinib Axitinib Ceritinib Crizotinib Dabrafenib Enzalutamide Regorafenib Trametinib	4	100	3		Intra: 15 Inter: 15	5	6 blanks 6 LLOQ	Cross-analyte/IS	2 blanks
Sunitinib	8	200	4		Intra: 15 Inter: 15		6 blanks 6 LLOQ	Cross-IS	2 blanks
Imatinib	6	200	3		Intra: 5 Inter: 10	10	5 blanks 5 LLOQ		1 blank
Methotrexate	7	1000	4		Intra: 30 Inter: 30		10 blanks 10 LLOQ		1 blank
Abiraterone Anastrozole Bicalutamide Enzalutamide Exemestane Letrozole Z-Endoxifen	4	20-200	3		Intra: 15 Inter: 15	5	6 blanks 6 LLOQ		2 blanks

Abbreviations: S/N = signal-to-noise ratio, Ref = reference, replic. = replicates, RT = room temperature, F/T = freeze/thaw, FE = final extract, h = hours, w = weeks, d = days, LLOQ = lower limit of quantifications, IS = internal standard, OTC = over the counter, Hemo = hemolytic, Lipi = lipidemic, Icte = icteric, DOA = drugs of abuse, ACD = anticancer drugs, IMS = immunosuppressants, AB = antibiotics, TKI = tyrosine kinase inhibitors, ART = antiretroviral therapy, AFT = antifungal therapy

Dilution integrity	Matrix effect	Recovery	Internal standards	Short-term stability		Ref
Levels Replic.	Levels Blanks Replic.	Levels Blanks Replic.		Levels	Conditions	
	3 levels 1 blank (19)	3 levels	$[^2H_9]$-Bosutinib $[^{13}C]$-Cobimetinib $[^2H_9]$-Dabrafenib $[^2H_8]$-Dasatinib $[^{13}C_6]$-Erlotinib $[^2H_5]$-Ibrutinib $[^2H_8]$-Imatinib $[^{13}C,^2H_7]$-Lapatinib $[^{13}C,^2H_3]$-Nilotinib $[^2H_8]$-Ponatinib $[^{13}C,^2H_3]$-Sorafenib $[^2H_{10}]$-Sunitinib $[^{13}C_6]$-Trametinib $[^{13}C_6]$-Vemurafenib	3	RT 48h F/T 4 FE 24h 4°C 48h	(70)
2 blanks	6 blanks 1 replic		$[^2H_5]$-Z-endoxifen	2	RT 7d F/T 3 FE 7d -20°C 7d 2-8°C 7d	(32)
	1 level 6 blanks 1 replic	1 level 3 replic	$[^{13}C_2,^2H_4]$-Binimetinib $[^{13}C_6]$-Cobimetinib $[^2H_9]$-Dabrafenib $[^{13}C_6]$-Trametinib $[^{13}C_6]$-Vemurafenib	2	RT 24h 4°C 3d F/T 3 -20°C 1m	(71)
1 level 5 replic	2 levels 6 blanks 1 replic		$[^{13}C_6]$-Afatinib $[^{13}C,^2H_3]$-Axitinib $[^2H_7]$-Ceritinib $[^{13}C_2]$-Crizotinib $[^2H_9]$-Dabrafenib $[^2H_6]$-Enzalutamide $[^{13}C,^2H_3]$-Regorafenib- $[^{13}C_6]$-Trametinib	2	RT 48h F/T 3 FE 48h -20°C 1m	(6)
1 level 5 replic	2 levels 1 blank 3 replic	2 levels 3 replic	$[^2H_{10}]$-Sunitinib	2	RT 72h F/T 3 FE 7d	(24)
	1 level 4 blanks 1 replic	3 levels	$[^2H_8]$-Imatinib			(72)
2 levels	4 levels 6 blanks 3 replic	4 levels 3 replic	$[^2H_3]$-Methotrexate	4	F/T 3 -20°C 48h 4°C 72h -80°C 34d	(73)
			$[^2H_4]$-Abiraterone $[^2H_{12}]$-Anastrozole $[^2H_4]$-Bicalutamide $[^2H_6]$-Enzalutamide $[^2H_3]$-Exemestane $[^2H_4]$-Letrozole $[^2H_5]$-Endoxifen	2	RT 5d F/T 3 4°C 5d FE 5d -20°C 21w	(49)

Table 2. Recommendations for bioanalytical method validation as given by the European Medicines Agency (EMA), the US Food and Drug Administration (FDA) and proposed recommendations specifically for therapeutic drug monitoring (TDM) assays

Validation parameter	Experiments/ criteria*	EMA	FDA	TDM
Calibration model	Experiments	Consists of a blank sample, a zero sample and 6-8 calibration standards (incl. LLOQ)	Consists of a blank sample, a zero sample and 6-8 calibration standards (incl. LLOQ)	Consists of a blank sample, a zero sample and 4 calibration standards (incl. LLOQ)
	Acceptance criteria	85-115% 80-120% for LLOQ	85-115% 80-120% for LLOQ	85-115% 80-120% for LLOQ
		75% should meet the criteria, including LLOQ and ULOQ	75% should meet the criteria, including LLOQ and ULOQ	75% should meet the criteria, including LLOQ and ULOQ
LLOQ	Experiments	Lowest calibration standard level	Lowest calibration standard level	Lowest calibration standard level
	Acceptance criteria	80-120% ≥5 S/N	80-120% ≥5 S/N	80-120% ≥10 S/N
Carry-over	Experiments	Blank sample injected after a high sample	Should be monitored during analysis	At least 2 blank samples injected after the ULOQ
	Acceptance criteria	≤20% of LLOQ ≤5% of IS	≤20% of LLOQ	≤20% of LLOQ ≤5% of IS
Accuracy & precision	Experiments	4 Concentration levels 5 samples per level	4 Concentration levels 5 samples per level	3 Concentration levels (LLOQ, Mid=target concentration, ULOQ), 5 samples per level
	Acceptance criteria	85-115% 80-120% for LLOQ	85-115% 80-120% for LLOQ	85-115% 80-120% for LLOQ
Dilution integrity	Experiments	Dilute sample >ULOQ (n=5) with blank matrix	Dilute sample >ULOQ (n=5) with blank matrix	Not applicable
	Acceptance criteria	85-115% 80-120% for LLOQ	85-115% 80-120% for LLOQ	
Endogenous Selectivity	Experiments	6 Batches, blank samples	6 Batches, blank samples and at LLOQ	6 Batches, blank samples and at LLOQ
	Acceptance criteria	≤20% of LLOQ ≤5% of IS	≤20% of LLOQ ≤5% of IS	≤20% of LLOQ ≤5% of IS
Exogenous Selectivity	Experiments	Potential interfering substances should be tested separately	Cross-interference when >1 analyte in the assay	If applicable: interference of structural analogues

Table 2. Continued

Validation parameter	Experiments/ criteria*	EMA	FDA	TDM
Stability	Experiments	Low and High concentrations: Stock solutions, Working solutions, F/T short-term at RT, Long-term. If applicable: dry extract, autosampler stability	Low and High concentrations: Stock solutions, Working solutions, F/T 3, short-term at RT, Long-term. If applicable: dry extract, autosampler stability	LLOQ and ULOQ concentrations: Stock solutions, Working solutions, F/T 3, short-term at RT, prolonged at RT during transport, long-term, influence of exposure to light. If applicable: dry extract, autosampler stability
	Acceptance criteria	85-115%	85-115%	85-115%
Matrix effect	Experiments	6 Batches of blank matrix, Low and High samples	Matrix effect should be evaluated	Not applicable if a stable isotopically-labeled internal standard is used co-eluting with the analyte
	Acceptance criteria	CV of IS-normalized should be <15%		
Recovery	Experiments	Not applicable	Extracted compared to unextracted at 3 concentration levels	Not applicable

* % of nominal concentration unless otherwise specified. Abbreviations: EMA = European Medicines Agency, FDA = US Food and Drug Administration, TDM = therapeutic drug monitoring, LLOQ = lower limit of quantification, ULOQ = upper limit of quantification, S/N = signal-to-noise, CV = coefficient of variance, IS = internal standard.

sample (processed matrix sample without analyte). These samples are not included in the calculation of the regression line. The EMA recommends the analysis of calibration standards on three occasions in duplicate (total n=6) to evaluate linearity of the calibration model. Acceptance criteria for calibration standards are 85-115% of the nominal concentration, and 80-120% for the LLOQ. At least 75% of calibration standards should meet these criteria, including the LLOQ (and the upper limit of quantification (ULOQ) in EMA guidelines).

Calibration standards
Included analytical assays all used a matrix similar to study samples for preparation of calibration standards. Most papers do not describe whether calibration standards were produced freshly before each validation run. The number of calibration standards ranged from four to nine, with a median number of seven and a median calibration range of 100-fold. The median number of calibration standards is in line with the recommended guidelines. However, nine articles use <6 calibration standards for the calibration model. When dividing the calibration range by the number of calibration standards, a median of 24 nominal concentration units per standard is calculated.

Based on this median, a 100-fold calibration range would only need four calibration standards. Reducing the analysis time by using fewer calibration standards (n=3) was previously demonstrated by Lankheet et al. in a method comparison of LC-MS/MS assays for the quantification of sunitinib (24). Reducing the number of calibration standards from six to three increased the turnaround while preserving accuracy and precision. To further investigate this concept, we performed a similar experiment in our lab using data from previously published TDM assays for quantification of pazopanib, trametinib and dasatinib (25,26). QC samples at LLOQ, low, mid and high level (n=15) were analyzed using both the original method with eight calibration standards and an adjusted method with four calibration standards. The results of the method comparison are shown in Figure 2. A regression test was performed for all three analytes and showed no significant constant error (y-axis intercept 95% confidence intervals contained zero; -0.0719 to 0.0607 for pazopanib, -0.0599 to 0.0433 for trametinib and -5.55 to 9.03 for dabrafenib). Furthermore, the slopes of the regression lines were not significantly different from one for pazopanib and dabrafenib (95% confidence interval; 0.996 to 1.00 and 0.997 to 1.00, respectively). Although the regression line for trametinib was found to be significantly different from one by reducing the number of calibration standards, with a slope of 1.01 (95% confidence interval; 1.01 to 1.02), the accuracy and precision improved compared to the original method from ±4.3% to ±3.8% and from ≤5.6% to ≤3.0%, respectively. These data suggest that reducing the number of calibration standards from eight to four when using calibration ranges of 100 fold or less does not affect the accuracy and precision of the method.

From a clinical point of view, target attainment is the final objective for decision making in TDM. Therefore, a one-level calibration could be considered with a calibration point being the target concentration. In a previous study, bias and precision of multiple-point and one-point calibration were compared. One-point calibration with a calibration close to the center of the complete calibration range (e.g. proposed target) shows bias and precision within the acceptance criteria for the majority of drugs (27). However, dose adjustments following TDM may depend on the quantitative determination of the concentration of an anti-cancer agent; patients with a concentration around the target could receive minimal or no dose adaptations, while large deviations from the target may ask for other interventions. Therefore a concentration range should be chosen per analyte depending on the decision making in TDM. A calibration range that spans 2 orders of magnitude using 4 calibration standards is in most cases sufficient for these purposes and this reduction in the number of calibrations standards increasis the turnaround time of TDM assays and has no impact on the quality of the reported data as demonstrated in Figure 2. Furthermore a one-level calibration assumes a linear model and a variance independent of the analyte concentration (no weighting factor is applied). This assumption is in most MS methods not justified. Therefore the calibration model should be established in each analytical run by analyzing (4) calibration standards in the chosen, validated range.

Pazopanib

Trametinib

Dabrafenib
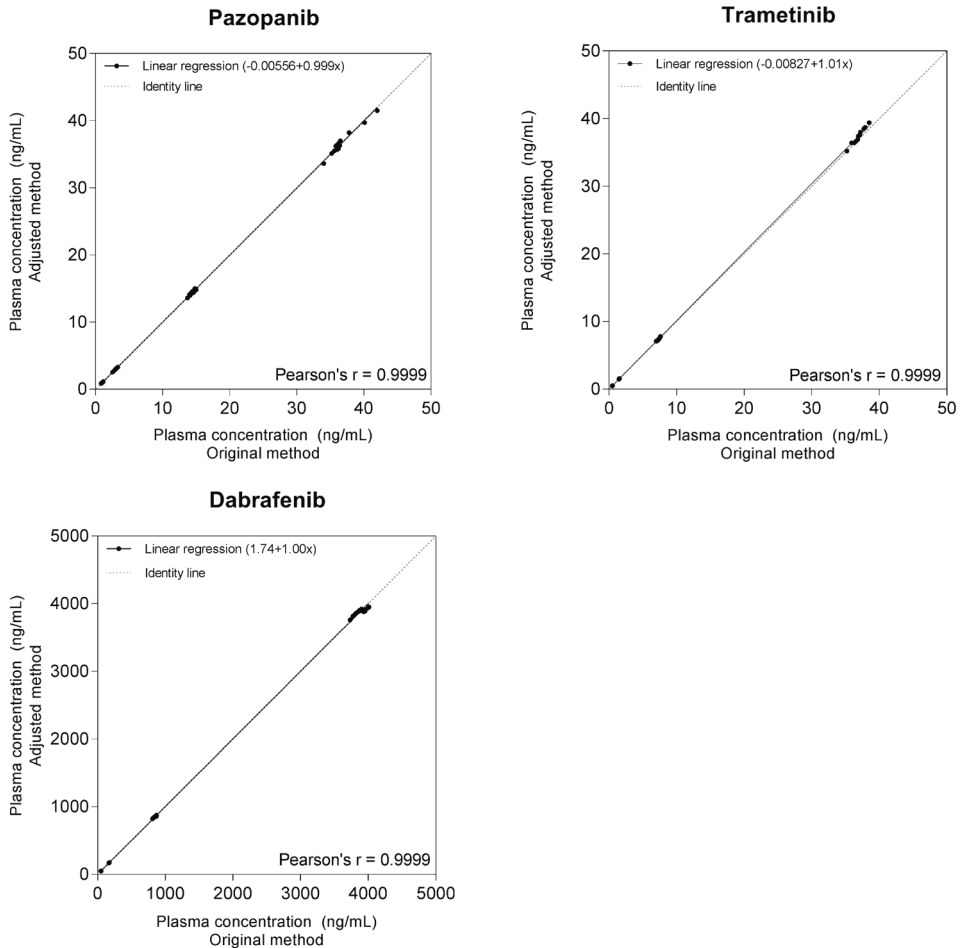
Figure 2. Scatter plots of method comparison showing plasma concentrations of four quality control (QC) levels (n=15) measured with the original method (eight calibration standards) and the adjusted method (four calibration standards). The black line represents the linear regression line and the dotted line represents the line of identity.

Regression line

All but one paper (28) used a weighted linear regression ($1/x$ or $1/x^2$) for the calibration model. A linear relationship is the simplest mathematical relationship with a constant accuracy over the complete range in contrast to quadratic fitting (17). Therefore, linear regression is the preferred mathematical method for calibration of analytical methods (29). A weighting factor of 1, $1/x$ or $1/x^2$ is selected if the standard deviation of the instrument response is proportional to x (29). Weighted regression of $1/x$ or $1/x^2$ should be used when the absolute variance is not constant for all observations, which is generally the case with a calibration range covering over one magnitude (29).

Therefore, 1/x or $1/x^2$ weighting may be used to improve the accuracy at lower concentrations. If a quadratic fit is chosen to compensate for saturation of the ion detector, the method could be de-optimized to reduce saturation, or the MRM channel could be modified (+1 or +2) to monitor the *m/z* values of isotopes and thereby avoid signal saturation (30). All but five articles report a determination coefficient (R^2) and a minimum of 0.99 is generally strived for. However, deviations from the nominal concentrations provide more information about linearity of the calibration model. Therefore, back-calculated concentrations should be reported instead of R^2. Acceptance criteria for the back-calculated calibration standards are provided by 24 papers, being 85-115% of the nominal concentration (80-120% for the LLOQ).

Quantitation range

The quantitation range of bioanalytical assays should be chosen on the basis of concentrations expected in clinical samples. TDM assays are developed to determine whether individual concentrations are above or below a certain target and, therefore, the concentration range should be built around this target concentration. A median calibration range of 100-fold was used in included assays for TDM purpose. The calibrations range should be as narrow as possible for high accuracy and precision, covering the concentration of the majority of samples as seen in the clinic, from the minimum reported concentration to the maximum reported concentration after drug intake. Accordingly, the range will depend on inter-patient variability of anticipated concentrations. In our experience, a range of 20 to 100-fold is in most cases sufficient.

Accuracy and precision

Accuracy of the LC-MS/MS method describes the closeness of mean measured concentrations to the nominal concentrations of the analyte and is expressed as a percentage, while the precision of the method describes the closeness of repeated measurements of an analyte. For PK-TK assays, both parameters should be assessed using quality control (QC) samples, i.e. spiked samples at known concentrations. QC samples are generally produced at LLOQ, low (within three times the LLOQ), mid (in the midrange) and high (approaching the end, >75% of ULOQ, of the calibration range) level. Accuracy and precision can be further subdivided into within-assay and between-assay accuracy and precision. According to the EMA and FDA, within-assay accuracy and precision should be determined by measuring a minimum of five samples at a minimum of four concentration levels (LLOQ, low, mid, high). Furthermore, between-assay accuracy and precision should be assessed by measuring four concentration levels in at least three runs or batches on at least two different days. Mean concentrations should be 85-115% of the nominal values for QC samples, except for LLOQ for which 80-120% is considered acceptable. It is recommended by the EMA to demonstrate accuracy and precision over at least one of the runs in a size equivalent to a prospective analytical run containing study samples.

Included analytical papers for TDM purpose determine accuracy and precision, with a minimum of three concentration levels. Although a variable number of QC samples was used for determining accuracy and precision, all papers included at least five samples to determine within-assay accuracy and precision and a minimum of three runs were performed for between- assay accuracy and precision. Only seven papers did not give acceptance criteria for accuracy and precision, while other papers reported acceptance criteria in line with FDA and EMA guidelines. These results suggest that recommendations in FDA and EMA guidelines are generally acceptable for determining accuracy and precision of TDM assays. Regarding the short calibration range of TDM assays and the aim for a fast turnaround, we believe that a minimum of three concentration levels (LLOQ, medium or target concentration an ULOQ) is sufficient. As most papers do not provide information on how accuracy and precision were calculated, we recommend using the following equations (31):

Within-assay accuracy (%) =
100% · (*mean measured conc.per run-nominal conc.*)/(*nomimal conc.*)   (a)

Between-assay accuracy (%) =
100% · (*overall mean measured conc.-nominal conc.*)/(*nominal conc.*)   (b)

Within-assay precision (%) =
100% (*SD of the measured conc.per run*)/(*mean measured conc.per run*)   (c)

Between-assay precision (%) =

(d)

$$\sqrt{\dfrac{\left(\dfrac{s^2_{overall}/((n_1+\cdots+n_a-1)-\left((n_1-1)s^2_1+\cdots+\left((n_a-1)s^2_{\bar{a}}\right)\right))}{a-1}\right)-\left(\dfrac{(n_1-1)s^2_1+\cdots+(n_a-1)s^2_{\bar{a}}}{n_1+\ldots+n_a-a}\right)}{\dfrac{\left(\dfrac{n}{a}\right)}{\text{Mean of runs}}}} \times 100\%$$

Where conc. = concentration, SD = standard deviation, $s^2_{overall}$ = overall SD^2, S^2x = variance (SD^2) of mean of replicates on a concentration level for run x, a = number of runs and n = number of replicates.

Lower limit of quantification
For assays for PK-TK studies, the LLOQ is the lowest level of the calibration standards which can determined with an accuracy and precision of ≤20% of the nominal concentration. Both EMA and FDA guidelines state that the LLOQ should be at least five times the signal of a blank sample.
The LLOQ in TDM assays is the lowest level of the calibration standards, however, it is generally not the lowest concentration of an analyte which can be quantified reliably as the concentration range is higher. Therefore, the LLOQ in TDM assays is rather a lower limit of the measuring interval (LLMI). In 34 of 36 papers of TDM assays, the LLOQ

was defined as the lowest level of the calibration range, witth an acceptance criterion of 80-120% of the nominal concentration. Based on these results, a maximum of ±20% deviation from the nominal concentration seems to be accepted in TDM assays. The signal-to-noise (S/N) ratio was provided in 19 papers, being at least five (n=12) or ten (n=7). Furthermore, the limit of detection was determined in 10 papers, with a S/N ratio of at least three (n=8), five (n=1) or six (n=1). To set an example; In our lab, we perform weekly TDM measurements of Z-endoxifen with a validated LC-MS/MS assay (32), and we have recorded the S/N ratio of the LLOQ (1 ng/mL) for 49 weeks. Figure 3 displays the S/N ratio of the LLOQ to range from 20 to 200 in this time period, demonstrating a factor 10 inter-occasion variability when the method is applied for a longer period. Although the EMA and FDA recommend a S/N ratio of at least five for the LLOQ, we believe this limit should be increased for TDM assays regarding the between-assay variability of the LC-MS/MS signal over a long time period. Therefore, we aim for a S/N ratio of at least ten instead of five. Increasing the S/N ratio is supported by the CLSI guidelines, in which a S/N ratio of at least 20 is recommended (33). Moreover, TDM assays are developed to measure steady-state drug concentrations and while choosing calibration standards to cover concentrations in a 20- to 100-fold range, the LLOQ will generally exceed an S/N ratio of 10. For example, enzalutamide is known to have a mean trough concentration at steady-state (at a 160 mg dose) of 11.4 mg/L (34). A validated method in our lab showed a S/N ratio of over 200 for the LLOQ of 5 ng/mL (35). Taken the variability in account over time and the intended use of TDM methods, we strongly advice to increase the S/N ratio at the LLOQ to increase the robustness of the validated method.

Selectivity

The selectivity of the analytical method is investigated during validation to assess whether the method is able to differentiate the analyte of interest from endogenous and exogenous components within the sample. EMA and FDA guidelines state that selectivity should be proven in at least six independently prepared and analyzed batches of the used biomatrix for PK-TK assays. The interference in these should be ±20% and 5% of the LLOQ for the analyte and the internal standard, respectively. According to the FDA, selectivity should also be ensured at the LLMI. These experiments focus on interference from endogenous source, while it may also be necessary to investigate potential interference from exogenous components, such as metabolites, co-medication, degradation products, excipients of the formulation and other xenobiotics. The FDA specifically adds that 'if the method is intended to quantify more than one analyte, each analyte should be tested to ensure that there is no interference'.

Endogenous selectivity
In 26 of 36 articles for TDM assays, endogenous selectivity was tested in accordance with the guidelines, in at least six different batches of blank matrix. One paper included
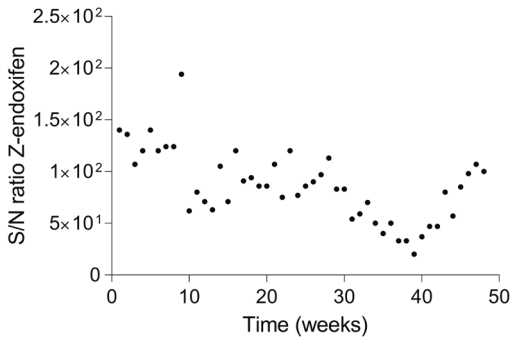
Figure 3. Z-endoxifen signal-to-noise (S/N) ratios of the LLOQ (1 ng/mL) as measured by LC-MS/MS for therapeutic drug monitoring for 49 weeks

10 different batches and two papers investigated endogenous interference in one batch of plasma. Testing for selectivity is important, as it shows that the substance quantified is indeed the analyte. Therefore, selectivity experiments should be performed in different batches of plasma, also for TDM assays. Selectivity at LLOQ was ensured in 14 papers, all analyzing LLOQ samples in six different batches. Although the EMA does not recommend to do such an experiment, we believe it is important to investigate the effect of different matrices and endogenous interference on quantification of the analyte. Endogenous components may cause suppression or enhancement of the MS signal and thereby influence quantification of the analyte. This can only be characterized if selectivity has been investigated in biological samples spiked with the analyte of interest. Therefore, we advice to assess endogenous selectivity in control matrix spiked at the LLOQ in six different batches of plasma. One of the papers included in this review investigated the selectivity in hemolyzed, lipidemic and icteric plasma and showed that the assay was not affected. If samples from a special population are included in TDM, such as renally or hepatically impaired populations, it is recommended to study the selectivity in such related samples (16)

Exogenous selectivity
Potential interferences from non-endogenous sources were investigated in 23 articles for TDM assays; six papers assessed interference of co-medication, 14 papers investigated cross-analyte interferences, two papers studied metabolite interference and one paper analyzed potential interference of photodegradation products of the analyte. Commonly investigated co-medication are over the counter drugs, drugs of abuse, immunosuppressants, antibiotics, antiretroviral therapy, and antifungal therapy. Testing for potential interference of co-medication and cross-analyte interference is adviced if these are structural analogues of the analyte of interest (36). Otherwise, no further testing is required. For some analytes, such as endoxifen and abiraterone, one needs to be aware of the presence of isomers (37,38). To preserve selectivity, isomers

should be separated at baseline from the analyte. In addition to testing for interferences of other drugs, the EMA recommends to investigate potential interference of excipients in the drug formulation, such as polyethylene glycol or polysorbate. This may be important for intravenously administered drugs, however, TDM will mainly be applied to orally administered drugs, and therefore is of less relevance.

Carry-over

Sample carry-over can be a major problem, which influences accuracy and precision of the method. Carry-over is caused by residual analyte from a sample analyzed earlier in the analytical run or batch (39). Both EMA and FDA guidelines recommend monitoring the carry-over during validation of PK-TK assays by injecting blank samples after the ULOQ. These blanks should contain ≤20% of the LLOQ response and ≤5% of the internal standard response.

Surprisingly, carry-over was investigated in only 20 papers of TDM assays. This simple experiment is important for TDM assays, as high concentrations may occur in patient samples and it should be ensured that these levels do not influence quantification in the next injected sample. In 17 papers, carry-over was determined by injecting matrix blanks after the ULOQ. Two papers assessed carry-over by injecting QC low samples before and after QC high samples (40,41). The carry-over was defined as the mean difference of QC low samples injected prior to QC high samples and QC low samples injected after QC high samples. Only one article provided acceptance criteria for this experiment, with the mean difference between the low samples before and after the high samples being ≤20% (41). The carry-over in such experiments is difficult to observe, because it involves an additive effect rather than the absence/presence of a peak. Furthermore, the carry-over was determined after injection of a QC high sample instead of the ULOQ. One article assessed carry-over by injecting an organic solvent sample after the ULOQ instead of a matrix blank (42). Matrix blanks have a similar composition and ion strength as study samples and should therefore be used to determine carry-over, while organic blank samples generally do not show carry-over. Determining carry-over according to EMA and FDA guidelines is rapid and easy to perform and interpret, therefore we recommend using these guidelines for the evaluation of carry-over during the validation and for routine assessment in each analytical run because carry-over may vary from run to run.. It is, however, important to be aware of the difference between carry-over and memory-effect as these problems may be resolved differently. A memory-effect is observed as a downward-drifting baseline in a blank sample that is analyzed after a high sample and suggests that the analyte was still eluting off the column from the previous injection (39). Both carry-over and memory-effect may affect quantification of low concentrations by a residual analyte peak or by an increased baseline, respectively, and should therefore be minimized. A procedure to evaluate the carry-over during the application phase of the validated assay is described under 'Analysis of study samples".

Dilution integrity

Dilution integrity is evaluated with the purpose of measuring samples above the upper limit of quantification (ULOQ). The dilution of samples should not affect the accuracy and precision of the measurement. According to EMA and FDA, dilution integrity should be demonstrated by spiking a sample at a concentration above the ULOQ and consequently diluting this sample to a concentration within the calibration range. The accuracy and precision of a sample set (n=5) should be ±15% of the nominal concentration. Dilution integrity was evaluated in 16 papers for TDM assays. Only ten papers provided acceptance criteria for the conducted experiments and more than one dilution step was investigated in seven of 15 papers. Dilution of samples is not common practice for TDM as it is time-consuming and therefore decreases the throughput. Furthermore, exceeding the ULOQ in general means that the target was attained. Therefore, samples exceeding the calibration range can be reported as above the ULOQ without further analysis. However, we would prefer to minimize the number of samples exceeding the ULOQ by choosing a calibration range that covers clinically observed concentrations. TDM can also be used for monitoring toxicities in which quantification of high concentrations could be important for the clinical perspective and treatment strategy. When a TDM assay is developed for this purpose, dilution integrity should be demonstrated to cover a larger calibration range and we would recommend incorporating the EMA/FDA experiments.

Matrix effect and recovery

Matrix effect can be assessed using a variety of methods described in literature, for example post-column infusion and post-extraction techniques (43). Post-column infusion was first described by Bonfiglio et al. (23) and consists of injecting a blank pretreated biological sample during continuous post-column infusion of the analyte of interest. A matrix effect may be observed by comparing changes from baseline across the chromatographic run. For post-extraction techniques a set of samples with and without biomatrix is used. The matrix effect can be calculated by comparison of the analyte response in presence and in absence of biomatrix. The latter method is recommended by the EMA for PK-TK assays, using at least six different batches of blank matrix. For each analyte, the matrix factor (MF) and internal standard (IS)-normalized matrix factor should be calculated and the coefficient of variation (CV) is found to be acceptable when ≤15%. A version of the post-extraction spike method has also been described by Matuszewski et al. (19). Peak areas are compared in three sets of five samples; set one consists of samples in neat solution (mobile phase), set two of matrix blanks spiked with the analyte after sample preparation and set three of processed samples spiked before sample preparation. Set two and three should be constructed in five different batches of blank matrix. The matrix factor is then calculated by the ratio of set one and set three, while the recovery is calculated by the ratio of set two

and three. FDA guidelines state that matrix effect should be evaluated for PK-TK assays, but do not describe how to achieve this. However, the FDA does describe recovery experiments by comparing the area of extracted samples with unextracted samples at three concentrations (low, mid, high).

Two papers of TDM assays performed matrix effect experiments according the post-column infusion method of Bonfiglio et al. (22,23). The effect of a blank matrix can be monitored with this method, however, the effect on quantification of the analyte is not investigated. Therefore, post-extraction is the preferred method for determination of the matrix effect (19–21). This is also reflected by the results of the literature search, as 26 papers investigated the matrix effect with this technique. Whether and how the matrix effect should be examined is still a matter of debate. Especially, since no acceptance criteria are given by guidelines as to what extent the matrix effect is thought to be acceptable. Poor reproducibility due to matrix effects will be reflected by a low accuracy and precision. This is already investigated in six different batches at LLOQ in the endogenous selectivity experiments. Furthermore, the use of isotopically labeled internal standards can compensate for matrix effects regarding reproducible quantification of the target analyte, and therefore, it is not necessary to determine the matrix factor in different batches (44). In 27 papers, a stable isotopically labeled internal standard was included in the assay; 16 papers used a ^{13}C- or ^{15}N-labeled internal standard, and 11 papers used a deuterated internal standard. Other articles used structural analogues as internal standard. As isotopically labeled internal standards are structurally similar to the analyte of interest, they will have a similar matrix effect and are therefore able to correct for matrix-related variability (45). However, deuterated internal standards may have a slightly different retention time than the analyte, caused by deuterium isotope effects, which is not observed for ^{13}C- or ^{15}N-labeled internal standard (46). Wang et al. demonstrated that a deuterated internal standard had a different degree of ion suppression due to a slight difference in retention time, causing a significant matrix effect (46). Therefore, ^{13}C- or ^{15}N-labeled internal standards should, if available, be first choice rather than deuterated internal standards. Furthermore, since a compound and its internal standard will theoretically co-elute, it is important to have a mass difference between those compounds to be able to separate them in the mass spectrometer to prevent cross talk. For small molecules a mass difference of at least 3 mass units is in most cases sufficient (47).

Recovery was studied in 27 TDM assays according to the post-extraction method. These experiments show the degree of analyte that is extracted during sample preparation. Recovery might be of interest if the extraction is low and the sensitivity is not sufficient for the purpose of the method. Such problems should already be addressed during method development to optimize the assay before method validation. Inconsistent and irreproducible recoveries have not been described in the selected TDM assays. Taking the above into account, determining matrix effect and recovery are not mandatory for validation of TDM methods when an isotopically labeled internal standard is used co-eluting with the analyte of interest.

Stability

Stability should be evaluated to ensure that storage conditions do not affect the concentration of the analyte. Therefore, stability needs to be established at every step of the analytical method. EMA and FDA guidelines recommend to test stock stability and the EMA advices to also test the stability of working solutions for PK-TK assays. Furthermore, the following stability conditions should be evaluated: freeze/thaw (F/T) stability of at least 3 cycles, short-term stability at room temperature, long-term stability under the same conditions as study samples are kept and, if applicable, other stability experiments, such as dry extract stability and the stability of processed samples. Stability experiments should be executed at low and high concentrations.

Although stability in stock- and working solution was described in only 14 papers for TDM assays, all papers reported stability in biomatrix, either experimental or from literature. Stability experiments were performed at least at low and high concentrations. Most papers did not describe how many replicates were used. Freeze/thaw stability was assessed in 24 papers, of which 4 tested more than 3 F/T cycles. For TDM, F/T stability of 3 cycles should be sufficient, as samples are frozen after withdrawal and generally measured after the first thaw cycle. Additional F/T stability of up to 3 cycles is important for potential reanalysis of samples. Short-term stability at room temperature was tested in 28papers, varying from 4 hours up to 28 days. Stability at room temperature is pivotal for transporting samples to the lab and during sample preparation. TDM assays are not always available in the hospital where blood withdrawal takes place. Therefore, it should be investigated whether samples can be transported at room temperature or should be transported on dry-ice. Furthermore, it is relevant to investigate the stability when exposed to light as blood collection tubes are generally transparent. Nonetheless, stability at room temperature while exposed to light and in the dark was examined in only five papers (6,25,32,48,49). The stability of processed samples was examined in 23 papers, either as re-injection reproduciblity or as final extract stability. EMA and FDA guidelines state that stability of processed samples should be measured if applicable, which is certainly the case for TDM to safeguard the possibility of re-analysis after system failure. When investigating the stability in processed samples, final extract stability is recommended instead of re-injection stability to facilitate re-analysis of samples with fresh calibration standards. Long-term stability (>1 month) was described in nine studies. Although long-term stability is not per se important for TDM measurements, because results are reported directly for routine clinical care, it might be useful for determining the shelf-life of calibration standards and quality control samples.

Analysis of study samples

EMA and FDA guidelines on bioanalytical validation also provide recommendations for application of the validated method for PK-TK assays. Before starting analysis of study

samples, the performance of the bioanalytical method should be verified. Similar to validation runs, the analytical run should consist of a blanks sample, a zero sample and at least 6 calibration standards. At least one set of calibration standards should be analyzed and ≥75% of the standards should be within 85-115% of their nominal concentration (80-120% for the LLOQ). If the LLOQ or ULOQ should be rejected in one analytical run, then the second lowest sample will become the LLOQ and the second highest sample the ULOQ. A minimum of three QC concentration levels in duplicate should be interspersed with study samples. The FDA and EMA recommend a minimum number of QC samples of at least 5% of the number of the clinical study samples or a total of six samples, whichever is greater. The accuracy at each concentration level should be ±15% of the nominal concentration and at least two out of three QC samples (one at each level) should be within the acceptance criteria. According to the FDA, the carry-over should be assessed and monitored during sample analysis.

Literature reporting analysis of study samples in TDM are sparse. Only one paper described the use of a system suitability test (SST) to prime the system (42) and two papers specified routine sample analysis (24,50). An SST is an integral part of the analytical procedure to ensure the performance of the analytical system. Critical elements of the analytical system should be included in the SST, such as the check for chromatographic separation of isomers. Methods for routine TDM should aim for a rapid turnaround by implementation of a short analytical run. Therefore, a method with fewer calibration standards and QC samples is proposed, consisting of a blank sample, a zero sample and four calibration standards, and three QC Mid samples (or at least 5% of the study samples whichever is higher). The calibration standards should be injected at the beginning of each analytical run and at least three out of four (75%) calibration standards should be within 85-115% of their nominal concentration (80-120% for the LLOQ), including the LLOQ and the ULOQ to maintain the anticipated range. QC Mid samples are injected after the calibration standards and at the end of the sequence to ensure adequate accuracy and precision for the whole analytical run. A similar strategy with only three calibration standards and one QC Mid sample proved accurate and robust for the quantification of sunitinib (24). The concentration of the QC Mid should have a similar concentration as the TDM target, which is the concentration at which dose adjustments are recommended. This concentration is the most critical value to be quantified accurately as results will be reported as being below or above this target. Therefore, we recommend the concentration of QC Mid samples to be similar to the target. Furthermore, carry-over should be assessed and monitored in each analytical run by injection two blanks samples after the ULOQ. If the carry-over exceeds ±20% of the LLOQ response, the integrity of the bioanalytical data should be assessed by calculation the carry-over matrix factor for all samples with the following equation:

$$Carry-over\ factor = \frac{\left(\dfrac{Response_x \cdot Mean\ response_{CB}}{Mean\ response_{ULOQ}}\right)}{Response_{x+1}} \times 100\%$$

In which x = sample x, CB = carry-over in the blank, ULOQ = upper limit of quantification and x+1 = the sample injected after sample x.

If the CF is >5%, there is a significant carry-over effect of sample x on sample x+1 and therefore, sample x+1 should be reanalyzed. However, if the CF is ≤5%, there is no significant effect of sample x on samples x+1 and the result of sample x+1 can be accepted. This carry-over protocol gives the opportunity to determine the impact of the carry-over on each sample and to accept those results that are not affected by it. In contrast to the analysis of multiple samples of one subject in PK studies, TDM sample concentrations may vary in concentration from sample to sample. It is important to establish that the carry-over has no impact on the quality of the generated data in each study run.

Overview of recommendations

In this review, method validation of TDM assays is described as compared to method validation of assays for PK-TK studies. For each validation parameter, recommendations of FDA and EMA guidelines for validation of PK-TK studies were described, followed by recommendations that could serve as a guide for future validations and analysis of study samples of TDM assays. A summary of recommendations specifically for validation of TDM assays is included in Table 2. The literature search showed that TDM assays are generally validated based on FDA and EMA guidelines, however, most articles do not fully comply with recommendations given in these guidelines, which is in line with what we recommend in this review. Calibration model and accuracy & precision were investigated in all included assays, which suggests that these parameters are regarded pivotal for validation of TDM assays. Furthermore, the majority of included articles describe stability and selectivity experiments, stressing the importance of these procedures. Although validation procedures differ among these assays, all articles based their experiments and criteria upon accepted bioanalytical method validation guidelines. In order to harmonize method validation of TDM assays, we aim to provide guidance for future assay validation of TDM methods. Differences in regard to FDA and EMA guidelines are proposed for the calibration model, LLOQ, selectivity, dilution factor, matrix effect and recovery. All proposed adjustments are made considering the importance of high-throughput assays and to simplify validation and implementation of such assays, keeping confidence in the fit-for-use purpose of the bioanalytical method. At least 4 calibration standards instead of 6 to 8 will be sufficient for TDM methods, as a short calibration range is recommended. Furthermore, a S/N ratio of at least 10 for the LLOQ will increase robustness of the assay regarding large between-assay variability of the MS signal. Endogenous selectivity experiments are of high importance during method validation of TDM methods, in which it is recommended to include blanks and LLOQ samples in 6 different batches of plasma. Interference of co-medications, degradation products or other xenobiotics only needs to be examined for structural analogous or

when there is reason to believe that an interference may occur. Determining the dilution factor is generally not necessary for TDM assays, as concentrations above ULOQ indicate that the target was attained. Matrix effect and recovery experiments are of no additional value in TDM methods, if stable isotopically-labeled internal standards are used co-eluting with the analytes of interest.. Therefore, we propose to not include matrix effect and recovery in validation procedures. Accuracy and precision, carry-over and stability experiments should be assessed according to FDA and EMA guidelines at three levels (Table 2). Analysis of study samples should be focussed on rapid turnaround. This can be achieved by analyzing only four calibration standards and at least three QC Mids at TDM target level.

Conclusions

A wide diversity of assays, for the purpose of TDM in oncology, have been developed and validated. This review presents an overview of publications in which LC-MS/MS assays have been validated for application in TDM. The focus of TDM assays is on developing and validating routine assays in which target attainment is strived for, rather than generating data for PK-TK studies. This is a different type of analytical procedure and, therefore, recommendations from FDA and EMA guidelines on bioanalytical method validation are comprehensive for LC-MS/MS assays specifically designed for TDM purpose. In addition to evaluating current practice, we recommend a minimal validation protocol for TDM assays while preserving a bioanalytical validation approach resulting in reliable bioanalytical results.

Future perspectives

The first validation paper of an LC-MS/MS assay specifically designed for TDM in oncology was published in 2003. Since then, many TDM assays have been developed and validated, also in other fields (Figure 1). With individualized drug dosing gaining popularity, implementation of TDM will further increase. Moreover, the class of oral anticancer therapies is rapidly growing and these drugs have a high inter-patient variable bioavailability and narrow therapeutic windowt. TDM of anticancer drugs is becoming an important tool in treatment of patients with cancer, especially with increased use of oral anticancer drugs with highly variable bioavailability (2–7). TDM has been shown to be a valuable intervention to optimize dosing of some anticancer drugs (4,5,7–9), however, prospective research is needed to further confirm these TDM targets. With the growing class of oral anticancer therapies, there is an increasing demand for TDM for which new assays have to be developed and validated. Shortened validation protocols could help to provide in this demand, while still offering sufficient confidence in the fit-for-purpose of the bioanalytical method. Simplifying the validation of TDM methods will shorten the time needed for validation and will increase the clinical implementation of such assays. In this review we focus on TDM assays in oncology,

however, recommendations can be applied to other fields and we advise bioanalytical laboratories to consider integrating our recommendations into standard validation of TDM assays.

References

1. de Jonge ME, Huitema ADR, Schellens JHM, Rodenhuis S, Beijnen JH. Individualised cancer chemotherapy: strategies and performance of prospective studies on therapeutic drug monitoring with dose adaptation: a review. Clin Pharmacokinet. 2005;44:147–73.

2. Gao B, Yeap S, Clements A, Balakrishnar B, Wong M, Gurney H. Evidence for therapeutic drug monitoring of targeted anticancer therapies. J Clin Oncol. 2012;30:4017–25.

3. Lankheet NAG, Knapen LM, Schellens JHM, Beijnen JH, Steeghs N, Huitema ADR. Plasma concentrations of tyrosine kinase inhibitors imatinib, erlotinib, and sunitinib in routine clinical outpatient cancer care. Ther Drug Monit. 2014;36:326–34.

4. Widmer N, Bardin C, Chatelut E, Paci A, Beijnen J, Leveque D, et al. Review of therapeutic drug monitoring of anticancer drugs part two--targeted therapies. Eur J Cancer. 2014;50:2020–36.

5. Paci A, Veal G, Bardin C, Leveque D, Widmer N, Beijnen J, et al. Review of therapeutic drug monitoring of anticancer drugs part 1--cytotoxics. Eur J Cancer. 2014;50:2010–9.

6. Herbrink M, de Vries N, Rosing H, Huitema ADR, Nuijen B, Schellens JHM, et al. Development and validation of a liquid chromatography-tandem mass spectrometry analytical method for the therapeutic drug monitoring of eight novel anticancer drugs. Biomed Chromatogr. 2018;32.

7. Yu H, Steeghs N, Nijenhuis CM, Schellens JHM, Beijnen JH, Huitema ADR. Practical Guidelines for Therapeutic Drug Monitoring of Anticancer Tyrosine Kinase Inhibitors: Focus on the Pharmacokinetic Targets. Clin Pharmacokinet. 2014;53:305–25.

8. Verheijen RB, Yu H, Schellens JHM, Beijnen JH, Steeghs N, Huitema ADR. Practical Recommendations for Therapeutic Drug Monitoring of Kinase Inhibitors in Oncology. Clin Pharmacol Ther. 2017;102:765–76.

9. Groenland SL, van Nuland M, Verheijen RB, Schellens JHM, Beijnen JH, Huitema ADR, et al. Therapeutic Drug Monitoring of Oral Anti-Hormonal Drugs in Oncology. Clin Pharmacokinet. 2019;58:299–308.

10. Adaway JE, Keevil BG. Therapeutic drug monitoring and LC-MS/MS. J Chromatogr B, Anal Technol Biomed life Sci. 2012;883–884:33–49.

11. Schellens JHM, McLeod HL, Newell DR. Cancer Clinical Pharmacology. Oxford University Press; 2005. p. 1-17.

12. Dasgupta A. Chapter 2 - Immunoassays and Issues With Interference in Therapeutic Drug Monitoring. In: Clinical Challenges in Therapeutic Drug Monitoring. San Diego: Elsevier; 2016. p. 17–44.

13. Zhang Y, Zhang R. Recent advances in analytical methods for the therapeutic drug monitoring of immunosuppressive drugs. Drug Test Anal. 2018;10:81–94.

14. Miura M, Takahashi N. Routine therapeutic drug monitoring of tyrosine kinase inhibitors by HPLC-UV or LC-MS/MS methods. Drug Metab Pharmacokinet. 2016;31:12–20.

15. US Food and Drug Administration (FDA). FDA Guidance for Industry: Bioanalytical Method Validation. Silver Spring, Maryland: US Food and Drug Administration. 2018 [cited 2018 Jun]. Available from: https://www.fda.gov/downloads/drugs/guidances/ucm070107.Pdf

16. European Medicines Agency (EMA). Guideline on Bioanalytical Method Validation. Committe for Medicinal Produts for Human Use and European Medicines Agency. 2011 [cited 2019 May]. Available from: http://www.ema.europa.eu/docs/en_GB/document_library/Scientific_guideline/2011/08/WC500109686.pdf

17. Clinical and Laboratory Standards Institute (CLSI). Evaluation of the Linearity of Quantitative Measurement Procedures: A Statistical Approach; Approved Guideline. EP06-A2. 2003.

18. Clinical and Laboratory Standards Institute (CLSI). Preliminary Evaluation of Quantitative Clinical Laboratory Measurement Procedures. EP10-A3. 2006.

19. Matuszewski BK, Constanzer ML, Chavez-Eng CM. Strategies for the assessment of matrix effect in quantitative bioanalytical methods based on HPLC-MS/MS. Anal Chem. 2003;75:3019–30.

20. Marchi I, Viette V, Badoud F, Fathi M, Saugy M, Rudaz S, et al. Characterization and classification of matrix effects in biological samples analyses. J Chromatogr A. 2010;1217:4071–8.

21. Taylor PJ. Matrix effects: the Achilles heel of quantitative high-performance liquid chromatography-electrospray-tandem mass spectrometry. Clin Biochem. 2005;38:328–34.

22. King R, Bonfiglio R, Fernandez-Metzler C, Miller-Stein C, Olah T. Mechanistic investigation of ionization suppression in electrospray ionization. J Am Soc Mass Spectrom. 2000;11:942–50.

23. Bonfiglio, King, Olah, Merkle. The effects of sample preparation methods on the variability of the electrospray ionization response for model drug compounds. Rapid Commun Mass Spectrom. 1999;13:1175–85.

24. Lankheet NAG, Steeghs N, Rosing H, Schellens JHM, Beijnen JH, Huitema ADR. Quantification of sunitinib and N-desethyl sunitinib in human EDTA plasma by liquid chromatography coupled with electrospray ionization tandem mass spectrometry: validation and application in routine therapeutic drug monitoring. Ther Drug Monit. 2013;35:168–76.

25. Nijenhuis CM, Haverkate H, Rosing H, Schellens JHM, Beijnen JH. Simultaneous quantification of dabrafenib and trametinib in human plasma using high-performance liquid chromatography-tandem mass spectrometry. J Pharm Biomed Anal. 2016;125:270–9.

26. Verheijen RB, Thijssen B, Rosing H, Schellens JHM, Nan L, Venekamp N, et al. Fast and Straightforward Method for the Quantification of Pazopanib in Human Plasma Using LC-MS/MS. Ther Drug Monit. 2018;40:230–6.

27. Peters FT, Maurer HH. Systematic comparison of bias and precision data obtained with multiple-point and one-point calibration in six validated multianalyte assays for quantification of drugs in human plasma. Anal Chem. 2007;79:4967–76.

28. Cardoso E, Mercier T, Wagner AD, Homicsko K, Michielin O, Ellefsen-Lavoie K, et al. Quantification of the next-generation oral anti-tumor drugs dabrafenib, trametinib, vemurafenib, cobimetinib, pazopanib, regorafenib and two metabolites in human plasma by liquid chromatography-tandem mass spectrometry. J Chromatogr B, Anal Technol Biomed life Sci. 2018;1083:124–36.

29. Gu H, Liu G, Wang J, Aubry A-F, Arnold ME. Selecting the correct weighting factors for linear and quadratic calibration curves with least-squares regression algorithm in bioanalytical LC-MS/MS assays and impacts of using incorrect weighting factors on curve stability, data quality, and assay perfo. Anal Chem. 2014;86:8959–66.

30. Liu H, Lam L, Dasgupta PK. Expanding the linear dynamic range for multiple reaction monitoring in quantitative liquid chromatography-tandem mass spectrometry utilizing natural isotopologue transitions. Talanta. 2011;87:307–10.

31. Rosing H, Man WY, Doyle E, Bult A, Beijnen JH. Bioanalytical liquid chromatographic method validation. A review of current practices and procedures. J Liq Chromatogr Relat Technol. 2000;23:329–54.

32. de Krou S, Rosing H, Nuijen B, Schellens JHM, Beijnen JH. Fast and Adequate Liquid Chromatography-Tandem Mass Spectrometric Determination of Z-endoxifen Serum Levels for Therapeutic Drug Monitoring. Ther Drug Monit. 2017;39:132–7.

33. Lynch KL. CLSI C62-A: A New Standard for Clinical Mass Spectrometry. Clin Chem. 2016;62:24–9.

34. Gibbons JA, Ouatas T, Krauwinkel W, Ohtsu Y, van der Walt J-S, Beddo V, et al. Clinical Pharmacokinetic Studies of Enzalutamide. Clin Pharmacokinet. 2015;54:1043–55.

35. van Nuland M, Hillebrand MJ., Rosing H, Schellens JHM, Beijnen JH. Development and validation of an LC-MS/MS method for the simultaneous quantification of abiraterone, enzalutamide, and their major metabolites in human plasma. Ther Drug Monit. 2017;39:243–51.

36. de Zwart M, Lausecker B, Globig S, Neddermann D, Le Bras B, Guenzi A, et al. Co-medication and interference testing in bioanalysis: a European Bioanalysis Forum recommendation. Bioanalysis. 2016;8:2065–70.

37. Jager NGL, Rosing H, Linn SC, Schellens JHM, Beijnen JH. Importance of highly selective LC-MS/MS analysis for the accurate quantification of tamoxifen and its metabolites: focus on endoxifen and 4-hydroxytamoxifen. Breast Cancer Res Treat. 2012;133:793–8.

38. van Nuland M, Hillebrand MJX, Rosing H, Schellens JHM, Beijnen JH. Development and Validation of an LC-MS/MS Method for the Simultaneous Quantification of Abiraterone, Enzalutamide, and Their Major Metabolites in Human Plasma. Ther Drug Monit. 2017;39:243–51.

39. Hughes NC, Wong EYK, Fan J, Bajaj N. Determination of carryover and contamination for mass spectrometry-based chromatographic assays. AAPS J. 2007;9:e353-60.

40. French D, Sujishi KK, Long-Boyle JR, Ritchie JC. Development and validation of a liquid chromatography-tandem mass spectrometry assay to quantify plasma busulfan. Ther Drug Monit. 2014;36:169–74.

41. Heideloff C, Payto D, Wang S. Comparison of a stable isotope-labeled and an analog internal standard for the quantification of everolimus by a liquid chromatography-tandem mass spectrometry method. Ther Drug Monit. 2013;35:246–50.

42. Rezende VM, Rivellis AJ, Gomes MM, Dorr FA, Novaes MMY, Nardinelli L, et al. Determination of serum levels of imatinib mesylate in patients with chronic myeloid leukemia: validation and application of a new analytical method to monitor treatment compliance. Rev Bras Hematol Hemoter. 2013;35:103–8.

43. Bergeron A, Garofolo F. Importance of matrix effects in LC–MS/MS bioanalysis. Bioanalysis. 2013;5:2331–2.

44. Viswanathan CT, Bansal S, Booth B, DeStefano AJ, Rose MJ, Sailstad J, et al. Workshop/conference report—Quantitative bioanalytical methods validation and implementation: Best practices for chromatographic and ligand binding assays. AAPS J. 2007;E30–42.

45. Annesley TM. Ion Suppression in Mass Spectrometry. Clin Chem. 2003;49:1041–4.

46. Wang S, Cyronak M, Yang E. Does a stable isotopically labeled internal standard always correct analyte response? A matrix effect study on a LC/MS/MS method for the determination of carvedilol enantiomers in human plasma. J Pharm Biomed Anal. 2007;43:701–7.

47. Stokvis E, Rosing H, Beijnen JH. Stable isotopically labeled internal standards in quantitative bioanalysis using liquid chromatography/mass spectrometry: necessity or not? Rapid Commun Mass Spectrom. 2005;19:401–7.

48. Escudero-Ortiz V, Perez-Ruixo JJ, Valenzuela B. Development and validation of a high-performance liquid chromatography ultraviolet method for lapatinib quantification in human plasma. Ther Drug Monit. 2013;35:796–802.

49. van Nuland M, Venekamp N, de Vries N, de Jong KAM, Rosing H, Beijnen JH. Development and validation of an UPLC-MS/MS method for the therapeutic drug monitoring of oral anti-hormonal drugs in oncology. J Chromatogr B. 2019;1106–1107:26–34.

50. Dennison JB, Renbarger JL, Walterhouse DO, Jones DR, Hall SD. Quantification of vincristine and its major metabolite in human plasma by high-performance liquid chromatography/tandem mass spectrometry. Ther Drug Monit. 2008;30:357–64.

51. Rood JJM, van Bussel MTJ, Schellens JHM, Beijnen JH, Sparidans RW. Liquid chromatography-tandem mass spectrometric assay for the T790M mutant EGFR inhibitor osimertinib (AZD9291) in human plasma. J Chromatogr B, Anal Technol Biomed life Sci. 2016;1031:80–5.

52. van Dyk M, Miners JO, Kichenadasse G, McKinnon RA, Rowland A. A novel approach for the simultaneous quantification of 18 small molecule kinase inhibitors in human plasma: A platform for optimised KI dosing. J Chromatogr B, Anal Technol Biomed life Sci. 2016;1033–1034:17–26.

53. Danso D, Jannetto PJ, Enger R, Langman LJ. High-Throughput Validated Method for the Quantitation of Busulfan in Plasma Using Ultrafast SPE-MS/MS. Ther Drug Monit. 2015;37:319–24.

54. Meesters RJW, Cornelissen R, van Klaveren RJ, de Jonge R, den Boer E, Lindemans J, et al. A new ultrafast and high-throughput mass spectrometric approach for the therapeutic drug monitoring of the multi-targeted anti-folate pemetrexed in plasma from lung cancer patients. Anal Bioanal Chem. 2010;398:2943–8.

55. Bobin-Dubigeon C, Heurgue-Berlot A, Bouche O, Amiand M-B, Le Guellec C, Bard J-M. A new rapid and sensitive LC-MS assay for the determination of sorafenib in plasma: application to a patient undergoing hemodialysis. Ther Drug Monit. 2011;33:705–10.

56. Taylor PJ, Franklin ME, Graham KS, Pillans PI. A HPLC-mass spectrometric method suitable for the therapeutic drug monitoring of everolimus. J Chromatogr B Analyt Technol Biomed Life Sci. 2007;848:208–14.

57. Kosovec JE, Egorin MJ, Gjurich S, Beumer JH. Quantitation of 5-fluorouracil (5-FU) in human plasma by liquid chromatography/electrospray ionization tandem mass spectrometry. Rapid Commun Mass Spectrom. 2008;22:224–30.

58. Wu D, Wang Y, Sun Y, Ouyang N, Qian J. A simple, rapid and reliable liquid chromatography-mass spectrometry method for determination of methotrexate in human plasma and its application to therapeutic drug monitoring. Biomed Chromatogr. 2015;29:1197–202.

59. Gao S, Zhou J, Zhang F, Miao H, Yun Y, Feng J, et al. Rapid and sensitive liquid chromatography coupled with electrospray ionization tandem mass spectrometry method for the analysis of paclitaxel, docetaxel, vinblastine, and vinorelbine in human plasma. Ther Drug Monit. 2014;36:394–400.

60. Morgan PE, Brown NW, Tredger JM. A direct method for the measurement of everolimus and sirolimus in whole blood by LC-MS/MS using an isotopic everolimus internal standard. Ther Drug Monit. 2014;36:358–65.

61. Capron A, Destree J, Maiter D, Wallemacq P. Validation of a rapid liquid chromatography-tandem mass spectrometric assay for the determination of octreotide plasma concentrations. Clin Biochem. 2014;47:139–41.

62. Shao R, Yu L, Lou H, Ruan Z, Jiang B, Chen J. Development and validation of a rapid LC-MS/MS method to quantify letrozole in human plasma and its application to therapeutic drug monitoring. Biomed Chromatogr. 2016;30:632–7.

63. Schofield RC, Ramanathan L V, Murata K, Grace M, Fleisher M, Pessin MS, et al. Development and validation of a turbulent flow chromatography and tandem mass spectrometry method for the quantitation of methotrexate and its metabolites 7-hydroxy methotrexate and DAMPA in serum. J Chromatogr B, Anal Technol Biomed life Sci. 2015;1002:169–75.

64. Kirchherr H, Shipkova M, von Ahsen N. Improved method for therapeutic drug monitoring of 6-thioguanine nucleotides and 6-methylmercaptopurine in whole-blood by LC/MSMS using isotope-labeled internal standards. Ther Drug Monit. 2013;35:313–21.

65. Lankheet NAG, Hillebrand MJX, Rosing H, Schellens JHM, Beijnen JH, Huitema ADR. Method development and validation for the quantification of dasatinib, erlotinib, gefitinib, imatinib, lapatinib, nilotinib, sorafenib and sunitinib in human plasma by liquid chromatography coupled with tandem mass spectrometry. Biomed Chromatogr. 2013;27:466–76.

66. Pressiat C, Huynh H-H, Plé A, Sauvageon H, Madelaine I, Chougnet C, et al. Development and Validation of a Simultaneous Quantification Method of Ruxolitinib, Vismodegib, Olaparib, and Pazopanib in Human Plasma Using Liquid Chromatography Coupled With Tandem Mass Spectrometry. Ther Drug Monit. 2018;40:337–43.

67. Couchman L, Birch M, Ireland R, Corrigan A, Wickramasinghe S, Josephs D, et al. An automated method for the measurement of a range of tyrosine kinase inhibitors in human plasma or serum using turbulent flow liquid chromatography-tandem mass spectrometry. Anal Bioanal Chem. 2012;403:1685–95.

68. Wojnicz A, Colom-Fernandez B, Steegmann JL, Munoz-Calleja C, Abad-Santos F, Ruiz-Nuno A. Simultaneous Determination of Imatinib, Dasatinib, and Nilotinib by Liquid Chromatography-Tandem Mass Spectrometry and Its Application to Therapeutic Drug Monitoring. Ther Drug Monit. 2017;39:252–62.

69. Herbrink M, de Vries N, Rosing H, Huitema ADR, Nuijen B, Schellens JHM, et al. Quantification of 11 Therapeutic Kinase Inhibitors in Human Plasma for Therapeutic Drug Monitoring Using Liquid Chromatography Coupled With Tandem Mass Spectrometry. Ther Drug Monit. 2016;38:649–56.

70.   Huynh HH, Pressiat C, Sauvageon H, Madelaine I, Maslanka P, Lebbe C, et al. Development and Validation of a Simultaneous Quantification Method of 14 Tyrosine Kinase Inhibitors in Human Plasma Using LC-MS/MS. Ther Drug Monit. 2017;39:43–54.

71.   Rousset M, Titier K, Bouchet S, Dutriaux C, Pham-Ledard A, Prey S, et al. An UPLC-MS/MS method for the quantification of BRAF inhibitors (vemurafenib, dabrafenib) and MEK inhibitors (cobimetinib, trametinib, binimetinib) in human plasma. Application to treated melanoma patients. Clin Chim Acta. 2017;470:8–13.

72.   Arellano C, Gandia P, Lafont T, Jongejan R, Chatelut E. Determination of unbound fraction of imatinib and N-desmethyl imatinib, validation of an UPLC-MS/MS assay and ultrafiltration method. J Chromatogr B Analyt Technol Biomed Life Sci. 2012;907:94–100.

73.   Mei S, Shi X, Du Y, Cui Y, Zeng C, Ren X, et al. Simultaneous determination of plasma methotrexate and 7-hydroxy methotrexate by UHPLC-MS/MS in patients receiving high-dose methotrexate therapy. J Pharm Biomed Anal. 2018;158:300–6.

Development and validation of an UPLC-MS/MS method for the therapeutic drug monitoring of oral anti-hormonal drugs in oncology

Merel van Nuland
Nikkie Venekamp
Niels de Vries
Karen A.M. de Jong
Hilde Rosing
Jos H. Beijnen

Abstract

A liquid chromatography-mass spectrometry assay was developed and validated for simultaneous quantification of anti-hormonal compounds abiraterone, anastrozole, bicalutamide, Δ(4)-abiraterone (D4A), *N*-desmethyl enzalutamide, enzalutamide, Z-endoxifen, exemestane and letrozole for the purpose of therapeutic drug monitoring (TDM). Plasma samples were prepared with protein precipitation. Analyses were performed with a triple quadrupole mass spectrometer operating in the positive and negative ion-mode. The validated assay ranges from 2-200 ng/mL for abiraterone, 0.2-20 ng/mL for D4A, 10-200 ng/mL for anastrozole and letrozole, 1-20 ng/mL for *Z*-endoxifen, 1.88 – 37.5 ng/mL for exemestane and 1,500-30,000 ng/mL for enzalutamide, *N*-desmethyl enzalutamide and bicalutamide. Due to low sensitivity for exemestane, the final extract of exemestane patient samples should be concentrated prior to injection and a larger sample volume should be prepared for exemestane patient samples and QC samples to obtain adequate sensitivity. Furthermore, we observed a batch-dependent stability for abiraterone in plasma at room temperature and therefore samples should be shipped on ice. This newly validated method has been successfully applied for routine TDM of anti-hormonal drugs in cancer patients.

Introduction

Breast cancer and prostate cancer are the most common malignancies in women and men in the Western world (1). As these cancer types are highly dependent on growth-stimulating hormones, anti-hormonal therapy is a first-line treatment strategy. Anti-hormonal drugs are generally administered orally or subcutaneously. Oral drugs for treatment of breast cancer include tamoxifen, anastrozole, letrozole and exemestane and oral drugs for prostate cancer therapy include bicalutamide, abiraterone acetate and enzalutamide. The group of oral anticancer drugs is rapidly expanding (2–5), however, most oral anti-hormonal agents have been on the market for a longer period of time.

Although many patients benefit from anti-hormonal therapy in terms of progression-free survival, treatment outcome is variable. This may be attributed to variability in drug levels and exposure. For some anti-hormonal drugs, such as tamoxifen and abiraterone acetate, a clear exposure-response relationship has been described (6–8). This relationship is the basis for therapeutic drug monitoring (TDM); individualized drug dosing by monitoring drug concentrations in patient blood, plasma or serum. In current practice, oral anti-hormonal drugs are administered at fixed doses, which could lead to suboptimal exposure or high blood concentrations and adverse-events. Recommendations for pharmacokinetic TDM are based on clinical studies and guidelines and proposed targets for anti-hormonal drugs for the treatment of breast cancer and prostate cancer can be found in literature (8). Ultimately, implementation of individualized dosing with TDM may be an important tool to improve treatment outcome and efficacy in breast cancer and prostate cancer patients.

To facilitate TDM, there is a need for bioanalytical assays to quantify drugs of interest. Liquid chromatography-mass spectrometry (LC-MS/MS) is a useful and often applied analytical technique for determining drug concentrations. When developing an analytical method for TDM, it is important to choose a clinically relevant calibration range. This quantitation range should be built around the proposed target concentration, covering the majority of samples as seen in the clinic. Our lab has experience developing and validating methods for TDM of anticancer agents (9–11). Previously published LC-MS/MS assays for quantification of abiraterone (11–16), anastrozole (17), bicalutamide (13,18–20), Z-endoxifen (21–24), enzalutamide (9,11,13,25–28), exemestane (29,30) and letrozole (31,32) are limited to measuring one to four analytes. Furthermore, there are no articles reporting steady-state concentrations of anastrozole, letrozole and exemestane in humans for TDM purpose, and no articles describing Z-endoxifen analysis in plasma. To our knowledge this is the first bioanalytical assay for simultaneous quantification of six anti-hormonal drugs in oncology, including the active metabolites Z-endoxifen, N-desmethyl enzalutamide and Δ(4)-abiraterone (D4A), which enables concurrent quantification of these analytes to

efficiently determine plasma concentrations for TDM purpose. Although methods have been developed for the combined analysis of anti-hormonal drugs for either prostate cancer or breast cancer, the development of an assay for both types of anti-hormonal drugs is complicated due to different chemical drug properties. Furthermore, the development of such an assay is challenging because target concentration ranges span from 0.2 – 30,000 ng/mL, compounds show a variety in MS response and a highly selective chromatographic method is needed to separate isomers of abiraterone and Z-endoxifen.

Materials and methods

Chemicals
Abiraterone, bicalutamide, enzalutamide, *N*-desmethyl enzalutamide, $^2H_4$-abiraterone, $^2H_4$-bicalutamide, $^2H_6$-enzalutamide and $^2H_6$-*N*-desmethyl enzalutamide were purchased from Alsachim (Illkirch Graffenstaden, France). Anastrozole, Z/E-endoxifen, exemestane, letrozole, $^2H_{12}$-anastrozole, $^2H_5$-Z/E-endoxifen, $^2H_3$-exemestane and $^2H_4$-letrozole were purchased from Toronto Research Chemistry (Toronto, Canada). D4A was produced at the Chemical Immunology laboratory, Leiden University Medical Centre (LUMC, Leiden, the Netherlands) according to a previously published method by Li et al. (33). Acetonitrile, methanol, water and formic acid 99%, used to prepare mobile phase, were obtained from Biosolve Ltd (Valkenswaard, The Netherlands). Water (distilled) used for sample preparation came from B. Braun Medical (Melsungen, Germany). Dimethyl sulfoxide (DMSO, seccosolv grade) was obtained from Merck (Darmstadt, Germany) and K_2EDTA plasma from Bioreclamations LLC (Hicksville, NY, USA).

Stock solutions and working solutions
Stock solutions containing abiraterone, anastrozole, bicalutamide, D4A, *N*-desmethyl enzalutamide enzalutamide, *Z*-endoxifen, exemestane or letrozole were stored in amber-colored containers. Separate stock solutions were prepared for calibration standards and quality control samples, according to Table 1. Stock solutions of the internal standards (IS) were prepared as 1 mg/mL concentration in the same solvent as the corresponding analyte. For D4A, no internal standard was available and therefore $^2H_4$-abiraterone was used as an internal standard for quantification. A mixture of IS stock solutions (IS working solution) was prepared in acetonitrile at concentrations of 125 ng/mL for $^2H_5$-Z-endoxifen, 250 ng/mL for $^2H_4$-abiraterone, $^2H_{12}$-anastrozole, $^2H_4$-bicalutamide and $^2H_4$-letrozole and 5,000 ng/mL for $^2H_6$-enzalutamide and $^2H_6$-*N*-desmethyl enzalutamide.

Working solutions were prepared in control human K_2EDTA plasma to spike the calibration and quality control samples. Working solutions for spiking calibration standards were prepared at concentrations of 10, 20, 100, 200, 2,000 ng/mL for *Z*-endoxifen, at 2, 10, 100, 200, 2,000 ng/mL for D4A, 20, 100, 1,000, 2,000, 20,000 ng/mL

Table 1. Concentrations of analytes in stock solution, calibration standards and quality control samples.

Analyte	Stock (mg/mL)	Calibration standards (ng/mL)	Quality control samples (ng/mL)
Abiraterone	1.00 (DMSO)	2; 10; 100; 200	2; 100; 200
Anastrozole	1.00 (Methanol)	10; 20; 100; 200	10; 10; 200
Bicalutamide	3.00 (DMSO)	1,500; 3,000; 15,000; 30,000	1,500; 15,000; 30,000
D4A	0.05 (DMSO)	0.2; 1; 10; 20	0.2; 10; 20
N-Desmethyl enzalutamide	3.00 (DMSO)	1,500; 3,000; 15,000; 30,000	1,500; 15,000; 30,000
Z-Endoxifen	0.05 (Methanol)	1; 2; 10; 20	1; 10; 20
Enzalutamide	3.00 (Acetonitrile)	1,500; 3,000; 15,000; 30,000	1,500; 15,000; 30,000
Exemestane	1.00 (DMSO)	62.5; 125; 625; 1,250	1,88; 18,8; 37.5 *
Letrozole	1.00 (DMSO)	10; 20; 100; 200	10; 100; 200

Abbreviations: D4A = Δ(4)-abiraterone, DMSO = Dimethylsulfoxide
* Exemestane QC samples were concentrated prior to analysis.

for abiraterone, 100, 200, 1,000, 2,000, 20,000 ng/mL for anastozole and letrozole, at 625, 1,250, 6,250, 12,500 ng/mL for exemestane and at 15,000, 30,000, 150,000, 300,000 ng/mL for bicalutamide, enzalutamide and *N*-desmethyl enzalutamide. Working solutions for spiking quality control (QC) samples were prepared at concentrations of 10, 20, 100, 200, 2,000 ng/mL for *Z*-endoxifen, at 2, 100, 200, 2,000 ng/mL for D4A, 20, 1,000, 2,000, 20,000 ng/mL for abiraterone, 100, 1,000, 2,000, 20,000 ng/mL for anastozole and letrozole and at 15,000, 150,000, 300,000 ng/mL for bicalutamide, enzalutamide and *N*-desmethyl enzalutamide. Separate working solutions were prepared to spike exemestane quality control samples at 125, 1,250, 25,000 ng/mL. All stock- and working solutions were stored at -20 °C.

Calibration standards, quality control samples
Calibration standards and QC samples were prepared by spiking 100 μL working solution to 900 μL K$_2$EDTA plasma. Independent working solutions were used for the preparation of calibration standards and QC samples. Combined QC samples were prepared for abiraterone, anastrozole, bicalutamide, D4A, *N*-desmethyl enzalutamide, enzalutamide and letrozole, while separate QC samples were prepared for exemestane. Final concentrations of calibration standards and quality control samples are depicted in Table 1. Calibration standards and QC samples were stored at -20 °C.

Sample preparation of calibration standards and combined QC samples
This paragraph describes the sample preparation of calibration samples containing abiraterone, anastrozole, bicalutamide, D4A, *N*-desmethyl enzalutamide, enzalutamide, exemestane and letrozole and of QC samples containing abiraterone, anastrozole, bicalutamide, D4A, *N*-desmethyl enzalutamide, enzalutamide and letrozole.

Directly after sample collection in the clinic, whole blood samples were centrifuged for 10 minutes at 2,000 x g at 4 °C and plasma was stored at -20 °C. To each 50 µL of plasma, a volume of 20 µL of IS working solution was added, except for double blank calibration samples. Proteins were precipitated to extract the analytes from the biomatrix with 100 µL of acetonitrile. Samples were then vortex-mixed for 10s and centrifuged for 5 minutes at 23,000 x g. The supernatant was transferred to amber-colored autosampler vials with insert.

Sample preparation of exemestane patient samples and QC samples

Directly after sample collection in the clinic, whole blood samples were centrifuged for 10 minutes at 2,000 x g at 4 °C and plasma was stored at -20 °C. For exemestane patient- and QC samples, 500 µL of plasma was aliquoted and a volume of 20 µL of IS working solution was added to each sample. Proteins were precipitated using 1,000 µL of acetonitrile. Samples were vortex-mixed for 10s and centrifuged for 5 minutes at 23,000 x g. The supernatant was transferred to 2 mL containers and the samples were dried under a gentle stream of nitrogen at 40 °C. The residue was reconstituted in 50 µL water-methanol (1:1 v/v), vortex-mixed for 10s and centrifuged for 5 minutes at 23,000 x g. The supernatant was transferred to amber-colored autosampler vials with insert. To correct for the difference in sample preparation of exemestane calibration samples and QC samples, a dilution factor of 0.03 and an internal standard concentration of 3.4 was used for quantification of patient samples and quality control samples.

Analytical equipment and conditions

Analytes were separated chromatographically using a Shimadzu LC system with a binary pump, a degasser, an autosampler and a valco valve (Nexera 2 series, Shimadzu corporation, Kyoto, Japan). The temperature of the autosampler was kept at 4 °C and the column oven at 50 °C. Mobile phase A consisted of 0.1% formic acid in water and mobile phase B consisted of acetonitrile-methanol (50:50, v/v). Gradient elution was applied at a flow rate of 0.6 mL/min through an Acquity BEH C$_{18}$ column (100Å, 2.1 x 15 mm, 1.8 µm) with an additional Acquity BEH C$_{18}$ Vanguard pre-column (100Å, 2.1 x 5 mm, 1.8 µm) (Waters, Milford, MA, USA). The following gradient was applied: 45% B (0.0–4.0 min), 100% B (4.0-5.0 min), 45% B (5.0–6.0 min). The divert valve directed the flow to the mass spectrometer between 0.5 and 5 minutes and the remainder to the waste container.

A triple quadropole mass spectrometer 6500 (Sciex, Framingham, MA, USA) with a turbo ion spray (TIS) interface operating in the positive and negative mode was used as a detector. Bicalutamide was determined in negative ion mode to obtain adequate assay sensitivity, while all the other compounds were measured in positive ion mode. For quantification, multiple reaction monitoring (MRM) chromatograms were acquired and processed using Analyst® 1.6.2 software (AB Sciex). General and analyte specific mass spectrometric parameters are listed in Table 2 and the structures and the proposed fragmentation patterns of the analytes are depicted in Figure 1.

Table 2. Above: General mass spectrometric parameters. Below: Analyte specific mass spectrometric parameters for abiraterone, anastrozole, bicalutamide, Δ(4)-abiraterone (D4A), *N*-desmethyl enzalutamide, endoxifen, enzalutamide, exemestane and letrozole. Bicalutamide is measured in negative ion mode, while the other analytes are measured in positive ion mode.

	Positive mode	Negative mode
Run duration	6 min	6 min
Ionspray voltage	5500 V	-4500 V
Nebulizer gas	40 au	30 au
Turbo gas / heater gas	60 au	40 au
Curtain gas	25 au	40 au
Collision gas	9 au	10 au
Temperature	450 °C	450 °C
Dwell time	20 ms	20 ms

	MRM (Da)	Collision energy (V)	Collision exit potential (V)	Declustering potential (V)	Retention time (min)
Abiraterone	350.1 → 156.1	63	10	186	2.3
Anastrozole	294.3 → 225.2	29	10	86	0.78
Bicalutamide	429.6 → 255.2	-20	-19	-35	1.7
D4A	348.3 → 156.1	57	6	111	2.2
N-Desmethyl enzalutamide	453.0 → 197.1	37	18	131	2.0
Z-Endoxifen	374.3 → 58.1	25	14	31	2.4
Enzalutamide	467.0 → 211.1	61	18	171	2.4
Exemestane	297.1 → 121.1	37	8	81	2.1
Letrozole	286.2 → 217.1	17	8	56	0.76

Validation procedures

The assay was validated for calibration model, accuracy and precision, LLOQ, sensitivity and selectivity, dilution integrity, carry-over and stability. Adjustments were made to typical validation practices to fit TDM purposes; four instead of six to eight calibrators were investigated, QC concentrations were prepared at three levels (LLOQ, medium, and high concentrations) and no matrix effects were evaluated. A reduced number of calibration standards increases the turnaround of the assay. We choose not to evaluate matrix effects as poor reproducibility due to the use of different matrices will also be reflected in the sensitivity experiments and because we use isotopically labeled internal standards to correct for matrix related effects. Accuracy and precision were calculated as described previously (9).
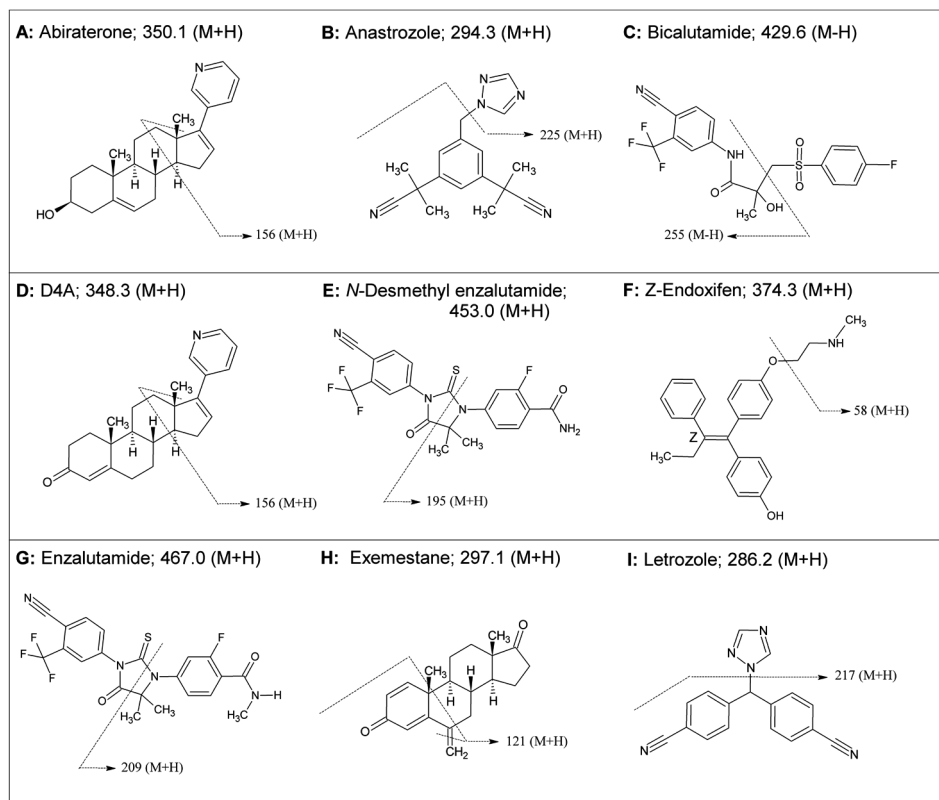
Figure 1. Proposed fragmentation patters of abiraterone (A), anastrozole (B), bicalutamide (C), Δ(4)-abiraterone (D4A;D), N-desmethyl enzalutamide (E), enzalutamide (F), endoxifen (G), exemestane (H) and letrozole (I). The mass of both the parent ion and the product ion are given for each analyte.

Clinical application

This assay was developed to support pharmacokinetic monitoring of abiraterone, anastrozole bicalutamide, D4A, N-desmethyl enzalutamide, Z-endoxifen, enzalutamide, exemestane and letrozole. As part of routine clinical care, K_2EDTA blood samples (4 mL) were collected from patients who were treated with one of these drugs at the Antoni van Leeuwenhoek – The Netherlands Cancer Institute. Plasma samples were collected and processed as described in this report.

Results and discussion

Sample preparation

Previous validation procedures showed that abiraterone is not stable in acetonitrile (34), therefore, working solutions were prepared in K_2EDTA plasma. Protein precipitation was chosen as high-throughput method for sample preparation with a sample:acetonitrile ratio of 50:100 (v/v). With this composition of the final extract, no further dilution was necessary prior to injection. However, with this simple sample preparation we were unable to quantify exemestane in patient samples due to low sensitivity. Therefore, we developed a method for the quantification of exemestane in patient samples and QC samples, using a 10-fold larger volume of plasma (500 µL instead of 50 µL). The final extracts of these samples were evaporated to dryness and reconstituted in 50 µL of reconstitution solvent. To preserve a fast turn-around, we prepared combined calibration standards containing all analytes including exemestane at a higher concentration range (62.5 to 1,250 ng/mL) these calibration standards were prepared with simple protein precipitation, without the need for concentrating the final extract. During development and validation it was shown that we could easily correct for the difference in sample preparation of exemestane calibration samples and QC samples by applying a dilution factor in the processing software.

Mass spectrometry and chromatography

The analytical setup was developed for simultaneous quantification of anti-hormonal drugs to monitor drug exposure. Chromatographic separation was pivotal and challenging for Z-endoxifen and abiraterone, as both analytes show extensive metabolism, including the formation of isomers. Therefore, baseline separation of these isomers was required. This was achieved by using an ultra-pressure liquid-chromatography (UPLC) column. Orbitrap MS (Thermo Fischer) spectra were obtained of the abiraterone metabolites to determine the accurate mass. These spectra confirm that both metabolites and abiraterone have the same accurate mass (349.24 g/mole) and are therefore considered isomers. Representative chromatograms of QC LLOQ and blank samples are presented in Figure 2 for each analyte. Furthermore, Figure 3 depicts the MRM chromatograms of Z-endoxifen and abiraterone of a patient sample, showing that the chromatographic system is capable of separating the isomers of these drugs. Calibration ranges were chosen so that analyte concentrations in patient samples were within this range. Reported C_{trough} concentrations of enzalutamide and *N*-desmethyl enzalutamide are 11.4 mg/L and 13.0 mg/L, respectively (35). A calibration range around these high plasma concentrations, however, caused saturation of the MS detector resulting in non-linearity of the calibration model. To overcome this, the MRM channel was adjusted (+2) to monitor m/z values of naturally occurring isotopes of both parent and product ions (36). With this modification, enzalutamide and *N*-desmethyl enzalutamide could both be measured in a clinically relevant concentration range without the need for sample dilution.
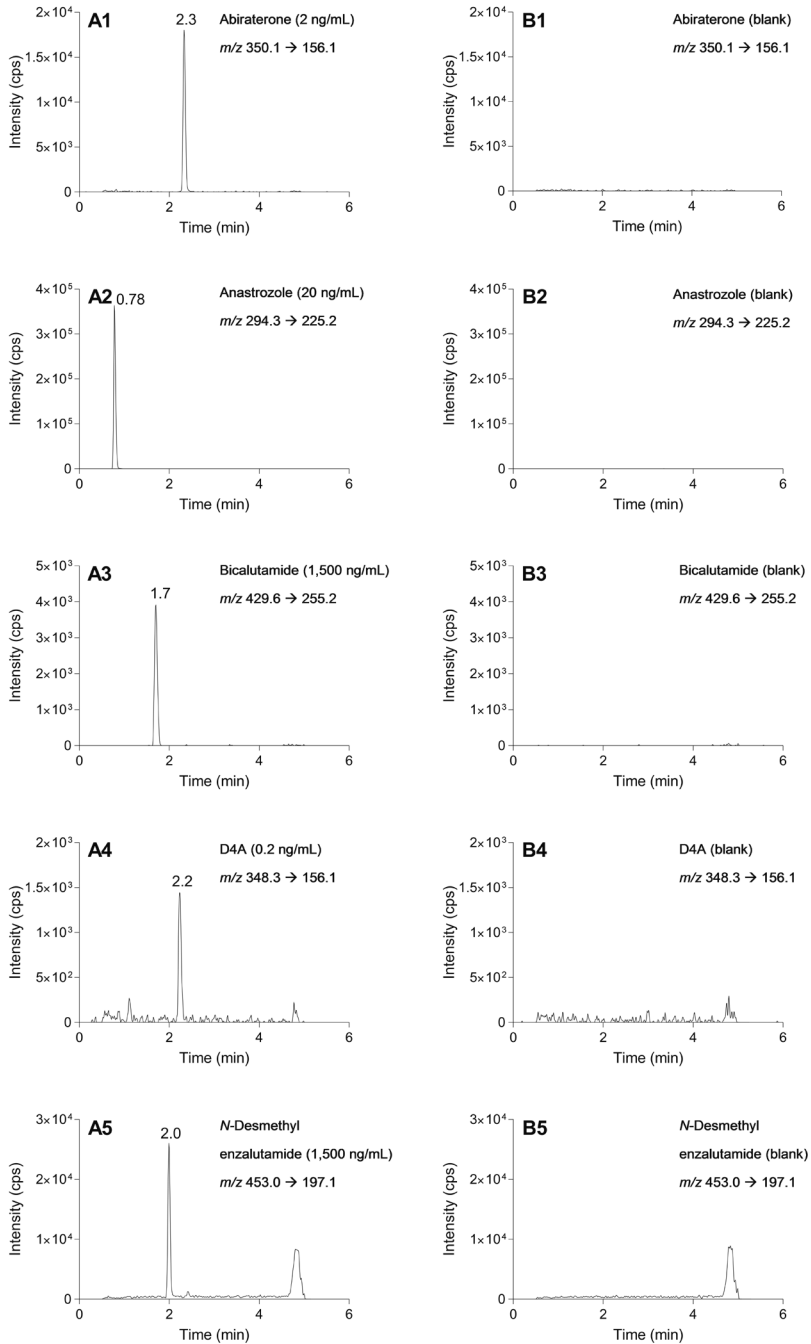
Figure 2. Representative LC-MS/MS chromatograms of the lower limit of quantification (A-series) and a blank sample (B-series): abiraterone (1), anastrozole (2), bicalutamide (3), D4A (4), *N*-desmethyl enzalutamide (5), enzalutamide (6), Z-endoxifen (7), exemestane (8) and letrozole (9). The isomer E-endoxifen (7) elutes at 2.1 minutes.
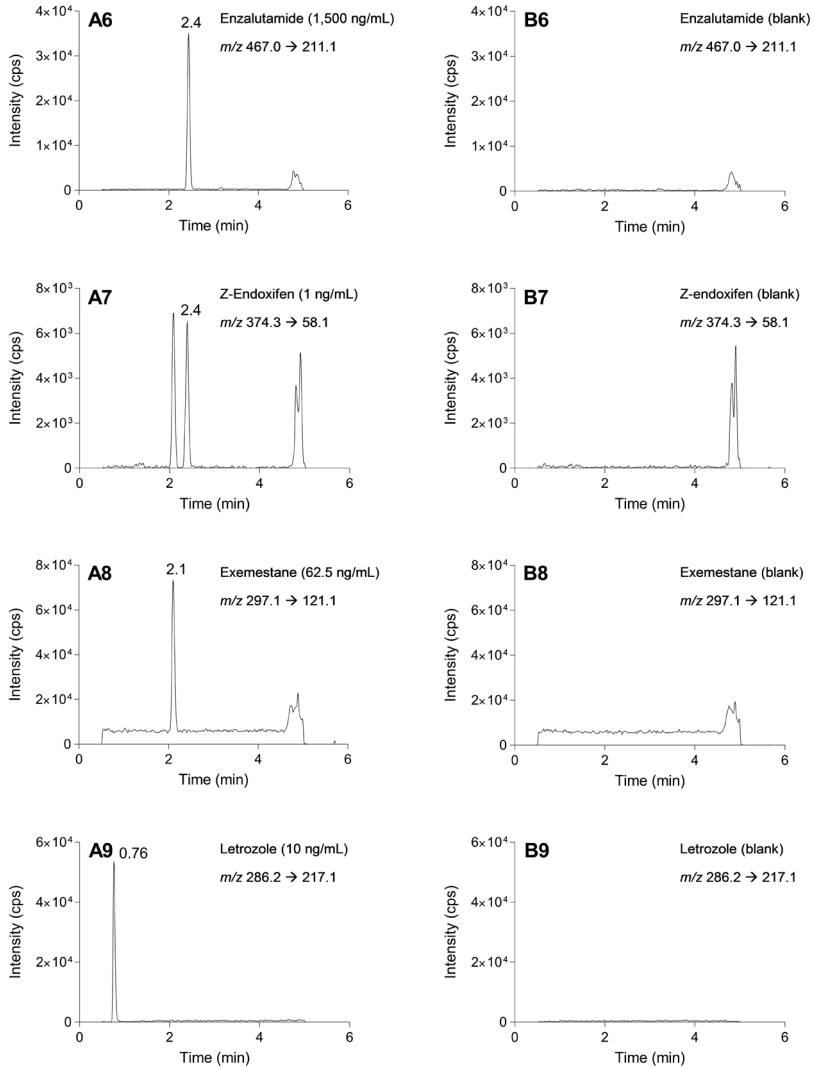
Continued: Figure 2. Representative LC-MS/MS chromatograms of the lower limit of quantification (A-series) and a blank sample (B-series): abiraterone (1), anastrozole (2), bicalutamide (3), D4A (4), *N*-desmethyl enzalutamide (5), enzalutamide (6), Z-endoxifen (7), exemestane (8) and letrozole (9). The isomer E-endoxifen (7) elutes at 2.1 minutes.
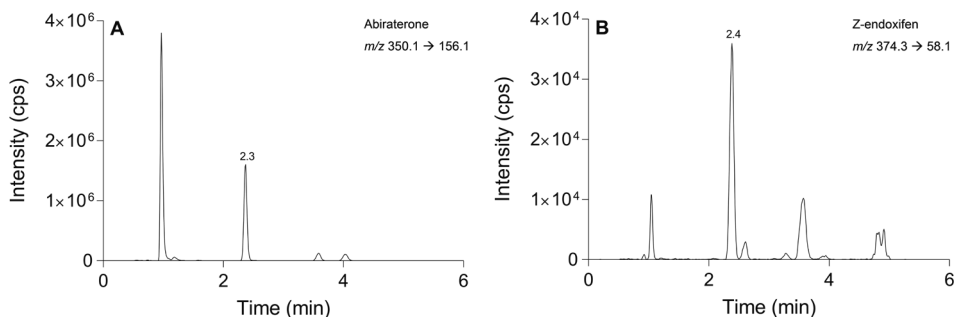
Figure 3. Representative LC-MS/MS chromatograms of abiraterone (A: 2.3 min) and Z-endoxifen (B: 2.4 min), showing the isomer patterns as seen in patient samples from a patient using abiraterone acetate and tamoxifen, respectively.

Calibration model

Four non-zero calibration standards were prepared and analyzed in three separate runs. Linearity of the calibration model was determined by plotting the peak area ratio of the analyte/IS against the corresponding concentration (x) of the calibration standard. The reciprocal of the squared concentrations ($1/x^2$) was used as a weighting factor for all analytes. For each calibration curve the calibration concentrations were back-calculated from the response ratios. The deviations of the nominal concentrations should be within ±15%. At the LLOQ level a deviation of ±20% was permitted. All calibration curves (n=3) of all analytes met these criteria. The assay was linear for the validated concentration ranges of 2-200 ng/mL voor abiraterone, 0.2-20 ng/mL for D4A, 10-200 ng/mL for anastrozole and letrozole, 1-20 ng/mL for *Z*-endoxifen, 62.5-1,250 ng/mL for exemestane and 1,500-30,000 ng/mL for enzalutamide, *N*-desmethyl enzalutamide and bicalutamide.

Accuracy and precision

Intra- and inter-assay bias and precisions of the method were determined by analyzing five replicate QC samples in three consecutive runs at LLOQ, mid and upper limit of quantification (ULOQ) concentration levels. The intra- and inter-assay biases and precisions should be within ±20% and ≤20%, respectively, for the LLOQ concentration and within ±15% and ≤15%, respectively, for other concentrations. Table 3 summarizes the intra- and inter-assay biases and precisions of the assay. All values were within the acceptance criteria.

Carry-over

Carry-over was investigated by injecting two double blank samples subsequently after an ULOQ sample in three independent runs. The peak area in the blank processed samples should be ≤20% of the peak area in the LLOQ sample and ≤5% of the internal standard area. There were no peaks observed in the first blank processed sample for any analyte, which means that there was no carry-over.
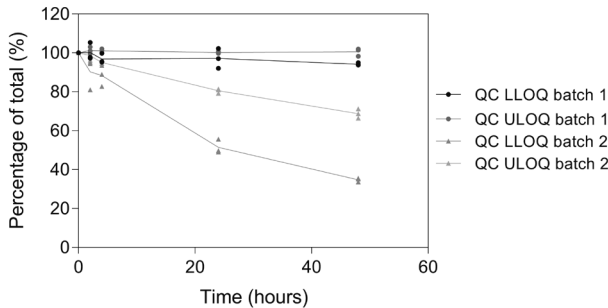
Figure 4. Short-term stability of abiraterone at lower limit of quantification (LLOQ) and upper limit of quantification (ULOQ) concentration in 2-year old K_2EDTA plasma (batch 1) and fresh K_2EDTA plasma (batch 2).

Specificity and selectivity

Six individual batches of K_2EDTA plasma were used to assess the specificity and selectivity of the method. A double blank sample and a sample spiked at the LLOQ were processed of each batch. The samples were prepared to determine whether endogenous compounds interfere at the mass transitions chosen for the analytes and internal standards. Samples were processed and analyzed according to the described procedures. Interferences co-eluting with the analytes or internal standards in the blanks were all ≤20% of the peak area of the analytes at LLOQ or ≤5% of the internal standard areas. Deviations of the nominal concentrations were within ±20% for at least 4 out of 6 batches for all analytes. Selectivity was therefore considered acceptable.

Stability

Stability of the analytes was tested under various conditions. All stability experiments were performed in triplicate. The analytes were considered stable in the plasma or processed sample when 85%–115% of the initial concentration was recovered. Furthermore, analytes were considered stable in the stock solution when 95%-105% of the original concentration was recovered.

All analytes were stable at -20 °C in plasma for at least 21 weeks. Short-term stability in plasma was determined after five days at room temperature (20-25 °C) and at 4°C in dark and exposed to light. Analytes were stable under these short-term storage conditions, except for abiraterone, which was unstable at room temperature in both light and dark. Additional stability experiments showed that abiraterone was stable for only 4 hours in plasma at room temperature. However, when the experiment was repeated in a two-year old batch of plasma, abiraterone was proven stable at room temperature up to 48 hours. Figure 4 shows the stability of abiraterone, given as the recovery (%) of the original concentration up to 48 hours in two different batches of plasma. The underlying mechanism for this batch-dependent stability remains to be elucidated but could possibly be caused by enzymes, which are active in fresh plasma and less active in older plasma.

Table 3. Assay performance data for abiraterone, anastrozole, bicalutamide, Δ(4)-abiraterone (D4A), *N*-desmethyl enzalutamide, endoxifen, enzalutamide, exemestane and letrozole.

Analyte	Nominal conc. (ng/mL)	Intra-assay (n=15)		Inter-assay (n=15)	
		Bias (%)	Precision (%)	Bias (%)	Precision (%)
Abiraterone	2	4.9-5.8	1.8-2.5	5.1	*
	100	-1.1-10	2.7-5.5	2.9	5.7
	200	2.1-7.6	1.4-4.5	4.9	2.2
Anastrozole	10	-5.7--4.2	1.2-1.8	-5.0	0.5
	100	-14.4--7.0	1.9-5.0	-10.0	4.1
	200	-10.5--6.1	1.5-4.0	-8.4	2.0
Bicalutamide	1,500	-10.0--7.2	1.7-3.1	-8.3	1.2
	15,000	-7.3--0.8	1.2-2.4	-4.8	3.6
	30,000	-7.3--1.1	1.4-3.2	-3.8	3.1
D4A	0.2	-16.6-7.5	2.5-12.5	-4.7	12.2
	10	-13.4--5.9	1.7-4.2	-10.6	4.3
	20	-11.1--8.9	2.2-2.8	-10.2	0.7
N-Desmethyl enzalutamide	1,500	-6.1-2.1	3.4-5.9	0.0	5.0
	15,000	-8.9--5.5	2.3-5.2	-7.6	1.2
	30,000	-9.3--2.9	4.7-5.8	-5.5	2.7
Z-Endoxifen	1	2.7-16.2	2.9-6.6	8.2	6.2
	10	2.2-14.8	3.1-5.1	6.7	6.3
	20	2.6-13.8	0.7-3.2	7.0	5.5
Enzalutamide	1,500	-5.9--2.1	1.6-4.7	-4.0	1.1
	15,000	-12.4-0.0	1.2-3.7	-6.6	6.6
	30,000	-3.5-0.7	0.7-3.4	-3.3	3.9
Exemestane	1.88	-19.0-5.1	0.8-3.1	-6.8	12.9
	18.8	-0.9-2.9	0.8-3.2	1.1	1.6
	37.5	-4.4-2.1	1.2-3.0	-0.4	3.4
Letrozole	10	-12.2--9.8	2.0-2.8	-10.9	0.7
	100	-10.0--6.0	1.3-4.4	-7.4	2.0
	200	-13.4--10.1	2.3-3.9	-11.2	1.6

* No significant additional variation was found due to the performance of the assay in different batches. Abbreviations: D4A = Δ(4)-abiraterone, conc. = concentration, C.V. = coefficient of variation.

The effect of three freeze (-20 ºC)/thaw cycles on the stability of each compound was investigated after thawing samples to room temperature with a minimum interval of 12 hours on three separate occasions and comparison with freshly prepared calibration samples. All analytes were stable for three freeze/thaw cycles. Five-day stability was proven for all analytes in final extract at 4 ºC. Furthermore, exemestane was stable in dried extract at 4 ºC for at least five days. Stability in stock solution was demonstrated at 124 days at -20 ºC.

Clinical application

This analytical assay was used to determine plasma concentrations of abiraterone, anastrozole bicalutamide, D4A, *N*-desmethyl enzalutamide, *Z*-endoxifen, enzalutamide,

Table 4. Plasma concentrations of the analytes in patient samples of patients treated with these drugs (n=10). Z-Endoxifen was measured in plasma from patients using tamoxifen and abiraterone and Δ(4)-abiraterone (D4A) were determined in plasma from patients using abiraterone acetate. Abbreviation: o.d. = once daily.

Analyte	Recommended dose (mg)	Mean plasma concentrations (ng/mL)	Range (ng/mL)	Validated range (ng/mL)
Abiraterone	1000 o.d.	43.0	3.31 - 136	2 – 200
Anastrozole	1 o.d.	38.9	19.6 - 64.6	10 – 200
Bicalutamide	50 o.d.	16,714	7,270 - 31,200	1,500 – 30,000
D4A	- *	4.67	0.382 - 9.45	0.2 – 20
N-desmethyl enzalutamide	- *	11,069	9,000 - 14,400	1,500 – 30,000
Endoxifen	- *	9.73	2.38 - 17.1	1 - 20
Enzalutamide	160 o.d.	11,946	8,320 - 17,800	1,500 – 30,000
Exemestane	25 o.d.	12.4	0.62** - 48.9	1.88 – 37.5
Letrozole	2.5 o.d.	107	37.9 – 356***	10 – 200

* D4A, *N*-desmethyl enzalutamide and endoxifen are active metabolites of abiraterone, enzalutamide and tamoxifen, respectively. The recommended dose of these drugs are 1000 mg o.d. for abiraterone, 160 mg o.d. for enzalutamide and 20 mg o.d. for tamoxifen.
** Two exemestane samples were below the lower limit of quantification (LLOQ).
*** One letrozole samples was above the upper limit of quantification (ULOQ).

exemestane and letrozole in samples from patients using these drugs. The chromatograms of abiraterone and Z-endoxifen show additional peaks with identical transitions, belonging to isomeric metabolites. The presence of these isomeric metabolites has been previously described (12,14,34,37). Applicability of the assay was shown in samples from patients treated with these drugs and the results are listed in Table 4. Ten patients were included for each drug and one sample was drawn from each patient. All values were within the validated range, except for two exemestane samples being below the LLOQ and one letrozole sample being above the ULOQ. The quantitation ranges of previously published methods (exemestane 0.2-0.4 ng/mL, (29,30); letrozole 6-430 ng/mL (32)) might be sufficient to determine exemestane and letrozole concentrations within the validated range. However, our method was developed for the purpose of therapeutic drug monitoring and therefore the quantitation range was chosen to measure the majority of samples from the clinic. These results demonstrate the applicability of this method for quantification of the selected oral anti-hormonal drugs and three active metabolites for therapeutic drug monitoring.

Conclusion

The development and validation of a combined assay for the quantification of abiraterone, anastrozole bicalutamide, D4A, *N*-desmethyl enzalutamide, *Z*-endoxifen,

enzalutamide, exemestane and letrozole in plasma is described. The validated assay ranges from 2-200 ng/mL voor abiraterone, 0.2-20 ng/mL for D4A, 10-200 ng/mL for anastrozole and letrozole, 1-20 ng/mL for *Z*-endoxifen, 1.88 – 37.5 ng/mL for exemestane and 1,500-30,000 ng/mL for enzalutamide, *N*-desmethyl enzalutamide and bicalutamide. Exemestane patient samples and QC samples should be concentrated to increase the sensitivity of the assay, and enzalutamide and *N*-desmethyl enzalutamide should be monitored at +2 m/z values to prevent detector saturation and therefore the need for sample dilution. Furthermore, the chromatographic method of this assay is highly selective and capable of separating isomers of abiraterone and Z-endoxifen Due to instability of abiraterone in plasma at room temperature, abiraterone patient samples should be shipped on dry ice. In conclusion, the presented assay is considered suitable to support therapeutic drug monitoring of oral anti-hormonal drugs in clinical daily oncology practice.

References

1. Siegel RL, Miller KD, Jemal A. Cancer statistics. CA Cancer J Clin. 2016;66:7–30.

2. US Food and Drug Administration (FDA). CDER 2014 Report to the Nation. 2014.

3. US Food and Drug Administration (FDA). CDER 2015 Report to the Nation. 2015.

4. US Food and Drug Administration (FDA). CDER 2016 Report to the Nation. 2016.

5. US Food and Drug Administration (FDA). CDER 2017 Report to the Nation. 2017.

6. Carton E, Noe G, Huillard O, Golmard L, Giroux J, Cessot A, et al. Relation between plasma trough concentration of abiraterone and prostate-specific antigen response in metastatic castration-resistant prostate cancer patients. Eur J Cancer. 2017;72:54–61.

7. Madlensky L, Natarajan L, Tchu S, Pu M, Mortimer J, Flatt SW, et al. Tamoxifen metabolite concentrations, CYP2D6 genotype, and breast cancer outcomes. Clin Pharmacol Ther. 2011;89:718–25.

8. Groenland SL, van Nuland M, Verheijen RB, Schellens JHM, Beijnen JH, Huitema ADR, et al. Therapeutic Drug Monitoring of Oral Anti-Hormonal Drugs in Oncology. Clin Pharmacokinet. 2019;58:299–308.

9. Herbrink M, de Vries N, Rosing H, Huitema ADR, Nuijen B, Schellens JHM, et al. Development and validation of a liquid chromatography-tandem mass spectrometry analytical method for the therapeutic drug monitoring of eight novel anticancer drugs. Biomed Chromatogr. 2018;32.

10. Herbrink M, de Vries N, Rosing H, Huitema ADR, Nuijen B, Schellens JHM, et al. Quantification of 11 Therapeutic Kinase Inhibitors in Human Plasma for Therapeutic Drug Monitoring Using Liquid Chromatography Coupled With Tandem Mass Spectrometry. Ther Drug Monit. 2016;38:649–56.

11. van Nuland M, Hillebrand MJ., Rosing H, Schellens JHM, Beijnen JH. Development and validation of an LC-MS/MS method for the simultaneous quantification of abiraterone, enzalutamide, and their major metabolites in human plasma. Ther Drug Monit. 2017;39:243–51.

12. Benoist GE, van der Meulen E, Lubberman FJE, Gerritsen WR, Smilde TJ, Schalken JA, et al. Analytical challenges in quantifying abiraterone with LC-MS/MS in human plasma. Biomed Chromatogr. 2017;31.

13. Kim K-P, Parise RA, Holleran JL, Lewis LD, Appleman L, van Erp N, et al. Simultaneous quantitation of abiraterone, enzalutamide, N-desmethyl enzalutamide, and bicalutamide in human plasma by LC-MS/MS. J Pharm Biomed Anal. 2017;138:197–205.

14. Alyamani M, Li Z, Upadhyay SK, Anderson DJ, Auchus RJ, Sharifi N. Development and validation of a novel LC-MS/MS method for simultaneous determination of abiraterone and its seven steroidal metabolites in human serum: Innovation in separation of diastereoisomers without use of a chiral column. J Steroid Biochem Mol Biol. 2017;172:231–9.

15. Gurav S, Punde R, Farooqui J, Zainuddin M, Rajagopal S, Mullangi R. Development and validation of a highly sensitive method for the determination of abiraterone in rat and human plasma by LC-MS/MS-ESI: application to a pharmacokinetic study. Biomed Chromatogr. 2012;26:761–8.

16. Martins V, Asad Y, Wilsher N, Raynaud F. A validated liquid chromatographic-tandem mass spectroscopy method for the quantification of abiraterone acetate and abiraterone in human plasma. J Chromatogr B Analyt Technol Biomed Life Sci. 2006;843:262–7.

17. Apostolou C, Dotsikas Y, Kousoulos C, Loukas YL. Development and validation of an improved high-throughput method for the determination of anastrozole in human plasma by LC-MS/MS and atmospheric pressure chemical ionization. J Pharm Biomed Anal. 2008;48:853–9.

18. Sharma K, Pawar G V, Giri S, Rajagopal S, Mullangi R. Development and validation of a highly sensitive LC-MS/MS-ESI method for the determination of bicalutamide in mouse plasma: application to a pharmacokinetic study. Biomed Chromatogr. 2012;26:1589–95.

19. P S S, Vijay Kumar S, Kumar A, Mullangi R. Development of an LC-MS/MS method for determination of bicalutamide on dried blood spots: application to pharmacokinetic study in mice. Biomed Chromatogr. 2015;29:254–60.

20. Kim B, Shim J, Lee S, Sang Yu K-, Yoon SH. Liquid Chromatography Tandem Mass Spectrometry Determination of Bicalutamide in Human Plasma and Application to a Bioequivalence Study. Lee S, editor. J Bioanal Biomed. 2011;03:098-102.

21. de Krou S, Rosing H, Nuijen B, Schellens JHM, Beijnen JH. Fast and Adequate Liquid Chromatography-Tandem Mass Spectrometric Determination of Z-endoxifen Serum Levels for Therapeutic Drug Monitoring. Ther Drug Monit. 2017;39:132–7.

22. Tre-Hardy M, Capron A, Antunes MV, Linden R, Wallemacq P. Fast method for simultaneous quantification of tamoxifen and metabolites in dried blood spots using an entry level LC-MS/MS system. Clin Biochem. 2016;49:1295–8.

23. Jager NG, Rosing H, Schellens JH, Beijnen JH. Determination of tamoxifen and endoxifen in dried blood spots using LC-MS/MS and the effect of coated DBS cards on recovery and matrix effects. Bioanalysis. 2014;6:2999–3009.

24. Antunes MV, Raymundo S, de Oliveira V, Staudt DE, Gossling G, Peteffi GP, et al. Ultra-high performance liquid chromatography tandem mass spectrometric method for the determination of tamoxifen, N-desmethyltamoxifen, 4-hydroxytamoxifen and endoxifen in dried blood spots--development, validation and clinical application during breast c. Talanta. 2015;132:775–84.

25. Benoist GE, van der Meulen E, van Oort IM, Beumer JH, Somford DM, Schalken JA, et al. Development and Validation of a Bioanalytical Method to Quantitate Enzalutamide and its Active Metabolite N-Desmethylenzalutamide in Human Plasma: Application to Clinical Management of Patients With Metastatic Castration-Resistant Prostate Cancer. Ther Drug Monit. 2018;40:222–9.

26. Song JH, Kim TH, Jung JW, Kim N, Ahn SH, Hwang SO, et al. Quantitative determination of enzalutamide, an anti-prostate cancer drug, in rat plasma using liquid chromatography-tandem mass spectrometry, and its application to a pharmacokinetic study. Biomed Chromatogr. 2014;28:1112–7.

27. Bennett D, Gibbons JA, Mol R, Ohtsu Y, Williard C. Validation of a method for quantifying enzalutamide and its major metabolites in human plasma by LC-MS/MS. Bioanalysis. 2014;6:737–44.

28. Sulochana SP, Saini NK, Daram P, Polina SB, Mullangi R. Validation of an LC-MS/MS method for simultaneous quantitation of enzalutamide, N-desmethylenzalutamide, apalutamide, darolutamide and ORM-15341 in mice plasma and its application to a mice pharmacokinetic study. J Pharm Biomed Anal. 2018;156:170–80.

29. Wang L-Z, Goh S-H, Wong AL-A, Thuya W-L, Lau J-YA, Wan S-C, et al. Validation of a rapid and sensitive LC-MS/MS method for determination of exemestane and its metabolites, 17beta-hydroxyexemestane and 17beta-hydroxyexemestane-17-O-beta-D-glucuronide: application to human pharmacokinetics study. PLoS One. 2015;10:e0118553.

30. Corona G, Elia C, Casetta B, Diana C, Rosalen S, Bari M, et al. A liquid chromatography-tandem mass spectrometry method for the simultaneous determination of exemestane and its metabolite 17-dihydroexemestane in human plasma. J Mass Spectrom. 2009;44:920–8.

31. Shao R, Yu L, Lou H, Ruan Z, Jiang B, Chen J. Development and validation of a rapid LC-MS/MS method to quantify letrozole in human plasma and its application to therapeutic drug monitoring. Biomed Chromatogr. 2016;30:632–7.

32. Precht JC, Ganchev B, Heinkele G, Brauch H, Schwab M, Murdter TE. Simultaneous quantitative analysis of letrozole, its carbinol metabolite, and carbinol glucuronide in human plasma by LC-MS/MS. Anal Bioanal Chem. 2012;403:301–8.

33. Li R, Evaul K, Sharma KK, Chang K-H, Yoshimoto J, Liu J, et al. Abiraterone inhibits 3beta-hydroxysteroid dehydrogenase: a rationale for increasing drug exposure in castration-resistant prostate cancer. Clin Cancer Res. 2012;18:3571–9.

34. van Nuland M, Hillebrand MJX, Rosing H, Schellens JHM, Beijnen JH. Development and Validation of an LC-MS/MS Method for the Simultaneous Quantification of Abiraterone, Enzalutamide, and Their Major Metabolites in Human Plasma. Ther Drug Monit. 2017;39:243–51.

35. Gibbons JA, Ouatas T, Krauwinkel W, Ohtsu Y, van der Walt J-S, Beddo V, et al. Clinical Pharmacokinetic Studies of Enzalutamide. Clin Pharmacokinet. 2015;54:1043–55.

36. Liu H, Lam L, Dasgupta PK. Expanding the linear dynamic range for multiple reaction monitoring in quantitative liquid chromatography-tandem mass spectrometry utilizing natural isotopologue transitions. Talanta. 2011;87:307–10.

37. Jager NGL, Rosing H, Linn SC, Schellens JHM, Beijnen JH. Importance of highly selective LC-MS/MS analysis for the accurate quantification of tamoxifen and its metabolites: focus on endoxifen and 4-hydroxytamoxifen. Breast Cancer Res Treat. 2012;133:793–8.

Development and validation of an LC-MS/MS method for the simultaneous quantification of abiraterone, enzalutamide, and their major metabolites in human plasma

Merel van Nuland
Michel J.X. Hillebrand
Hilde Rosing
Jan H.M. Schellens
Jos H. Beijnen

Abstract

Background
Abiraterone acetate and enzalutamide are two novel drugs for the treatment of metastatic castration-resistant prostate cancer (mCRPC). The metabolism of these drugs is extensive. Major metabolites are *N*-desmethyl enzalutamide, enzalutamide carboxylic acid, abiraterone N-oxide sulfate, and abiraterone sulfate, of which *N*-desmethyl enzalutamide is reported to possess anti-androgen capacities. A liquid chromatography-tandem mass spectrometry (LC-MS/MS) method for simultaneous quantification of abiraterone, enzalutamide, and the main metabolites has been developed and validated to support therapeutic drug monitoring.

Methods
Human plasma samples of patients treated with abiraterone or enzalutamide were harvested at the clinic and stored at -20ºC. Proteins were precipitated by acetonitrile and the final extract was injected on a Kinetex C18 column and separated with gradient elution. Analytes were detected by liquid chromatography-mass spectrometry (Triple Quad 6500).

Results
The method was validated over various linear ranges: 1-100 ng/mL for abiraterone, 5-500 ng/mL for enzalutamide and enzalutamide carboxylic acid, 10-1,000 ng/mL for *N*-desmethyl enzalutamide, 30-3,000 ng/mL for abiraterone N-oxide sulfate, and 100-10,000 ng/mL for abiraterone sulfate. Intra-assay and inter-assay variabilities were within ±15% of the nominal concentrations for quality control (QC) samples at medium and high concentrations and within ±20% at the lower limit of quantification (LLOQ), respectively.

Conclusion
The described method for simultaneous determination of abiraterone and enzalutamide was validated successfully and provides a useful tool for therapeutic drug monitoring in patients treated with these agents.

Introduction

Prostate cancer is a highly prevalent malignancy and accounts for approximately 20% of new oncological diagnoses in men (1,2). Abiraterone acetate and enzalutamide are both oral anti-androgen drugs approved for treatment of metastatic castration-resistant prostate cancer (mCRPC). Abiraterone acetate was granted market access in 2011 and enzalutamide became available in 2012 (3,4). Both drugs inhibit tumor growth effects of androgens. Abiraterone acetate prevents the production of testosterone by inhibition of 17α-hydroxylase/C17,20-lyase (CYP17), while enzalutamide functions as an androgen receptor signaling inhibitor (5,6). In human intestinal fluid, abiraterone acetate is rapidly deacetylated into the active compound abiraterone, which is measured in this bioanalytical method. Hepatic metabolism of abiraterone and enzalutamide is extensive and the major metabolites *N*-desmethyl enzalutamide, enzalutamide carboxylic acid, abiraterone sulfate, and abiraterone N-oxide sulfate are produced in substantial quantities (7,8). *N*-desmethyl enzalutamide is known to have clinically relevant anti-androgen capacities similar to enzalutamide (4).

Pharmacokinetic monitoring of oral anti-cancer therapies has increased enormously over the past years (9). Interpatient variability in exposure, known to be 41-141% for abiraterone (10) and up to 31% for enzalutamide (11), could lead to undesirable toxicities or sub-therapeutic treatment. Therefore, plasma level measurement of abiraterone and enzalutamide could be beneficial in therapy optimization. It is currently unknown what target concentrations should be pursued and this is now assessed in pharmacokinetic studies. Previously published liquid chromatography-mass spectrometry (LC-MS/MS) assays for the determination of abiraterone (12–14), enzalutamide (15) and both metabolites of enzalutamide (16) are limited to either one anti-androgen drug and report no human clinical data. This assay enables concurrent quantification of these analytes to efficiently determine plasma concentrations of patients receiving abiraterone or enzalutamide. Quantification of the major metabolites gives insight into the metabolism of both drugs and provides information on hepatic clearance. We now report the development and validation of the simultaneous analysis of abiraterone, enzalutamide, and their major metabolites *N*-desmethyl enzalutamide, enzalutamide carboxylic acid, abiraterone sulfate, and abiraterone N-oxide sulfate in human plasma with LC-MS/MS. Additionally, the clinical application of this assay was demonstrated.

Materials and methods

Chemicals

Abiraterone, enzalutamide, *N*-desmethyl enzalutamide, and the internal standards (IS) $^2H_4$-abiraterone, $^2H_6$-enzalutamide, and $^2H_6$-*N*-desmethyl enzalutamide were purchased from Alsachim (Illkirch, France). Enzalutamide carboxylic acid was manufactured by TLC Pharmaceutical Standards Ltd. (Ontario, Canada) and abiraterone sulfate sodium

salt and abiraterone N-oxide sulfate sodium salt were obtained from Toronto Research Chemicals (Toronto, Canada). Acetonitrile, methanol (both Supra-Gradient grade), water, and formic acid (both LC-MS grade) were from Biosolve Ltd. (Valkenswaard, The Netherlands). Dimethyl sulfoxide (DMSO, seccosolv grade) was obtained from Merck (Darmstadt, Germany) and K_2EDTA plasma from the Medical Center Slotervaart (Amsterdam, The Netherlands) and Bioreclamations LLC (Hicksville, NY, USA).

Stock solutions
Stock solutions, working solutions, calibrators, and all quality control (QC) samples were prepared in amber colored 1.5 mL tubes. Separate stock solutions in DMSO were prepared for calibrators and QC samples. These contained 1 mg/mL of one of abiraterone, enzalutamide, or *N*-desmethyl enzalutamide, and 0.5 mg/mL of enzalutamide carboxylic acid, abiraterone sulfate, or abiraterone N-oxide sulfate. Stock solutions of 1 mg/mL in methanol were produced for the internal standards $^2H_4$-abiraterone, $^2H_6$-enzalutamide, and $^2H_6$-*N*-desmethyl enzalutamide.

Calibrators, quality control samples
The stock solutions were diluted with plasma in order to obtain working solutions. A combined working solution of abiraterone, enzalutamide, *N*-desmethyl enzalutamide, enzalutamide carboxylic acid, and abiraterone N-oxide sulfate was prepared. Since an interfering impurity of abiraterone was present in the reference standard of abiraterone sulfate, a separate working solution was prepared for this compound. A combined IS working solution was prepared in methanol at final concentrations of 25 ng/mL and 100 ng/mL for $^2H_4$-abiraterone and both $^2H_6$-enzalutamide and $^2H_6$-*N*-desmethyl enzalutamide, respectively. Stock solutions and working solutions were stored at -20ºC. Both calibrators and QC samples were freshly prepared prior to each validation run by adding 80 µL of each working solution to 320 µL of blank human plasma. Concentrations of the calibrators were 1, 5, 50, and 100 ng/mL for abiraterone; 5, 25, 250, and 500 ng/mL for enzalutamide and enzalutamide carboxylic acid; 10, 50, 500, and 1,000 ng/mL for *N*-desmethyl enzalutamide, and 30, 150, 1,500, and 3,000 ng/mL for abiraterone N-oxide sulfate. A separate set of calibrators was produced for abiraterone sulfate containing 100, 500, 5,000, and 10,000 ng/mL. Concentrations of the lower limit of quantification (LLOQ) QC, QC mid, and QC high samples were 5, 40, and 100 ng/mL for abiraterone; 5, 200, and 500 ng/mL for enzalutamide and enzalutamide carboxylic acid; 10, 400, and 1,000 ng/mL for N-desmethyl enzalutamide; 30, 1,200, and 3,000 ng/mL for abiraterone N-oxide sulfate and 100, 4,000, and 10,000 ng/mL for the separately spiked abiraterone sulfate. Both calibrators and QC samples were processed in aliquots of 50 µL.

Sample preparation
Whole venous blood was obtained from treated patients and centrifuged for 5 minutes at 4ºC at 1,800 g. The supernatant (plasma fraction) was isolated and stored at -20ºC

until analysis. Samples were thawed prior to processing and a 50 µL aliquot was transferred to amber colored 1.5 mL containers. A volume of 15 µL IS working solution was added to each sample. Proteins were precipitated with 150 µL of acetonitrile, after which the samples were vortexed, shaken (10 minutes at 11,300g, and centrifuged (10 minutes at 20°C at 23,100 g). A volume of 100 µL of the supernatant was transferred to 1.5 mL tubes and diluted with 100 µL water (LC-MS grade). The final extracts were transferred to amber colored glass autosampler vials.

Analytical equipment and conditions
The analytical system was composed of a liquid chromatography (LC) Nexera 2 series (Shimadzu Corporation, Kyoto, Japan) coupled to a triple quadropole mass spectrometer 6500 (Sciex, Framingham, MA, USA) with a turbo ion spray (TIS) interface. The LC was equipped with a Nexera 2 series binary pump, a degasser, an autosampler, and a valco valve (Shimadzu Corporation, Kyoto, Japan).
Chromatographic separation was acquired using a Kinetex C18 column (15 x 2.1 mm, particle size 2.6 µm; Phenomenex, Torrance, CA, USA). The mobile phase A consisted of formic acid-water (0.1:100, v/v) and mobile phase B was composed of formic acid-methanol (0.1:100, v/v). Analytes were eluted under isocratic conditions with 70% mobile phase B following a 2-minute hold of 30% mobile phase B at a flow rate of 0.3 mL/min. To elute hydrophobic compounds from the column, a 3-minute rinsing step with a 100% mobile phase B was applied before conditions were stabilized to initial settings. During the first 2.5 minutes and the last 4.5 minutes, the eluate was directed to waste.
The mass spectrometer operated in the positive ion mode and was configured in multiple reaction monitoring mode at unique transitions for each analyte and IS. Analyst software version 1.6.2 (Sciex) was used for system control and data analysis. A summary of general and specific mass spectrometric settings is provided in Table 1 and Table 2. ^{2}H$_4$-Abiraterone was used as IS for abiraterone, ^{2}H$_6$-*N*-desmethyl enzalutamide for *N*-desmethyl enzalutamide, and ^{2}H$_6$-enzalutamide for enzalutamide, enzalutamide carboxylic acid, abiraterone N-oxide sulfate, and abiraterone sulfate. The structures and the proposed fragmentation patterns of the analytes are depicted in Figure 1.

Validation procedures
Validation of the assay was completed based on the United States Food and Drug Administration (FDA) and European Medicines Agency (EMA) guidelines for bioanalytical method validation (17,18). These guidelines apply for clinical and pre-clinical pharmacology and toxicology studies. For this TDM assay, all aspects of the validation were investigated; however, four instead of six to eight calibrators were investigated and QC concentrations were prepared at three levels: LLOQ, medium, and high concentrations. Calibration model, accuracy and precision, carry-over, selectivity (endogenous, cross analyte/IS interferences), matrix effect, recovery, dilution integrity, and stability were established during the validation.

Table 1. Above: general mass spectrometric parameters. Below: Analyte specific mass spectrometric parameters for abiraterone, enzalutamide and both major metabolites.

Parameter	Setting
Run duration	13.5 min
Ionspray voltage	5500 V
Nebulizer gas	40 au
Turbo gas / heater gas	40 au
Curtain gas	20 au
Collision gas	8 au
Temperature	350 ºC
Dwell time	50 msec

	Parent mass	Product mass	Collision energy	Collision exit potential	Declustering potential	Retention time
Enzalutamide	465.0 *m/z*	209.1 *m/z*	37.0 V	18.0 V	131.0 V	4.77 min
N-desmethyl enzalutamide	451.1 *m/z*	195.2 *m/z*	37.0 V	18.0 V	186.0 V	4.64 min
Enzalutamide carboxylic acid	452.1 *m/z*	196.1 *m/z*	37.0 V	18.0 V	131.0 V	4.95 min
Abiraterone	350.1 *m/z*	156.1 *m/z*	63.0 V	10.0 V	186.0 V	7.10 min
Abiraterone N-oxide sulfate	446.0 *m/z*	348.3 *m/z*	63.0 V	10.0 V	186.0 V	5.10 min
Abiraterone sulfate	430.0 *m/z*	332.1 *m/z*	63.0 V	10.0 V	186.0 V	5.44 min
$^2H_6$-enzalutamide	471.2 *m/z*	215.1 *m/z*	37.0 V	18.0 V	131.0 V	4.76 min
$^2H_6$-*N*-desmethyl enzalutamide	457.1 *m/z*	201.2 *m/z*	37.0 V	18.0 V	131.0 V	4.63 min
$^2H_4$-abiraterone	354.1 *m/z*	160.1 *m/z*	63.0 V	10.0 V	186.0 V	6.95 min

Calibration model

Calibration linearity was determined by plotting the peak area ratio of the analyte/IS against the corresponding concentration (x) of the calibrator. Linear regression analysis was performed with $1/x^2$ weighting. Deviations from the mean calculated concentrations should be within ±15% (±20% for LLOQ calibrators) of nominal concentrations in at least 75% of non-zero calibrators.

Accuracy and precision

Five replicated QC samples were analyzed in three consecutive runs at LLOQ, mid-, and high concentrations. Accuracy was expressed as the relative error (RE%) and precision was calculated as the relative standard deviation (RSD%). Intra-assay variability (%) was determined from mean measured concentrations per run and the inter-assay bias (%) was calculated from the overall mean measured concentrations. A one-way ANOVA was used to calculate inter-run variation. The acceptance criteria for both parameters were ±15% for QC mid and QC high and ±20% for QC LLOQ.
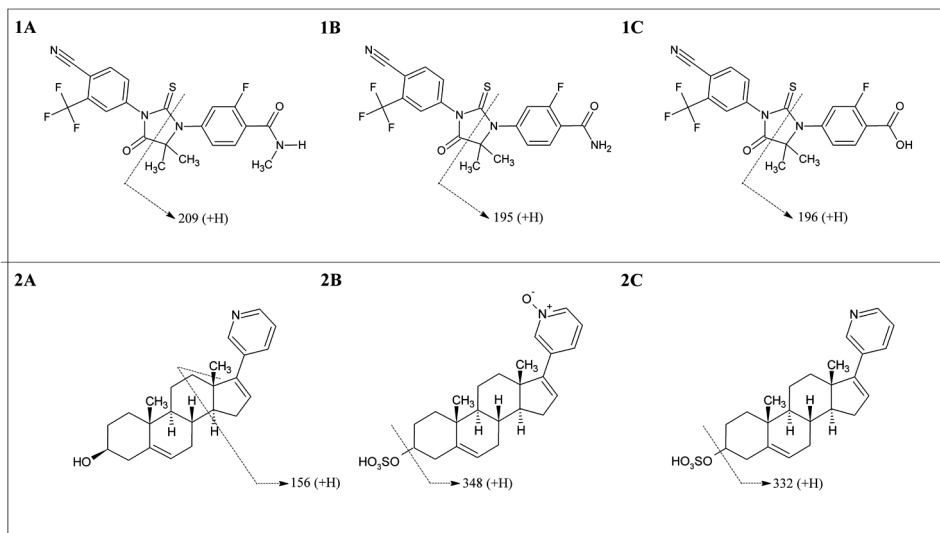
Figure 1. Molecular structures and proposed fragmentation of enzalutamide (1A), *N*-desmethyl enzalutamide (1B), enzalutamide carboxylic acid (1C), abiraterone (2A), abiraterone N-oxide sulfate (2B), and abiraterone sulfate (2C). Precursor ions m/z (+H) are 465.0, 451.1, 452.1, 350.1, 446.0, and 430.0, respectively.

Carry-over

Carry-over was determined by injecting two double blank samples after a calibrator with the highest concentration (upper limit of quantification, ULOQ). The peak area in the blank sample should not be higher than 20% of the peak area in the LLOQ.

Selectivity

Six separate batches of blank human plasma were spiked at the LLOQ level with one of abiraterone, enzalutamide, *N*-desmethyl enzalutamide, enzalutamide carboxylic acid, and abiraterone N-oxide sulfate or abiraterone sulfate. An accuracy of within 80-120% of the nominal concentration was strived for in at least 5 out of 6 samples. Endogenous selectivity was assessed by analysis of six separate batches of blank human plasma. Interfering peak areas at the analyte retention time should not exceed 20% of the peak area at LLOQ level (n = 6). The cross-analyte and IS interference assay was performed with single samples that were separately spiked with one analyte or IS at ULOQ concentration. To ensure that compounds do not interfere with the quantification of the analyte, the cross-analyte or IS interference should be ≤20% of the peak area in LLOQ samples and ≤5% for the IS.

Matrix effect and recovery

The matrix effect was investigated with six different batches of blank human plasma at QC LLOQ and QC high concentrations. Peak areas of QC samples spiked after protein precipitation were compared to peak areas of QC samples of equivalent concentrations

Table 2. Assay performance data for abiraterone, enzalutamide and both major metabolites in human plasma tested at LLOQ, mid and high concentrations.

Analyte	Nominal conc. (ng/mL)	Intra-assay (n=15)		Inter-assay (n=15)	
		Bias (%)	C.V. (%)	Bias (%)	C.V. (%)
Enzalutamide	94.4	5.7	4.2	5.1	0.4
	189	-4.3	5.6	-0.1	3.3
	494	6.4	4.2	3.7	1.9
N-desmethyl enzalutamide	10	4.7	3.6	2.9	0.9
	400	-10.4	3.2	-6.3	3.9
	1,000	-5.1	2.6	-4.8	-*
Enzalutamide carboxylic acid	5	7.4	9.0	-4.0	5.6
	200	-7.2	4.3	-7.2	2.6
	500	-9.1	3.8	2.0	5.9
Abiraterone	0.998	7.0	4.7	1.8	5.1
	40	-6.8	2.2	-4.6	1.9
	99.8	-8.3	3.7	-4.1	3.7
Abiraterone N-oxide sulfate	30	2.6	10.0	1.6	-*
	1,200	12.7	7.4	8.2	4.0
	3,000	13.5	4.4	4.7	8.0
Abiraterone sulfate	100	-15.2	5.0	-11.2	6.8
	4,000	-13.9	3.9	-9.2	5.0
	10,000	-13.3	4.0	-12.5	-*

* No significant additional variation was found due to the performance of the assay in different batches.
Abbreviation: C.V. = coefficient of variation.

in acetonitrile-water (50:50, v/v). Additionally, the IS-normalized matrix factor was calculated by dividing the matrix factor of the analyte by the matrix factor of the IS. Determination of the recovery was also performed at QC LLOQ and QC high (n = 6) concentrations. The recovery was calculated by dividing the peak area of processed QC samples by the peak area of blank plasma extract spiked with reference compound at equal concentrations. A total recovery of >70% and coefficients of variance (CV) of below 15% were required.

Dilution integrity
Five replicate plasma samples with a concentration above the ULOQ were diluted 200-fold with control human plasma. A volume of 30 μL sample was diluted with 570 μL of control human plasma. Subsequently, 30 μL of this solution was added to 270 μL of control human plasma. An accuracy of within -15% and +15% of the nominal concentration was acceptable.

Stability
Short-term stability experiments were performed in plasma after storage at room temperature (20-25ºC) and at -20ºC. Further stability assessments were done in the final extracts at 4ºC. The effect of three freeze (-20ºC)/thaw cycles on the stability of

each compound was investigated after thawing samples to room temperature for at least 12 hours on three separate occasions and comparison with freshly prepared samples. Long-term stability in plasma was determined after 1 months of storage at -20°C. Stock stability was described as the recovery percentage after 3 months storage at -20°C. All stability experiments were performed in triplicate at QC LLOQ and QC high levels. Analytes were considered stable under specific conditions when 85-115% of the initial concentration at QC high levels and when 80-120% of the initial concentration at QC LLOQ were recovered.

Clinical application

This assay was developed to facilitate pharmacokinetic monitoring of abiraterone and enzalutamide in patients with mCRPC at the Antoni van Leeuwenhoek-Netherlands Cancer Institute. Whole blood was collected at the clinic as routine standard of care at steady-state situation, which is reached after at least 1 month of treatment with enzalutamide (half-life of 5.8 days (4)) and 1 week of treatment with abiraterone (half-life of 16.3 hours (10)). Samples were stored at -20°C. Further processing is performed as previously described in this report (Section *2.4 Sample preparation).*

Results and discussion

Sample preparation

Several sample pretreatment methods have been tested. Protein precipitation was initially performed with methanol instead of acetonitrile to obtain a final extract similar to the composition of the mobile phase. This resulted, however, in large peak area variation (>50%) of the IS. Sample pretreatment with acetonitrile improved this variability to a nominal <5% per batch.

Mass spectrometry and chromatography

During the development, carry-over was observed for abiraterone, enzalutamide, and abiraterone N-oxide. Accordingly, a 3-minute rinsing step with 100% methanol was incorporated after each injection. Furthermore, an impurity of abiraterone was present in the abiraterone sulfate reference standard. As the abiraterone sulfate was expected to be a 100-fold more abundant, the cross-analyte interference would exceed 20%. Therefore, separate calibrators and QC samples were produced for both abiraterone sulfate and a combination of abiraterone, enzalutamide, *N*-desmethyl enzalutamide, enzalutamide carboxylic acid, and abiraterone N-oxide sulfate. Representative chromatograms of QC LLOQ are presented in Figure 2 for each analyte and IS. Baseline separation was necessary for the metabolites *N*-desmethyl enzalutamide and enzalutamide carboxylic acid, since *N*-desmethyl enzalutamide interferes at the transitions of enzalutamide carboxylic acid.

Three internal standards were incorporated in the analysis. $^2H_6$-Enzalutamide was used to normalize concentrations of the compounds without a deuterated IS (enzalutamide
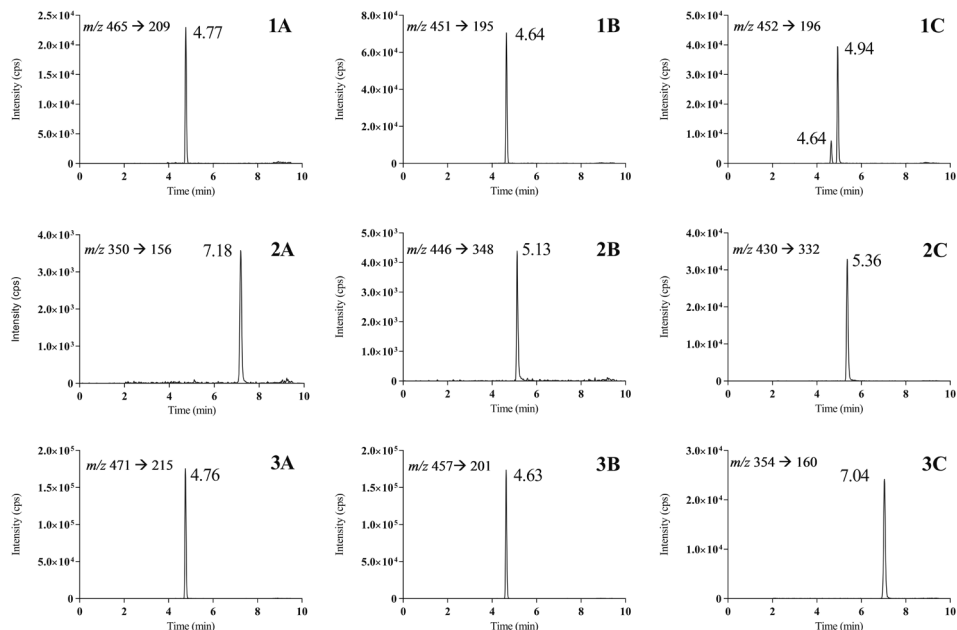
Figure 2. Representative LC-MS/MS chromatograms of enzalutamide (1A), *N*-desmethyl enzalutamide (1B), enzalutamide carboxylic acid (the additional peak belongs to enzalutamide carboxylic acid, the first peak corresponds with *N*-desmethyl enzalutamide) (1C), abiraterone (2A), abiraterone N-oxide sulfate (2B) abiraterone sulfate (2C), and the internal standards $^2H_6$-enzalutamide (3A), $^2H_6$-*N*-desmethyl enzalutamide (3B), $^2H_4$-abiraterone (3C).

carboxylic acid, abiraterone N-oxide sulfate, and abiraterone sulfate). Although $^2H_6$-Enzalutamide is not a structural analogue of the abiraterone sulfated metabolites, this internal standard was able to compensate for variations in responses, resulting in acceptable accuracy and precision values.

After receiving clinical samples, it became clear that plasma concentrations of enzalutamide, *N*-desmethyl enzalutamide, enzalutamide carboxylic acid, abiraterone N-oxide sulfate, and abiraterone sulfate exceeded the upper limit of quantification and therefore needed 10- to 100-fold dilution before analysis. Changing the calibration range was not possible due to nonlinearity at higher concentrations and increased carry-over. It could be suggested, if available, to transfer this method to a less sensitive instrument with adjusted calibration ranges.

Calibration model

Consistent with the requirement, at least 75% of the calibrators were within ±15% (±20% for the LLOQ) of the nominal concentrations. Calibration ranges of 1-100 ng/mL for abiraterone, 5-500 ng/mL for enzalutamide and enzalutamide carboxylic acid, 10-1,000 ng/mL for *N*-desmethyl enzalutamide, 30-3,000 ng/mL for abiraterone N-oxide sulfate, and 100-10,000 ng/mL for abiraterone sulfate fulfilled the criteria.

Accuracy and precision

Assay performance data are presented in Table 3. Inter-assay accuracy, intra-assay accuracy, and the precision were within the acceptance criteria at LLOQ, mid-, and high concentrations.

Specificity and selectivity

Mean measured QC LLOQ concentrations in six different batches of plasma were all within ±20% of the nominal concentrations for all tested analytes. In the double blank samples, no peaks were observed, with areas exceeding 20% of the analyte peak areas measured in QC LLOQ samples in the different batches of plasma. Cross-interference of co-eluting peaks in separately spiked samples was <20% of the QC LLOQ samples and thus within the required limits. Hence, this method was proven to be selective.

Dilution integrity

The concentrations of 200-fold diluted samples were within ±15% of the nominal concentration in five replicates. Intra-assay bias and intra-assay variability were between -5.9% and 2.8% for abiraterone, 5.1% and 4.0% for enzalutamide, -4.1% and 14% for *N*-desmethyl enzalutamide, -7.7% and 5.4% for enzalutamide carboxylic acid, 2.4% and 14% for abiraterone N-oxide sulfate, and 1.6% and 3.5% for abiraterone sulfate. These results show that samples with concentrations >ULOQ can be diluted up to 200-fold to obtain plasma concentrations within the validated range.

Carry-over

Criteria were fulfilled in three separate runs, with a maximum carry-over of 12% for abiraterone N-oxide sulfate. No carry-over was observed for the internal standards.

Matrix factor and recovery

The CV for the IS-normalized matrix factor was below 15% at the tested concentrations for each compound. Furthermore, the total recovery was >70% for all analytes and the variance did not exceed 15%. These results show that the internal standard effectively minimizes the influence of matrix effects and that protein precipitation with acetonitrile is an adequate sample pretreatment.

Stability

Stability results of the tests are shown in Table 4. Abiraterone N-oxide and enzalutamide carboxylic acid are unstable in DMSO after 3 months storage at -20ºC. To minimize degradation of these metabolites, working solutions were produced in plasma with freshly prepared abiraterone N-oxide and enzalutamide carboxylic acid stock solutions. All other experiments demonstrated adequate stability, because results were within the acceptance criteria. Long-term stability assessment in plasma was measured up to 1 month and is still ongoing.

Table 3. Stability of abiraterone, enzalutamide and their major metabolites in several matrixes. All experiments are performed in triplicate at LLOQ and high concentrations.

Matrix	Conditions	Compound	Nominal conc. (ng/mL)	Dev. (%)	C.V. (%)
DMSO	-20 °C, 3 months	Enzalutamide	1,000,000	-1.2	3.9
		N-desmethyl enzalutamide	1,000,000	-3.7	6.2
		Enzalutamide carboxylic acid	500,000	-7.0	3.7
		Abiraterone	1,000,000	-4.8	3.5
		Abiraterone N-oxide sulfate	500,000	-8.8	2.4
		Abiraterone sulfate	500,000	0. 8	0.5
Plasma	RT, 5 days	Enzalutamide	4.94	0.29	2.5
			494	-1.0	1.2
		N-desmethyl enzalutamide	10	-1.5	1.1
			1,000	-2.9	1.7
		Enzalutamide carboxylic acid	5	0.84	2.6
			500	-0.073	2.6
		Abiraterone	0.998	-2.9	0.99
			99.8	-2.3	3.2
		Abiraterone N-oxide sulfate	30	1.1	3.1
			3,000	-0.78	2.4
		Abiraterone sulfate	100	2.7	-2.3
			10,000	-3.5	-3.3
Plasma	-20 °C/RT, Freeze/thaw, 3 cycles	Enzalutamide	4.94	0.29	2.5
			494	-0.72	2.1
		N-desmethyl enzalutamide	10	-1.5	2.9
			1,000	1.1	-2.6
		Enzalutamide carboxylic acid	5	0.44	3.3
			500	3.1	2.7
		Abiraterone	0.998	-3.1	1.3
			99.8	0.20	0.79
		Abiraterone N-oxide sulfate	30	1.1	3.1
			3,000	2.0	2.4
		Abiraterone sulfate	100	0.95	-3.9
			10,000	2.5	-1.2
Plasma	-20 °C, 1 month	Enzalutamide	4.94	1.1	2.3
			494	0.26	1.5
			2,470	-0.97	2.7
		N-desmethyl enzalutamide	10	0.83	1.9
			1,000	0.56	1.5
			5,000	-1.4	4.8
		Enzalutamide carboxylic acid	5	4.1	1.0
			500	0.45	5.2
			2,500	2.0	2.8
		Abiraterone	0.998	4.7	1.7
			99.8	5.3	2.2
			499	3.8	2.3
		Abiraterone N-oxide sulfate	30	-2.4	4.9
			3,000	3.3	2.6
			15,000	3.1	3.2
		Abiraterone sulfate	100	-5.4	3.6
			10,000	-2.7	1.0
			50,000	-0.59	2.6

Table 3. Continued

Matrix	Conditions	Compound	Nominal conc. (ng/mL)	Dev. (%)	C.V. (%)
Final extract	2-8 °C 5 days	Enzalutamide	4.94	1.9	4.0
			494	-1.0	1.2
		N-desmethyl enzalutamide	10	-1.0	4.7
			1,000	-3.0	2.4
		Enzalutamide carboxylic acid	5	-0.64	3.8
			500	2.8	0.93
		Abiraterone	0.998	-0.22	5.6
			99.8	-0.12	2.0
		Abiraterone N-oxide sulfate	30	5.4	6.1
			3,000	0.47	0.64
		Abiraterone sulfate	100	9.9	-4.4
			10,000	9.2	-3.6

Abbreviations: RT = room temperature. DMSO = dimethyl sulfoxide. Dev = deviation. C.V. = coefficient of variance.

Table 4. Mean steady-state plasma concentrations and the range of 10 patients receiving either abiraterone (1000 mg per day) or enzalutamide (160 mg per day).

	Time after dosing			
	0-12 hours (n=5)		12-24 hours (n=5)	
Compound	Mean conc. (ng/mL)	Range (ng/mL)	Mean conc. (ng/mL)	Range (ng/mL)
Enzalutamide	13,640	11,900 – 17,600	11,436	9,620 – 13,100
N-desmethyl enzalutamide	10,737	6,990 – 13,500	9,120	5,050 – 14,100
Enzalutamide carboxylic acid	4,375	4,160 – 4,590	5,560	2,880 – 12,300
Abiraterone	37.4	12.7 – 121	19.6	7.70 – 30.7
Abiraterone N-oxide sulfate	7,341	833 – 17,200	3,234	1,270 – 5,270
Abiraterone sulfate	10,050	7,000 – 14,000	11,936	7,540 – 22,400

Clinical application

In order to establish applicability of the validated assay, steady-state plasma of patients receiving a regular dose of either abiraterone acetate or enzalutamide was analyzed. The mean measured plasma concentrations are presented in Table 5 and representative chromatograms are depicted in Figure 3. A second peak with identical transitions to abiraterone is observed in the augmented image presenting plasma from a patient using abiraterone acetate. The peak area of this additional peak differs per patient, and suggests that it belongs to an isomeric metabolite that is produced in varying quantities *in vivo*. Measurements were within the validated ranges after 100-fold dilution of enzalutamide samples and 10-fold dilution of abiraterone samples. One abiraterone concentration was below the LLOQ after 10-fold dilution and was therefore
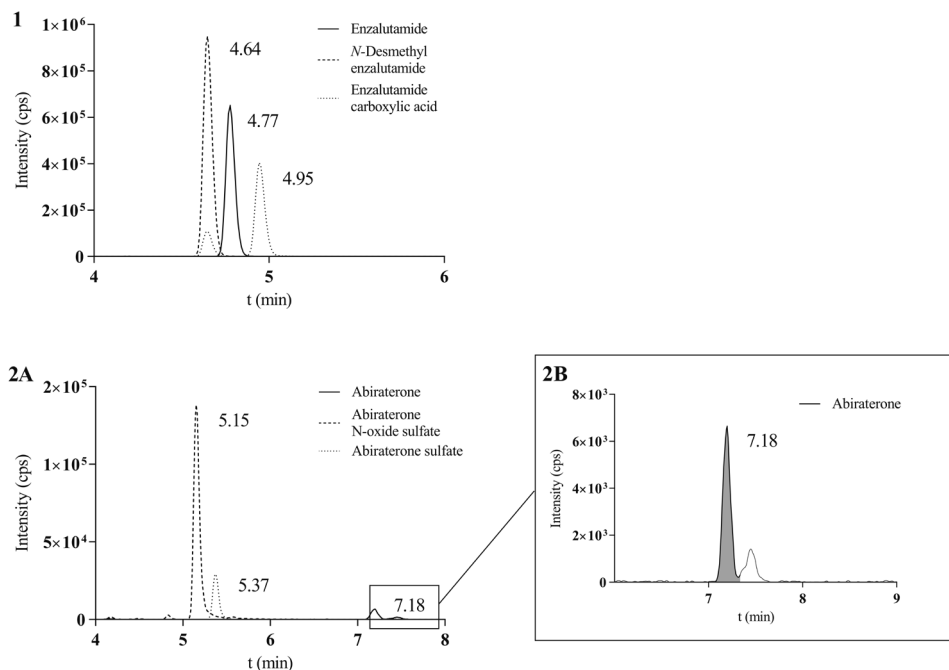
Figure 3. LC-MS/MS chromatograms of 100 times diluted steady-state plasma from a patient using enzalutamide (1, from 4-6 min) and of 10-fold diluted steady-state plasma from a patient using abiraterone (2A, from 4-8 min). A limited part of the chromatogram is shown to provide a better image of the peaks and the abiraterone chromatogram is enlarged to show the additional peak detected at the abiraterone transition (2B, from 6-9 min).

reanalyzed undiluted. The large range of the abiraterone concentrations can be explained by the sampling time after dosing and by reported variability in exposure and C_{max} that is caused by intake with food or by decreased hepatic function (3). These results also demonstrate the potential relevance of this assay for pharmacokinetic monitoring of abiraterone, enzalutamide, and their metabolites.

Conclusion

An LC-MS/MS method was developed and validated for the simultaneous analysis of abiraterone, enzalutamide, *N*-desmethyl enzalutamide, enzalutamide carboxylic acid, abiraterone N-oxide sulfate, and abiraterone sulfate. Due to low stability of abiraterone N-oxide sulfate and enzalutamide carboxylic acid in DMSO, working solutions were produced in plasma with freshly prepared stock solutions. Concentration ranges of 1-100 ng/mL for abiraterone, 5-500 ng/mL for enzalutamide and enzalutamide carboxylic acid, 10-1,000 ng/mL for *N*-desmethyl enzalutamide, 30-3,000 ng/mL for abiraterone N-oxide sulfate, and 100-10,000 ng/mL for abiraterone sulfate were chosen

to measure compound concentrations in steady-state plasma of patients. A combined assay for these analytes provides an efficient approach to measure plasma concentrations. This assay has now been successfully implemented to facilitate therapeutic drug monitoring of abiraterone, enzalutamide, and both major metabolites.

1.3

References

1. Siegel RL, Miller KD, Jemal A. Cancer statistics, 2016. CA Cancer J Clin. 2016;66:7–30.

2. American Cancer Society. Global Cancer Facts & Figures 3rd Edition. American Cancer Society. 2015.

3. US Food and Drug Administration. Prescribing information: Zytiga (abiraterone acetate). Silver Spring, Maryl US Food Drug Adm. 2011 [cited 2017 May] p. 1-11. Available from: http://www.janssenlabels.com/package-insert/product-monograph/prescribing-information/ZYTIGA-pi.pdf

4. US Food and Drug Administration. Prescribing information: Xtandi (enzalutamide). Silver Spring (MD). 2012 [cited 2017 May]. p. 1–16. Available from: https://www.accessdata.fda.gov/drugsatfda_docs/label/2012/203415lbl.pdf

5. O'Donnell A, Judson I, Dowsett M, Raynaud F, Dearnaley D, Mason M, et al. Hormonal impact of the 17alpha-hydroxylase/C(17,20)-lyase inhibitor abiraterone acetate (CB7630) in patients with prostate cancer. Br J Cancer. 2004;90:2317–25.

6. Tran C, Ouk S, Clegg NJ, Chen Y, Watson PA, Arora V, et al. Development of a second-generation antiandrogen for treatment of advanced prostate cancer. Science. 2009;324:787–90.

7. Acharya M, Gonzalez M, Mannens G, De Vries R, Lopez C, Griffin T, et al. A phase I, open-label, single-dose, mass balance study of 14C-labeled abiraterone acetate in healthy male subjects. Xenobiotica. 2013;43:379–89.

8. Gibbons JA, Ouatas T, Krauwinkel W, Ohtsu Y, van der Walt J-S, Beddo V, et al. Clinical Pharmacokinetic Studies of Enzalutamide. Clin Pharmacokinet. 2015;54:1043–55.

9. Yu H, Steeghs N, Nijenhuis CM, Schellens JHM, Beijnen JH, Huitema ADR. Practical Guidelines for Therapeutic Drug Monitoring of Anticancer Tyrosine Kinase Inhibitors: Focus on the Pharmacokinetic Targets. Clin Pharmacokinet. 2014;53:305–25.

10. European Medicines Agency. European Public Assessment Report (EPAR): Zytiga (Abiraterone Acetate). London. 2016;

11. US Food and Drug Administration. Clinical Pharmacology and Biopharmaceutics Review: Xtandi (Enzalutamide). Silver Spring (MD). 2012 [cited 2017 May]. p. 1–75. Available from: https://www.accessdata.fda.gov/drugsatfda_docs/nda/2012/203415Orig1s000ClinPharmR.pdf

12. Alyamani M, Li Z, Upadhyay SK, Anderson DJ, Auchus RJ, Sharifi N. Development and validation of a novel LC-MS/MS method for simultaneous determination of abiraterone and its seven steroidal metabolites in human serum: innovation in separation of diastereoisomers without use of a chiral column. J Steroid Biochem Mol Biol. 2017;172:231-9.

13. Gurav S, Punde R, Farooqui J, Zainuddin M, Rajagopal S, Mullangi R. Development and validation of a highly sensitive method for the determination of abiraterone in rat and human plasma by LC-MS/MS-ESI: application to a pharmacokinetic study. Biomed Chromatogr. 2012;26:761–8.

14. Martins V, Asad Y, Wilsher N, Raynaud F. A validated liquid chromatographic-tandem mass spectroscopy method for the quantification of abiraterone acetate and abiraterone in human plasma. J Chromatogr B Analyt Technol Biomed Life Sci. 2006;843:262–7.

15. Song JH, Kim TH, Jung JW, Kim N, Ahn SH, Hwang SO, et al. Quantitative determination of enzalutamide, an anti-prostate cancer drug, in rat plasma using liquid chromatography-tandem mass spectrometry, and its application to a pharmacokinetic study. Biomed Chromatogr. 2014;28:1112–7.

16. Bennett D, Gibbons JA, Mol R, Ohtsu Y, Williard C. Validation of a method for quantifying enzalutamide and its major metabolites in human plasma by LC-MS/MS. Bioanalysis. 2014;6:737–44.

17. US Food and Drug Administration (FDA). FDA Guidance for Industry: Bioanalytical Method Validation. Silver Spring, Maryland: US Food and Drug Administration. 2018 [cited 2018 Jun]. Available from: https://www.fda.gov/downloads/drugs/guidances/ucm070107.pdf

18. European Medicines Agency (EMA). Guideline on Bioanalytical Method Validation. Committe for Medicinal Produts for Human Use and European Medicines Agency. 2011 [cited 2017 May]. Available from: http://www.ema.europa.eu/docs/en_GB/document_library/Scientific_guideline/2011/08/WC500109686.pdf

1.3

An LC-MS/MS method for quantification of the active abiraterone metabolite Δ(4)-abiraterone (D4A) in human plasma

Merel van Nuland
Hilde Rosing
Jelle de Vries
Huib Ovaa
Jan H.M. Schellens
Jos H. Beijnen

Abstract

Δ(4)-Abiraterone (D4A) is a recently discovered active metabolite of the oral anti-androgen drug abiraterone acetate. For quantification of this metabolite in human plasma, a liquid chromatography-tandem mass spectrometry (LC-MS/MS) method was developed and validated. Human plasma samples of patients treated with abiraterone acetate were prepared by protein precipitation with acetonitrile. The method was validated over a linear range of 0.2 to 20 ng/mL. Intra-assay and inter-assay variabilities were within ±15% of the nominal concentrations for quality control (QC) samples at medium and high concentrations and within ±20% at the lower limit of quantification (LLOQ), respectively. The described method for quantification of D4A was validated successfully and implemented to support therapeutic drug monitoring in patients treated with abiraterone acetate.

Introduction

Abiraterone acetate is an oral drug for the treatment of metastatic castration-resistant prostate cancer (1). Its anti-androgen capacities can be allocated to 17α-hydroxylase/ C17,20-lyase (CYP17) inhibition (2). CYP17 is responsible for the production of androgens, such as testosterone, which are natural ligands for the androgen receptor. Inhibition of this receptor reduces testosterone levels and prolongs the survival of prostate cancer patients (3).

Abiraterone undergoes extensive hepatic metabolism. The main circulating metabolites abiraterone sulfate and abiraterone N-oxide sulfate account for about 43% of exposure each and are inactive (1,4). Li et al. recently discovered the active metabolite Δ(4)-Abiraterone (D4A), that is formed by conversion of abiraterone by the enzyme 3β-hydroxysteroid-dehydrogenase (3βHSD). D4A inhibits multiple steroidic enzymes and blocks androgen receptor signaling. This combined mechanism of action makes D4A even more active than abiraterone (5).

We recently published a liquid chromatography-mass spectrometry (LC-MS/MS) method for determination of abiraterone, enzalutamide and their major metabolites to support therapeutic drug monitoring (TDM) of these compounds (6). D4A possesses relevant anti-androgen capacities that contribute to the efficacy of abiraterone treatment in prostate cancer and is therefore a relevant metabolite to be incorporated in the previously published assay. The aim of the presented study was to include D4A in the existing assay for quantification of abiraterone, enzalutamide and their major metabolites to obtain further insight into the metabolism of these drugs to optimize the treatment of prostate cancer patients.

Experiments

Chemicals

D4A was produced at the Chemical Immunology laboratory, Leiden University Medical Centre (LUMC, Leiden, the Netherlands) according to a previously published method by Li et al (7). Abiraterone and $^2H_4$-abiraterone were purchased from Alsachim (Illkirch, France). Acetonitrile, methanol (both Supra-Gradient grade), water, and formic acid (both LC-MS grade) were from Biosolve Ltd. (Valkenswaard, The Netherlands). Dimethyl sulfoxide (DMSO, seccosolv grade) was obtained from Merck (Darmstadt, Germany) and K_2EDTA plasma from Bioreclamations LLC (Hicksville, NY, USA).

Calibration and quality control samples

Stock solutions of D4A and the internal standard (IS) $^2H_4$-abiraterone were prepared at a concentration of 1 mg/mL in DMSO and methanol, respectively. Calibration standards and quality control (QC) samples were prepared from stock solutions in K_2EDTA plasma. The calibration standards were freshly produced before each validation run in a concentration range of 0.2-20 ng/mL. QC samples were produced in batches

at concentrations of 0.2, 8 and 20 ng/mL. The IS working solution contained 25 ng/mL of $^2H_4$-abiraterone. Stock solutions, working solutions and QC samples were stored at -20ºC.

Sample preparation

Samples were collected in the clinic by venipuncture and centrifuged for 5 minutes at 4ºC at 1,800 g. After centrifugation, plasma was isolated and stored at -20ºC until further analysis. Samples were thawed and vortex-mixed prior to processing, and a 50 µL aliquot was used for analysis. Fifteen microliters of IS working solution and, after mixing, 150 µL of acetonitrile were added to precipitate proteins. Samples were shaken for 10 minutes at 1,250 rpm and centrifuged for 10 minutes at 20ºC at 23,100 g. The supernatant was transferred to an autosampler vial.

Liquid chromatography-tandem mass spectrometry

The chromatographic separation was performed using a Nexera 2 series liquid chromatograph equipped with a Nexera 2 series binary pump, a degasser, an autosampler, and a valco valve (Shimadzu Corporation, Kyoto, Japan). The autosampler temperature was kept at 4ºC and the column oven at 45ºC. Analytes were separated using a Kinetex C18 column (15 x 2.1 mm ID, particle size 2.6 µm; Phenomenex, Torrance, CA, USA) with mobile phase A consisting of formic acid-water (0.1:100, v/v) and mobile phase B consisting of formic acid-methanol (0.1:100, v/v). The following gradient program was used to achieve separation: 30% B (0.0-2.0 min), 70% B (2.0-10 min), 30% B (10-13 min) at a flow rate of 0.3 mL/min. A triple quadrupole mass spectrometer API6500 (Sciex, Framingham, MA, USA) operating in positive mode was used for quantification of D4A. The instrument was equipped with a turbo ion spray (TIS) interface and was configured in multiple reaction monitoring (MRM) mode. Analyst software version 1.6.2 (Sciex) was used for system control and data analysis. Table 1 summarizes the general and specific mass spectrometric settings.

Identification and purity of the reference standard D4A

The identity and purity of the D4A reference standard were determined. Identification was performed by nuclear magnetic resonance (NMR) and LC-MS and the purity was determined by LC-UV (diode array detection, DAD) and LC-MS. For NMR, a solution of 7.5 mg/mL D4A was prepared in deuterated chloroform and this solution was further diluted to 0.26 mg/mL in formic acid-acetonitrile-water (0.1:1:100, v/v) for LC-MS and LC-UV analysis.

NMR was performed with a Bruker Avance 300 (75.00 MHz for 13C) using the residual solvent as internal standard. LC-MS and UV for identification were done with an LCT Premier equipped with an LC Alliance 2795 and PDA1996 (Waters, Milford, MA, USA). Chromatographic separation was performed using an XBridge column (30 x 2.1 mm ID, particle size 10 µm, Waters), using mobile phase A consisting of formic acid-acetonitrile-water (0.1:1:100, v/v) and mobile phase B consisting of formic acid-water-acetonitrile (0.1:1:100, v/v). The following gradient was applied to the column with a

Table 1. General and analyte specific mass spectrometric parameters

Parameter	Setting
Run duration (min)	13.5
Ion spray voltage (V)	5500
Nebulizer gas (au)	40
Turbo gas/heater gas (au)	40
Curtain gas (au)	20
Collision gas (au)	8
Temperature °C	350
Dwell time (msec)	50

	D4A	$^2H_4$-abiraterone
Parent mass	348.3 *m/z*	354.1 *m/z*
Product mass	156.1 *m/z*	160.1 *m/z*
Collision energy	61 V	63 V
Collision exit potential	18 V	10 V
Declustering potential	171 V	186 V
Retention time	6.16 min	7.08 min

0.8 mL/min flow: 5% B (0.0-0.2 min), 5% → 95% B (0.2-3.2 min), 95% B (3.2-4.2 min), 95% → 5% B (4.2-4.4 min), 5% B (4.4-6.2 min).

To establish the D4A purity we used an LC-20AD pump with a SIL-HTc autosampler (Shimadzu, Kyoto, Japan) coupled to a LTX-XL linear ion trap mass spectrometer (Thermo Electron, Waltham, MA, USA) in combination with diode array detection (DAD). Chromatographic conditions were as described for the LC-MS identification method However, the flow was reduced to 0.2 mL/min in order not to exceed the upper pressure limit. After chromatographic separation, a post column splitter directed 1/4th of the flow to the MS/MS and 3/4th to the DAD. The peaks in the UV chromatogram could therefore be directly correlated with the retention time of the peaks in the LC chromatogram. Peak identification of D4A and abiraterone were assessed with LC-MS/MS and purity was determined by LC-DAD 254 nm.

Additional peaks in the chromatograms beside the D4A and abiraterone peaks and not observed in the blanks, were assigned as unknown impurities. The total area of these unknown impurities was expressed as relative impurity compared to the peak area of D4A. Furthermore, the amount of abiraterone in the D4A reference standard was determined with a validated LC-MS/MS method [6].

Validation procedures

Validation of the assay was based on the United States Food and Drug Administration (FDA) and European Medicines Agency (EMA) guidelines for bioanalytical method

validation (8,9). All aspects of the validation were investigated. However, four instead of six to eight calibrators were included and three instead of four QC concentrations were prepared. These adaptations were made since the method will be used for routine TDM. Therefore, we focused on the development of a fast turn-around method, while still offering a bioanalytical validation approach.

Clinical application

The applicability of the assay for TDM was demonstrated with steady-state plasma samples of patients receiving abiraterone acetate, collected after at least one week after the start of the abiraterone treatment (half-life of 16.3 hours (10)). Samples were collected for routine TDM at the Netherlands Cancer Institute according to the declaration of Helsinki.

Results and discussion

Identification and purity of the reference standard D4A

The identity of D4A was determined using NMR and LC-MS. The position and number of chemical shifts in the NMR spectrum were diagnostic of the structure of D4A, as presented in literature (7). Furthermore, the MS spectrum clearly showed a response at *m/z* 348 corresponding to the protonated parent mass of D4A.

The percentage of unknown impurities was determined with LC-UV. Figure 1 shows the UV chromatograms of D4A, abiraterone and a blank sample. D4A and abiraterone elute at a retention time of 9.23 min and 10.8 min, respectively. Ten unknown impurities were visible in the D4A chromatogram and the total peak area of these impurities accounted for 8.30% of the D4A peak area. The percentage of abiraterone in the reference standard, determined with LC-MS/MS, was 0.938%. Taken together, the assigned purity of the reference standard was 90.8% (100%-8.30%-0.938%) and a correction factor of 0.908 was used to calculate the D4A concentration in the stock solutions that were used for the preparation of calibration standards and QC samples during the validation and routine application of the method.

Calibration curve

Calibration standards were analyzed in duplicate in three separate analytical runs. Linear regression was used with a weighting factor of $1/x^2$ to fit the calibration data (peak area ratios versus the concentration of D4A). The calibration range of D4A consisted of four calibration standards with concentrations of 0.2, 1, 10 and 20 ng/mL. The calibration plots were consistent and the back-calculated D4A concentrations were within the requirements, as at least 75% of the calibration standards were within ±15% (±20% for the lower limit of quantification (LLOQ)) of the nominal concentrations.

Accuracy and precision

Five replicates of QC LLOQ (0.182 ng/mL), QC Mid (7.28 mg/mL) and QC High (18.2 g/mL) were analyzed in three consecutive runs. Accuracy was expressed as the relative
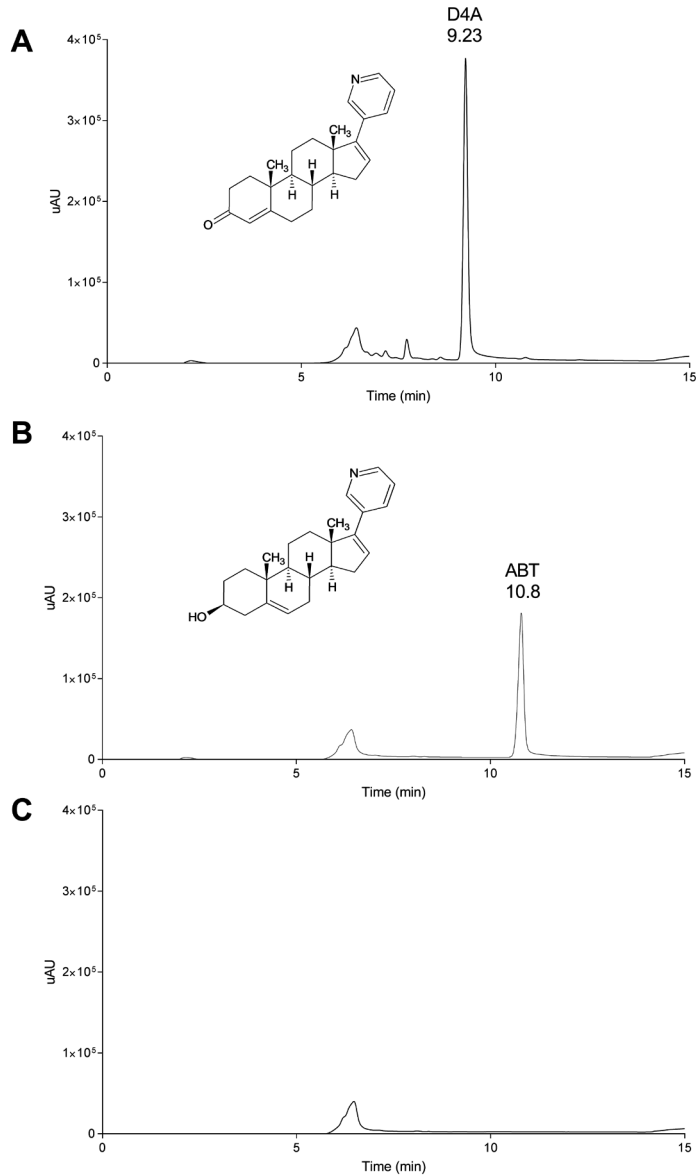
Figure 1. Representative UV chromatograms of D4A (A), abiraterone (ABT) (B) and water (C) at λ=254 nm.

error (% deviation) and one-way ANOVA was used to calculate the intra- and inter-assay variation. The acceptance criteria for accuracy were within ±15% for QC mid and QC high and within ±20% for QC LLOQ. Precisions should be ≤15% for QC mid and QC high and for QC LLOQ the criterion was set to ≤20%. As shown in Table 2, all parameters were within the acceptance criteria.

Table 2. Assay performance data for D4A in human plasma tested at LLOQ, mid-, and high concentrations.

Run	Nominal conc. (ng/mL)	Measured conc. (ng/mL)	Inaccuracy (% deviation)	Precision (%)	No. of replicates
1	0.182	0.183	0.8	10	5
2	0.182	0.170	-6.6	5.8	5
3	0.182	0.186	2.2	8.1	5
Inter-assay	0.182	0.180	-1.2	3.0	15
1	7.28	7.01	-3.8	5.2	5
2	7.28	6.74	-7.4	6.7	5
3	7.28	7.27	-0.1	2.2	5
Inter-assay	7.28	7.01	-3.8	3.1	15
1	18.2	18.8	3.5	5.3	5
2	18.2	19.4	6.6	5.3	5
3	18.2	19.4	6.8	4.9	5
Inter-assay	18.2	19.2	5.6	-[1]	15

[1] Inter-run precision could not be calculated because mean square between group was less then mean square within groups

Specificity and selectivity

Six separate batches of blank human K_2EDTA plasma were spiked at the LLOQ level and were processed together with blank samples to assess whether endogenous constituents interfere with the assay. The accuracy of the LLOQ samples was within 80-120% of the nominal concentration in all batches of plasma and no interference was observed in the blanks at the retention time of the analyte with areas >20% (or >5% for the internal standards) of the LLOQ areas in all tested batches.

Cross-analyte interference was tested by spiking blank human plasma separately at the highest concentration of the calibration range (upper limit of quantification, ULOQ) with D4A, abiraterone, abiraterone sulfate, abiraterone N-oxide sulfate, enzalutamide, desmethyl-enzalutamide or enzalutamide carboxylic acid. Internal standard interference was tested by spiking blank samples separately at nominal concentrations of internal standard. To ensure that compounds do not interfere with the quantification of the analyte, the cross-analyte or IS interference should be ≤20% of the peak area in LLOQ samples and ≤5% for the IS.

The interference of D4A at the retention time of abiraterone was 49% and the interference of abiraterone sulfate at the retention time of D4A was 100%. These percentages exceeded the acceptance criteria of 20% which can be explained by impurities in the reference standards of D4A and abiraterone sulfate . The impurity of abiraterone in the D4A reference standard will have no significant influence in the quantification of abiraterone, since the calibration range of D4A is 5-fold lower than the calibration range of abiraterone. Therefore, this interference was considered

acceptable. However, the interference of abiraterone sulfate at the retention time of D4A was unacceptably high as the concentration range of abiraterone sulfate is 500-fold higher than the calibration range of D4A. Therefore, separate calibration standards should be prepared for abiraterone sulfate while combined calibration standards can be prepared for D4A, abiraterone, abiraterone N-oxide sulfate, enzalutamide, desmethyl-enzalutamide and enzalutamide carboxylic acid. The interference of other analytes and internal standards was ≤20% (≤5% for the IS) of the peak area in LLOQ samples and therefore within the acceptance criteria.

Dilution integrity
The concentrations of 10-fold diluted samples (30 μL sample in 270 μL control K_2EDTA plasma) were within the criteria of ±15% for accuracy and ≤15% for precision in five replicates. From these data it can be concluded that samples exceeding the ULOQ can be diluted up to 10-fold to obtain plasma concentrations within the validated range.

Carry-over
Two blank samples were injected after the ULOQ to determine the carry-over. In three separate analytical runs, the peak areas in blank samples were ≤20% of the peak areas in the LLOQ and therefore considered acceptable.

Matrix effect
The matrix effect was investigated for six different batches of blank human K_2EDTA plasma at QC LLOQ and QC high concentration. The matrix factor (MF) was calculated by comparison of the D4A response in presence and in absence (acetonitrile-water (50:50, v/v)) of the biomatrix. The following formula was used to calculate the IS-normalized MF:

$$IS-normalized\ MF = \frac{MF\ of\ the\ analyte}{MF\ of\ the\ internal\ standard}$$

The IS-normalized MF ranged from 1.23 to 1.45. The CV for the IS-normalized matrix factor at LLOQ and high concentration was respectively 3.1% and 7.9% and fulfilled the criteria (≤15%).

Stability
Stability experiments were performed in triplicate at QC LLOQ and QC high levels. D4A was considered stable under specific conditions when 85-115% of the initial concentration at QC high levels and when 80-120% of the initial concentration at QC LLOQ were recovered. In plasma, D4A was stable for at least 5 days at ambient temperature (20-25ºC), for at least a month at -20 ºC and after 3 freeze/thaw cycles (4ºC/20-25ºC). Final extracts could be injected up to 3 days after sample preparation.
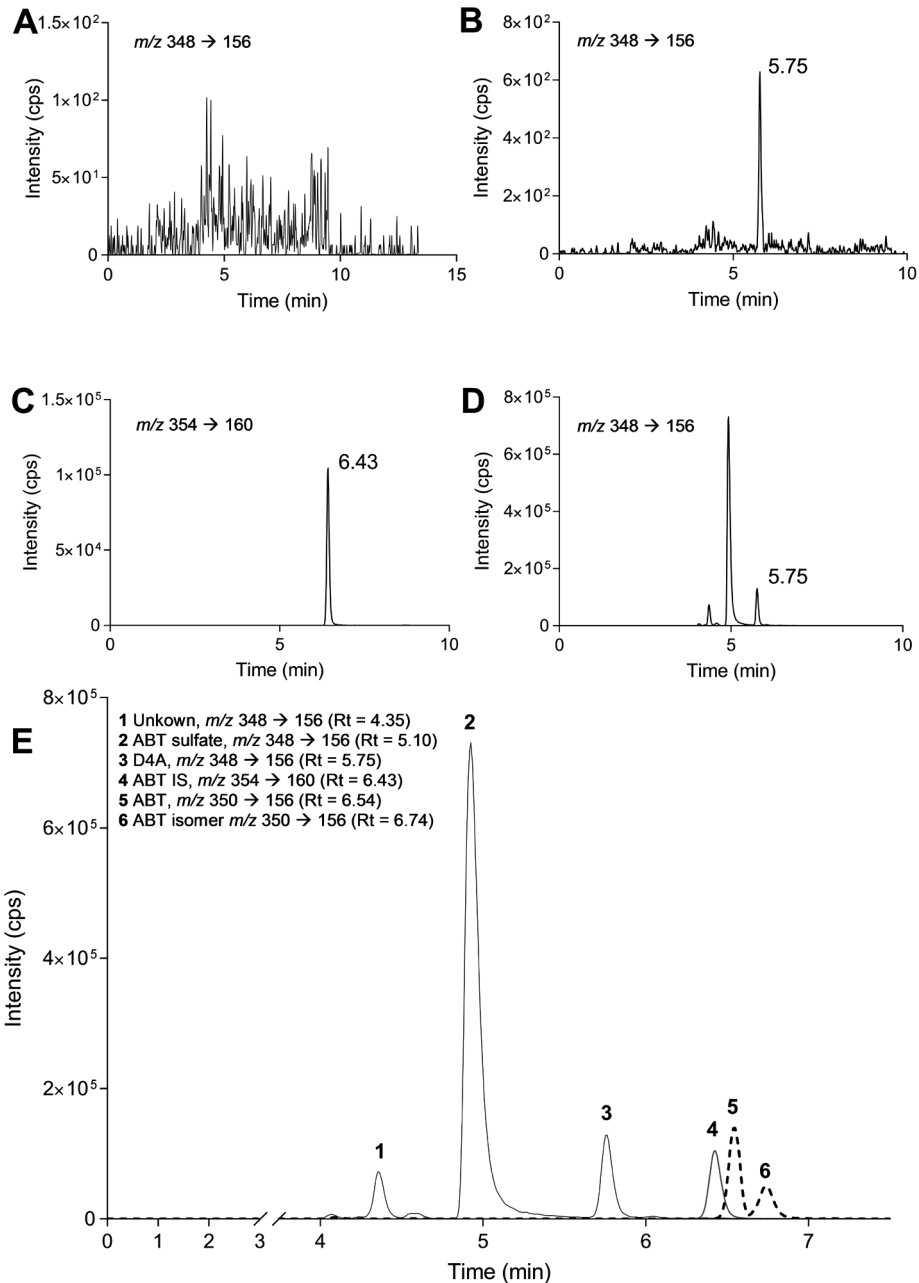
Figure 2. Representative LC-MS/MS chromatograms of a blank sample (A), D4A LLOQ (B), $^2H_4$-abiraterone (C), D4A in steady-state plasma from a patient using abiraterone acetate (D) and a chromatogram showing abiraterone, D4A and $^2H_4$-abiraterone in a steady-state plasma sample collected from a patient using abiraterone acetate (E).

Table 3. Steady-state plasma concentrations of D4A and abiraterone and the conversion ratio.

Patient number	D4A conc. (ng/mL)	ABT conc. (ng/mL)	Conversion ratio (%, ABT/D4A)
1	1.30	5.06	25.7
2	1.00	15.9	6.30
3	2.54	38.7	6.56
4	2.13	32.6	6.53
5	12.1	452	2.69
6	1.99	44.8	4.44
7	0.329	4.47	7.36
8	0.458	0.980	46.7
9	0.361	1.00	36.1
10	1.50	14.8	10.1
11	1.70	32.0	5.31
12	7.91	417	1.90
13	3.31	41.5	7.98
14	3.35	44.1	7.60
15	10.4	207	5.02
Median (range)	1.99 (0.329–12.1)	32.6 (0.980-452)	6.56 (1.90-46.7)

Abbreviations: conc = concentration, ABT = abiraterone

1.4

Clinical application

Steady-state plasma samples of 15 patients receiving abiraterone acetate were analyzed; all results were within the validated range. Representative selective ion chromatograms of a blank sample, spiked calibration standards and a patient sample at steady-state (abiraterone acetate 1000 mg daily dose) is depicted in Figure 2. D4A elutes at 5.75 min and abiraterone at 6.54 min. Another peak at a retention time of 5.10 min belongs to the metabolite abiraterone sulfate and is observed in the transitions of abiraterone and D4A. Measured plasma concentrations of D4A and abiraterone are presented in Table 3 with a median concentration of 1.99 ng/mL (0.329-12.1 ng/mL) and 32.6 ng/mL (0.980-452 ng/mL), respectively. The median conversion ratio of abiraterone to D4A was 6.56%, which is comparable to the 5% conversion ratio as described in literature (11). Interpatient variability of D4A plasma concentrations and conversion ratios demonstrate the additional relevance of monitoring D4A in plasma of patients treated with abiraterone acetate.

Conclusion

An LC-MS/MS method for the quantification of D4A was validated successfully over a concentration range of 0.2-20 ng/mL. A median D4A steady-state plasma concentration

of 1.99 ng/mL and a 6.56% conversion ratio of abiraterone to D4A were determined for 15 patients treated with abiraterone acetate. The active metabolite D4A has been successfully incorporated in the assay for quantification of abiraterone, enzalutamide and their major metabolites to support TDM.

References

1. US Food and Drug Administration. Prescribing information: Zytiga (abiraterone acetate). Silver Spring, Maryl US Food Drug Adm. 2011 [cited 2017 May] p. 1-11. Available from: http://www.janssenlabels.com/package-insert/product-monograph/prescribing-information/ZYTIGA-pi.pdf

2. O'Donnell A, Judson I, Dowsett M, Raynaud F, Dearnaley D, Mason M, et al. Hormonal impact of the 17alpha-hydroxylase/C(17,20)-lyase inhibitor abiraterone acetate (CB7630) in patients with prostate cancer. Br J Cancer. 2004;90:2317–25.

3. Fizazi K, Scher HI, Molina A, Logothetis CJ, Chi KN, Jones RJ, et al. Abiraterone acetate for treatment of metastatic castration-resistant prostate cancer: final overall survival analysis of the COU-AA-301 randomised, double-blind, placebo-controlled phase 3 study. Lancet Oncol. 2012;13:983–92.

4. Acharya M, Gonzalez M, Mannens G, De Vries R, Lopez C, Griffin T, et al. A phase I, open-label, single-dose, mass balance study of 14C-labeled abiraterone acetate in healthy male subjects. Xenobiotica. 2013;43379–89.

5. Li Z, Bishop AC, Alyamani M, Garcia JA, Dreicer R, Bunch D, et al. Conversion of abiraterone to D4A drives anti-tumour activity in prostate cancer. Nature. 2015;523:347–51.

6. van Nuland M, Hillebrand MJ., Rosing H, Schellens JHM, Beijnen JH. Development and validation of an LC-MS/MS method for the simultaneous quantification of abiraterone, enzalutamide, and their major metabolites in human plasma. Ther Drug Monit. 2017;39:243–51.

7. Li R, Evaul K, Sharma KK, Chang K-H, Yoshimoto J, Liu J, et al. Abiraterone inhibits 3beta-hydroxysteroid dehydrogenase: a rationale for increasing drug exposure in castration-resistant prostate cancer. Clin Cancer Res. 2012;18:3571–9.

8. US Food and Drug Administration (FDA). FDA Guidance for Industry: Bioanalytical Method Validation. Silver Spring, Maryland: US Food and Drug Administration. 2018 [cited 2017 Jun]. Available from: https://www.fda.gov/downloads/drugs/guidances/ucm070107.Pdf

9. European Medicines Agency (EMA). Guideline on Bioanalytical Method Validation. Committe for Medicinal Produts for Human Use and European Medicines Agency. 2011 [cited 2017 May]. Available from: http://www.ema.europa.eu/docs/en_GB/document_library/Scientific_guideline/2011/08/WC500109686.pdf

10. European Medicines Agency. European Public Assessment Report (EPAR): Zytiga (Abiraterone Acetate). London. 2016 [cited 2017 May]. Available from: https://www.ema.europa.eu/en/documents/variation-report/zytiga-h-c-2321-ii-0004-g-epar-assessment-report-variation_en.pdf

11. Emamekhoo H, Li Z, Sharifi N. Clinical significance of D4A in prostate cancer therapy with abiraterone. Cell cycle. 2015;14:3213–4.

1.4

LC-MS/MS assay for the quantification of testosterone, dihydrotestosterone, androstenedione, cortisol and prednisone in plasma from castrated prostate cancer patients treated with abiraterone acetate or enzalutamide

Merel van Nuland
Nikkie Venekamp
Willemijn M.E. Wouters
Huub H. van Rossum
Hilde Rosing
Jos H. Beijnen

Abstract

Prostate cancer is the most common malignancy among men in the Western world. Treatment of this patient population, e.g. by (chemical) castration, is primarily focused on depletion of tumor-stimulating androgens, with testosterone being the major androgenic hormone. After initial therapy, prostate cancer may progress to metastatic castration-resistant prostate cancer. Anti-hormonal drugs abiraterone acetate and enzalutamide are commonly used to treat patients with this disease as both drugs reduce tumor growth and increase time to tumor progression. To evaluate the pharmacodynamic effects of anti-hormonal drugs in this patient population, we developed an LC-MS/MS method for the quantification of testosterone, dihydrotestosterone, androstenedione, cortisol and prednisone in human plasma. The validated assay ranges from 10-10,000 pg/mL for testosterone and androstenedione, 100-10,000 pg/mL for dihydrotestosterone, 50-5,000 pg/mL for cortisol and 500-50,000 pg/mL for prednisone. Intra-assay and inter-assay variabilities were within ±15% of the nominal concentrations for quality control (QC) samples at low, medium and high concentrations and within ±20% at the lower limit of quantification (LLOQ), respectively. The applicability of the method was demonstrated in plasma from patients with metastatic castrated-resistant prostate cancer using either abiraterone acetate or enzalutamide.

Introduction

Prostate cancer is the most common malignancy in men in het Western world (1–3). Treatment of this patient population is primarily focused on depletion of tumor-stimulating androgens, with testosterone being the major androgenic hormone (4). Testosterone is produced from cholesterol in the testes and the adrenal cortex (5). Furthermore, tumor cells may develop the ability to produce testosterone to autonomously stimulate growth (6). Figure 1 represents the simplified biosynthesis of testosterone from cholesterol via cytochrome P450 17 (CYP17) and 3β-hydroxysteroid dehydrogenase (3βHSD) (5). A similar pathway is depicted for cortisol, which is also produced from cholesterol by CYP17 and 3βHSD. Testosterone is further metabolized to the active metabolite dihydrotestosterone by 5α-reductase (5).

Androgen-deprivation therapy is the basis for prostate cancer treatment. After initial therapy, prostate cancer may progress to metastatic castration-resistant prostate cancer (mCRPC) (7). In this phase of the disease, abiraterone acetate and enzalutamide can be prescribed to prolong time to tumor progression. Abiraterone acetate, co-administered with prednisone, inhibits the enzyme CYP17, which is pivotal in the production of testosterone (Figure 1) (7), while enzalutamide inhibits the androgen receptor (AR) by competitive binding and thereby antagonizes AR activation (8).

Baseline testosterone and androstenedione serum levels in castrated patients prior to abiraterone acetate therapy are generally 0.1-309 pg/mL and 0.1-185 pg/mL, respectively (9). Although enzalutamide itself does not decrease androgen levels, it is co-administered with a gonadoreline agonist (i.e. gosereline) to suppress testosterone concentrations below the castration limit of 500 pg/mL (10). Circulating androgen concentrations could be used as biomarkers for efficacy of anti-androgen therapy. However, routine assays often lack sensitivity to measure below the testosterone castration level of 500 pg/mL (11). Our institute has previously shown that these low testosterone concentrations can be quantified in human serum using liquid chromatography-mass spectrometry (LC-MS/MS) (12). Previously published assays providing the possibility to quantify testosterone among other androgens at low concentrations do not focus on measuring these analytes in plasma from prostate cancer patients using androgen-deprivation therapy (13–15). Besides androgen concentrations, plasma anti-androgenic drug concentrations are relevant to investigate whether the exposure is adequate to suppress androgenic effects. Recently, we published the bioanalytical validation of an LC-MS/MS method to measure plasma concentrations of anti-hormonal drugs for treatment of prostate- and breast cancer, among which abiraterone and enzalutamide (16). The assay that we present here consists of the same analytical system but with a different sample preparation and including four hormones to evaluate treatment effects. To our knowledge this is the first assay that combines quantification of androgens, cortisol and prednisone with the quantification of anti-hormonal drugs. Furthermore, this sensitive method is fast and easy to implement with the possibility to determine hormones and prednisone in

1.5

human plasma instead of human serum, as is predominantly described in literature. In conclusion, we present now the development, validation and clinical application of this sensitive and high-throughput LC-MS/MS assay for measuring testosterone, dihydrotestosterone, androstenedione, cortisol and prednisone in plasma from castrated prostate cancer patients using abiraterone acetate or enzalutamide.

Experimental

Chemicals

Testosterone, androstenedione, cortisol, $^2H_4$-testosterone, $^2H_7$-androstenedione and $^2H_4$-cortisol were purchased from Alsachim (Illkirch Graffenstaden, France). Dihydrotestosterone and $^2H_3$-Dihydrotestosterone were from Sigma Aldrich (Zwijndrecht, the Netherlands). Prednisone and $^2H_6$-Prednisone were purchased from Toronto Research Chemistry (Toronto, Canada). Acetonitrile, methanol, water and formic acid 99% (all ULC/MS-grade) were from Biosolve Ltd (Valkenswaard, The Netherlands). Water (distilled) used for sample preparation came from B. Braun Medical (Melsungen, Germany) and tert-butyl-methylether originated from Merck (Amsterdam, the Netherlands).

Charcoal-stripped fetal bovine serum

Testosterone, androstenedione, dihydrotestosterone and cortisol are present in human plasma. Therefore, we were unable to use control human plasma for the preparation of calibration standards and quality control (QC) samples. Charcoal-stripping human plasma reduced hormone levels, however, plasma concentrations of testosterone, androstenedione, dihydrotestosterone and cortisol were still elevated and too high for preferred assay sensitivity. Ultimately, we choose to use charcoal-stripped fetal bovine serum (CCS-FBS) as matrix for calibration standards and quality control samples, as this matrix did not contain interfering hormones. The matrix was produced by stripping FBS in triplicate with charcoal at the Division of Molecular Pathology of the Netherlands Cancer Institute (Amsterdam, The Netherlands).

Stock solutions and working solutions

Separate stock solutions were made for the preparation of calibration standards and QC samples according to Table 1. Working solutions were prepared in acetonitrile at concentrations of 0.4, 0.8, 2, 4, 40, 100, 320 and 400 ng/mL for testosterone and androstenedione, at concentrations of 4, 8, 20, 40, 80, 200, 320 and 400 ng/mL for dihydrotestosterone, at concentrations of 2, 4, 10, 20, 40, 100, 160 and 200 ng/mL for cortisol and at concentrations of 20, 40, 100, 200, 400, 1,000, 1,600 and 2,000 ng/mL for prednisone. Stock solutions for the internal standards (IS) were produced at a concentration of 1 mg/mL in DMSO for $^2H_4$-testosterone and $^2H_6$-prednisone, in methanol for $^2H_7$-androstenedione and in acetonitrile for $^2H_4$-cortisol. $^2H_3$-dihydrotestosterone was purchased as a 0.1 mg/mL stock solution in acetonitrile.

Table 1. Concentrations of analytes in stock solution, calibration standards and quality control samples.

Analyte	Stock (mg/mL)	Calibration standards (pg/mL)	Quality control samples (pg/mL)
Androstenedione	1.00 (Methanol)	10; 20; 50; 100; 1,000; 2,500; 8,000; 10,000	10; 30; 100; 7,500
Cortisol	1.00 (Acetonitrile)	50; 100; 250; 500; 1,000; 2,500; 4,000; 5,000	50; 150; 500; 3,750
Dihydro-testosterone	1.00 (Methanol)	100; 200; 500; 1,000; 2,000; 5,000; 8,000; 10,000	100; 300; 1,000; 7,500
Prednisone	1.00 (DMSO)	500; 1,000; 2,500; 5,000; 10,000; 25,000; 40,000; 50,000	500; 1,500; 5,000; 37,500
Testosterone	1.00 (DMSO)	10; 20; 50; 100; 1,000; 2,500; 8,000; 10,000	10; 30; 100; 7,500

Abbreviations: DMSO = Dimethylsulfoxide

1.5

A mixture of IS stock solutions was prepared and diluted with water to obtain a working solution IS that was used for sample pretreatment. This working solution IS (WIS) contained 5 ng/mL $^2H_4$-testosterone and $^2H_7$-androstenedione, 0.5 ng/mL $^2H_3$-dihydrotestosterone, 2.5 ng/mL $^2H_4$-cortisol and 25 ng/mL $^2H_6$-prednisone. Stock- and working solutions were stored at -20 ºC.

Calibration standards, quality control samples
Calibration samples were prepared freshly prior to each validation run, by spiking 25 µL working solution to 975 µL charcoal-stripped FBS. QC samples were prepared in batches and stored at -20 ºC. Calibration standards and QC samples were prepared in charcoal-stripped FBS according to Table 1.

Sample preparation
All samples were thawed prior to processing and 250 µL was aliquoted in 2 mL containers. Each sample was spiked with 20 µL WIS, except for double blank calibration samples, and 1,5 mL tert-butyl-methylether (TBME). Samples were vortex-mixed for 10 seconds, shaken for 5 minutes at 1,250 rpm and centrifuged for 3 minutes at 23,000 x *g*. The aqueous layer was frozen in a bath of ethanol and dry ice and the organic layer was transferred into a clean 2 mL Eppendorf container. The samples were dried under a gentle stream of nitrogen at 40 ºC. The residue was reconstituted in 50 µL water-methanol (1:1 v/v), vortex-mixed for 10 seconds and centrifuged for 3 minutes at 23,000 x *g*. The final extracts were transferred to autosampler vials with glass insert.

LC-MS equipment and conditions
The LC-MS system was similar to the previously published method for quantification of anti-hormonal drugs in the treatment of prostate- and breast cancer (16). Table 2 depicts general and analyte specific mass spectrometric parameters and the chemical

structures of the analytes are shown in Figure 1. The most sensitive transition was used for quantitation (quantifier, quan), while less abundant ions were monitored for confirmation (qualifier, qual). The ratio of quantifier/qualifier peak areas in unknown samples were compared to the average ratio of the calibration standards. The proposed fragmentation patterns of the quantifier transitions are given in Figure 2.

Table 2. Above: General mass spectrometric parameters. Below: Analyte specific mass spectrometric parameters for testosterone, dihydrotestosterone (DHT), androstenedione, cortisol, prednisone and the internal standards. The most sensitive transition was used for quantitation (quantifier, quan) and the second one was used for confirmation (qualifier, qual).

Parameter	Setting
Run duration	7 min
Ionspray voltage	5500 V
Nebulizer gas	60 au
Turbo gas / heater gas	40 au
Curtain gas	25 au
Collision gas	11 au
Temperature	550 ºC
Dwell time	30 ms

	MRM (Da)	Collision energy (V)	Collision exit potential (V)	Declustering potential (V)	Retention time (min)
Testosterone quan	289.1 → 97.1	27	12	27	2.8
Testosterone qual	289.1 → 109.1	27	12	27	2.8
Testosterone IS	293.1 → 98.1	27	12	27	2.8
DHT quan	291.3 → 225.3	21	10	86	4.6
DHT qual	291.3 → 159.1	21	10	86	4.6
DHT IS	294.2 → 258.3	21	10	86	4.6
Androstenedione quan	287.3 → 97.1	25	10	121	3.0
Androstenedione qual	287.3 → 109.1	25	10	121	3.0
Androstenedione IS	294.2 → 100.1	25	10	121	3.0
Cortisol quan	363.0 121.0	29	19	91	1.2
Cortisol qual	363.0 81.1	29	19	91	1.2
Cortisol IS	367.3 121.0	29	19	91	1.2
Prednison quan	359.3 79.0	57	10	81	1.0
Prednison IS	367.2 → 79.0	57	10	81	1.0

MRM = multiple reaction monitoring, IS = internal standard

Validation procedure

A full validation of the assay was performed based on the United States Food and Drug Administration (FDA) and European Medicines Agency (EMA) guidelines for bioanalytical method validation (17,18). The following aspects were established during the validation: calibration model, accuracy, precision, carry-over, selectivity, matrix effect, dilution integrity, suitability of CCS-FBS as blank matrix, cross-validation and stability.

Clinical application

This assay was developed to quantify of testosterone, androstenedione, dihydrotestosterone, cortisol and prednisone in samples from patients using abiraterone acetate or enzalutamide. Surplus plasma was collected from samples obtained during treatment with abiraterone acetate or enzalutamide at the Antoni van Leeuwenhoek – The Netherlands Cancer Institute as part of routine clinical care. These samples had been collected in K_2EDTA tubes and stored at -20 ℃ until further processing as described in this report. This study was in accordance with the code of conduct for responsible use of human tissue and medical research (19).

Results and discussion

Sample preparation

Starting method development, charcoal-stripped human plasma was used as a biomatrix for calibration standards and quality control samples. Endogenous testosterone, dihydrotestosterone, androstenedione, and cortisol levels, however, were too high to use as a matrix blank. Therefore, we decided to use charcoal-stripped fetal bovine serum to use as matrix to spike calibration standards and quality control samples as this matrix did not contain interfering hormones. Protein precipitation and liquid-liquid extraction were tested as a method for sample preparation. Protein precipitation showed poor sensitivity due to high background noise. Therefore, sample pretreatment was further developed with liquid-liquid extraction. Different extraction solvents were tried: TBME, ethyl acetate and a combination of both solvents in a 80:20 and 20:80 ratio, respectively. Furthermore, extraction ratios of 1:4, 1:9 and 1:14 (sample:extraction solvent) were tested to optimize sample preparation. The extraction recovery using TBME and ethylacetate was comparable, however, TBME was chosen for further development because this organic solvent has a lower boiling point and therefore the evaporation time was shortened. Extraction was optimal with a ratio of 1:14 (sample:extraction solvent), as the recovery did not improve by further increasing the volume of TBME.

Mass spectrometry and chromatography

We developed an analytical system for the quantification of anti-hormonal drugs and for quantification of testosterone, dihydrotestosterone, androstenedione, cortisol and prednisone. Developing such an assay is challenging because a highly selective
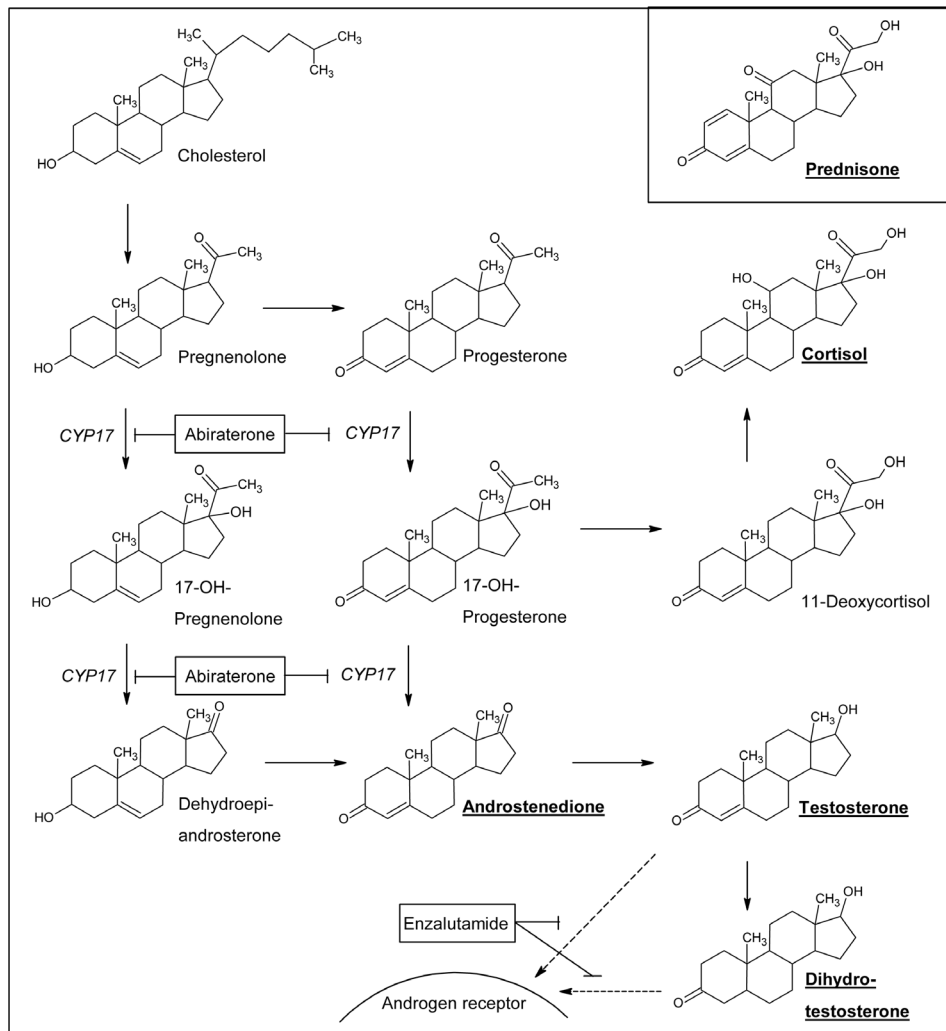
Figure 1. Biosynthesis of testosterone and cortisol from cholesterol. Prednisone is not included in this pathway, but the chemical structure is visible in the top of the figure. Hormones in bold and underlined are included in this assay. Abiraterone inhibits CYP17 and enzalutamide inhibits androgen receptor activation by testosterone and dihydrotestosterone. Abbreviation: CYP17 = cytochrome P450 17.

chromatographic method is needed to separate structural analogues, such as testosterone, dihydrotestosterone and androstenedione. The composition of mobile phase B was pivotal for obtaining this high selectivity and could only be achieved by a combination of methanol-acetonitril (50:50 v/v). Furthermore, high sensitivity was necessary for quantification of these hormones in plasma from patients treated with androgen-deprivation therapy. During assay development, the noise was high (>1000
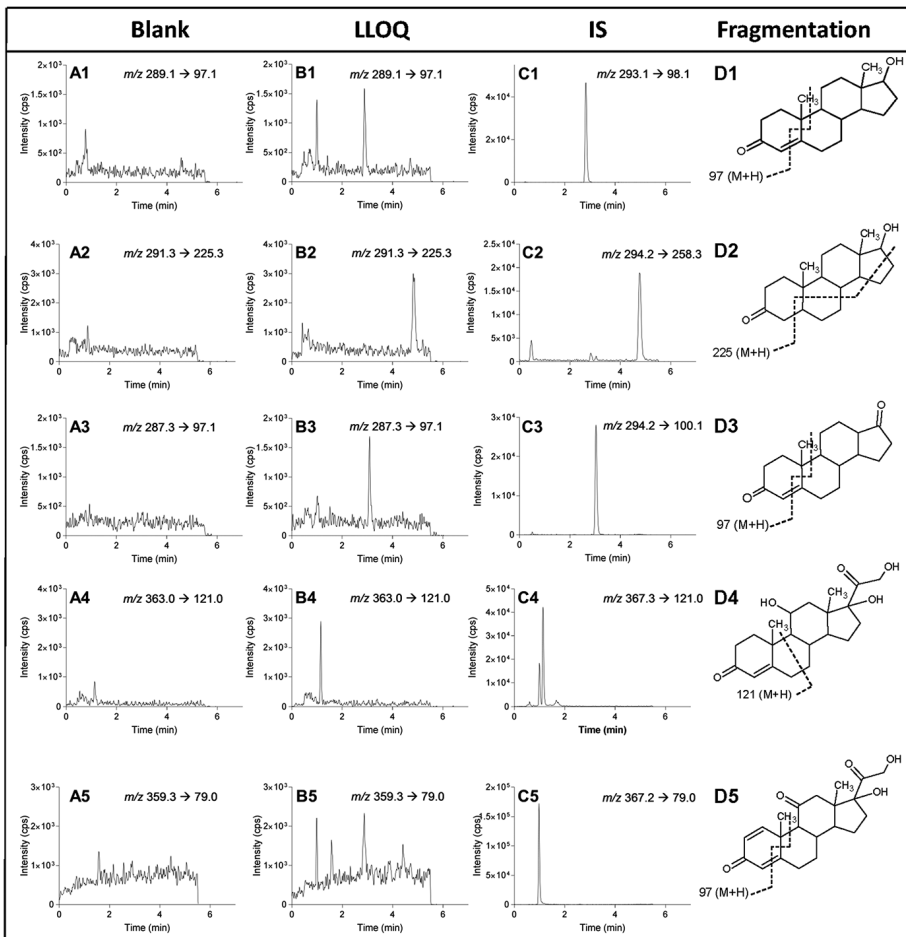
Figure 2. Representative LC-MS/MS chromatograms of a blank sample (A-series) lower limit of quantification (LLOQ; B-series) and the internal standard (C-series), including proposed fragmentation patterns, for testosterone (1, t= 2.8 min), dihydrotestosterone (2, t=4.8 min), androstenedione (3, t=3.0 min), cortisol (4, t=1.2 min) and prednisone (5, t=1.0 min).

cps) for the transitions of testosterone, dihydrotestosterone and androstenedione, which made it difficult to achieve this. However, by using ULC-quality solvents, the noise could be reduced to 200 cps thereby substantially improving assay sensitivity.

Calibration model

Eight non-zero calibration standards were freshly prepared in duplicate prior to each run and were analyzed in three separate runs. All the calibration data were fitted linearly using a weighting factor of $1/x^2$, where x is the analyte concentration. For every calibration curve the calibration concentrations were back-calculated from the response

Table 3. Assay performance data for testosterone, dihydrotestosterone, androstenedione, cortisol and prednisone.

Analyte	Nominal conc. (pg/mL)	Intra-assay (n=15)		Inter-assay (n=15)	
		Bias (%)	C.V. (%)	Bias (%)	C.V. (%)
Testosterone	10	-8.7 to 11.6	4.4 to 11.6	3.1	8.9
	30	-7.2 to 5.7	3.5 to 9.2	-1.4	6.0
	100	-4.1 to 5.6	3.2 to 3.6	-0.9	5.5
	7500	-1.4 to 2.6	0.5 to 8.1	0.4	*
Dihydrotestosterone	100	-6.6 to 1.1	10.1 to 12.5	-2.1	*
	300	2.1 to 7.2	1.7 to 6.9	4.2	0.6
	1000	-5.7 to -0.7	2.7 to 7.2	-2.5	2.0
	7500	-3.3 to -0.4	2.7 to 2.9	-1.9	0.8
Androstenedione	10	-4.9 to -1.4	6.6 to 13.3	-3.7	*
	30	-3.6 to 1.1	4.3 to 8.8	2.0	5.4
	100	-2.0 to 5.9	3.8 to 5.7	2.7	3.5
	7500	0.3 to 4.7	1.7 to 4.5	2.0	1.8
Cortisol	50	-9.2 to -1.0	8.6 to 13.0	-4.5	*
	150	-6.8 to -0.4	8.0 to 9.7	-3.3	*
	500	-7.0 to 0.3	3.4 to 5.0	-2.4	3.6
	3750	-4.1 to 0.4	1.6 to 5.4	-1.9	1.6
Prednisone	500	-10.5 to 11.5	6.3 to 10.9	0.0	10.4
	1500	-11.2 to 9.3	3.5 to 7.7	-1.1	10.1
	5000	-5.5 to 1.4	4.7 to 7.3	-2.9	2.7
	37500	-12.7 to 0.6	1.3 to 5.5	-7.1	7.2

* No significant additional variation was found due to the performance of the assay in different batches.
Abbreviations: conc. = concentration, C.V. = coefficient of variation.

ratios. Deviations of the nominal concentrations were within ±15% and within ±20% for the LLOQ. The assay was linear for the validated concentration ranges of 10-10,000 pg/mL for testosterone and androstenedione, 100-10,000 pg/mL for dihydrotesto-sterone, 50-5,000 pg/mL for cortisol and 500-50,000 pg/mL for prednisone.

Accuracy and precision
Intra- and inter-assay accuracies and precisions of the method were assessed by analyzing five replicate QC samples in three consecutive runs at LLOQ, low, mid and high concentration levels. Accuracy and precision were calculated as described previously (20). Assay performance data of all analytes are presented in Table 3. Inter-assay accuracy, intra-assay accuracy and the precision were ≤15% for low, mid and high concentrations and ≤20% for the LLOQ concentrations. Therefore, accuracy and precision were within the acceptance criteria.

Carry-over

Carry-over was investigated by injecting two double blank samples subsequently after an upper limit of quantification (ULOQ) sample in three independent runs. There were no peaks observed in the first and second blank processed sample, which means that there was no carry-over for testosterone, dihydrotestosterone, androstenedione, cortisol, prednisone and the internal standards.

Specificity and selectivity

Six individual batches of charcoal-stripped FBS were used to assess the specificity and selectivity of the method. A double blank sample and a sample spiked at the LLOQ were processed of each batch. The samples were prepared to determine whether endogenous compounds interfere at the mass transition chosen for the analytes and internal standards. Samples were processed according to the described procedures and analyzed. MRM chromatograms of the six batches of charcoal-stripped FBS contained no co-eluting peaks >20% of the area at the LLOQ level of the analytes and no co-eluting peaks >5% of the area of both internal standards. The accuracies at LLOQ level were within ±20% of the nominal concentration for at least 4 out of 6 batches charcoal-stripped FBS.

Cross-analyte interferences was assessed by preparing samples containing only one of the analytes at ULOQ concentration in control charcoal-stripped FBS. An interference was found for testosterone in the sample spiked with androstenedione. To further investigate this interference, an androstenedione sample at ULOQ concentration was prepared in methanol-water (50:50 v/v) and measured. This sample showed a similar cross-analyte interference for testosterone. Based on this information, we concluded that testosterone is not formed during sample preparation, but present in the reference standard of androstenedione. We quantified the amount of testosterone in the androstenedione reference standard to be 0.33% (w/w). Since the concentration ranges of both analytes are equal (10-10,000 pg/mL) and individual analyte concentrations per calibration standard were the same, we concluded that a bias of 0.33% was acceptable for this bioanalytical assay. For dihydrotestosterone, androstenedione, cortisol and prednisone, cross-interference of co-eluting peaks in separately spiked samples were ≤20% of the QC LLOQ samples and thus within the required limits. For the internal standards, the interference was ≤5% and thus also within the acceptance criteria (17,18).

To investigate the selectivity of the method, structurally related hormones and anti-hormonal drugs were injected onto the system. The method was selective with regard to 17-hydroxy-progesterone, estradiol, epitestosterone, dehydroepiandrosteron (DHEA), progesterone, abiraterone, Δ(4)-abiraterone (D4A) and exemestane. Estradiol, progesterone, abiraterone, Δ(4)-abiraterone (D4A) and exemestane showed no peak in the mass windows of analytes of interest. Furthermore, 17-Hydroxy-progesterone, epitestosterone and DHEA were baseline separated from testosterone, androstenedione and DHT, and therefore will not interfere with analyte quantification.

Matrix factor
The matrix effect was determined in six different batches of charcoal-stripped FBS at low and high concentration levels in singular. Peak areas of QC samples spiked after liquid-liquid extraction were compared to peak areas of QC samples of equivalent concentrations in methanol-water (50:50, v/v). Additionally, the IS-normalized matrix factor was calculated by dividing the matrix factor of the analyte by the matrix factor of the IS. The normalized matrix factor was between 0.957 and 1.09 for testosterone, between 0.915 and 1.04 for dihydrotestosterone, between 1.00 and 1.40 for androstenedione, between 0.912 and 1.29 for cortisol and between 0.474 and 0.707 for prednisone. The CVs for the IS-normalized matrix factor were ≤15% at the tested concentrations for each compound. Prednisone showed a lower normalized matrix factor than the other compounds, which was caused by the presence of a small endogenous peak at the transition and retention time of the internal standard. Overall, the results indicate that the stable-isotopically labelled internal standards are most effective in minimizing the influence of matrix effects as the CV for IS-normalized matrix factor was ≤15% for all analytes.

Dilution integrity cortisol
Dilution integrity was established for cortisol only, as plasma concentrations of the other hormones in patient samples were not expected to exceed the ULOQ. Five replicate charcoal-stripped FBS samples spiked with a cortisol concentration above the ULOQ (100 ng/mL) were diluted 100-fold with charcoal-stripped FBS. The concentrations of 100-fold diluted samples were within ±15% of the nominal concentration. Intra-assay bias and intra-assay variability were 11.0% and 3.9%, respectively. These results show that samples with cortisol concentrations >ULOQ can be diluted with charcoal-stripped FBS up to 100-fold to obtain plasma concentrations within the validated range.

Suitability charcoal-stripped FBS as blank matrix
Testosterone, androstenedione, dihydrotestosterone and cortisol are endogenous compounds and thus CCS-FBS was used as a matrix for calibration standards and QC samples. However, our method was applied to quantify testosterone, dihydrotestosterone, androstenedione, cortisol and prednisone in K_2EDTA plasma and, therefore, the suitability of CCS-FBS as a surrogate matrix was determined by spiking K_2EDTA plasma from patients using abiraterone acetate with unmeasurable testosterone, androstenedione, dihydrotestosterone, cortisol and prednisone concentrations. Three batches of this 'hormone-free' plasma were used for the preparation of QC mid samples in triplicate. These QC samples where measured against a calibration curve in CCS-FBS. Accuracy and precision were ≤15% for all analytes. From these data it can be concluded that CCS-FBS is a suitable surrogate matrix for the quantification of these analytes.

Cross-validation

The assay was cross-validated for testosterone, androstenedione and cortisol with an LC-MS/MS method that was standardized against National Institute of Standards and Technology (NIST) reference material SRM 971 (12). QC samples at three concentration levels and 17 patient samples were measured on both systems to check whether both methods were able to generate the same results. Accuracy of the QC samples was within ±15% and the bias between concentrations measured in patient samples was within ±20% of the mean for at least 67% of the repeats.

Stability

Stability experiments were performed under various conditions at low and high concentrations in triplicate. Analytes were considered stable in the stock solution when 95%-105% of the original concentration was recovered. Stability experiments demonstrate adequate stability in biomatrix of all analytes after 7 days at room temperature and 4ºC, both in the dark and exposed to light. Prednisone was unstable in final extract and dry extract after 7 days at nominally 4ºC, however, 2-day stability of prednisone in final extract and dry extract (4ºC) was established. Other analytes were stable in final extract and dry extract for at least 7 days at nominally 4ºC. Furthermore, analytes were stable undergoing 4 freeze/thaw cycles. Long-term stability assessment in charcoal-stripped FBS was demonstrated up to five months and is still ongoing. Stock solutions were stable for at least 124 days at -20ºC and working solutions were stable for at least 62 days at -20ºC.

Clinical application

The validated assay was used to quantify testosterone, dihydrotestosterone, androstenedione, cortisol and prednisone in K_2EDTA plasma from prostate cancer patients with androgen deprivation therapy. Mean plasma concentrations in 20 patients using abiraterone acetate (1000 mg QD) were <10 pg/mL for testosterone, <10 pg/mL for androstenedione, <10 pg/mL for dihydrotestosterone, 9.6 ng/mL for cortisol and 9.8 ng/mL for prednisone, and mean plasma concentrations in 20 patients using enzalutamide (160 mg QD) were 97 pg/mL for testosterone, 289 pg/mL for androstenedione and <10 pg/mL for dihydrotestosterone. Testosterone and androstenedione could be determined in only two samples from patients using abiraterone acetate, indicating adequate androgen deprivation far below the castration limit of 0.50 ng/mL. Cortisol and prednisone were only quantified in plasma from patients using abiraterone acetate. Cortisol levels were lower in patients with adequate androgen suppression and a measurable prednisone concentration (3.4 vs 16 ng/mL, both n=10). Figure 3 shows representative chromatograms of plasma obtained from three separate patients: one patient using abiraterone acetate with adequate androgen deprivation, one patient using abiraterone acetae with measurable hormone levels and one patient using enzalutamide. Testosterone levels were <10 pg/mL, 92 pg/mL and 67 pg/mL, respectively. Androstenedione showed a similar trend, with plasma
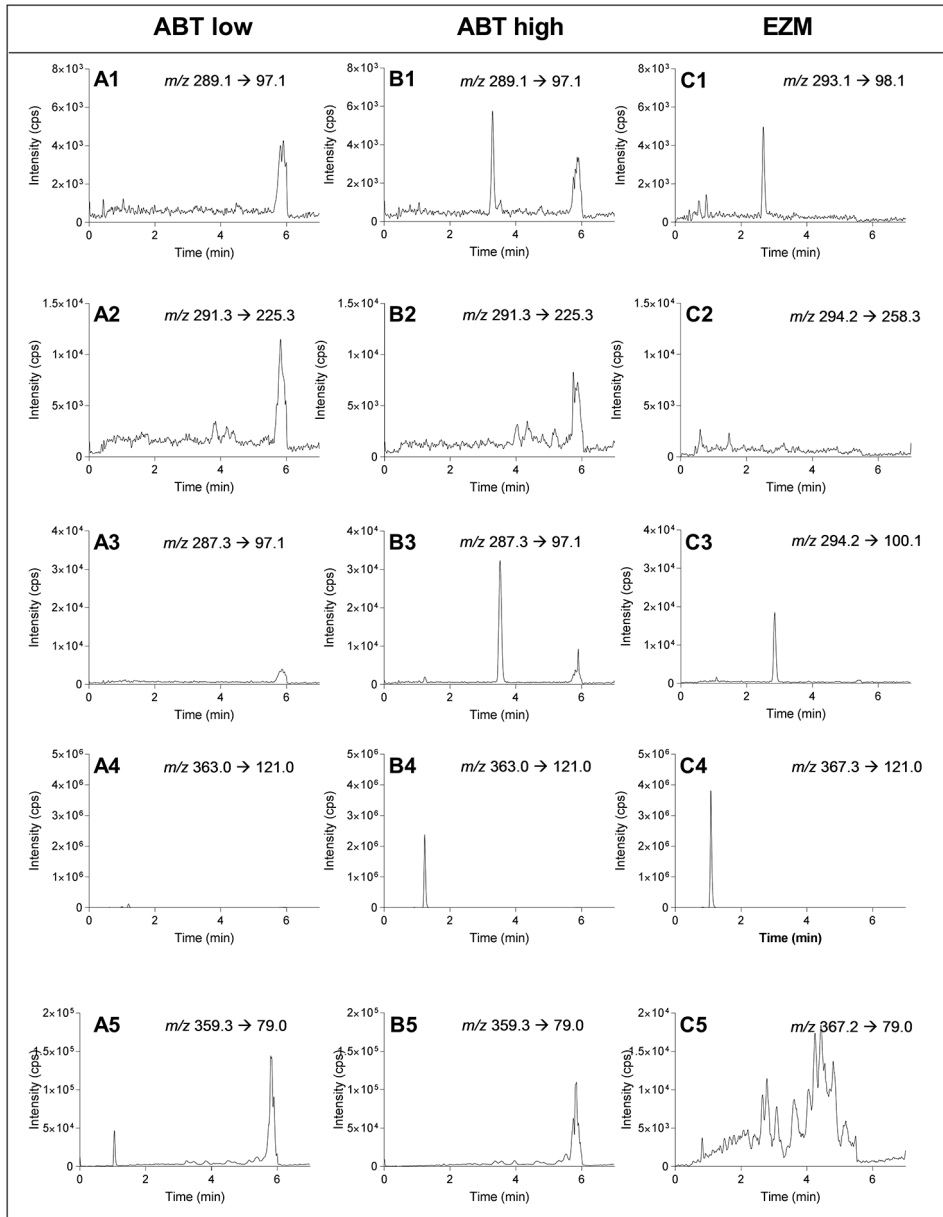
Figure 3. Representative LC-MS/MS chromatograms of plasma from a patient using abiraterone acetate with adequate testosterone suppression (ABT low), a patient using abiraterone with insufficient testosterone suppression (ABT high), and a patient using enzalutamide (EZM) for testosterone (1, t= 2.8 min), dihydrotestosterone (2, t=4.8 min), androstenedione (3, t=3.5 min), cortisol (4, t=1.2 min) and prednisone (5, t=1.0 min).

concentrations of <10 pg/mL, 576 pg/mL and 182 pg/mL, respectively. These results are in line with our expectations based on the mechanism of actions of both drugs. Abiraterone acetate inhibits the production of testosterone, androstenedione, dihydrotestosterone and cortisol via CYP17, while enzalutamide inhibits androgen receptor activation and does not directly inhibits androgen production. Thus, lower plasma concentrations of androgens and cortisol are expected in patients using abiraterone acetate compared to patients using enzalutamide. Furthermore, patients with measurable testosterone and androstenedione levels showed higher cortisol levels. Anti-androgen drugs, such as abiraterone acetate and enzalutamide, can be measured with the same analytical conditions for therapeutic drug monitoring, providing information on both the exposure to anti-androgen drugs and their effects on testosterone, dihydrotestosterone, androstenedione and cortisol.

1.5

Conclusion

The development and validation of a combined assay for the quantification of testosterone, dihydrotestosterone, androstenedione, cortisol and prednisone in samples from drug-treated castrated prostate cancer patients is described. The validated range was 10-10,000 pg/mL for testosterone and androstenedione, 100-10,000 pg/mL for dihydrotestosterone, 50-5,000 pg/mL for cortisol and 500-50,000 pg/mL for prednisone. We are the first to describe a method to monitor plasma drug levels as well as hormones affected by the treatment. The method has been successfully implemented to support clinical pharmacology studies in castrated prostate cancer patients.

References

1. Fitzmaurice C, Allen C, Barber RM, Barregard L, Bhutta ZA, Brenner H, et al. Global, regional, and national cancer incidence, mortality, years of life lost, years lived with disability, and disability-adjusted life-years for 32 cancer groups, 1990 to 2015: A Systematic Analysis for the Global Burden of Disease Study Global Burden . JAMA Oncol. 2017;3:524–48.

2. Siegel RL, Miller KD, Jemal A. Cancer statistics, 2016. CA Cancer J Clin. 2016;66:7–30.

3. American Cancer Society. Global Cancer Facts & Figures 3rd Edition. American Cancer Society. 2015.

4. Sharifi N, Gulley JL, Dahut WL. Androgen deprivation therapy for prostate cancer. JAMA. 2005;294:238–44.

5. Rommerts FFG. Testosterone: an overview of biosynthesis, transport, metabolism and action BT - Testosterone: Action · Deficiency · Substitution. In: Nieschlag E, Behre HM, editors. Berlin, Heidelberg: Springer Berlin Heidelberg; 1990. p. 1–22.

6. Cai C, Balk SP. Intratumoral androgen biosynthesis in prostate cancer pathogenesis and response to therapy. Endocr Relat Cancer. 2011;18:R175-82.

7. US Food and Drug Administration (FDA). Clinical Pharmacology and Biopharmaceutics Review: Zytiga (abiraterone acetate). 2010 [cited 2019 May]. p. 1–86. Available from: https://www.accessdata.fda.gov/drugsatfda_docs/nda/2011/202379orig1s000clinpharmr.pdf

8. US Food and Drug Administration. Clinical Pharmacology and Biopharmaceutics Review: Xtandi (Enzalutamide). Silver Spring (MD). 2012 [cited 2019 Jan]. p. 1–75. Available from: https://www.accessdata.fda.gov/drugsatfda_docs/nda/2012/203415Orig1s000ClinPharmR.pdf

9. Ryan CJ, Molina A, Li J, Kheoh T, Small EJ, Haqq CM, et al. Serum androgens as prognostic biomarkers in castration-resistant prostate cancer: results from an analysis of a randomized phase III trial. J Clin Oncol. 2013;31:2791–8.

10. US Food and Drug Administration. Prescribing information: Xtandi (enzalutamide). Silver Spring (MD). 2012 [cited 2018 Jun]. p. 1–16. Available from: https://www.accessdata.fda.gov/drugsatfda_docs/label/2012/203415lbl.pdf

11. Taieb J, Mathian B, Millot F, Patricot M-C, Mathieu E, Queyrel N, et al. Testosterone measured by 10 immunoassays and by isotope-dilution gas chromatography-mass spectrometry in sera from 116 men, women, and children. Clin Chem. 2003;49:1381–95.

12. van Winden LJ, van Tellingen O, van Rossum HH. Serum Testosterone by Liquid Chromatography Tandem Mass Spectrometry for Routine Clinical Diagnostics. Methods Mol Biol. 2018;1730:93–102.

13. Hakkinen MR, Heinosalo T, Saarinen N, Linnanen T, Voutilainen R, Lakka T, et al. Analysis by LC-MS/MS of endogenous steroids from human serum, plasma, endometrium and endometriotic tissue. J Pharm Biomed Anal. 2018;152:165–72.

14. Buttler RM, Martens F, Ackermans MT, Davison AS, van Herwaarden AE, Kortz L, et al. Comparison of eight routine unpublished LC-MS/MS methods for the simultaneous measurement of testosterone and androstenedione in serum. Clin Chim Acta. 2016;454:112–8.

15. Taylor DR, Ghataore L, Couchman L, Vincent RP, Whitelaw B, Lewis D, et al. A 13-Steroid Serum Panel Based on LC-MS/MS: Use in Detection of Adrenocortical Carcinoma. Clin Chem. 2017;63:1836–46.

16. van Nuland M, Venekamp N, de Vries N, de Jong KAM, Rosing H, Beijnen JH. Development and validation of an UPLC-MS/MS method for the therapeutic drug monitoring of oral anti-hormonal drugs in oncology. J Chromatogr B. 2019;1106–1107:26–34.

17. US Food and Drug Administration (FDA). FDA Guidance for Industry: Bioanalytical Method Validation. Silver Spring, Maryland: US Food and Drug Administration. 2018 [cited 2018 Jun]. Available from: https://www.fda.gov/downloads/drugs/guidances/ucm070107.Pdf

18. European Medicines Agency (EMA). Guideline on Bioanalytical Method Validation. Committe for Medicinal Produts for Human Use and European Medicines Agency. 2011 [cited 2019 May]. Available from: http://www.ema.europa.eu/docs/en_GB/document_library/Scientific_guideline/2011/08/WC500109686.pdf

19. Federation of Dutch Medical Scientific Societies. Human Tissue and medical Research: Code of conduct for responsible use. 2011. p. 21. Available from: https://www.federa.org/sites/default/files/digital_version_first_part_code_of_conduct_in_uk_2011_12092012.pdf

20. Herbrink M, de Vries N, Rosing H, Huitema ADR, Nuijen B, Schellens JHM, et al. Development and validation of a liquid chromatography-tandem mass spectrometry analytical method for the therapeutic drug monitoring of eight novel anticancer drugs. Biomed Chromatogr. 2018;32.

1.5

Ultra-sensitive LC-MS/MS method for the quantification of gemcitabine and its metabolite 2′,2′-difluorodeoxyuridine in human plasma for a microdose clinical trial

Merel van Nuland
Michel J.X. Hillebrand
Hilde Rosing
Sjaak A. Burgers
Jan H.M. Schellens
Jos H. Beijnen

Abstract

In microdose clinical trials a maximum of 100 μg of drug substance is administered to participants, in order to determine the pharmacokinetic properties of the agents. Measuring low plasma concentrations after administration of a microdose is challenging and requires the use of ulta-sensitive equipment. Novel liquid chromatography-mass spectrometry (LC-MS/MS) platforms can be used for quantification of low drug plasma levels. Here we describe the development and validation of an LC-MS/MS method for quantification of gemcitabine and its metabolite 2',2'-difluorodeoxyuridine (dFdU) in the low picogram per milliliter range to support a microdose trial. The validated assay ranges from 2.5-500 pg/mL for gemcitabine and 250-50,000 pg/mL for dFdU were linear, with a correlation coefficient (r^2) of 0.996 or better. Sample preparation with solid phase extraction provided a good and reproducible recovery. All results were within the acceptance criteria of the latest US FDA guidance and EMA guidelines. In addition, the method was successfully applied to measure plasma concentrations of gemcitabine in a patient after administration of a microdose of gemcitabine.

Introduction

Microdose studies are exploratory investigational new drug (eIND) trials that can be conducted in a phase 0 context. The aim of such trials is to accelerate drug development by early selection of promising candidates. A microdose is defined as 1/100th of the therapeutic dose or the dose calculated to yield a pharmacological effect, with a maximum dose of 100 µg (1,2). As no clinical effect is expected after administration of such a low dose, microdoses are considered harmless. After administration of a microdose, pharmacokinetic data of the investigated drug are acquired and evaluated. Early establishment of such parameters might shorten the overall development time and increase success rates of drug approval.

Administration of a microdose results in low systemic plasma concentrations. Determining such low concentrations requires the use of sensitive analytical techniques. Commonly used analytical tools in these cases are accelerator mass spectrometry (AMS) and liquid chromatography-mass spectrometry (LC-MS/MS) (3). Although AMS is known for its high sensitivity and specificity, the low availability and the use of radiolabeled drugs makes this technique expensive. Therefore, the new generation of ultra-sensitive LC-MS/MS provides a good alternative with measurements that have reached the picogram per milliliter level without using radioactive labeled drugs.

An LC-MS/MS method was developed and validated for simultaneous quantification of gemcitabine (dFdC) and its metabolite 2',2'-difluorodeoxyuridine (dFdU) to support a microdose trial. Gemcitabine is a nucleoside analog that can be prescribed for treatment of several cancer types. The main antitumor effect is caused by its triphosphate metabolite dFdCTP, inhibiting DNA synthesis after being incorporated into the DNA (4). Previously published methods for the quantification of gemcitabine and dFdU have insufficient sensitivity to be applied in a microdose trial. The lower limit of quantification (LLOQ) in these assays ranges from 0.25-125 ng/mL and 1-1250 ng/mL for gemcitabine and dFdU, respectively (5–11). We developed a method with 100-fold increased sensitivity to enable analysis of patient samples with low picogram per milliliter concentrations. The focus of this paper is on the development and validation of such a highly sensitive LC-MS/MS method by preserving accurate and precise measurements.

Materials and methods

Chemicals

Gemcitabine hydrochloride (dFdC HCl), 2',2'-difluorodeoxyuridine, ^{13}C,^{15}N$_2$-gemcitabine hydrochloride and ^{13}C,^{15}N$_2$-2',2'-difluorodeoxyuridine were purchased from Alsachim (Illkirch Graffenstaden, France). Acetonitrile, methanol and water (all Supra-Gradient grade) were from Biosolve Ltd (Valkenswaard, The Netherlands). Ammonium acetate (98%) and tetrahydrouridine were supplied from Merck (Amsterdam, the Netherlands).

Water (distilled) used for sample preparation came from B. Braun Medical (Melsungen, Germany). Blank human dipotassium ethylenediaminetetraacetic acid (K_2EDTA) plasma was obtained from the department of clinical chemistry (MC Slotervaart, the Netherlands).

THU stabilized plasma
In human plasma, gemcitabine is deaminated by cytidine deaminase leading to the formation of dFdU. Tetrahydrouridine (THU) is a potent inhibitor of cytidine deaminase and can be added to plasma to prevent deamination. THU was dissolved in water to obtain a 10 mg/mL solution. Consequently, control human K_2EDTA plasma was spiked with this solution at a final concentration of 0.1 mg/mL. This THU stabilized control human K_2EDTA plasma was used for making working solutions, calibration standards and quality control (QC) samples.

Stock solutions and working solutions
Separate stock solutions of 1 mg/mL for calibration standards and QC samples were prepared in water for each analyte (corrected for potency). The stock solutions were further diluted with THU stabilized control K_2EDTA plasma to obtain separate working solutions. Stock solutions of the internal standards (IS) were also prepared at 1 mg/mL in water. A mixture of internal standard stock solutions was prepared and diluted with water to obtain a working solution IS (WIS) that was used for sample pretreatment. This WIS contained 10 ng/mL $^{13}C,^{15}N_2$-gemcitabine and 100 ng/mL $^{13}C,^{15}N_2$-2',2'-dFdU. Stock solutions and working solutions were stored at -20 °C.

Calibration standards, quality control samples
Calibration samples were prepared freshly prior to each validation run, by spiking 25 µL working solution to 475 µL THU stabilized control K_2EDTA plasma. QC samples were prepared in batches and stored at -20 °C. Eight calibration standards were used in this assay and a limit of detection (LOD) was added to determine the lowest analyte concentration to be reliably distinguished from the noise. Concentrations of the calibration standards were 5, 10, 25, 50, 100, 250, 400 and 500 pg/mL with an LOD of 2.5 pg/mL for gemcitabine and 500, 1,000, 2,500, 5,000, 10,000, 25,000, 40,000, 50,000 pg/mL with an LOD of 250 pg/mL for dFdU. Quality control samples were prepared at concentrations 5, 15, 50 and 375 for gemcitabine and 500, 1,500, 5,000, 37,500 for dFdU.

Sample preparation
Samples were thawed prior to processing and 200 µL was aliquoted in 1.5 mL containers. Each sample was spiked with 20 µL WIS, except for double blank calibration samples. Samples were prepared with solid phase extraction (SPE) using Oasis HLB 1cc vac cartridges (Waters, Milford, MA, USA). The cartridges were first equilibrated with 0.5 mL methanol and 0.5 mL water, respectively. After equilibration, plasma

samples were transferred to the cartridges and washed with 0.5 mL water. The cartridges were dried under a maximal vacuum for 10 minutes and samples were eluted with 0.4 mL methanol. Afterwards, the samples were dried under a gentle stream of nitrogen at 40 °C and the dried extract was subsequently reconstituted with 80 μL of reconstitution solvent (10 mM ammonium acetate in water-acetonitrile (93:7, v/v)) by vortex mixing and shaking (10 minutes at 1,250 rpm). The final extracts were transferred to autosampler vials with insert.

LC equipment and conditions

Gemcitabine and dFdU were chromatographically separated using a Shimadzu LC system with a binary pump, a degasser, an autosampler and a valco valve (Nexera 2 series, Shimadzu corporation, Kyoto, Japan). The autosampler temperature was kept at 4 °C and the column oven at 30 °C. Mobile phase A consisted of 10 mM ammonium acetate in water-acetonitrile (93:7, v/v) and mobile phase B of 100% acetonitrile. Gradient elution was applied at a flow rate of 0.2 mL/min through a Acquity UPLC HSS T3 column (100Å, 2.1 x 150 mm, 1.8 μm) with an additional Acquity UPLC HSS T3 Vanguard pre-column (100Å, 2.1 x 5.0 mm, 1.8 μm) (Waters, Milford, MA, USA). The following gradient was applied: 0% B (0.0–7.0 min), 0-80% B (7.0–7.5 min), 80% B (7.5–10 min), 0% B (10–13 min). The divert valve directed the flow to the mass spectrometer between 2.0 and 7.0 minutes and the remainder to the waste container.

MS equipment and conditions

A triple quadropole mass spectrometer 6500 (Sciex, Framingham, MA, USA) with a turbo ion spray (TIS) interface operating in the positive mode was used as a detector. For quantification, multiple reaction monitoring (MRM) chromatograms were acquired and processed using Analyst® 1.6.2 software (AB Sciex). General and analyte specific mass spectrometric parameters are listed in Table 1 and the structures and the proposed fragmentation patterns of the analytes are depicted in Figure 1.

Validation procedures

A full validation of the assay was performed based on the United States Food and Drug Administration (FDA) and European Medicines Agency (EMA) guidelines for bioanalytical method validation (12,13). The following aspects were established during the validation: calibration model, accuracy, precision, carry-over, selectivity (endogenous and cross analyte/IS interferences), matrix effect, recovery, dilution integrity and stability.

Calibration model

Eight non-zero calibration standards were prepared freshly in duplicate for each run and were analyzed in three separate runs. Calibration linearity was determined by plotting the peak area ratio of the analyte/IS against the corresponding concentration (x) of the calibration standard. For all analytes, the reciprocal of the squared concentrations ($1/x^2$) was used as a weighting factor. Deviations from the mean

calculated concentrations should be within 85-115% of the nominal concentrations in at least 75% of non-zero calibration standards. At the LLOQ, a deviation of 20% was permitted.

Limit of detection
A limit of detection was included to determine the lowest analyte concentration to be reliably distinguished from the noise. The signal-to-noise ratio of the LOD should be ≥3.

Table 1. Above: General mass spectrometric parameters. Below: Analyte specific mass spectrometric parameters for gemcitabine, 2',2'-difluorodeoxyuridine (dFdU) and the internal standards. Abbreviations: min = minutes, V = voltage, au = arbitrary units, ms = milliseconds, *m/z* = mass-to-charge ratio

Parameter	Setting
Run duration	13 min
Ionspray voltage	3000 V
Nebulizer gas	40 au
Turbo gas / heater gas	70 au
Curtain gas	35 au
Collision gas	10 au
Temperature	450 °C
Dwell time	150 ms

	Gemcitabine	Gemcitabine IS	dFdU	dFdU IS
Parent mass	264 *m/z*	267 *m/z*	265 *m/z*	268 *m/z*
Product mass	112 *m/z*	115 *m/z*	113 *m/z*	116 *m/z*
Collision energy	21	21	21	21
Collision exit potential	14	14	14	14
Declustering potential	51	51	71	71
Retention time	3.42	3.42	5.35	5.35
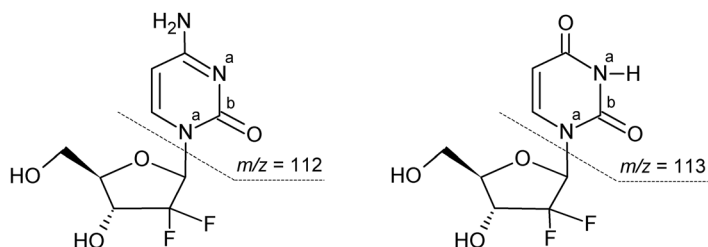
Figure 1. Chemical structures of gemcitabine and dFdU, including the proposed *m/z* fragments. The stable isotopes in the internal standards are indicated with [a] (^{15}N) and [b] (^{13}C).

Accuracy and precision

Intra- and inter-assay accuracies and precisions of the method were determined by analyzing five replicate QC samples in three consecutive runs at LLOQ, low, mid and high concentration levels. Accuracy was expressed as the bias and precision was calculated as the coefficient of variance (CV) according to the following equations (14): Intra-assay bias (%) =

$$100\% \cdot (\textit{mean measured conc.per run-nominal conc.})/(\textit{nomimal conc.})$$

Inter-assay bias (%) =

$$100\% \cdot (\textit{overall mean measured conc.-nominal conc.})/(\textit{nominal conc.})$$

Intra-assay CV (%) =

$$100\% \; (\textit{SD of the measured conc.per run})/(\textit{mean measured conc.per run})$$

$$\sqrt{\frac{\left(\frac{s^2_{overall} /((n_1 + \cdots + n_a - 1) - \left((n_1 - 1)s^2_1 + \cdots + ((n_a - 1)s^2_a) \right))}{a - 1} \right) - (\frac{(n_1 - 1) + \cdots + (n_a - 1)s^2_a}{n_1 + \ldots + n_a - a})}{(\frac{n}{a})}}$$

The acceptance criteria for both parameters were ±15% for QC low, QC mid and QC high and ±20% for QC LLOQ.

Carry-over

Carry-over was investigated by injecting two double blank samples after a calibration standard with the highest concentration (upper limit of quantification, ULOQ). The peak areas in the blank processed samples were expected to be <20% of the peak area in the LLOQ sample.

Selectivity

Six individual batches of THU stabilized control K_2EDTA plasma were used to assess the specificity and selectivity of the method. A double blank sample and a sample spiked at the LLOQ were processed of each batch. The areas of co-eluting peaks in the double blank samples should be <20% of the peak area in LLOQ samples in each batch. Furthermore, the areas of peaks in the double blanks co-eluting with internal standards were expected to be <5% of the peak area of the mean internal standard response. For LLOQ samples, sample inaccuracies were expected to be within 80-120% of the nominal concentration in at least 5 out of 6 samples. Cross-analyte and IS interference was determined with single samples that were separately spiked with one analyte or IS at ULOQ concentration or nominal concentration, respectively. To ensure that compounds did not interfere with the quantification of other analytes, the cross-analyte/IS interference should be ≤20% of the peak area in LLOQ samples and ≤5% for the IS.

Matrix effect and recovery

The matrix effect was determined in six different batches of THU stabilized control human plasma at low and high concentration levels in singular. The following samples were prepared: QC samples in the presence of matrix (each lot of blank sample processed to dried extract, spiked with an academic solution at low and high concentrations) and QC samples in the absence of matrix (a pure solution of the analyte at low and high concentrations). The matrix factor was calculated for each batch by calculating the ratio of the peak area in the presence of matrix to the peak area in absence of matrix. Additionally, the IS-normalized matrix factor was calculated by dividing the matrix factor of the analyte by the matrix factor of the IS.

The recovery was investigated at low and high concentration levels (n=3) in one batch of THU stabilized control human plasma. The recovery was determined by calculating the ratio of the peak area of processed QC samples to the peak area in presence of matrix (blank sample processed to dried extract, spiked with an academic solution at low and high concentrations). The coefficient of variance (CV) for the matrix factor and the recovery should be <15%. (12)

Dilution integrity

Dilution integrity was investigated with five replicate plasma samples with a concentration above the ULOQ. These samples were diluted 10-fold by adding 30 µL sample to 270 µL THU stabilized control human plasma. An accuracy of within -15% and +15% of the nominal concentration was acceptable.

Stability

Short-term stability experiments were performed in plasma after storage at room temperature (20-25 ºC) and at -20 ºC. Further stability assessments were done in dried extracts and final extracts at 4 ºC. The effect of 3 freeze (-20 ºC)/thaw cycles on the stability of each compound was investigated after thawing samples to room temperature with a minimum interval of 12 hours on 3 separate occasions and comparison with freshly prepared calibration samples. Short-term stability in plasma was determined after 1 month and long-term stability will be investigated after 3 months, 6 months and 1 year of storage at -70 ºC. Above described stability experiments were performed in triplicate at low and high concentration levels. Analytes were considered stable under specific conditions when 85-115% of the initial concentration were recovered. Short-term stock stability of one month was previously established (5). The results of 26-month stock stability at -20 ºC are described in this manuscript. Analytes are considered stable in the stock solution when 95%-105% of the original concentration is recovered.

Clinical application

This analytical assay was used for sample analysis in a microdose trial with gemcitabine. The study was conducted in accordance with the International Conference on

Harmonisation guidelines for Good Clinical Practice and the Declaration of Helsinki. The protocol was approved by the Independent Ethics Committee of the Netherlands Cancer Institute. Patients with advanced cancer received 100 µg of gemcitabine via a 30-minute infusion. Blood was drawn at the following time points: t=0 (predose), t=15 min (1/2th of infusion), t=30 min (end of infusion), t=45 min, t=60 min, t=75 min, t=90 min, t=105 min, t=2 h, t=4 h and t=8 h. Blood was collected in 4 mL tubes pre-spiked with 40 µL THU to obtain a final concentration of 0.1 mg/mL. Whole venous blood was centrifuged for 10 minutes at 2,000 g at 4 °C and the plasma was transferred to 2.0 mL containers. Samples were stored at -70 °C directly after processing. Afterwards, the patients went off study and were treated in their best interest with standard of care gemcitabine.

Results and discussion

Sample preparation
Several conventional sample preparation methods were considered during method development, such as protein precipitation and solid phase extraction (SPE). Protein precipitation showed a low recovery and high background noise, while SPE efficiently removed interferences and thereby produced well purified final extracts. To meet sensitivity requirements, SPE was chosen as the method for sample preparation. Oasis® MCX, MAX and HLB SPE cartridge sorbents were evaluated during method development. Since gemcitabine and dFdU are polar compounds, SPE with Oasis® HLB cartridges gave the highest recovery compared to other cartridges.

During the development of this assay, K_2EDTA plasma from Bioreclamations LLC (Hicksville, NY, USA) was used for the preparation of calibration standards and QC samples. Double blank samples of this batch showed an interference at the retention time of gemcitabine, which interfered with low calibration standards. To further develop this method, a new batch of plasma was collected at the department of clinical chemistry (MC Slotervaart, the Netherlands) that did not contain this interference . This batch was used for development and validation of the assay. During the microdose trial, pre-dose samples were collected. These samples did not contain the described interference.

Mass spectrometry and chromatography
Previously published methods for the quantification of gemcitabine and dFdU required improvements regarding sensitivity to measure low plasma concentrations. Use of an ultra-sensitive MS system (i.e. QTRAP6500) already improved selectivity, but optimization of the assay was necessary to reach a sufficient LLOQ. Therefore, we used an UPLC column to improve separation of the compounds and to improve peak shape. Since using a UPLC column clearly increased resolution and the shape of eluting peaks, a nano-LC system with similar column material was tested to further enhance peak separation and signal to noise ratio. Implementation of this nano-LC system, however,
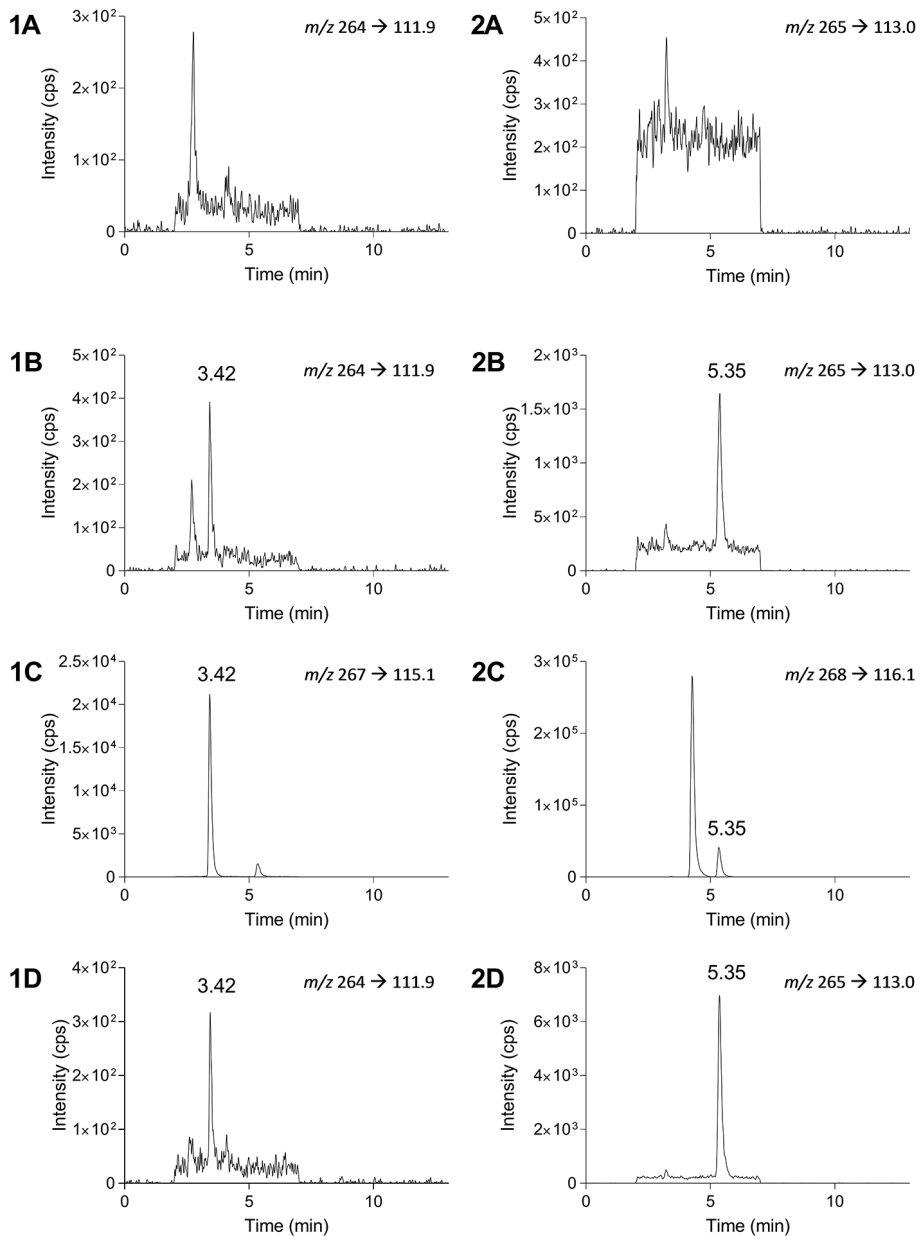
Figure 2. Representative LC-MS/MS chromatograms of a blank sample (1A and 2A), gemcitabine LLOQ (1B), dFdU LLOQ (2B), gemcitabine internal standard (1C), dFdU internal standard (2C), gemcitabine and dFdU in a patient sample at t=8 hours (1D and 2D). The second peak in 1C at 5.35 minutes belongs to the isotopically labeled dFdU, and the first peak in 2C at 4.27 minutes is an unknown endogenous interference.

Table 2. Assay performance data for gemcitabine and its metabolite 2′,2′-difluorodeoxyuridine (dFdU).

Analyte	Nominal conc. (pg/mL)	Intra-assay (n=15)		Inter-assay (n=15)	
		Bias (%)	C.V. (%)	Bias (%)	C.V. (%)
Gemcitabine	5	6.4-11.5	2.8-6.2	8.9	1.3
	15	-2.5-4.7	4.8-7.2	1.0	2.3
	50	2.9-5.5	3.8-6.0	4.5	*
	375	2.5-10.6	2.2-13.2	7.4	2.2
dFdU	500	2.1-11.6	5.3-8.0	8.0	3.7
	1500	2.3-3.7	4.1-8.5	3.2	*
	5000	-0.6-4.7	2.6-6.2	2.4	1.8
	37500	6.7-11.9	1.2-3.3	9.9	2.4

* The inter-assay precision could not be calculated because there is no significant additional variation due to the performance of the assay in different batches. Abbreviations: conc. = concentration, C.V. = coefficient of variation.

1.6

did not further improve the sensitivity of the assay. Thus, an UPLC system was used to develop and to validate this method. Representative chromatograms of a blank sample, QC LLOQ and a patient sample at t=8 hours are presented in Figure 2 for both analytes. Gemcitabine and dFdU were baseline separated. The first peak in the gemcitabine chromatogram corresponds to THU at the transition of gemcitabine (*m/z* 164 → 111.9), as non THU stabilized control plasma does not show this peak.

Calibration model
All the calibration curves were constructed using a weighting factor of $1/x^2$ and were fitted linearly with a minimum correlation coefficient (r^2) of 0.9964 for gemcitabine and 0.9962 for dFdU. The assay was linear for the validated concentration ranges of 5-500 pg/mL for gemcitabine and 500-50,000 pg/mL for dFdU.

Limit of detection
All LOD samples had a single-to-noise ratio of at least 3. To determine plasma concentrations between the LOD and the LLOQ, the LOD could be included in the calibration range. The calibration model (linear fit with a weighting factor of $1/x^2$) remained the same and all calibration samples and QC samples remained within the acceptance criteria. In the application phase of the method it is feasible to include the LOD in the calibration model to quantify plasma concentrations between the LLOQ and the LOD as long as the signal-to-noise ratio is at least 3. In pharmacokinetic analysis, incorporation of the concentrations between the LLOQ and LOD show superior pharmacokinetic models in terms of bias and precision compared to models that exclude these concentration data (15).

Accuracy and precision

Assay performance data of gemcitabine and dFdU are presented in Table 2. Inter-assay accuracy, intra-assay accuracy and the precision were ≤15% for low, mid and high concentrations and ≤20% for the LLOQ concentrations. Therefore, accuracy and precision were within the acceptance criteria.

Specificity and selectivity

MRM chromatograms of six batches of control human plasma contained no co-eluting peaks larger than 20% of the area at the LLOQ level of the analytes and no co-eluting peaks larger than 5% of the area of both internal standards. The influence of different batches control human plasma on the accuracy and precision at LLOQ level was investigated. The accuracies at LLOQ level were in all six batches of control human plasma within 20% of the nominal concentration. Cross-interference of co-eluting peaks in separately spiked samples were <20% of the QC LLOQ samples and thus within the required limits. For the internal standards, the interference was less than 5% and thus also within the acceptance criteria.

Dilution integrity

The concentrations of 10-fold diluted samples were within 85-115% of the nominal concentration in five replicates. Intra-assay bias and intra-assay variability were 2.2% and 5.5% for gemcitabine and 3.6% and 2.9% for dFdU, respectively. These results show that samples with concentrations >ULOQ can be diluted up to 10-fold.

Carry-over

There were no peaks observed in the first blank processed sample, which means that there was no carry-over for gemcitabine, dFdU or the internal standards.

Matrix factor and recovery

The CV for the IS-normalised matrix factor was below 15% at the tested concentrations for each compound. The total recovery was determined at two concentration levels and was >64.8% for gemcitabine, >64.5% for dFdU, >70.7% for $^{13}C,^{15}N_2$-gemcitabine and >82.6% for $^{13}C,^{15}N_2$-dFdU. Although the recovery of the analytes was below 65%, the method was sufficient to reach an LOD of 2.5 pg/mL and 250 pg/mL for gemcitabine and dFdU, respectively. The coefficient of variance did not exceed 15%.

Stability

The results of the investigated stability are presented in Table 3. Gemcitabine and dFdU are stable in stock solution for 26 months. All other experiments demonstrate adequate stability of both analytes in biomatrix, dried extract and final extract. Long-term stability assessment in THU stabilized control human plasma was measured up to 1 month and is still ongoing.

Table 3. Stability parameters for gemcitabine and 2′,2′-difluorodeoxyuridine (dFdU).

Analyte	Conditions	Matrix	Nominal concentration (pg/mL)	Measured concentration (pg/mL)	Bias (%)	C.V. (%)	n
Gemcitabine	-20°C, 26 m	Water (stock)	1.05 ng/mL	1.01 ng/mL	-0.44	0.63	3
	3 F/T (20°C/RT)	Plasma	15	16.2	8.9	1.9	3
			375	391	3.2	6.0	
	RT, 3 d	Plasma	15	13.9	-6.9	1.8	3
			375	416	10	1.8	
	-70°C, 1 m	Plasma	15	16.2	8.0	5.7	3
			375	360	-5.0	3.0	
	2-8 °C, 4 d	Dried extract	15	15.4	2.9	3.7	3
			375	415	10	2.5	
	2-8 °C, 7 d	Final extract	15	14.5	-2.0	3.1	3
			375	409	8.0	3.2	
dFdU	-20°C, 26 m	Water (stock)	1.03 ng/mL	1.03 ng/mL	0.06	3.2	3
	3 F/T (20°C/RT)	Plasma	1500	1443	-2.4	6.3	3
			37500	39900	6.4	3.8	
	RT, 3 d	Plasma	1500	1437	-2.7	0.7	3
			37500	42233	11	2.4	
	-70°C, 1 m	Plasma	1500	1600	6.7	2.3	3
			37500	39033	4.1	1.5	
	2-8 °C, 4 d	Dried extract	1500	1613	7.6	0.9	3
			37500	41967	12	1.7	
	2-8 °C, 7 d	Final extract	1500	1640	11	2.6	3
			37500	41733	10	1.0	

Abbreviations: C.V. = coefficient of variation, m = months, d = days, RT = room temperature, F/T = freeze/thaw.

1.6

Clinical application

The validated gemcitabine assay is used to support a clinical microdose trial. A plasma concentration-time profile of gemcitabine after administration of a microdose is depicted in Figure 3. The patient received a single 100 μg dose of gemcitabine via a 30-minute infusion. This dose is at least 10,000-fold lower than a therapeutic gemcitabine dose of 1,000-1,250 mg/m^2. All measurements were within the validated range after 4-fold dilution of plasma samples at 1/2th (t=15 min) of infusion and end of infusion (t=30 min). The LLOQ was sufficiently low to measure gemcitabine and dFdU up to eight hours after start of the infusion with a plasma concentration of a 3 pg/mL at the final time point. From this plasma concentration-time profile, we can deduce pharmacokinetic data. These results demonstrate the applicability of this method for clinical gemcitabine microdose studies.
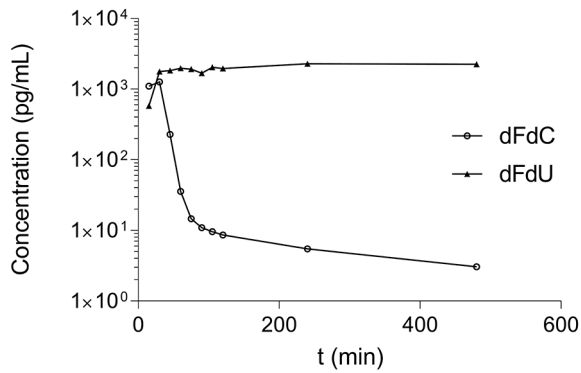
Figure 3. Plasma concentration-time profile of gemcitabine (dFdC) and 2',2'-difluorodeoxyuridine (dFdU) following an intravenous dose of 100 µg gemcitabine in a patient with non-small cell lung cancer via a 30-minute infusion.

Conclusion

A ultra-sensitive LC-MS/MS method was developed and validated for the quantification of gemcitabine and its metabolite dFdU. The validated range is from 2.5-500 pg/mL and 250-50,000 pg/mL for gemcitabine and dFdU, respectively. The assay shows great improvement regarding sensitivity compared to previously published methods, while preserving the accuracy and precision. The method has been successfully implemented to support a microdose trial with gemcitabine.

References

1. FDA/CDER. Guidance for Industry, Investigators, and Reviewers: Exploratory IND Studies. Biotechnol Law Rep. 2006;25:167–74.

2. European Medicines Agency (EMA). ICH guideline M3(R2) on non-clinical safety studies for the conduct of human clinical trials and marketing authorisation for pharmaceuticals. 2009 [cited 2017 May]. Available from: https://www.ema.europa.eu/en/documents/scientific-guideline/international-conference-harmonisation-technical-requirements-registration-pharmaceuticals-human-use_en-2.pdf

3. Burt T, John CS, Ruckle JL, Vuong LT. Phase-0/microdosing studies using PET, AMS, and LC-MS/MS: a range of study methodologies and conduct considerations. Accelerating development of novel pharmaceuticals through safe testing in humans - a practical guide. Expert Opin Drug Deliv. 2016;14:1–16.

4. European Medicines Agency. Gemcitabine. Summary of Product Characteristics. 2017;

5. Vainchtein LD, Rosing H, Thijssen B, Schellens JHM, Beijnen JH. Validated assay for the simultaneous determination of the anti-cancer agent gemcitabine and its metabolite 2′,2′-difluorodeoxyuridine in human plasma by high-performance liquid chromatography with tandem mass spectrometry. Rapid Commun Mass Spectrom. 2007;21:2312–22.

6. Bapiro TE, Richards FM, Goldgraben MA, Olive KP, Madhu B, Frese KK, et al. A novel method for quantification of gemcitabine and its metabolites 2′,2′-difluorodeoxyuridine and gemcitabine triphosphate in tumour tissue by LC-MS/MS: comparison with (19)F NMR spectroscopy. Cancer Chemother Pharmacol. 2011;68:1243–53.

7. Bjanes T, Kamceva T, Eide T, Riedel B, Schjott J, Svardal A. Preanalytical Stability of Gemcitabine and its Metabolite 2′, 2′-Difluoro-2′-Deoxyuridine in Whole Blood-Assessed by Liquid Chromatography Tandem Mass Spectrometry. J Pharm Sci. 2015;104:4427–32.

8. Bowen C, Wang S, Licea-Perez H. Development of a sensitive and selective LC-MS/MS method for simultaneous determination of gemcitabine and 2,2-difluoro-2-deoxyuridine in human plasma. J Chromatogr B, Anal Technol Biomed life Sci. 2009;877:2123–9.

9. Honeywell R, Laan AC, van Groeningen CJ, Strocchi E, Ruiter R, Giaccone G, et al. The determination of gemcitabine and 2′-deoxycytidine in human plasma and tissue by APCI tandem mass spectrometry. J Chromatogr B, Anal Technol Biomed life Sci. 2007;847:142–52.

10. Wickremsinhe ER, Lee LB, Schmalz CA, Torchia J, Ruterbories KJ. High sensitive assay employing column switching chromatography to enable simultaneous quantification of an amide prodrug of gemcitabine (LY2334737), gemcitabine, and its metabolite dFdU in human plasma by LC-MS/MS. J Chromatogr B, Anal Technol Biomed life Sci. 2013;932:117–22.

11. Zhou J, Gao S, Zhang F, Jiang B, Zhan Q, Cai F, et al. Liquid chromatography-tandem mass spectrometry method for simultaneous determination of seven commonly used anticancer drugs in human plasma. J Chromatogr B, Anal Technol Biomed life Sci. 2012;906:1–8.

12. US Food and Drug Administration (FDA). FDA Guidance for Industry: Bioanalytical Method Validation. Silver Spring, Maryland: US Food and Drug Administration. 2018 [cited 2017 Jun]. Available from: https://www.fda.gov/downloads/drugs/guidances/ucm070107.Pdf

13. European Medicines Agency (EMA). Guideline on Bioanalytical Method Validation. Committe for Medicinal Produts for Human Use and European Medicines Agency. 2011 [cited 2017 May]. Available from: http://www.ema.europa.eu/docs/en_GB/document_library/Scientific_guideline/2011/08/WC500109686.pdf

14. Rosing H, Man WY, Doyle E, Bult A, Beijnen JH. Bioanalytical liquid chromatographic method validation. A review of current practices and procedures. J Liq Chromatogr Relat Technol. 2000;23:329–54.

15. Keizer RJ, Jansen RS, Rosing H, Thijssen B, Beijnen JH, Schellens JHM, et al. Incorporation of concentration data below the limit of quantification in population pharmacokinetic analyses. Pharmacol Res Perspect. 2015;3:e00131.

1.6

Therapeutic drug monitoring of anti-hormonal drugs in oncology

Therapeutic drug monitoring of oral anti-hormonal drugs in oncology

Stefanie L. Groenland
Merel van Nuland
Remy B. Verheijen
Jan H.M. Schellens
Jos H. Beijnen
Alwin D.R. Huitema
Neeltje Steeghs

Abstract

Oral anti-hormonal drugs are essential in the treatment of breast and prostate cancer. It is well-known that the interpatient variability in pharmacokinetic exposure is high for these agents and exposure-response relationships exist for many oral anti-hormonal drugs. Yet, they are still administered at fixed doses. This could lead to under dosing and thus suboptimal efficacy in some patients, while other patients could be over dosed resulting in unnecessary side effects. Therapeutic drug monitoring (TDM), individualized dosing based on measured blood concentrations of the drug, could therefore be valid to further optimize treatment. In this review, we provide an overview of relevant clinical pharmacokinetic and pharmacodynamic characteristics of oral anti-hormonal drugs in oncology and translate these into practical guidelines for TDM.

For some agents, TDM-targets are not well established yet and as reference the median exposure could be targeted (exemestane: C_{min} 4.1 ng/mL and enzalutamide: C_{min} 11.4 mg/L). However, for most drugs exposure-efficacy analyses could be translated into specific targets (abiraterone: C_{min} 8.4 ng/mL, anastrozole: C_{min} 34.2 ng/mL and letrozole: C_{min} 85.6 ng/mL). Moreover, prospective clinical trials have shown TDM to be feasible for tamoxifen, for which the exposure-efficacy threshold of its active metabolite endoxifen is 5.97 ng/mL. Based on the available data we therefore conclude that individualized dosing based on drug levels is feasible and promising for oral anti-hormonal drugs and should be developed further and implemented into clinical practice.

Introduction

Breast and prostate cancer are both highly prevalent malignancies, with breast cancer being the most commonly diagnosed malignancy in women and prostate cancer in men in the Western world. Breast and prostate cancer represent the second cause of cancer deaths in women and men, respectively (1). As these tumors are often dependent on estrogens and androgens for their growth, anti-hormonal drugs are imperative in their treatment.

Even though many oral anti-hormonal drugs show exposure-response relationships and the interpatient variability in pharmacokinetic (PK) exposure is high (up to 141% for abiraterone) (2), they are still administered at fixed doses. As a result, some patients may be underdosed, which could lead to suboptimal efficacy, while other patients might be overdosed, causing unnecessary toxicity. Treatment could be optimized by therapeutic drug monitoring (TDM), which is individualized dosing based on measured blood concentrations of the drug (3–8).

Use of TDM in oncology has been previously advocated and for other targeted therapies, such as kinase inhibitors, TDM targets have been described previously (3,4,6,7,9). The aim of this review is to summarize the available PK and pharmacodynamic (PD) data on oral anti-hormonal drugs, to discuss exposure-toxicity and exposure-efficacy relationships and to propose pharmacokinetic targets, which can be used for TDM.

Table 1 provides a summary of selected (steady state) PK parameters of these drugs. The proposed targets and TDM recommendations have been summarized in Table 2.

Methods

Although this is not a systematic review, literature was searched as comprehensive as possible. For all oral anti-hormonal drugs, the FDA Clinical Pharmacology & Biopharmaceutics Review and the CHMP European Public Assessment Report were consulted. Also, PubMed searches were performed using the term pharmacokinetics in combination with the different oral anti-hormonal drugs. In addition, citation snowballing was used to find other relevant studies.

2.1

Table 1. Overview of oral anti-hormonal drugs in oncology with selected (steady state) pharmacokinetic parameters.

Drug	Indication	(Primary) Target	Approved Dose	t_{max} (h)	C_{min} (ng/mL ± SD or [range] if reported)	Inter-patient variability (CV%)	Intra-patient variability (CV%)	$t_{1/2}$ (h)	Time to steady-state plasma concentration (days)	References
Anastrozole	BC	Aromatase	1 mg QD	2	33.2 [0.0 – 132.1]	41-44[e]	7-12[f]	50	7	(34,43–45,61–63)
Exemestane	BC	Aromatase	25 mg QD	2	4.1 [1.3 – 38.1][b]	33-39[f]	40[f]	24	7	(36,48,64)
Letrozole	BC	Aromatase	2.5 mg QD	1-2	88.4 [0.0 – 349.2]	43-55[e]	10-21[f]	48	60	(35,44,51,65)
Tamoxifen[a]	BC	ER	20 mg QD	2	9.72 [1.73-30.8][c]	40-49[g]	11[g]	336	70	(24–26,66)
Abiraterone	PC	CYP17	1000 mg QD	2	10.9[d] ± 4.8	46[e]	33[e]	12	3	(10,13)
Enzalutamide	PC	AR	160 mg QD	1	11,400 ± 2,950	26[e]	not reported	139	29	(19)

[a] Pharmacokinetic data shown for the active metabolite endoxifen
[b] Calculated C_{min} based on median C_{max} (7.7 ng/mL, range: 2.5 – 72.0) and $t_{1/2}$, calculated with the formula proposed by Wang et al.(50)
[c] Steady-state concentration
[d] Weighted average
[e] Variability in C_{min}
[f] Variability in AUC
[g] Variability in steady state concentration
Abbreviations: AR = androgen receptor, AUC = area under plasma concentration-time curve, BC = breast cancer, C_{min} = minimum plasma concentration / trough concentration, C_{max} = maximum concentration, CYP17 = 17α-hydroxylase, ER = estrogen receptor, PC = prostate cancer, QD = once daily, T_{max} = time until maximum concentration, $T_{1/2}$ = terminal elimination half-life

Practical Recommendations for Therapeutic Drug Monitoring of Oral Anti-Hormonal Drugs in Oncology

Anti-androgens

Abiraterone

Abiraterone acetate (Zytiga®) is the prodrug of abiraterone, which is a steroidal irreversible inhibitor of 17α-hydroxylase (CYP17) thereby blocking the androgen synthesis. Abiraterone acetate is currently indicated for metastatic castration-resistant prostate cancer (mCRPC) (10). In the near future, this indication might be expanded to patients with locally advanced or metastatic prostate cancer who are naive to anti-hormonal treatment (11).

According to the Summary of Product Characteristics (SmPC), abiraterone acetate should be ingested in modified fasting state, which means no food 2 hours before or 1 hour after drug intake. Chi *et al* studied the food-effect of the PK of abiraterone acetate and found a 7- and 5-fold increase in C_{max} and area under plasma concentration-time curve (AUC), respectively, with a low-fat meal and a 17-fold and 10-fold increase in C_{max} and AUC, respectively, with a high-fat meal, compared to overnight fasting in healthy subjects. However, in mCRPC patients the food effect was compared to a modified fasting state, showing a less pronounced effect (similar exposure with low-fat meals and a 2-fold increase with high-fat meals). Adverse events (all grade ≤ 3) were similar in the different groups (mainly hot flushes, fatigue and hypokalemia) (12).

Abiraterone acetate has a high inter-patient variability of 41 – 141% for $AUC_{0-\infty}$ and 46% for C_{min}, with an intra-patient variability of 33% (2,13). In the population PK model described by Stuyckens *et al* food and hepatic impairment appeared to be relevant covariates that influence abiraterone exposure, while 70% of the inter-patient variability remained unexplained (14).

Unfortunately, insufficient PK data have been collected in the pivotal trial and phase II trials to evaluate the exposure-toxicity relationships.(10) Abiraterone acetate was generally well tolerated, and no dose limiting toxicities were reported for doses up to 2000 mg once daily (15).

A model has been developed in which a relationship between PK and prostate specific antigen (PSA)-reduction has been established (2,16). Also, in a prospective observational study in castration resistant prostate cancer patients (n=61) higher abiraterone trough concentrations (C_{min}) were found in PSA-responders compared to non-responders (12.0 versus 8.0 ng/mL, p=0.0015), in which PSA-response was defined as a PSA decline of at least 50% after 3 months of treatment (13). The most predictive C_{min} cut-off for PSA response was 8.4 ng/mL according to a receiver operator curve. Using this threshold, exposure-survival analysis found a progression free survival, defined as the time from treatment initiation to the first progression event (either PSA or radiologic progression), of 7.4 months in patients below and 12.2 months in patients above a C_{min} of 8.4 ng/mL (p=0.044). 19 of the 55 patients (35%) in this study had a C_{min} below 8.4 ng/mL. (13).

2.1

Table 2. Overview of practical TDM recommendations for oral anti-hormonal drugs in oncology.

Drug	TDM Recommendation[a]	Proposed Target (ng/mL)	Mean / Median Exposure (C_{min} in ng/mL)	Outcome Parameter Associated with TDM Target	References
Anastrozole	Exploratory	$C_{min} \geq 34.2$	33.2	Estradiol suppression	(43)
Exemestane	Exploratory		4.1[b]		(48)
Letrozole	Promising	$C_{min} \geq 85.6$	88.4	Increased time to tumor progression	(35)
Tamoxifen	Viable	$C_{min} \geq 5.97$	9.72	Lower recurrence rate	(24,29)
Abiraterone	Promising	$C_{min} \geq 8.4$	10.9	PSA reduction, progression free survival	(8,14)
Enzalutamide	Exploratory	$C_{min} \geq 5,000$	11,400	16β-[18]F-5α-dihydrotestosterone imaging	(21)

[a] The provided TDM recommendation is considered promising if a pharmacokinetic TDM target is available or viable if a prospective TDM study has been conducted. Otherwise the recommendations are considered exploratory.
[b] Calculated C_{min} based on median C_{max} and $t_{1/2}$, calculated with the formula proposed by Wang et al (50).
Abbreviations: C_{min} = minimum plasma concentration / trough concentration, C_{max} = maximum concentration, PSA = prostate specific antigen, TDM = therapeutic drug monitoring

Abiraterone is converted into the active metabolite Δ⁴-abiraterone (D4A) by the enzyme 3β-hydroxysteroid-dehydrogenase (3βHSD). Although the conversion ratio of abiraterone to D4A is low (~5%), it targets multiple steps of the androgen receptor signaling pathway, some of them more potently than abiraterone. An exposure-efficacy relationship has not been established for D4A hitherto, but given the dual mechanism of action of D4A (both inhibition of CYP17 and blockage of the androgen receptor), it is to be expected that such a relationship exists and may be identified. Therefore, measuring this metabolite could be interesting to refine TDM-guided dosing in the future (17,18).

Given the clear exposure-efficacy relationship, a target C_{min} of ≥ 8.4 ng/mL can be recommended for abiraterone. At the currently used fixed dose of 1000 mg QD, 35% of patients do not reach this threshold, with the potential to increase PFS by 4.8 months for this subpopulation. Although it is advised to administer abiraterone in a modified fasting state, in clinical practice patients often take it after an overnight fast. Since a clinically significant food-effect has been shown when compared to overnight fasting, a first step in case of low exposure could be to administer abiraterone concomitantly with a light meal or a snack, before escalating the dose.

Enzalutamide
Enzalutamide (Xtandi®) is an androgen-receptor antagonist indicated for the treatment of mCRPC (19). Enzalutamide is metabolized by CYP2C8 and CYP3A4/5 to an inactive carboxylic acid (M1) and an active N-desmethyl metabolite (M2). The mean ± SD C_{min}

of the approved 160 mg QD dose was 11.4 ± 3.0 mg/L for enzalutamide, 13.0 ± 3.8 mg/L for M2 and 8.4 ± 6.8 mg/L for M1.(20) Since M2 has a high abundancy and similar potency as enzalutamide, and concentrations of these two compounds can differ between patients (±25%), it could be scientifically interesting to measure both enzalutamide and its M2 metabolite (19). Future studies should clarify the role of this M2 metabolite in TDM.

No clinically significant exposure-toxicity relationships have been found so far (19). An exposure-efficacy analysis has been executed for enzalutamide in the pivotal phase III study, using the sum of the C_{min} for enzalutamide and M2 with overall survival as endpoint. All quartiles performed significantly better than placebo (p<0.0001), yet no differences between the exposure quartiles could be found (p≥0.5499) (20).

In the phase I/II trial, PSA decreases at 12 weeks were comparable in the different dose levels (range: 60 – 600 mg) (21). Although enzalutamide targets the androgen receptor and could therefore cause a PSA decline without reflecting tumor response, it has been shown that PSA decline after 12 weeks is still associated with progression-free survival and overall survival (22).

In the phase I trial, 16β-[18]F-5α-dihydrotestosterone PET imaging in 22 patients suggested androgen receptor binding was higher in the 150 mg (corresponding to a median C_{min} of 11.4 mg/L) than in the 60 mg dose group (corresponding to a median C_{min} of approximately 5 mg/L). No additional effect was seen at higher doses, suggesting a plateau at a dose of 150 mg and C_{min} of 12 mg/L (21).

Given the lack of exposure-toxicity relationship, the limited evidence for an exposure-efficacy relationship and the small interpatient variability in exposure (26% for C_{min}), enzalutamide may not be the ideal drug for TDM. In absence of an exposure-efficacy target, the mean C_{min} of 11.4 mg/L at the standard dose of 160 mg QD could be used as a reference. As this is the mean exposure, approximately 50% of patients will have concentrations below this reference. Based on the 16β-[18]F-5α-dihydrotestosterone data, dose increments could be considered in patients with very low (e.g. <5 mg/L) C_{min}. Taking into account the mean exposure and standard deviation, less than 2.5% of patients will have trough levels < 5 mg/L.

Anti-Estrogens

Tamoxifen

Tamoxifen (Nolvadex®) is an estrogen receptor antagonist indicated for the treatment of estrogen receptor positive breast cancer. Tamoxifen is extensively metabolized mainly by CYP2D6 and CYP3A4 into a range of active and inactive metabolites (23). Endoxifen is one of the most potent and abundant metabolites and therefore TDM of tamoxifen has focused on measuring endoxifen levels. Endoxifen shows a large inter-patient variability in steady-state concentrations of 40-49% , while the intra-patient variability is only 11% (24–26).

No clear relationship between endoxifen concentration and toxicity has been reported in the literature. A retrospective study (n=109) could not find evidence for an association between exposure and hot flashes, a major side effect of tamoxifen treatment (27). In another, prospective trial (n=122), no significant correlation was found between tamoxifen metabolites and hot flash score (p=0.07) (28).

A retrospective analysis of 1370 ER-positive breast cancer patients receiving tamoxifen in the adjuvant setting, found that patients in the lowest endoxifen exposure quintile (0 – 5.9 ng/mL) had a higher risk of recurrence than patients above this threshold (hazard ratio 0.74; 95% CI 0.55-1.00). The recurrence rate was 16% for patients in the lowest quintile versus 10.1-14.7% in the higher exposure quintiles. The investigators also explored dichotomized optimal cut-off points for the association between endoxifen levels and additional breast cancer events, in which an endoxifen level ≥ 5.97 ng/mL turned out to be the best threshold. This threshold corresponds closely to the lowest quintile (29).

With the same dataset, an anti-estrogenic activity score (AAS) was developed taking into account the IC_{50}-corrected concentrations of tamoxifen, endoxifen, 4-hydroxytamoxifen, and N- desmethyltamoxifen (30). An AAS threshold of 1798 was associated with a hazard ratio of 0.69 (95% CI 0.48–0.99). It should be noted, that this AAS was dominated by endoxifen, suggesting that endoxifen can serve as a proxy for the overall anti-estrogenic effect of tamoxifen and its metabolites.

While a clear exposure-efficacy relationship has been demonstrated in the adjuvant setting, Neven *et al* did not find this relationship in the neo-adjuvant and metastatic setting (31).

In a recent prospective clinical trial (n=122), tamoxifen doses were tailored based on endoxifen levels (28). Breast cancer patients with an endoxifen level <5.6 ng/mL (corresponding to 15 nmol/L) received a 20 mg dose increase, while patients with endoxifen levels between 5.6-11.2 ng/mL (or 15-30 nmol/L) were recommended a dose increase of 10 mg. All patients with endoxifen levels ≥ 11.2 ng/mL continued treatment at the fixed dose of 20 mg tamoxifen. In total, 68 of 122 patients had at least one dose increment, after which 96% of patients achieved an endoxifen level ≥ 5.6 ng/mL, compared to only 76% at baseline (28).

Although it is known that CYP2D6 intermediate and poor metabolizer phenotypes are associated with lower endoxifen concentrations, CYP2D6 phenotype only accounts for 18 – 43% of the interpatient variability in endoxifen levels (29,31–33). 24% of the poor metabolizers and 58% of the intermediate metabolizers still have an endoxifen concentration above the efficacy threshold, while 12% of the normal metabolizers does not reach this threshold (29). As endoxifen concentrations can not be adequately predicted by CYP2D6 phenotype, we advocate endoxifen-guided dosing instead of genotype-guided dosing.

At the currently used fixed dose of 20 mg QD, 20% of patients do not reach the proposed efficacy-threshold of 5.97 ng/mL, with the potential to lower the recurrence rate by 26% in this subpopulation. The presence of a large retrospective exposure-

efficacy study and prospective dose individualization study support the conclusion that it is feasible to dose tamoxifen based on measured endoxifen levels, using ≥ 5.97 ng/mL as a threshold, although no unequivocal evidence from a prospective trial is available yet which demonstrates that TDM really increases tamoxifen treatment efficacy.

Aromatase inhibitors

Estrogens are synthesized from androgens by the aromatase enzyme complex. This enzyme system is inhibited by aromatase inhibitors (AIs). After previous use of the first and second generation AIs (e.g. aminoglutethimide and formestane), the third generation AIs currently used in clinical practice are anastrozole, letrozole and exemestane. These drugs are indicated for the treatment of postmenopausal estrogen receptor positive breast cancer patients, either in the (neo)adjuvant or metastatic setting (34–36). Anastrozole and letrozole are nonsteroidal AIs that bind reversibly to aromatase while exemestane is a steroidal AI that binds irreversibly to aromatase (37).

Since AIs inhibit the synthesis of estrogens, measuring circulating estrogen concentrations would be a good biomarker for efficacy. However, the sensitivity of the currently most commonly used estrogen assays is insufficient to measure the low levels of circulating estradiol in postmenopausal women, especially in those on AI treatment (38,39). Patients on anastrozole, letrozole and exemestane treatment have estradiol concentrations of 1.26, 0.63 and 0.63 pg/mL, respectively (40,41). In daily clinical practice circulating estradiol is measured using immunoassays (optimized to measure concentrations between 40 – 2000 pg/mL (39)), while mass spectrometry would be a more sensitive method, although this method is more costly and labor intensive. Even mass spectrometry assays are not always sensitive enough to measure the low circulating levels of estradiol in patients on AI treatment, for which assays with an lower limit of quantification (LLOQ) of 0.1-0.2 pg/mL are needed (39). A recently published paper suggested measuring gonadotrophins as a possible surrogate marker for estrogen activity.(42) Future studies are needed to confirm the feasibility of gonadotrophins as a biomarker for efficacy of AIs.

Hypothetically, one could imagine dosing of AIs could be personalized using a PD biomarker, such as measured estradiol or gonadotrophin levels. In absence of these data, individualized dosing based on PK is more within reach.

Anastrozole

Ingle *et al* reported a high variability in anastrozole concentrations at the standard dose of 1 mg QD, with a median of 33.2 ng/mL, interquartile ranges 23.5 – 44.8 ng/mL and a range from LLOQ (0.1 ng/mL) to 132.1 ng/mL (n = 649) (43), while the intra-patient variability is small (7-12%)(44).

To our knowledge, no exposure-toxicity relationship has been described for anastrozole. In phase I studies patients received repeated doses up to 10 mg QD and single doses

2.1

up to 60 mg QD, which were well tolerated and did not cause any serious adverse events (45). A linear dose-exposure relationship was found for doses of 0.5 up to 10 mg (45).

Dose-efficacy and exposure-efficacy relationships have only been studied with estrogen suppression as a surrogate marker of effect. Although previous studies showed estradiol suppression to below the limits of detection (LLOQ: 2 pg/mL) for doses of 1 mg or higher (45,46), it could still be possible that higher doses suppress estradiol to a greater extend, which could not have been quantified with these assays.

In a prospective study (n=649), Ingle *et al* reported significantly lower anastrozole concentrations in patients with stable or increased estradiol concentrations compared to patients with decreased estradiol concentrations (LLOQ: 0.625 pg/mL) after start of anastrozole treatment (26.7 ng/mL vs. 34.2 ng/mL, p<0.001) (43). This indicates that TDM could be of value for anastrozole. However, since not all patients with decreased estradiol concentrations compared to baseline necessarily have sufficient estrogen suppression, higher anastrozole concentrations might be needed to attain adequate estrogen suppression.

No definitive exposure-efficacy target has been proposed yet for anastrozole. However, based on the available data dose-escalation could be considered for patients with C_{min} < 34.2 ng/mL (43). Since the median exposure is 33.2 ng/mL, approximately 50% of patients will have a C_{min} below this threshold at the currently used fixed dose of 1 mg QD. Future studies should further investigate the relationship of anastrozole plasma concentrations with both circulating estrogen levels and progression-free and recurrence-free survival.

Exemestane

Although exemestane is extensively metabolized, 17-hydroxy-exemestane is the only active metabolite. However, because the 17-hydroxy-exemestane concentration is ten times lower than the exemestane concentration and 17-hydroxy-exemestane is 2.6 times less potent than exemestane, its additional anti-estrogenic effect is limited (36). Estradiol and exemestane share the same steroidal backbone. This structural resemblance can lead to falsely elevated estradiol concentrations in immunoassays. Measuring estradiol concentrations with liquid chromatography tandem mass spectrometry instead of immunoassays therefore is to be preferred (47).

Hertz *et al* reported a median C_{max} of exemestane of 7.7 ng/mL (range: 2.5 - 72.0, n = 246) at the standard daily dose of 25 mg. Higher exemestane concentrations have been associated with CYP3A4*22 variant, white race, elevated liver enzymes, renal insufficiency, lower body-mass index (BMI) and not having received prior chemotherapy (all p < 0.05). However, these factors explained less than 10% of the overall inter-patient variability in exemestane concentrations (48).

No exposure-toxicity relationship has been shown for exemestane. In general, exemestane is well tolerated, with single doses up to 800 mg and multiple doses up to 200 mg administered in phase I studies (36).

Exposure increases proportionally with increasing dose. Estrogen suppression was maximal at a dose of 25 mg (used assay is not mentioned) (36). However, exemestane concentrations were not significantly different in patients who did and did not achieve estradiol suppression to undetectable levels (LLOQ: 1.25 pg/mL) (49).

No exposure-efficacy analyses have been reported yet for exemestane. Future studies need to explore any relationship between exemestane exposure and clinical response. In absence of an exposure- efficacy target, the median C_{max} of 7.7 ng/mL could be used as a reference for TDM, corresponding to a calculated trough level of 4.1 ng/mL (50). As this is the median exposure, approximately 50% of patients will have trough levels below this proposed reference.

Letrozole

Desta *et al* reported a high interpatient variability, with a median steady-state exposure of 88.4 ng/mL (range: LLOQ (7 ng/mL) – 349.2 ng/mL) at the standard dose of 2.5 mg QD (51). Higher exposure was associated with increasing age, lower BMI and CYP2A6 genetic variations. The lower exposure with increasing BMI can be explained by the fact that letrozole is a highly lipophilic drug with a large volume of distribution (183L), which increases with increasing BMI. These three variables explain only 32.3% of the inter-patient variability, so a large proportion remains to be elucidated (51).

In phase I studies single doses up to 30 mg and repeated doses up to 5 mg were well tolerated. Higher exposure did not cause increased toxicity (35). Exposure increases approximately linear with doses up to the standard dose of 2.5 mg QD, while at higher doses the exposure increases non-linearly (35).

No significant relationship was found between dose (range: 0.5 mg – 5.0 mg) and estrogen suppression albeit that the assay used may not have been sensitive enough (LLOQ: 2.5 pg/mL) (35). Furthermore, Hertz *et al* found that median steady-state concentrations of letrozole were comparable in patients who did and did not achieve E2 suppression to undetectable levels (LLOQ 1.25 pg/mL, 88.8 vs. 105.7 ng/mL, respectively, p=0.63) (49).

In an exposure- efficacy analysis patients were divided in groups reaching different letrozole plasma concentration. This analysis showed a tendency to an increase in time to tumor progression for those patients with a letrozole plasma concentration ≥ 85.6 ng/mL (35). Future studies need to confirm this exposure-efficacy relationship. Until then, the most appropriate target for TDM of letrozole is 85.6 ng/mL. Since the median exposure is 88.4 ng/mL, slightly less than 50% of patients will not reach this target at the currently used fixed dose of 2.5 mg QD.

Discussion

The data presented in this review point towards clear opportunities to improve and to optimize treatment with anti-hormonal agents in oncology through TDM. However, the evidence for this is not equally strong for all agents. Because of this, we evaluated

2.1

the available evidence and proposed TDM recommendations, which we considered either *exploratory*, *promising* or *viable*, as presented in Table 2. The provided TDM recommendation is considered *promising* if a pharmacokinetic TDM target is available or *viable* if a prospective TDM study has been conducted. Otherwise the recommendations are considered *exploratory*.

Future studies are needed to explore exposure-efficacy relationships for those oral anti-hormonal drugs which are classified as *exploratory* (anastrozole, enzalutamide and exemestane). In addition, prospective clinical studies should be performed to demonstrate the safety and feasibility of TDM for those oral anti-hormonal drugs which are classified as *promising* (abiraterone and letrozole). Ideally, for those drugs for which TDM is *viable* (tamoxifen), randomized controlled trials comparing TDM and fixed dosing with regard to relevant clinical efficacy endpoints such as progression free survival and overall survival would be needed. Then TDM could be fully integrated in clinical practice and become *standard of care*. However, given the large patient numbers needed to conduct adequately powered randomized controlled trials (RCTs), especially in the adjuvant setting, this will be a major challenge. Instead, future research could focus on prospective clinical studies strengthening the evidence of the PK target and confirming the safety and feasibility of TDM (52).

Currently, exposure-efficacy and exposure-toxicity analyses are pivotal parts of the drug development process (53). However, in the era in which most of the older oral anti-hormonal drugs were registered this was uncommon, resulting in a paucity of PK-PD data for these agents. Nonetheless, a PK target could be identified for four of the seven included agents. Overall, these targets amounted to 85% (±19%) of the mean population exposure (Figure 1). This is in accordance with the data for kinase inhibitors, as reported previously of 82% (±17%) (3,4). Thus, targeting the mean exposure, in the absence of exposure-efficacy analyses, generally leads to adequate concentrations.

While awaiting a TDM target based on exposure-response analyses, measuring drug concentrations and collecting data on efficacy and toxicity in routine patient care can provide us with valuable data on exposure-efficacy and exposure-toxicity relationships, comparable with safety monitoring as part of post-marketing surveillance.

In order to measure drug concentrations of oral anti-hormonal drugs, validated bio-analytical assays are needed. Our methods for the quantification of abiraterone, enzalutamide and endoxifen have been previously published (54–56). Also, methods on the quantification of anastrozole, letrozole and exemestane have been published by others (57–59). Currently, we are validating an assay for the simultaneous measurement of all mentioned oral anti-hormonal drugs, which makes this a suitable assay for TDM in clinical practice.

Apart from the apparent advantages of TDM, another potential advantage for anti-hormonal drugs could be monitoring of medication adherence, as it is has been shown that compliance decreases with long-term treatment (60). Also, TDM could help in detecting drug-drug interactions.
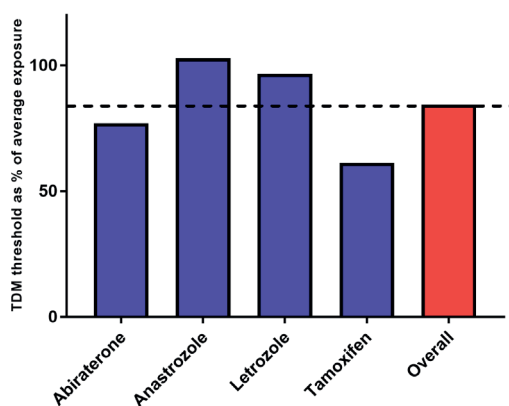
Figure 1. Proposed TDM-thresholds as percentage of the average exposure, on average the threshold amounted to 85% (± 19%) of the population average (indicated by the dotted line).

2.1

Since many of the anti-hormonal drugs have considerably long terminal elimination half-lives, PK sampling for TDM should be timed appropriately in order to ensure that steady state concentration has been achieved. In Table 1 the time until steady state concentration has been reached is specified for the different compounds.

In other disciplines than oncology, TDM is being broadly applied, for example in patients using antibiotics, antiretroviral drugs and immunosuppressants. An important difference, however, is the fact that in oncology we are reluctant to reduce the dose in case of high drug levels, since tumor progression is irreversible. For this reason, we advise to increase the dose in case of low drug concentrations, while reducing doses only in case of toxicity.

Conclusion

This review has summarized the clinical PK and PD properties of oral anti-hormonal drugs used in daily oncology practice and aimed to translate these data into practical guidelines for TDM.

For abiraterone, anastrozole and letrozole PK targets for TDM could be identified. Furthermore, for tamoxifen a prospective clinical trial has already demonstrated the feasibility of individualizing the dose based on the endoxifen concentration. However, prospective studies to correlate individualized dosing with tumor response or outcome parameters, such as progression free survival and overall survival, are lacking.

To conclude, the data presented in this review points towards clear opportunities to study and improve the treatment with oral anti-hormonal agents in oncology through TDM.

References

1.   Siegel RL, Miller KD, Jemal A. Cancer statistics. CA Cancer J Clin. 2016;66:7–30.

2.   Committee for Medicinal Products for Human Use (CHMP) European Medicines Agency. Abiraterone European Public Assessment Report . 2011 [Cited 2018 May]. Available from: http://www.ema.europa.eu/docs/en_GB/document_library/EPAR_-_Product_Information/human/002321/WC500112858.pdf

3.   Verheijen R, Yu H, Schellens J, Beijnen J, Steeghs N, Huitema A. Practical Recommendations for Therapeutic Drug Monitoring of Kinase Inhibitors in Oncology. Clin Pharmacol Ther. 2017;102:765–76.

4.   Yu H, Steeghs N, Nijenhuis C, Schellens J, Beijnen J, Huitema A. Practical guidelines for therapeutic drug monitoring of anticancer tyrosine kinase inhibitors: Focus on the pharmacokinetic targets. Clin Pharmacokinet. 2014;53:305–25.

5.   Beumer JH. Without therapeutic drug monitoring, there is no personalized cancer care. Clin Pharmacol Ther. 2013;93:228–30.

6.   Paci A, Veal G, Bardin C, Levêque D, Widmer N, Beijnen J, et al. Review of therapeutic drug monitoring of anticancer drugs part 1 - Cytotoxics. Eur J Cancer. 2014;50:2010–9.

7.   Widmer N, Bardin C, Chatelut E, Paci A, Beijnen J, Levêque D, et al. Review of therapeutic drug monitoring of anticancer drugs part two - Targeted therapies. Eur J Cancer. 2014;50:2020–36.

8.   Fox P, Balleine RL, Lee C, Gao B, Balakrishnar B, Menzies AM, et al. Dose escalation of tamoxifen in patients with low endoxifen level: Evidence for therapeutic drug monitoring - The TADE study. Clin Cancer Res. 2016;22:3164–71.

9.   De Wit D, Guchelaar HJ, Den Hartigh J, Gelderblom H, Van Erp NP. Individualized dosing of tyrosine kinase inhibitors: Are we there yet? Drug Discov Today. 2015;20:18–36.

10. Food and Drug Administration. Center for Drug Evaluation and Research. Abiraterone Clinical Pharmacology and Biopharmaceutics Review. 2011 [Cited 2018 May]. p1–183. Available from: http://www.accessdata.fda.gov/drugsatfda_docs/nda/2011/202379Orig1s000ClinPharmR.pdf

11. James ND, de Bono JS, Spears MR, Clarke NW, Mason MD, Dearnaley DP, et al. Abiraterone for Prostate Cancer Not Previously Treated with Hormone Therapy. N Engl J Med. 2017;377:338–51.

12. Chi KN, Spratlin J, Kollmannsberger C, North S, Pankras C, Gonzalez M, et al. Food effects on abiraterone pharmacokinetics in healthy subjects and patients with metastatic castration-resistant prostate cancer. J Clin Pharmacol. 2015;55:1406–14.

13. Carton E, Noe G, Huillard O, Golmard L, Giroux J, Cessot A, et al. Relation between plasma trough concentration of abiraterone and prostate-specific antigen response in metastatic castration-resistant prostate cancer patients. Eur J Cancer. 2017;72:54–61.

14. Stuyckens K, Saad F, Xu XS, Ryan CJ, Smith MR, Griffin TW, et al. Population Pharmacokinetic Analysis of Abiraterone in Chemotherapy-Naïve and Docetaxel-Treated Patients with Metastatic Castration-Resistant Prostate Cancer. Clin Pharmacokinet. 2014;53:1149–60.

15. Attard G, Reid AHM, Yap TA, Raynaud F, Dowsett M, Settatree S, et al. Phase I clinical trial of a selective inhibitor of CYP17, abiraterone acetate, confirms that castration-resistant prostate cancer commonly remains hormone driven. J Clin Oncol. 2008;26:4563–71.

16. Steven X, Charles X, Kim JR, Matthew S, Saad F, Griffin TW, et al. Modeling the Relationship Between Exposure to Abiraterone and Prostate-Specific Antigen Dynamics in Patients with Metastatic Castration-Resistant Prostate Cancer. Clin Pharmacokinet. 2017;56:55–63.

17. Li Z, Bishop AC, Alyamani M, Garcia JA, Dreicer R, Bunch D, et al. Conversion of abiraterone to D4A drives anti-tumour activity in prostate cancer. Nature. 2015;523:347–51.

18. Emamekhoo H, Li Z, Sharifi N. Clinical significance of D4A in prostate cancer therapy with abiraterone. Cell Cycle. 2015;14:3213–4.

19. Food and Drug Administration. Center for Drug Evaluation and Research. Enzalutamide Clinical Pharmacology and Biopharmaceutics Review. 2012 [Cited 2018 May]. Available from: http://www.accessdata.fda.gov/drugsatfda_docs/nda/2012/203415Orig1s000ClinPharmR.pdf

20. Gibbons JA, Ouatas T, Krauwinkel W, Ohtsu Y, van der Walt J-S, Beddo V, et al. Clinical Pharmacokinetic Studies of Enzalutamide. Clin Pharmacokinet. 2015;54:1043–55.

21. Scher HI, Anand A, Rathkopf D, Shelkey J, Morris MJ, Danila DC, et al. Antitumour activity of MDV3100 in castration-resistant prostate cancer: A phase 1-2 study. Lancet. 2010;375:1437–46.

22. Armstrong AJ, Saad F, Phung D, Dmuchowski C, Shore ND, Fizazi K, et al. Clinical outcomes and survival surrogacy studies of prostate-specific antigen declines following enzalutamide in men with metastatic castration-resistant prostate cancer previously treated with docetaxel. Cancer. 2017;123:2303–11.

23. de Vries Schultink AHM, Zwart W, Linn SC, Beijnen JH, Huitema ADR. Effects of Pharmacogenetics on the Pharmacokinetics and Pharmacodynamics of Tamoxifen. Clin Pharmacokinet. 2015;54:797–810.

24. Jager NGL, Rosing H, Schellens JHM, Linn SC, Beijnen JH. Tamoxifen dose and serum concentrations of tamoxifen and six of its metabolites in routine clinical outpatient care. Breast Cancer Res Treat. 2014;143:477–83.

25. Borges S, Desta Z, Li L, Skaar TC, Ward BA, Nguyen A, et al. Quantitative effect of CYP2D6 genotype and inhibitors on tamoxifen metabolism: Implication for optimization of breast cancer treatment. Clin Pharmacol Ther. 2006;80:61–74.

26. Mürdter TE, Schroth W, Bacchus-Gerybadze L, Winter S, Heinkele G, Simon W, et al. Activity Levels of Tamoxifen Metabolites at the Estrogen Receptor and the Impact of Genetic Polymorphisms of Phase I and II Enzymes on Their Concentration Levels in Plasma. Clin Pharmacol Ther. 2011;89:1–10.

27. Jager N, Koornstra R, Vincent A, van Schaik R, Huitema A, Korse C, et al. Hot flashes are not predictive for serum concentrations of tamoxifen and its metabolites. BMC Cancer. 2013;13.

28. Fox P, Balleine RL, Lee C, Gao B, Balakrishnar B, Menzies AM, et al. Dose Escalation of Tamoxifen in Patients with Low Endoxifen Level: Evidence for Therapeutic Drug Monitoring - The TADE Study. Clin Cancer Res. 2016;22:3164–71.

29. Madlensky L, Natarajan L, Tchu S, Pu M, Mortimer J, Flatt SW, et al. Tamoxifen Metabolite Concentrations, CYP2D6 Genotype, and Breast Cancer Outcomes. Clin Pharmacol Ther. 2011;89:718–25.

30. de Vries Schultink AHM, Alexi X, van Werkhoven E, Madlensky L, Natarajan L, Flatt SW, et al. An Antiestrogenic Activity Score for tamoxifen and its metabolites is associated with breast cancer outcome. Breast Cancer Res Treat. 2017;161:567–74.

31. Neven P, Jongen L, Lintermans A, Van Asten K, Blomme C, Lambrechts D, et al. Tamoxifen metabolism and efficacy in breast cancer- a prospective multicentre trial. Clin Cancer Res. 2018 [Cited 2018 May]. Available from: http://clincancerres.aacrjournals.org/lookup/doi/10.1158/1078-0432.CCR-17-3028

32. Jin Y, Desta Z, Stearns V, Ward B, Ho H, Lee KH, et al. CYP2D6 genotype, antidepressant use, and tamoxifen metabolism during adjuvant breast cancer treatment. J Natl Cancer Inst. 2005;97:30–9.

33. Dezentje V, Hartigh den J, Guchelaar H, Hessing T, Straaten van der T, Vletter-Bogaartz J. Association between endoxifen serum concentration and predicted CYP2D6 phenotype in a prospective cohort of patients with early-stage breast cancer. J Clin Oncol. 2011;15.

34. Food and Drug Administration. Center for Drug Evaluation and Research. Anastrozole Clinical Pharmacology and Biopharmaceutics Review. 2000 [Cited 2018 May]. Available from: https://www.accessdata.fda.gov/drugsatfda_docs/nda/2000/20-541S006_Arimidex_biopharmr.pdf

35. Food and Drug Administration. Center for Drug Evaluation and Research. Letrozole Clinical Pharmacology and Biopharmaceutics Review. 1997 [Cited 2018 May]. Available from: https://www.accessdata.fda.gov/drugsatfda_docs/nda/97/20726_FEMARA 2.5MG_BIOPHARMR.PDF

2.1

36. Food and Drug Administration. Center for Drug Evaluation and Research. Exemestane Clinical Pharmacology and Biopharmaceutics Review. 1999 [Cited 2018 May]. Available from: https://www.accessdata.fda.gov/drugsatfda_docs/nda/99/20-753_Aromasin_biopharmr_P1.pdf

37. Kelly CM, Buzdar AU. Anastrozole. Expert Opin Drug Saf. 2010;9:995–1003.

38. Pauwels S, Lintermans A, Neven P, Verhaeghe J, Jans I, Billen J, et al. Need for estradiol assays with a lower functional sensitivity in clinical studies examining postmenopausal women treated with aromatase inhibitors. J Clin Oncol. 2013;31:509.

39. Ketha H, Girtman A, Singh RJ. Estradiol assays - The path ahead. Steroids. 2015;99:39–44.

40. Ingle JN, Buzdar AU, Schaid DJ, Goetz MP, Batzler A, Robson ME, et al. Variation in anastrozole metabolism and pharmacodynamics in women with early breast cancer. Cancer Res. 2010;70:3278–86.

41. Folkerd EJ, Dixon JM, Renshaw L, A'Hern RP, Dowsett M. Suppression of plasma estrogen levels by letrozole and anastrozole is related to body mass index in patients with breast cancer. J Clin Oncol. 2012;30:2977–80.

42. Oberguggenberger A, Meraner V, Sztankay M, Beer B, Weigel G, Oberacher H, et al. Can we use gonadotropin plasma concentration as surrogate marker for BMI-related incomplete estrogen suppression in breast cancer patients receiving anastrozole? BMC Cancer. 2017;17:1–7.

43. Ingle JN, Kalari KR, Buzdar AU, Robson ME, Goetz MP, Desta Z, et al. Estrogens and their precursors in postmenopausal women with early breast cancer receiving anastrozole. Steroids. 2015;99:32–8.

44. Micheal F, Saranya S, Aparna N, Sridevi, Chithra R, Judith MP. Concepts of bioequivalence and it's impact on truncated area under curve (AUC) of drugs with long half life in point estimate and intra-subject variability. J Pharm Sci Res. 2012;4:1890–6.

45. Plourde P, Dyroff M, Dukes M. Arimidex: A potent and selective fourth-generation aromatase inhibitor. Breast Cancer Res Treat. 1994;30:103–11.

46. Geisler J, King N, Dowsett M, Ottestad L, Lundgren S, Walton P, et al. Influence of anastrozole (Arimidex), a selective, non-steroidal aromatase inhibitor, on in vivo aromatisation and plasma oestrogen levels in postmenopausal women with breast cancer. Br J Cancer. 1996;74:1286–91.

47. Mandic S, Kratzsch J, Mandic D, Debeljak Z, Lukic I, Horvat V, et al. Falsely elevated serum oestradiol due to exemestane therapy. Ann Clin Biochem. 2017;54:402-5.

48. Hertz DL, Kidwell KM, Seewald NJ, Gersch CL, Desta Z, Flockhart DA, et al. Polymorphisms in drug-metabolizing enzymes and steady-state exemestane concentration in postmenopausal patients with breast cancer. Pharmacogenomics J. 2017;17:521-7.

49. Hertz DL, Speth KA, Kidwell KM, Gersch CL, Desta Z, Storniolo AM, et al. Variable aromatase inhibitor plasma concentrations do not correlate with circulating estrogen concentrations in post-menopausal breast cancer patients. Breast Cancer Res Treat. 2017;1–10.

50. Wang Y, Chia Y, Nedelman J, Schran H, Mahon F, Molimard M. A therapeutic drug monitoring algorithm for refining the imatinib trough level obtained at different sampling times. Ther Drug Monit. 2009;31:579–84.

51. Desta Z, Kreutz Y, Nguyen AT, Li L, Skaar T, Kamdem LK, et al. Plasma letrozole concentrations in postmenopausal women with breast cancer are associated with CYP2A6 genetic variants, body mass index, and age. Clin Pharmacol Ther. 2011;90:693–700.

52. De Jonge ME, Huitema ADR, Schellens JHM, Rodenhuis S, Beijnen JH. Individualised cancer chemotherapy: Strategies and performance of prospective studies on therapeutic drug monitoring with dose adaptation: A review. Clin Pharmacokinet. 2005;44:147–73.

53. Food and Drug Administration. Center for Drug Evaluation and Research. Guidance for Industry: Exposure-Response Relationships - Study Design, Data Analysis and Regulatory Applications. 2003 [cited 2018 May. p. 1–25. Available from: https://www.fda.gov/media/71277/download

54. Van Nuland M, Hillebrand MJX, Rosing H, Schellens JHM, Beijnen JH. Development and Validation of an LC-MS/MS Method for the Simultaneous Quantification of Abiraterone, Enzalutamide, and Their Major Metabolites in Human Plasma. Ther Drug Monit. 2017;39:243–51.

55. De Krou S, Rosing H, Nuijen B, Schellens JHM, Beijnen JH. Fast and Adequate Liquid Chromatography– Tandem Mass Spectrometric Determination of Z-endoxifen Serum Levels for Therapeutic Drug Monitoring. Ther Drug Monit. 2017;39:132–7.

56. Van Nuland M, Rosing H, De Vries J, Ovaa H, Schellens JHM, Beijnen JH. An LC–MS/MS method for quantification of the active abiraterone metabolite Δ(4)-abiraterone (D4A) in human plasma. J Chromatogr B Anal Technol Biomed Life Sci. 2017;1068–1069:119–24.

57. Shao R, Yu L, Lou H, Ruan Z, Jiang B, Chen J. Development and validation of a rapid LC-MS/MS method to quantify letrozole in human plasma and its application to therapeutic drug monitoring. Biomed Chromatogr. 2016;30:632–7.

58. Yu J, He J, Zhang Y, Qin F, Xiong Z, Li F. Development of a liquid chromatography-tandem mass spectrometry method for determination of butoconazole nitrate in human plasma and its application to a pharmacokinetic study. Biomed Chromatogr. 2011;25:511–6.

59. Wang L-Z, Goh S-H, Wong AL-A, Thuya W-L, Lau J-YA, Wan S-C, et al. Validation of a rapid and sensitive LC-MS/MS method for determination of exemestane and its metabolites, 17beta-hydroxyexemestane and 17beta-hydroxyexemestane-17-O-beta-D-glucuronide: application to human pharmacokinetics study. PLoS One. 2015;10:e0118553.

60. Cardoso E, Csajka C, Schneider MP, Widmer N. Effect of Adherence on Pharmacokinetic/Pharmacodynamic Relationships of Oral Targeted Anticancer Drugs. Clin Pharmacokinet. 2017;1–6.

61. Gervasini G, Jara C, Olier C, Romero N, Martinez R, Carrillo JA. Polymorphisms in ABCB1 and CYP19A1 genes affect anastrozole plasma concentrations and clinical outcomes in postmenopausal breast cancer patients. Br J Clin Pharmacol. 2017;83:562–71.

62. Dowsett M, Cuzick J, Howell A, Jackson I, ATAC Trialists' Group. Pharmacokinetics of anastrozole and tamoxifen alone, and in combination, during adjuvant endocrine therapy for early breast cancer in postmenopausal women: A sub-protocol of the "Arimidex™ and tamoxifen alone or in combination" (ATAC) trial. Br J Cancer. 2001;85:317–24.

63. Hubalek M, Oberguggenberger A, Beer B, Meraner V, Sztankay M, Oberacher H, et al. Does obesity interfere with anastrozole treatment? Positive association between body mass index and anastrozole plasma levels. Clin Breast Cancer. 2014;14:291–6.

64. Committee for Medicinal Products for Human Use (CHMP) European Medicines Agency. Public Assessment Report Scientific discussion Exemestane. 2010 [Cited 2018 May]. Available from: https://db.cbg-meb.nl/Pars/h104327.pdf%0A

65. Bisagni G, Cocconi G, Scaglione F, Fraschini F, Pfister C, Trunet PF. Letrozole, a new oral non-steroidal aromatase inhibitor in treating postmenopausal patients with advanced breast cancer. A pilot study. Ann Oncol. 1996;:99–102.

66. Binkhorst L, Kloth JSL, de Wit AS, de Bruijn P, Lam MH, Chaves I, et al. Circadian variation in tamoxifen pharmacokinetics in mice and breast cancer patients. Breast Cancer Res Treat. 2015;152:119–28.

67. Food and Drug Administration. Center for Drug Evaluation and Research. Abiraterone Clinical Pharmacology and Biopharmaceutics Review. 2010 [Cited 2018 May]. Available from: https://www.accessdata.fda.gov/drugsatfda_docs/nda/2011/202379Orig1s000ClinPharmR.pdf

2.1

Exposure-response assessments of enzalutamide and its major metabolites in real-world metastatic castration-resistant prostate cancer patients

Merel van Nuland
Andries M. Bergman
Hilde Rosing
Niels de Vries
Alwin D.R. Huitema
Jos H. Beijnen

Abstract

Background

Enzalutamide is an oral agent for the treatment of metastatic castration-resistant prostate cancer (mCRPC). *N*-desmethyl enzalutamide is its active metabolite, which has clinically relevant anti-androgen capacities similar to enzalutamide, and carboxylic acid enzalutamide is an inactive metabolite. The aim of our study was to investigate the relationship between enzalutamide and *N*-desmethyl enzalutamide exposure and treatment response in a real-world patient cohort.

Patients and methods

Patients with mCRPC, treated with enzalutamide 160 mg daily, were included in this trial if at least one plasma concentration of enzalutamide was collected. Plasma concentrations, determined with liquid-chromatography tandem mass spectrometry (LC-MS/MS), were compared between responders and non-responders. Three clinical end points were evaluated separately in this study; prostate-specific antigen (PSA) independent progression-free survival (PFS), time to PSA progression (TTPP) and rate of PSA response (defined as ≥50% decrease in PSA level from baseline). Enzalutamide toxicity was defined as discontinuation due to adverse events, dose reductions due to adverse events, or temporary treatment interruption. For these analyses, plasma concentrations of enzalutamide and its active metabolite *N*-desmethyl enzalutamide were divided into quartiles.

Results

Sixty-five patients were included in this study, with a mean ± SD plasma concentrations of 11.2 ± 2.8 μg/mL for enzalutamide, 9.9 ± 2.9 μg/mL for *N*-desmethyl enzalutamide and 6.1 ± 4.3 μg/mL for carboxylic acid enzalutamide. Plasma concentrations were not significantly different in the responder (*n*=38) versus non-responder (*n*=27) group for enzalutamide (11.5 vs 10.6 μg/mL; *p*=0.20), *N*-desmethyl enzalutamide (10.1 vs 9.6 μg/mL; *p*=0.48), or carboxylic acid enzalutamide (6.5 vs 5.5 μg/mL; *p*=0.34). Univariate and multivariate analyses did not show a relationship between plasma concentrations and PSA independent PFS, TTPP or toxicity.

Conclusions

This study confirms that enzalutamide plasma concentrations are not related to PSA-independent PFS, TTPP, or toxicity in patients with mCRPC, and demonstrated that plasma concentrations of its major metabolites were also not associated with treatment response. Based on these findings, there is no role for therapeutic drug monitoring of enzalutamide in patients with mCRPC in daily practice.

Introduction

Enzalutamide is a potent inhibitor of the androgen receptor by blocking multiple steps in the androgen signaling pathway: it competitively inhibits androgen binding to the androgen receptor, prevents nuclear translocation of the androgen receptor and inhibits receptor association with DNA (1). Enzalutamide was approved for the treatment of metastatic castration-resistant prostate cancer (mCRPC), as it improves overall survival (OS) and progression-free survival (PFS) in this patient population (2,3).

After oral ingestion, enzalutamide is converted into its major metabolites *N*-desmethyl enzalutamide and carboxylic acid enzalutamide by CYP3A4/5 and CYP2C8, respectively (1). *N*-desmethyl enzalutamide has clinically relevant anti-androgen capacities similar to enzalutamide while carboxylic acid enzalutamide is inactive. Enzalutamide is administered orally once daily (QD) in a fixed dose of 160 mg, and is well tolerated in clinical practice (4). Mean ± SD steady-state trough concentrations (C_{min}) at this approved dose are 11.4 ± 3.0 μg/mL for enzalutamide, 13.0 ± 3.8 μg/mL for *N*-desmethyl enzalutamide and 8.4 ± 6.8 μg/mL for carboxylic acid enzalutamide (5). In a phase 3 pivotal trial, no significant enzalutamide exposure-response relationship was identified for the primary efficacy endpoint OS, as all exposure quartiles performed uniformly better relative to placebo ($p \leq 0.0001$) (1). Unfortunately, measurement of the active metabolite *N*-desmethyl enzalutamide concentration was not included in this study; however, due to its similar potency to enzalutamide and high abundance, an exposure-response analysis would be justified as well. In a phase 1 trial, positron emission tomography (PET) imaging with 16β-[18]F-5α-dihydrotestosterone showed higher androgen receptor binding at 150 mg enzalutamide QD compared to 60 mg QD, with corresponding C_{min} concentrations of 11.4 μg/mL and 5.0 μg/mL, respectively. At doses above 150 mg QD, plasma concentrations did not further increase, suggesting a concentration plateau at ~ 11 μg/mL (6). Based on these findings, our research group previously suggested a C_{min} of 5.0 μg/mL as a target for exposure to enzalutamide in a therapeutic drug monitoring (TDM) setting (7).

Although the pivotal trial suggests that there is no exposure-response relationship for enzalutamide (1), there is lack of real-world data from daily clinical practice to underscore these findings. Obtaining real-life data is relevant in medical research because patients from clinical trials may not fully reflect the patient population, given the clear set of inclusion and exclusion criteria such as having co-morbidities or the use of concomitant medication. Furthermore, the pivotal trial did not include exposure to the major metabolites in these analyses. Given the limited data from clinical practice, to our knowledge, we are the first to investigate the exposure-response relationship of enzalutamide and its major metabolites. Specifically, the objective of our study was to investigate the relationship between enzalutamide and *N*-desmethyl enzalutamide exposure and treatment response in a real-world cohort of patients with mCRPC.

2.2

Materials and methods

Patients and sampling
This retrospective, observational, pharmacokinetic study was performed in the outpatient clinic at the Antoni van Leeuwenhoek/Netherlands Cancer Institute, Amsterdam. Patients with mCRPC who were treated with enzalutamide 160 mg once daily and had at least one steady-state enzalutamide plasma concentration between May 2015 and June 2018 were included in the study. As part of routine clinical care, dipotassium ethylenediaminetetraacetic acid samples were collected for pharmacokinetic monitoring at each hospital visit from these patients. The frequency of the outpatient visits and blood draws were at the discretion of the treating physician. Data from routine clinical care were used retrospectively, as authorized by the Institute, and the following clinical characteristics were collected from medical records: demographic data, medical history, enzalutamide dose, treatment duration, reason for discontinuation, time of prostate-specific antigen (PSA) independent progression and time of PSA progression, concomitant medication and PSA levels. Furthermore, testosterone and androstenedione levels were quantified using a validated liquid chromatography-tandem mass spectrometry (LC-MS/MS) assay (8). The extent of adherence was not available due to the retrospective character of this analysis, however, plasma levels may serve as a potential indicator if compliance.

Pharmacokinetics
Blood samples were collected as part of routine clinical care. The date and time of the last drug intake and the time of blood withdrawal were recorded. Due to the long half-life of enzalutamide (5.8 days), steady-state was considered to be reached after at least 1 month of enzalutamide treatment (1). Enzalutamide and its metabolites were measured using a validated LC-MS/MS method (9). In short, 50 µL of plasma was prepared using protein precipitation. Analytes were quantified using a Triple Quad 6500 (Sciex, Framingham, MA, USA). The lower limit of quantification (LLOQ) was 5 ng/mL for enzalutamide and carboxylic acid enzalutamide, and 10 ng/mL for *N*-desmethyl enzalutamide, Intra-assay and inter-assay variabilities were within ±15% for all analytes. Measured plasma concentrations, collected at random time points during a dosing interval, were used in the further analyses without correction for time after intake, as the difference between maximal and minimal concentrations during a dosing interval at steady-state is negligible due to the long half-life of enzalutamide and its metabolites. Samples taken before steady-state or more than 24 hours after the last dose were excluded from further analysis.

Outcome measures
Three clinical end points were evaluated separately in this study; PSA independent progression-free survival (PFS), time to PSA progression (TTPP) and rate of PSA response. PFS was defined as the time from treatment start to the first event of

progression, being either radiographic progression, symptomatic progression (start of radiotherapy, samarium treatment, increase of analgesic dose, or an Eastern Cooperative Oncology Group (ECOG)/World Health Organization (WHO) Performance Status increase of at least 2, onset of next treatment or death from any cause. Radiographic progression was evaluated according to modified Response Evaluation Criteria in Solid Tumors (RECIST version 1.1) (10). TTPP was defined as the time from treatment start to a 25% or greater PSA increase from the nadir, with an absolute increase in PSA levels of at least 2 ng/mL (10). PSA response was defined as the rate of ≥50% decreases in PSA levels from baseline, according to the Prostate Cancer Working Group 3 criteria (11,12). Toxicity was defined as discontinuation due to adverse events, dose reductions due to adverse events or temporary treatment interruption.

Statistical analysis

For the purpose of exposure-response analyses, the mean of all available enzalutamide and metabolite levels per patient were used as parameter for exposure. Univariate analysis of PSA response and plasma concentrations involved two-sided t-tests. For progression-free survival and TTPP analyses, plasma concentrations were divided into quartiles. PFS functions were estimated using the Kaplan-Meier method and predictive factors were assessed using the univariate model (log-rank test). All statistical analyses were performed by using R statistical software, version 3.6.0, package 'survival' (R Foundation for Statistical Computing, Vienna, Austria). In multivariate analysis, age, ECOG/WHO performance status, previous lines of treatment, prior treatment with docetaxel and testosterone and androstenedione levels were included as covariates (1). A post hoc effect size analysis was conducted, comparing low versus high C_{min} with 80% power using a two-sided significance level of 0.05 and log-rank test with equal groups (n=31 per group). With our data, we would be able to detect a 30% increase in PFS with a hazard ratio of 0.42.

Results

Evaluable patients

From May 2015 to June 2018, 65 patients were included in this study. Patient characteristics are presented in Table 1. The median duration of treatment was 9.1 months (ranging from 0.8 to 35 months). All patients received enzalutamide in combination with a goserelin 10.8 mg subcutaneous depot injection every 12 weeks. Measured testosterone levels were below the castration level of 0.50 ng/mL, with a mean ± SD value of 0.10 ± 0.08 ng/mL. Mean ± SD levels of androstenedione were 0.31 ± 0.25 ng/mL. At data cut-off, 8 patients were still on treatment with enzalutamide. Three patients stopped treatment due to adverse events. No relevant CYP-inhibiting or inducing concomitant medication was used during this treatment period.

2.2

Table 1. Patient characteristics.

Patient characteristics	
Number of patients	65
Number of samples	235
Samples per patient	3 (1-11)
Age (yrs)	69 (49-99)
Weight (kg)	91 (59-147)
ECOG/WHO performance status	
0	19 (29)
1	35 (54)
2	7 (11)
NR	4 (6)
Previous lines of therapy	
0	32 (49)
1	20 (31)
2	9 (14)
3	2 (3)
4	2 (3)
Previous chemotherapy	30 (46)
Plasma concentrations (µg/mL): 　Enzalutamide 　*N*-desmethyl enzalutamide 　Carboxylic acid enzalutamide	 11 (3.3-18) 9.9 (3.1-17) 6.1 (1.1-22)
Patients with enzalutamide concentration < 5 µg/mL (n (%))	1 (1.5%)
Testosterone levels (ng/mL)	0.10 (<0.010*-0.50)
Androstenedione levels (ng/mL)	0.31 (<0.010*-1.5)

Abbreviations: NR = not reported, ECOG/WHO = Eastern Cooperative Oncology Group/World Health Organization
Data are mean (range) values or no. (%) of patients unless otherwise specified.
* Data points below the lower limit of quantification of this bioanalytical method.

Pharmacokinetics

In total, 235 samples were gathered, with a mean of 3 samples (range 1-11) per patient. Mean ± SD plasma concentrations were 11.2 ± 2.8 µg/mL for enzalutamide, 9.9 ± 2.9 µg/mL for *N*-desmethyl enzalutamide and 6.1 ± 4.3 µg/mL for carboxylic acid enzalutamide. Interpatient variability (coefficient of variation; CV%) of mean plasma concentrations was of 28% for enzalutamide, 31% for *N*-desmethyl enzalutamide and 67% for carboxylic acid enzalutamide. The mean intrapatient variability (CV%) was 18% for enzalutamide, 19% for *N*-desmethyl enzalutamide and 44% for carboxylic acid enzalutamide.

An overview of the distribution of mean enzalutamide, *N*-desmethyl enzalutamide and carboxylic acid enzalutamide concentrations per patient is provided in Figure 1. One patient had an enzalutamide concentration below the proposed target of 5.0 µg/mL. This patient also had the lowest *N*-desmethyl enzalutamide concentration of 3.1 µg/mL.
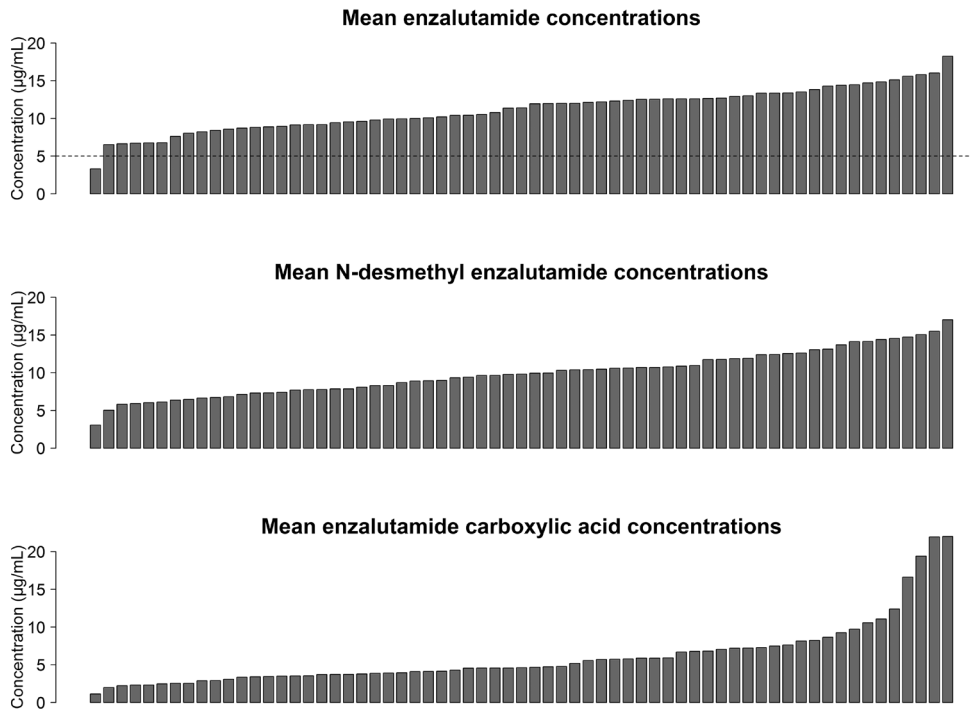
Figure 1. Distribution of plasma concentrations of enzalutamide (top panel), *N*-desmethyl enzalutamide (middle panel), and enzalutamide carboxylic acid (bottom panel) for the 65 study patients. The dotted line in the top panel represents the proposed target of 5.0 µg/mL for enzalutamide.

This patient received a reduced dose of 80 mg QD due to adverse events fatigue and dyspnea. Two more patients received a reduced dose of 80 and 120 mg QD due to adverse events (i.e. fatigue, nausea, loss of appetite and abdominal pain). While receiving treatment, these doses were increased back to the starting dose of 160 mg once daily since the drug became well tolerated by both patients. Mean enzalutamide plasma concentrations of these two patients at reduced dose were 5.8 and 9.2 µg/mL compared to 11.4 and 15.2 µg/mL at 160 mg QD, respectively. Linear regression indicated that patients who were older had higher *N*-desmethyl enzalutamide and carboxylic acid enzalutamide concentrations (p=0.046 and p=0.00032).

Exposure-response analyses
At time of analysis, the data from 62 patients were considered for calculation of PFS and TTPP. Three patients were excluded from survival analysis, as these patients discontinued treatment due to adverse events. Patients were divided into quartiles based on plasma concentrations of the active substances enzalutamide and *N*-desmethyl enzalutamide, and progression-free survival analyses were performed using the data from these groups.

For PSA independent PFS, the data from 62 patients and 54 events (87% of patients) were considered, with 36 radiographic progressions, 12 symptomatic progressions, 1 onset of next treatment and 5 deaths. Eight patients were still on treatment. There was no significant difference in the four quartiles regarding PSA independent PFS for enzalutamide (14 vs 11 vs 7.3 vs 13 months, p=0.44) and N-desmethyl enzalutamide (8.1 vs 13 vs 8.2 vs 13 months, p=0.33), as depicted in Figure 2 and 3, respectively. Furthermore, the sum of enzalutamide and N-desmethyl enzalutamide plasma concentrations was also not associated with PSA independent PFS (12 vs 8.4 vs 9.2 vs 12 months, p=0.40) (Figure 4). In univariate analysis, plasma concentrations of enzalutamide, N-desmethyl enzalutamide and a combination of both were not related to PFS. Similarly, no evidence to support a relationship between concentration levels of enzalutamide, N-desmethyl enzalutamide and a combination of both with PSA independent PFS was found; the hazard ratios (HRs) for enzalutamide, N-desmethyl enzalutamide and the combination of these two were 1.2 (95% confidence interval (CI), 0.90–1.5), 1.1 (95% CI, 0.81-1.4) and 1.2 (95% CI, 0.89-1.6) per quartile change in concentration, respectively.

For TTPP analysis, 62 patients were included with 53 events (85% of patients) of PSA progression. Six patients were still on treatment, 1 patient died prior to PSA progression, and 2 patients did not show PSA progression but discontinued treatment due to radiographic progression. These patients were censored in the survival analysis, as information about their survival was incomplete. Similar to PSA independent PFS, TTPP was no significantly different in the four quartiles for enzalutamide (6.7 vs 7.2 vs 4.8 vs 8.7 months, p=0.39), N-desmethyl enzalutamide (4.9 vs 8.0 vs 5.6 vs 7.2 months, p=0.41) and the sum of enzalutamide and N-desmethyl enzalutamide plasma concentrations (6.7 vs 7.6 vs 6.6 vs 8.7 months, p=0.50), as depicted in Figures 2, 3, and 4, respectively. In multivariate analysis, plasma concentrations were not related to TTPP, with HRs for enzalutamide, N-desmethyl enzalutamide and the combination of these two being 1.1 (95% confidence interval (CI), 0.86–1.5), 1.0 (95% CI, 0.76-1.4) and 1.1 (95% CI, 0.85-1.5) per quartile change in concentration, respectively.

Among 65 patients, 38 patients were PSA responders (58%). Figure 5 shows the relationship between plasma concentrations of enzalutamide, N-desmethyl enzalutamide and carboxylic acid enzalutamide, and PSA response. Plasma concentrations were not significantly different in the responder and non-responder group for enzalutamide (11.5 vs 10.6 µg/mL; p=0.20), N-desmethyl enzalutamide (10.1 vs 9.6 µg/mL; p=0.48), and carboxylic acid enzalutamide (6.5 vs 5.5 µg/mL; p=0.34). In addition, the number of previous lines of treatment, prior treatment with docetaxel and testosterone and androstenedione levels were included in multivariate analyses, which did not show an association between plasma concentrations of enzalutamide, N-desmethyl enzalutamide and carboxylic acid and PSA response (p=0.392, p=0.953 and p=0.208, respectively). Quartiles of enzalutamide and metabolite concentration levels and PSA response rates are presented in Table 2.

PSA independent PFS

No. at risk

Q1:	15	9	4	1	0	0
Q2:	16	8	3	2	1	0
Q3:	16	6	3	1	1	0
Q4:	15	9	4	4	1	0

Time To PSA Progression

No. at risk

Q1:	15	5	0	0	0	0
Q2:	16	5	1	1	1	0
Q3:	16	3	1	1	1	0
Q4:	15	7	3	3	1	0
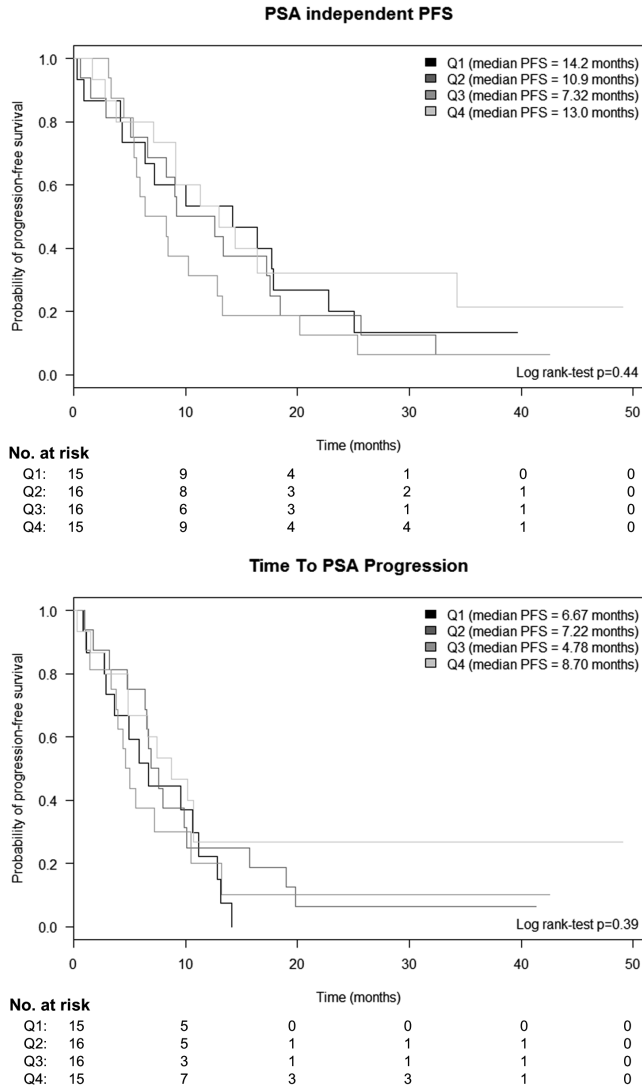
Figure 2. Kaplan-Meier plots of progression-free survival (PFS) for the 62 patients with metastatic castration-resistant prostate cancer included in the survival analysis for each enzalutamide concentration quartile (Q1–Q4). Prostate-specific antigen (PSA)-independent PFS is shown in the upper panel, and time to PSA progression is shown in the lower panel.
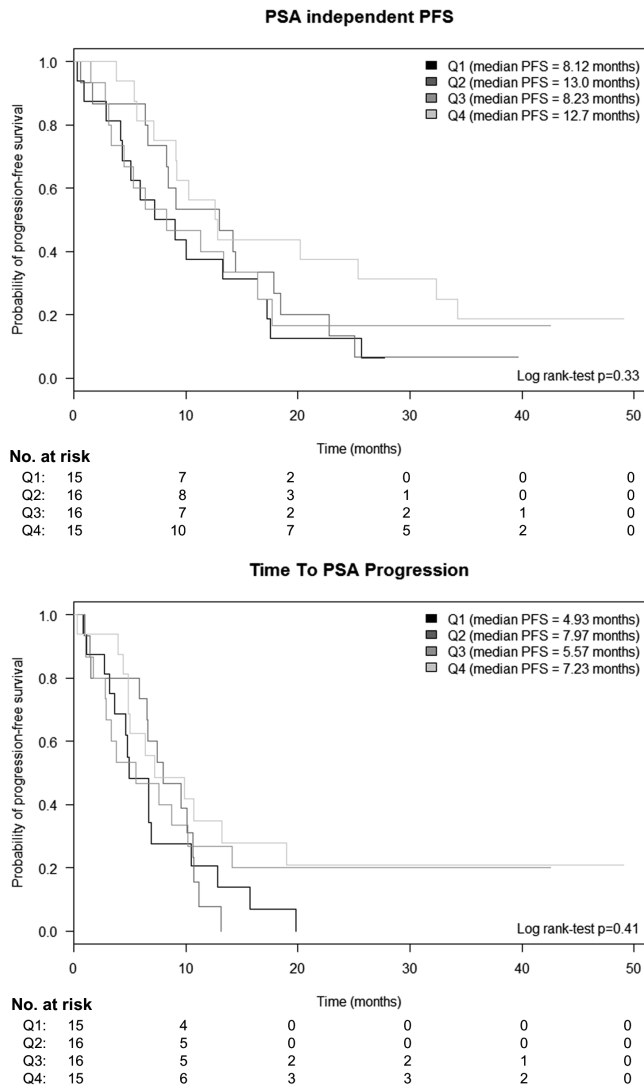
Figure 3. Kaplan-Meier plots of progression-free survival (PFS) for the 62 patients with metastatic castration-resistant prostate cancer in the survival analysis for each *N*-desmethyl enzalutamide concentration quartile (Q1–Q4). Prostate-specific antigen (PSA)-independent PFS is shown in the upper panel, and time to PSA progression is shown in the lower panel.

PSA independent PFS

No. at risk

Q1:	15	9	4	1	0	0
Q2:	16	6	1	0	0	0
Q3:	16	7	3	2	2	0
Q4:	15	10	6	5	1	0

2.2

Time To PSA Progression

No. at risk

Q1:	15	4	0	0	0	0
Q2:	16	5	0	0	0	0
Q3:	16	5	2	2	2	0
Q4:	15	6	3	3	1	0

Figure 4. Kaplan-Meier plots of progression-free survival (PFS) for the 62 patients with metastatic castration-resistant prostate cancer in the survival analysis for each quartile (Q1–Q4) of the sum of enzalutamide and *N*-desmethyl enzalutamide concentrations. Prostate-specific antigen (PSA)-independent PFS is shown in the upper panel, and time to PSA progression is shown in the lower panel.
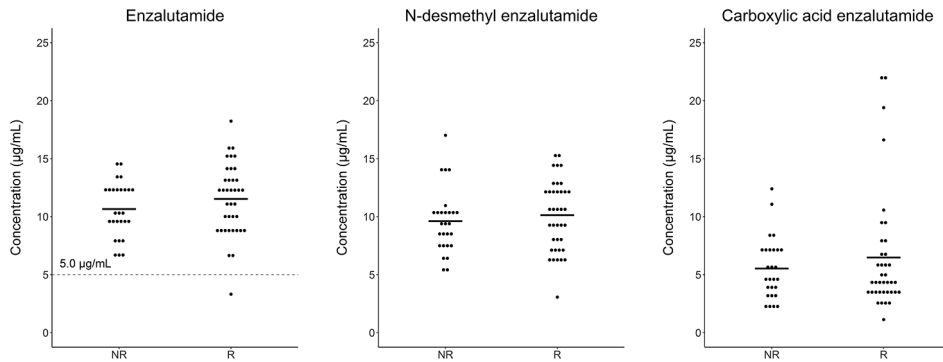
Figure 5. Relationship between prostate-specific antigen response and mean plasma concentrations of enzalutamide (left panel), *N*-desmethyl enzalutamide (middle panel), and carboxylic acid enzalutamide (right panel) in the 38 responders (R) versus the 27 nonresponders (NR). The horizontal black line represents the mean in each group, and the dotted line in the left panel represents the proposed target for enzalutamide. Mean plasma concentrations were not significantly different in the responder versus nonresponder groups for enzalutamide (11.5 vs 10.6 µg/mL, p=0.20), *N*-desmethyl enzalutamide (10.1 vs 9.6 µg/mL, p=0.48), and carboxylic acid enzalutamide (6.5 vs 5.5 µg/mL, p=0.34).

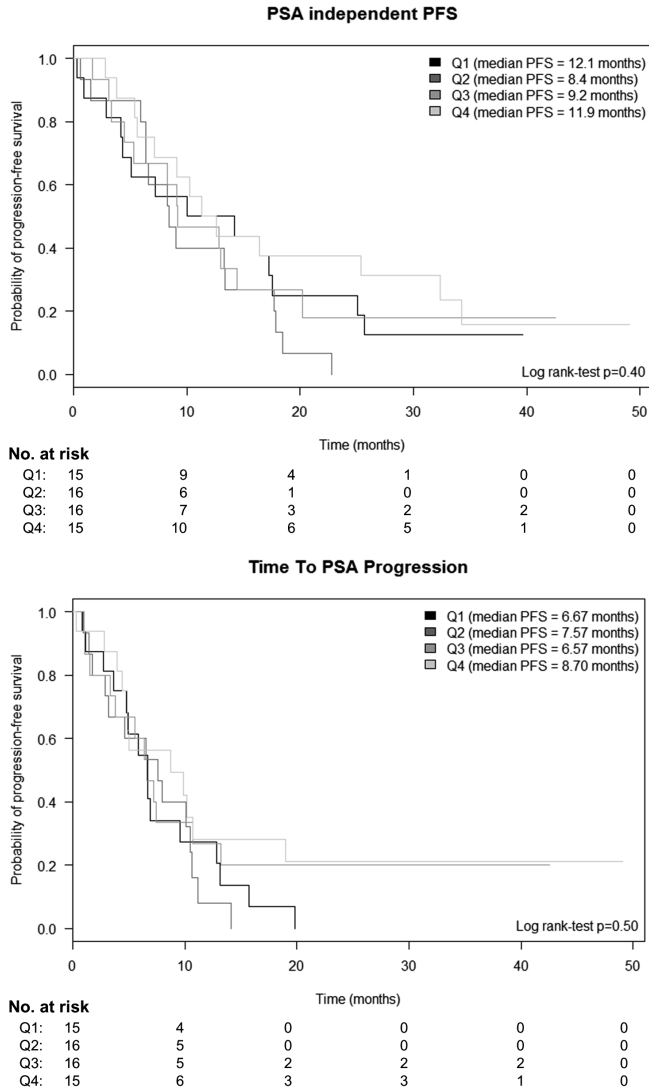Of 65 included patients, 3 patients discontinued treatment due to adverse events, 3 patients received a dose reduction due to adverse events and 1 patients interrupted enzalutamide treatment temporarily due to adverse events. Reasons for discontinuation were fatigue, nausea, abdominal pain, loss of appetite and dyspnea. Mean enzalutamide Cmin was 11.2 µg/mL in those who discontinued treatment due to adverse events, and also 11.2 µg/mL in the group of participants without adverse events (*p*=0.99). Furthermore, *N*-desmethyl enzalutamide concentrations were 9.3 and 10.0 µg/mL in patients whom experience adverse events compared with those who did not (*p*=0.67).

Discussion

In this study we investigated the enzalutamide plasma concentrations in patients treated at our outpatient clinic to gather data from daily clinical practice. To our knowledge, this is the first study to evaluate the relationship between exposure and response to enzalutamide and its metabolites in a real-world clinical dataset. Mean plasma concentrations of enzalutamide and its metabolites were in line with reported mean plasma concentrations, being 11.4 µg/mL for enzalutamide, 13.0 µg/mL for *N*-desmethyl enzalutamide and 8.4 µg/mL for carboxylic acid enzalutamide (1). Exposure to enzalutamide and its metabolites was not associated with PSA independent PFS, TTPP or PSA response. These data confirm previous findings from the pivotal phase 3 study and confirm our findings of no exposure-response relationship visible in clinical practice for enzalutamide and its metabolites. Furthermore, only one patient had a plasma concentration below the proposed target of 5.0 µg/mL and this patient

Table 2. Mean plasma concentrations of enzalutamide and its metabolites by quartile and prostate specific antigen (PSA)-response rate in 65 study patients.

	Mean plasma concentration (µg/mL)	Range (µg/mL)	PSA response rate (%)
Enzalutamide			
Q1	7.6	3.3-9.2	62.5
Q2	10.0	9.2-11.4	43.8
Q3	12.3	11.4-12.7	50.0
Q4	14.5	12.9-18.2	76.5
N-desmethyl enzalutamide			
Q1	6.4	3.1-7.7	62.5
Q2	8.7	7.8-9.8	50.0
Q3	10.6	9.8-11.8	43.8
Q4	13.7	11.9-17.0	76.5
Carboxylic acid enzalutamide			
Q1	2.7	1.1-3.5	56.3
Q2	4.1	3.6-4.6	68.8
Q3	5.7	4.6-7.1	56.3
Q4	11.5	7.2-22.0	52.9

Abbreviations: PSA = prostate-specific antigen, Q = quartile

2.2

responded well to treatment with a PSA independent PFS of 28 months. When combining enzalutamide and for N-desmethyl enzalutamide plasma concentrations, the difference in PFS between groups diminishes, suggesting that the total level of active substance is similar in all quartiles. The PFS analyses in this study included PSA-independent PFS and TTPP and did not focus on OS, because included patients received multiple and variable lines of treatment after cessation of enzalutamide. These different treatment regimens influence OS and therefore, OS is not solely related to enzalutamide treatment. Both PSA independent PFS and TTPP were included in our analyses, because PSA as a marker for progression is still being used as an indicator of disease activity, but does not fully reflect clinically relevant progression.

Enzalutamide and metabolite concentrations were divided into quartiles for the PSA-independent PFS and TTPP analysis, instead of studying a linear relationship between concentrations and PFS. This approach was chosen because of the expected type of exposure-response relationship, based on receptor occupancy. Enzalutamide and N-desmethyl enzalutamide show high affinity for the androgen receptor in vitro LNCaP cell lines, with inhibition concentration 50% (IC50) values of 0.0098 µg/mL and 0.079 µg/mL, respectively. Given that the plasma protein binding of enzalutamide is about 98% and of N-desmethyl enzalutamide is about 95%, plasma concentrations to achieve these IC50 values should be 0.49 and 1.6 µg/mL, respectively. Measured plasma

concentrations were far above these IC50 values, suggesting adequate inhibition of the androgen receptor. Based on this information, an exposure-response relationship in the measured concentration range was not anticipated, however, it should be of note that plasma concentrations are a surrogate marker for concentrations at the site of action.

Testosterone and androstenedione levels were measured in this study and showed no relationship with PSA independent PFS, TTPP or PSA response. Previous studies have shown that higher testosterone levels at baseline are associated with longer PFS in enzalutamide treated mCRPC patients (13,14). In our study, testosterone levels were determined at steady-state and no baseline values were available. All patients had adequate androgen suppression below the castration level of 0.5 ng/mL.

Our analysis has some limitations, such as the Antoni van Leeuwenhoek/Netherlands Cancer Institute being a tertiary referral center. Patients visiting this hospital are referred for specialized treatment, which may influence outcome. Second, due to the retrospective character of this analysis, there were limitations in identifying a sufficient number of patients for this study. The fact that we did not find statistically significant differences does not imply that these would not be found with a larger number of patients. However, our results fit with previously published data and the conclusion that enzalutamide does not seem suitable for TDM. Last, measured plasma concentrations at random time points during a dosing interval were used instead of actual C_{min}. Yet, despite these limitations, to our knowledge, this is the first pharmacokinetic study that reports the results of an enzalutamide exposure-response and exposure-toxicity assessment in a real-world cohort of patients with mCRPC.

Due to the lack of a relationship between exposure and response in the measured concentration range, we found that there is not sufficient evidence to implement TDM in daily practice. Requirements for drugs to be suitable for TDM include the absence of a measureable biomarker, the availability of a validated bioanalytical method, significant interpatient variability and low intra-patient variability, a narrow therapeutic range, long-term therapy and an exposure-response relationship (15). Although enzalutamide meets several of these requirements, such as the absence of a measurable biomarker and the availability of a validated LC-MS/MS assay for quantification, enzalutamide has only limited inter-patient variability (28%), has a broad therapeutic window and shows no exposure-response relationship at measured concentrations. Taken these data and our findings into account, we conclude that enzalutamide is not a suitable drug for TDM in daily practice, with the exception of some specific situations, such as monitoring compliance, drug-drug interactions or exposure in patients with impaired organ functions, such as end-stage renal disease (16).

Conclusion

In this observational study in a "real-world" population of patients with mCRPC, we found no significant relationship between exposure to enzalutamide or its major metabolites *N*-desmethyl enzalutamide and carboxylic acid enzalutamide and response. Furthermore, PSA independent PFS and TTPP was not significantly different in quartiles based on plasma drug levels. This study suggests that enzalutamide is not a suitable drug for TDM purpose in daily practice, as plasma concentrations do not show an association with treatment response in the measured concentration range.

2.2

References

1. US Food and Drug Administration. Clinical Pharmacology and Biopharmaceutics Review: Xtandi (Enzalutamide). Silver Spring (MD). 2012 [cited 2019 Jan]. p. 1–75. Available from: https://www.accessdata.fda.gov/drugsatfda_docs/nda/2012/203415Orig1s000ClinPharmR.pdf

2. Beer TM, Armstrong AJ, Rathkopf DE, Loriot Y, Sternberg CN, Higano CS, et al. Enzalutamide in metastatic prostate cancer before chemotherapy. N Engl J Med. 2014;371:424–33.

3. Scher HI, Fizazi K, Saad F, Taplin M-E, Sternberg CN, Miller K, et al. Increased survival with enzalutamide in prostate cancer after chemotherapy. N Engl J Med. 2012;367:1187–97.

4. US Food and Drug Administration. Prescribing information: Xtandi (enzalutamide) . Silver Spring (MD). 2012 [cited 2018 Jun]. p. 1–16. Available from: https://www.accessdata.fda.gov/drugsatfda_docs/label/2012/203415lbl.pdf

5. Gibbons JA, Ouatas T, Krauwinkel W, Ohtsu Y, van der Walt J-S, Beddo V, et al. Clinical Pharmacokinetic Studies of Enzalutamide. Clin Pharmacokinet. 2015;54:1043–55.

6. Scher HI, Anand A, Rathkopf D, Shelkey J, Morris MJ, Danila DC, et al. Antitumour activity of MDV3100 in castration-resistant prostate cancer: A phase 1-2 study. Lancet. 2010;375:1437–46.

7. Groenland SL, van Nuland M, Verheijen RB, Schellens JHM, Beijnen JH, Huitema ADR, et al. Therapeutic Drug Monitoring of Oral Anti-Hormonal Drugs in Oncology. Clin Pharmacokinet. 2019;58:299–308.

8. van Nuland M, Venekamp N, Wouters WME, van Rossum HH, Rosing H, Beijnen JH. LC–MS/MS assay for the quantification of testosterone, dihydrotestosterone, androstenedione, cortisol and prednisone in plasma from castrated prostate cancer patients treated with abiraterone acetate or enzalutamide. J Pharm Biomed Anal. 2019;170:161–8.

9. van Nuland M, Hillebrand MJ., Rosing H, Schellens JHM, Beijnen JH. Development and validation of an LC-MS/MS method for the simultaneous quantification of abiraterone, enzalutamide, and their major metabolites in human plasma. Ther Drug Monit. 2017;39:243–51.

10. Therasse P, Arbuck SG, Eisenhauer EA, Wanders J, Kaplan RS, Rubinstein L, et al. New Guidelines to Evaluate the Response to Treatment in Solid Tumors. JNCI J Natl Cancer Inst. 2000;92:205–16.

11. Scher HI, Morris MJ, Stadler WM, Higano CS, Halabi S, Smith MR, et al. The Prostate Cancer Working Group 3 (PCWG3) consensus for trials in castration-resistant prostate cancer (CRPC). J Clin Oncol. 2015;33:5000.

12. Scher HI, Halabi S, Tannock I, Morris M, Sternberg CN, Carducci MA, et al. Design and end points of clinical trials for patients with progressive prostate cancer and castrate levels of testosterone: recommendations of the Prostate Cancer Clinical Trials Working Group. J Clin Oncol. 2008;26:1148–59.

13. Hashimoto K, Tabata H, Shindo T, Tanaka T, Hashimoto J, Inoue R, et al. Serum testosterone level is a useful biomarker for determining the optimal treatment for castration-resistant prostate cancer. Urol Oncol. 2019;Epub ahead of print.

14. Sakamoto S, Maimaiti M, Xu M, Kamada S, Yamada Y, Kitoh H, et al. Higher Serum Testosterone Levels Associated with Favorable Prognosis in Enzalutamide- and Abiraterone-Treated Castration-Resistant Prostate Cancer. J Clin Med. 2019;8:E489.

15. de Jonge ME, Huitema ADR, Schellens JHM, Rodenhuis S, Beijnen JH. Individualised cancer chemotherapy: strategies and performance of prospective studies on therapeutic drug monitoring with dose adaptation: a review. Clin Pharmacokinet. 2005;44:147–73.

16. van Nuland M, Groenland S, Bergman AM, Rotmans JI, Rosing H, Beijnen JH, et al. Plasma Levels of Enzalutamide and Its Main Metabolites in a Patient With Metastatic Castration-resistant Prostate Cancer Undergoing Hemodialysis. Clin Genitourin Cancer. 2019;17:e383–6.

2.2

Exposure-response analyses of abiraterone and its metabolites in real-world patients with metastatic castration-resistant prostate cancer

Merel van Nuland
Stefanie L. Groenland
Andries M. Bergman
Neeltje Steeghs
Hilde Rosing
Nikkie Venekamp
Alwin D.R. Huitema
Jos H. Beijnen

Abstract

Background

Abiraterone acetate is an oral 17α-hydroxylase/C17,20-lyase (CYP17) inhibitor approved for the treatment of metastatic castration-resistant prostate cancer (mCPRC) patients. Previously, a prospective observational trial demonstrated a relationship between abiraterone trough concentrations (C_{min}) in plasma and treatment efficacy. The aim of our study was to investigate the exposure-response relationship of abiraterone and its metabolites, and to study if the proposed target for abiraterone of 8.4 ng/mL is feasible in a "real-world" patient cohort.

Patients and methods

mCRPC patients who had at least one abiraterone plasma concentration at steady-state were included in this study. Plasma abiraterone and its metabolites levels were analyzed using a validated liquid chromatography-mass spectrometry method. Using calculated C_{min} values of abiraterone and its active metabolite Δ(4)-abiraterone (D4A), univariate and multivariable Cox regression analyses were performed.

Results

Sixty-two patients were included in this retrospective analysis, of which 42% were underexposed (mean abiraterone C_{min} ≤8.4 ng/mL). In multivariable analysis, C_{min} ≥8.4 ng/mL was associated with longer prostate-specific antigen (PSA) independent progression-free survival (16.9 vs 6.1 months; p=0.033), which resulted in a hazard ratio of 0.44 (95% confidence interval: 0.23-0.82, p=0.01). D4A C_{min} did not show a relationship with treatment efficacy.

Conclusion

Our study shows that mCRPC patients with an abiraterone C_{min} ≥8.4 ng/mL have a better prognosis compared to patients with low C_{min}. Monitoring C_{min} of abiraterone can help to identify those patients at risk of suboptimal treatment for whom treatment optimization may be appropriate.

Introduction

Abiraterone is an inhibitor of 17α-hydroxylase/C17,20-lyase (CYP17), an enzyme involved in the intra- and extragonadal biosynthesis of androgens, including testosterone. Initially, abiraterone acetate was approved for treatment of metastatic castration-resistant prostate cancer (mCRPC) as it improves overall survival (OS) and progression-free survival (PFS) in this patient population compared to placebo (1,2). Following oral ingestion, abiraterone acetate is rapidly deacetylated to form the active substance abiraterone. Further metabolism into its major inactive metabolites abiraterone sulfate and abiraterone N-oxide sulfate is facilitated by cytochrome P450 family 3A member 4 (CYP3A4) and sulfotransferase family 2A member 1 (SULT2A1) (3). More recently, an active metabolite of abiraterone was discovered named Δ(4)-abiraterone (D4A), which is formed by the enzyme 3β-hydroxysteroid-dehydrogenase (3βHSD) (4,5). D4A blocks CYP17, several steroidogenic enzymes and the androgen receptor (5,6). Conversely, D4A is further metabolized to 3-keto-5-α-abiraterone, which stimulates the androgen receptor (7,8). The net result of these pharmacologic actions on therapeutic outcome remains to be elucidated.

Abiraterone acetate is administered in a fixed dose of 1000 mg once daily (QD). Mean steady-state trough concentrations (C_{min}) at this approved dose are 11.1 ng/mL for abiraterone and 1.6 ng/mL for D4A (3,9). In a prospective observational trial, abiraterone C_{min} has been associated with treatment response in mCRPC patients. In this study, plasma trough concentrations of abiraterone were significantly higher in prostate-specific antigen (PSA)-responders (n=38) compared to non-responders (n=23) (12.0 versus 8.0 ng/mL, p=0.0015) (10). Furthermore, a threshold of 8.4 ng/mL has been identified, above which patients had a longer PFS compared to patients with C_{min} below this target (12.2 versus 7.4 months, p=0.044) (10). The same research group reported that higher D4A C_{min} is related to shorter OS, but not PFS (n=30).

Abiraterone acetate has a large inter-patient variability in C_{min} of 46% (10). Part of this variability may be accounted for by the food-effect, causing a 7-fold increase in C_{max} with a low-fat meal and a 17-fold increase in C_{max} with a high-fat meal, compared to overnight fasting in healthy volunteers (11). A prospective clinical trial has shown that abiraterone acetate 250 mg QD taken with a low-fat meal was non-inferior to abiraterone acetate at a standard dose of 1000 mg QD in modified fasting state, in terms of PSA-response and PFS (n=72) (12). Furthermore, Stover et al. show that some men may benefit from taking abiraterone acetate concomitant with food (13).

Previous studies clearly show an exposure-efficacy relationship between plasma trough concentrations of abiraterone and PFS. Yet, abiraterone acetate is still administerd at fixed doses, which could lead to suboptimal treatment for some patients. Therapeutic drug monitoring (TDM), the clinical practice of measuring drug concentrations in biological fluids to individualize drug dosing, could be used to improve patient care. Based on current data, TDM of abiraterone may be implemented with a C_{min} threshold of 8.4 ng/mL. This threshold was established in a restrictive clinical study and needs

2.3

to be confirmed with real-life data from daily clinical practice.The aim of our study was to assess the exposure-efficacy relationship of abiraterone and its major metabolites for the purpose of TDM in a "real-world" patient cohort. We hypothesized that patients with abiraterone C_{min} ≥8.4 ng/mL will have a longer PFS compared to patients with a C_{min} <8.4 ng/mL. A retrospective study was conducted to test this hypothesis.

Methods

Patients and sampling

This was an observational study in the outpatient clinical of the Netherlands Cancer Institute – Antoni van Leeuwenhoek Hospital, Amsterdam. Abiraterone concentrations were monitored in all mCRPC patients using abiraterone acetate as part of routine clinical care. As authorized by the institute, data from clinical care were used retrospectively. Clinical characteristics were collected from medical records, including demographic data, medical history, abiraterone acetate dose, treatment duration, reason for discontinuation, concomitant medication and PSA levels. Furthermore, testosterone and androstenedione concentrations were determined during treatment using a validated liquid chromatography-mass spectrometry (LC-MS/MS) assay (14).

Pharmacokinetics

Blood samples were drawn as part of routine clinical care every three months on average. The date and time of blood withdrawal, and date and time of drug intake were recorded. Patients with at least one available abiraterone plasma concentration at steady-state were included in this study. Steady-state was considered to be reached after 1 week of treatment, taken into account the 15-hour half-life (3). Abiraterone and its metabolites D4A, abiraterone sulfate and abiraterone N-oxide sulfate were quantified using a validated LC-MS/MS method (15,16). Plasma samples were collected at random time points during a dosing interval at routine patient visits to the outpatient clinic, and therefore, C_{min} values were calculated from the measured concentrations. As abiraterone shows clear distribution pharmacokinetics, log-linear extrapolation was not feasible. Furthermore, the use of Bayesian estimates from a population pharmacokinetic model was considered, but this was complicated by high shrinkage. Therefore, we used the ratio of the observed concentration and median concentration as tool to calculate C_{min}. First, we simulated a full population concentration-time curve of abiraterone with the pharmacokinetic model published by Stuyckens et al. (17). Second, measured concentrations were divided by the simulated concentrations of the population curve at the recorded time points. Third, the ratio between measured concentrations and simulated concentrations was multiplied by the simulated C_{min} of the population curve to obtain the final calculated C_{min}. Our data show that the shape of the D4A concentration-time curve is similar to that of abiraterone, and therefore, it is suggested that metabolite formation is rate-limiting in the clearance of D4A. As there is no pharmacokinetic model available for D4A, C_{min} was calculated in the same manner

as the C_{min} of abiraterone. Measured concentrations of abiraterone sulfate and abiraterone N-oxide sulfate were divided into three groups based on the time of sampling after dosing (TAD), being 0-4 hours, 4-10 hours and 10-24 hours after drug intake. Samples taken before steady-state was reached or more than 24 hours after the last dose were excluded from further analysis.

Outcome measures
Three clinical end points regarding treatment response were evaluated separately in this study; PSA response, PSA independent PFS and time to PSA progression (TTPP). PSA response was defined as ≥50% decrease in PSA from baseline, both according to the Prostate Cancer Working Group 2 (PCWG2) criteria (18,19). PSA independent PFS was defined as the time from treatment start to the first event of progression, being either radiographic progression, symptomatic progression (start of radiotherapy, samarium treatment, increase of analgesic dose or a WHO performance level increase of at least 2), onset of next treatment or death from any cause. Radiographic progression was evaluated according to modified Response Evaluation Criteria in Solid Tumors (RECIST version 1.1) (20). TTPP was defined as the time from treatment start to a 25% or greater PSA increase from the nadir, with an absolute increase in PSA levels of at least 2 ng/mL (20), and had to be confirmed by a subsequent PSA value, also according to PCWG2 criteria. Toxicity was defined as discontinuation due to adverse events, dose reductions due to adverse events or temporary treatment interruption.

2.3

Statistics
For the purpose of exposure-response analyses, the mean of all available abiraterone and metabolite levels per patient were used as parameter for exposure. The association between abiraterone plasma concentrations and metabolite concentrations were determined using the Spearman correlation test. Mann-Whitney U tests were used for univariable analysis of PSA response and plasma concentrations of abiraterone and its metabolites. Using the abiraterone C_{min} target of 8.4 ng/mL as a cut-off value, patients were divided into two groups (adequate vs low C_{min}) for PFS analyses. As no exposure target is known for D4A, D4A plasma concentrations were divided into quartiles for further analyses. PFS functions were estimated using the Kaplan-Meier method and predictive factors were assessed using the univariable model (log rank-test). A stepwise logistic regression was performed for the determination of a predictive score of PFS. Variables significantly associated with outcome in univariate analysis were used in the multivariate analysis. Ultimately, in multivariable analysis, PSA levels at baseline, WHO performance status, number of previous lines of treatment and whether patients switched from prednisone to dexamethason during treatment were included as covariates. The following variables were tested but not included in the final model: age, weight, testosterone levels, androstenedione levels, prior treatment with docetaxel, hemoglobin, alkaline phosphatase, kidney and liver function. All statistical analyses were performed in R (version 3.6.0, package 'survival'). A post hoc power analysis was conducted to evaluate the statistical power of this study.

Results

Evaluable patients

From June 2016 to June 2018, 62 patients on treatment with abiraterone acetate were included in this study. A full overview of patient characteristics is provided in Table 1. The median time of treatment was 13.6 months (range 1.1 to 73.0 months). At data cut-off on May 13th 2019, 12 patients were still on abiraterone treatment. No relevant CYP-inhibiting or inducing co-medication was used during this treatment period. The Spearman correlation test showed that abiraterone and metabolite concentrations were statistically correlated, meaning that plasma samples with high abiraterone levels also contained high metabolite concentrations. Testosterone and androstenedione levels were below the lower limit of quantification (LLOQ) of 0.01 ng/mL in all patients.

Pharmacokinetics

In total, 244 plasma samples were included. The distribution of time of sampling after dosing is shown in Supplementary Figure 1. Overall, a median (range) of 4 (1-11) samples were available per patient. In aggregate, the median ± SD abiraterone C_{min} concentration was 9.3 ± 10 ng/mL, and median ± SD metabolite plasma concentrations were 1.0 ± 0.9 ng/mL for D4A, 8.7 ± 7.2 $\cdot 10^3$ ng/mL for abiraterone sulfate and 7.8 ± 3.9 $\cdot 10^3$ ng/mL for abiraterone N-oxide sulfate. Interpatient variability (coefficient of variation; CV%) of mean plasma concentrations at a 1,000 mg QD was 70% for abiraterone and 61% for D4A. Furthermore, mean intrapatient variability (CV%) at a 1,000 mg QD was 53% for abiraterone and 45% for D4A.

An overview of the distribution of mean abiraterone and D4A C_{min} concentrations per patient is provided in Figure 1. Twenty-six (42%) patients had an abiraterone C_{min} below the target of 8.4 ng/mL. Four patients received a dose reduction to 500 mg QD (n=2) or 750 mg QD (n=2) due to adverse events, including hepatotoxicity and fatigue. Two of these patients had an abiraterone C_{min} below the target of 8.4 ng/mL after dose reduction. Of all explored clinical parameters, none were found to be significantly predictive of abiraterone plasma concentrations, except for body weight at baseline. Linear regression indicated that patients with a higher body weight at baseline had a lower plasma concentration (p=0.014).

Exposure-response analyses abiraterone

Among 62 included patients, 35 (56%) patients were considered PSA-responders, versus 27 (44%) patients without a PSA response. Figure 2 shows the relationship between C_{min} of abiraterone PSA response. Mean plasma trough concentrations of abiraterone were 11.4 ng/mL in PSA-responders compared to 7.2 ng/mL non-responders (p=0.18). The maximal change in PSA from baseline (%) after start of treatment is shown for each patient in Figure 3. Plasma concentrations of the inactive metabolites abiraterone N-oxide sulfate and abiraterone sulfate are depicted in Supplementary Figure 2. As no

Table 1. Patient characteristics.

	Total	Abiraterone C$_{min}$	
		>8.4 ng/mL	≤8.4 ng/mL
Number of patients (n (%))	62 (100)	36 (58)	26 (42)
Age (mean, range)	72 (60-87)	72 (60-87)	71 (61-83)
Weight (mean, range)	89 (57-175)	91 (57-175)	85 (68-117)
WHO performance status (n (%))			
0	22 (36)	12 (33)	10 (38)
1	36 (58)	22 (61)	14 (54)
2	4 (6)	2 (5)	2 (8)
Dose reduction (n (%))	4 (6)	2 (6)	2 (8)
Number of previous lines of therapy (n (%))			
0	33 (53)	23 (64)	10 (38)
1	13 (21)	7 (19)	6 (23)
2	10 (16)	3 (8)	7 (27)
3	4 (7)	2 (5)	2 (8)
4	2 (3)	1 (3)	1 (4)
Previous chemotherapy	26 (42)	9 (25)	17 (65)
Switch to dexamethasone during treatment (n (%))	33 (53)	25 (69)	8 (69)
Number of samples (n)	244	165	79
Samples per patient (mean (range))	4 (1-11)	5 (1-10)	3 (1-8)
Median (range) C$_{min}$ (ng/mL): Abiraterone D4A	9.3 (2.0-49.8) 1.0 (0.3-4.4)	14.9 (8.5-49.8) 1.3 (0.4-4.4)	6.3 (2.0-8.4) 0.7 (0.3-1.8)
Median testosterone levels (ng/mL)	<0.010*	<0.010*	<0.010*
Median androstenedione levels (ng/mL)	<0.010*	<0.010*	<0.010*

Demographic data and androgen levels are at values at baseline. Abbreviations: D4A = Δ(4)-abiraterone
* Data points below the lower limit of quantification of the bioanalytical method.

2.3

trough concentrations could be calculated for these metabolites, plasma levels are given in three groups based on the time after dosing. Median plasma concentrations were higher in PSA-responders compared to non-responders in all groups but one.

For PSA independent PFS, 62 patients were included with 50 events (81% of patients) of progression. The remaining patients were still on treatment with abiraterone acetate. Median PSA independent PFS was 16.9 months in patients with an abiraterone C$_{min}$ ≥8.4 ng/mL compared to 6.1 months in patients with a C$_{min}$ below the target (p=0.077, see Figure 4). The multivariable analysis resulted in a hazard ratio (HR) of 0.44 (95% CI 0.23-0.82, p=0.01).

For TTPP analysis, 62 patients were included with 53 events (85% of patients) of PSA progression. Three patients were still on treatment, 1 patient died prior to PSA
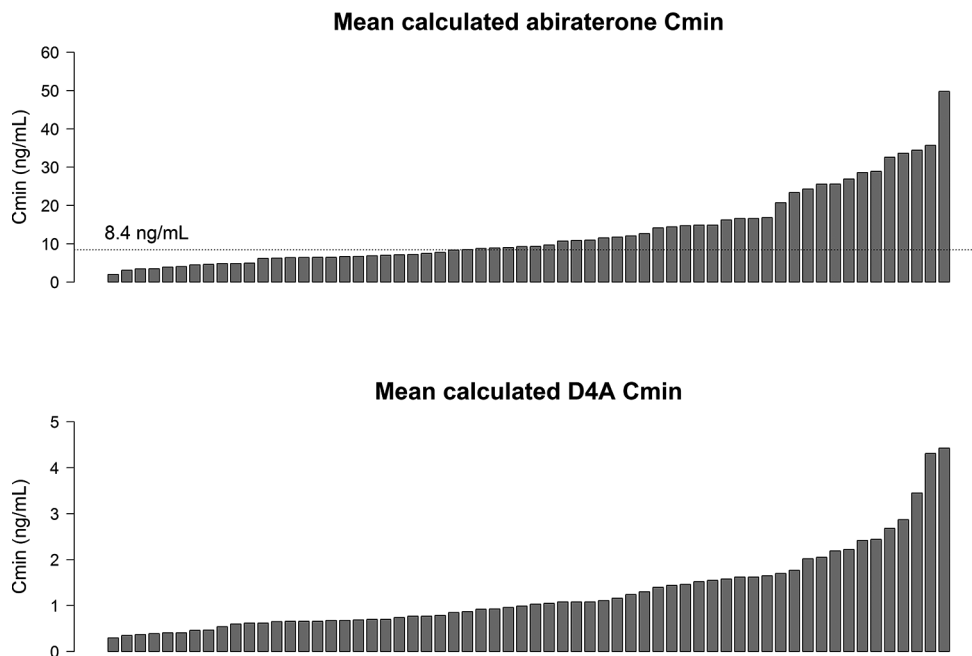
Figure 1. Distribution of plasma concentrations of abiraterone and Δ(4)-abiraterone (D4A) in patients with metastatic castration-resistant prostate cancer (mCRPC), including the proposed target concentration for abiraterone of 8.4 ng/mL. Each bar represents one patient.

progression, and 5 patients did not show PSA progression but discontinued treatment due to radiographic progression. These patients were censored for TTPP analysis. Median TTPP in patients with an abiraterone C_{min} ≥8.4 ng/mL was 19.8 months compared to 3.7 months in patients with a C_{min} below the target (p=0.062, see Figure 4). In multivariable analysis, C_{min} ≥8.4 ng/mL resulted in a HR of 0.52 (95% CI 0.29-0.97, p=0.038).

A post hoc power analysis was conducted using the above described results. The power to detect a difference in PFS from 16.1 months to 6.1 months (with a hazard ratio of 0.44) between patients with C_{min} ≥8.4 ng/mL versus <8.4 ng/mL, when there are 36 subjects in the first group and 26 in the second, using a two-sided log rank test with alpha=0.05, was 80%.

Exposure-response analyses D4A

Figure 2 shows the relationship between C_{min} of D4A and PSA response. Plasma concentrations were 1.0 ng/mL in both PSA-responders and non-responders (p=0.88). Patients were divided into quartiles based on plasma concentrations of D4A, and progression-free survival analyses were performed using these groups. There was no significant difference in the four quartiles regarding PSA independent PFS (7.7 vs 22
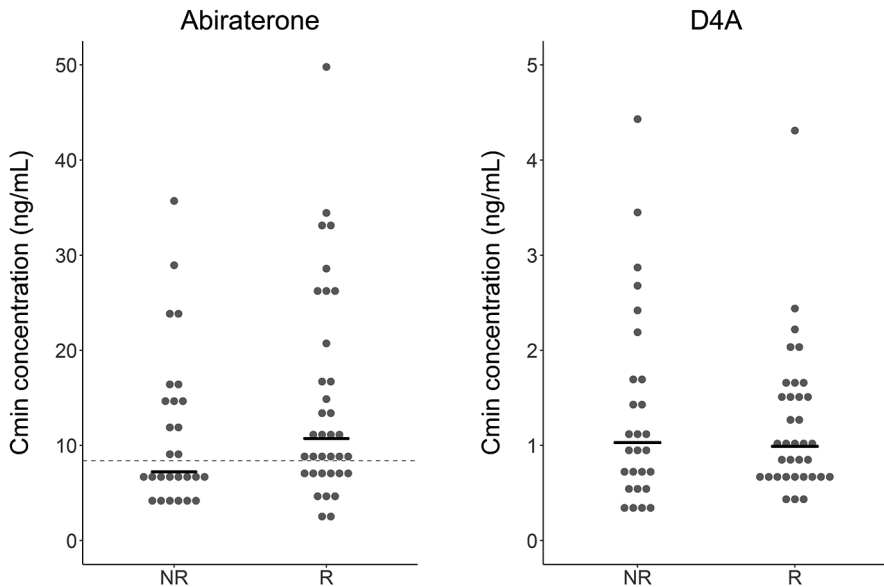
Figure 2. Relationship between prostate-specific antigen response and the calculated trough concentration of abiraterone (left), Δ(4)-abiraterone (D4A) (right). Horizontal lines represent the median concentration for PSA-responders (R, n=35) and non-responders (NR, n=27) and the dotted lines represent the proposed target for abiraterone of 8.4 ng/mL. Mean plasma trough concentrations of abiraterone were 11.4 ng/mL in PSA-responders compared to 7.2 ng/mL non-responders (p=0.18) and D4A plasma concentrations were 1.0 ng/mL in both PSA-responders and non-responders (p=0.88).

vs 13 vs 11 months, p=0.47). Furthermore, there was no significant differences in the four quartiles regarding TTPP (8.2 vs 15 vs 5.1 vs 11 months, p=0.57). Kaplan-meier curves are shown in Supplementary Figure 3. Both univariable and multivariable analysis did not support a relationship between D4A plama concentrations and PFS.

Exposure-toxicity analysis
Of 62 included patients, 4 patients received a dose reduction and 3 patients temporarily discontinued treatment due to the presence of adverse events. Reasons for dose reduction or treatment interruption included fatigue, hepatotoxicity and abdominal pain. Median abiraterone C_{min} was 9.0 ng/mL for patients experiencing clinically relevant adverse events, compared to 9.3 ng/mL in those who did not (p=1.0). Moreover, median D4A C_{min} concentrations were 1.1 versus 1.0 for patients with and without adverse events, respectively (p=0.60).

PSA change from baseline
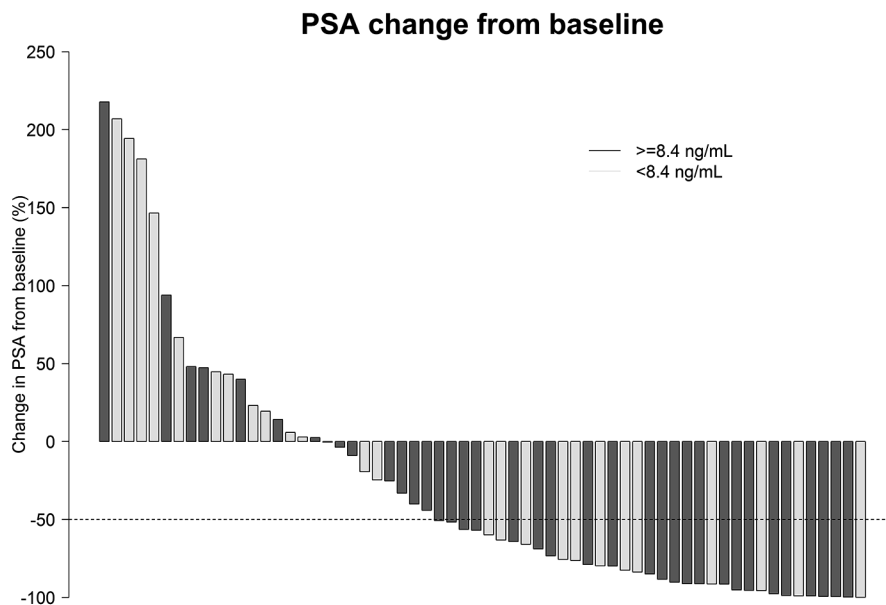
Figure 3. Waterfall plot showing the PSA change from baseline (%) after start of abiraterone acetate treatment. Each bar represents one patient and the colors indicate if this patient had an abiraterone C_{min} above or below 8.4 ng/mL, The dotted line indicates a 50% PSA decrease from baseline, representing the cut-off for patients to be regarded PSA responders (>50%) or non-responders.

Discussion

In this study, plasma concentrations of abiraterone and its metabolites were monitored in a clinical setting. To our knowledge, this is the first study to evaluate the correlation between abiraterone C_{min} and response in a real-world patient cohort, including D4A and other metabolite data. Obtaining real-life data is relevant for clinical practice, as this better reflects daily practice than data derived from clinical trials (21). Abiraterone acetate is administerd at a fixed dose of 1,000 mg QD. Our data show that patients with an abiraterone C_{min} ≥8.4 ng/mL have a longer PFS compared to patients with a pharmacokinetic exposure below this threshold. Furthermore, this study shows that 42% of patients with mCRPC may be underdosed with this standard fixed dosing regimen and could benefit from an individualized dosing strategy, which is in line with the previously reported 35% of patients having a C_{min} below the target (10).

D4A was included in PFS analyses as it shows anti-androgen activity. However, it may be furher converted to an androgen-stimulating metabolite and, therefore, the net contribution of D4A to the anti-tumor effect of abiraterone is ambiguous (7,8). Although a previous study has shown that a higher D4A C_{min} was associated with shorter OS (HR 1.54, 95% CI 1.06-2.22, p=0.022) but not with PFS (9), our study did not reveal a
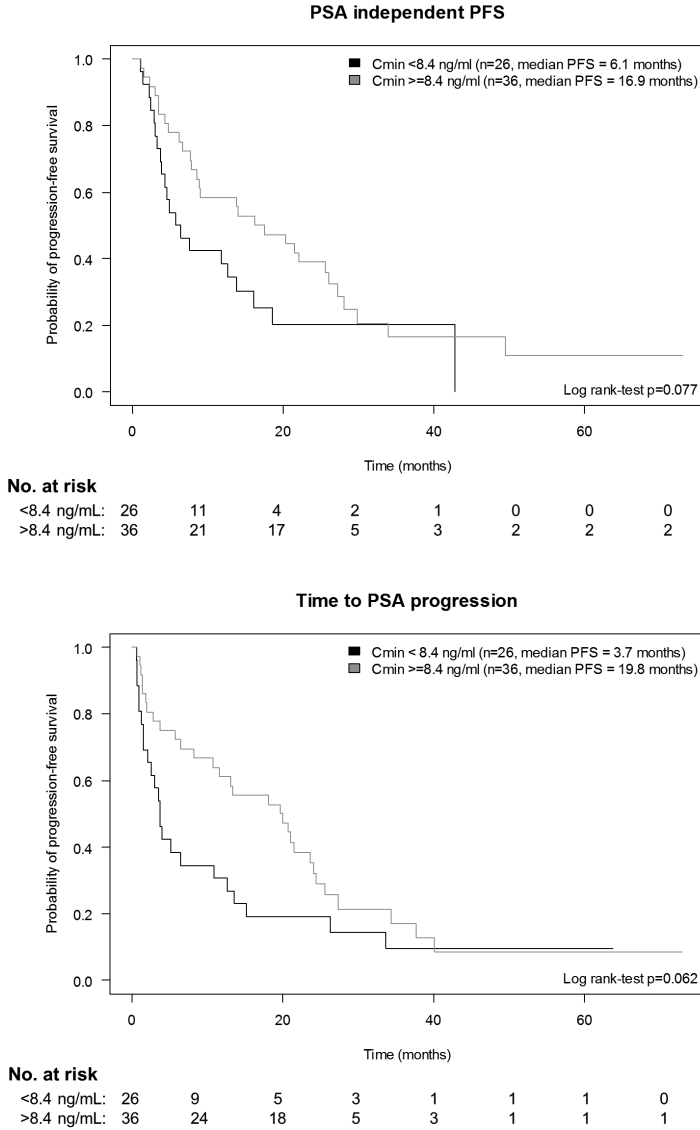
PSA independent PFS

No. at risk

<8.4 ng/mL:	26	11	4	2	1	0	0	0
>8.4 ng/mL:	36	21	17	5	3	2	2	2

Time to PSA progression

No. at risk

<8.4 ng/mL:	26	9	5	3	1	1	1	0
>8.4 ng/mL:	36	24	18	5	3	1	1	1

Figure 4. Kaplan-meier plots of PSA independent progression-free survival (PFS) in metastatic castration-resistant prostate cancer (mCRPC) patients with a mean abiraterone C_{min} above (n=36, grey line) or below (n=26, black line) the exposure target of 8.4 ng/mL. Prostate-specific antigen (PSA)-independent PFS is shown in the upper panel, and time to PSA progression is shown in the lower panel.

relationship between D4A C_{min} and treatment response, PSA independent PFS or TTPP. Moreover, abiraterone and D4A concentrations are correlated, which indicates that abiraterone C_{min} may serve as a proxy for the total antitumor effect of abiraterone and its metabolites.

The exposure target for abiraterone of 8.4 ng/mL was based on a prospective observational study (10). The CYP17 inhibitory concentrations 50% (IC50) value of abiraterone is 0.07 ng/mL. After correcting for plasma protein binding (99%), a minimum concentration of 7.0 ng/mL should be reached to inhibit 50% of CYP17 in plasma. The exposure target is close to this corrected IC50 value, which biologically substantiates the threshold. Moreover, the CYP17 IC50 of D4A is 0.035 ng/mL. Given a protein binding of 99%, a minimum concentration of 3.5 ng/mL should be achieved to inhibit 50% of the CYP17 enzyme (4,5). Only three patients reached this threshold, which could explain why no association was found between D4A plasma levels and response in this population.

Although we believe our study provides relevant information on exposure-response of abiraterone in real-life patients, our analysis does have some limitations. First, in thist study not actual C_{min} but calculated (from measured) plasma concentrations were used. Although actual C_{min} may be more accurate than calculated C_{min}, the practical implementation of TDM is more feasible if samples can be drawn at random times during the dosing interval as it can be combined with routine visits to the outpatient clinic. Second, the extent of adherence to abiraterone acetate was not available due to the retrospective nature of this analysis. Although treating physicians provided instructions on drug intake and usage, this may be a potentential source of variability in abiraterone C_{min}.

Based on our study and previously published data, an exposure target for abiraterone of 8.4 ng/mL seems appropriate for TDM. Patients with a C_{min} below this target may be advised to take the drug concomitant with food, thereby avoiding expensive dose increments. A single-dose study of abiraterone in healthy volunteers has shown that the area under the plasma concentration-time curve (AUC) and C_{max} increase 10- and 17-fold after intake with a high-fat meal, respectively, and 7- and 5-fold after intake with a low-fat meal compared to overnight fasting, respectively (11). The same study showed a less pronounced effect in mCRPC patients when comparing a modified fasting state with food intake (similar exposure with low-fat meals and a 2-fold increase with high-fat meals) (11). Furthermore, previous research has shown that some men may benefit from concomitant intake of abiraterone acetate with food in terms of PSA progression (13). This may be attributed to the a lower percentage of patients with C_{min} <8.4 ng/mL. Based on this information, concomitant intake of abiraterone with a low-fat meal may increase plasma levels up to 5-fold, which would be sufficient for the majority of included patients with C_{min} ≤8.4 ng/mL to reach plasma levels above the target. Treatment optimization by individualized dosing strategies could lead to better efficacy of abiraterone and higher treatment response. Furthermore, the lack of a relationship between exposure and toxicity suggests that increasing plasma levels will, in these ranges, not result in additional toxicity. Although more research is needed to confirm our findings and to furher study the 8.4 ng/mL threshold, we advise clinicians to consider integrating TDM of abiraterone into standard treatment of mCRPC patients. Currently, a study is performed in our Institute to investigate the feasibility of TDM

with abiraterone using a food intervention (22) by which we hope to improve outcome for mCRPC patients treated with abiraterone acetate.

Conclusion

Our study shows that patients with an abiraterone trough level above 8.4 ng/mL have a longer PFS compared to patients with a pharmacokinetic exposure below this threshold. Exposure to the active metabolite D4A did not show a relationship with treatment efficacy and therefore may not add to the prognostic value of abiraterone plasma levels. Monitoring abiraterone C_{min} can identify those patients who are underdosed and we advise clinicians to consider integrating TDM of abiraterone into standard treatment of mCRPC patients.

2.3
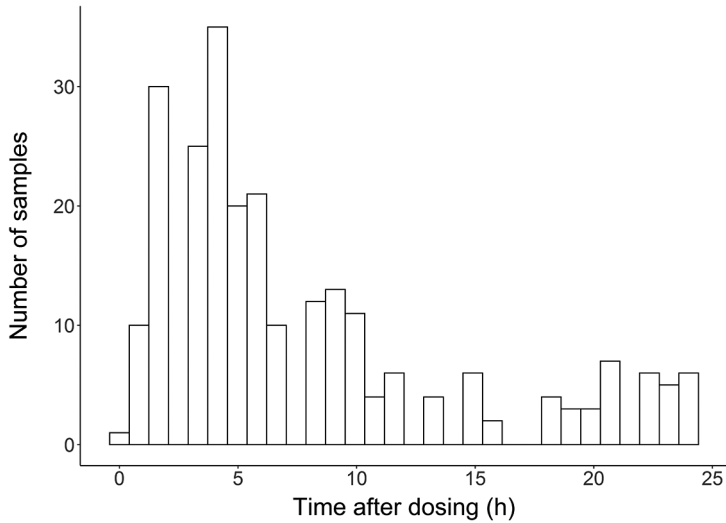
Supplementary

Supplementary Figure 1. Histogram showing the number of samples taken at a certain time after dosing (TAD).
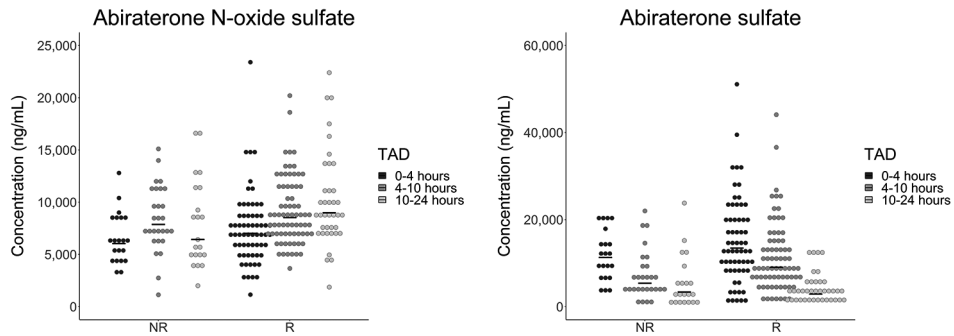
Supplementary Figure 2. Relationship between prostate-specific antigen response and plasma concentrations of abiraterone N-oxide sulfate (left) and abiraterone sulfate (right). Plasma concentrations are divided into three groups, based on the time of sampling after dosing (TAD), being 0-4 hours, 4-10 hours and 10-24 hours. Horizontal lines represent the median concentration for PSA-responders (R) and non-responders (NR). Median plasma concentrations of abiraterone N-oxide sulfate per group were $6.0 \cdot 10^3$, $7.9 \cdot 10^3$ and $6.4 \cdot 10^3$ ng/mL for the non-responders versus $7.0 \cdot 10^3$, $8.5 \cdot 10^3$ and $9.0 \cdot 10^3$ ng/mL for PSA-responders, respectively. Median plasma concentrations of abiraterone sulfate were $11 \cdot 10^3$, $5.4 \cdot 10^3$ and $3.4 \cdot 10^3$ ng/mL versus $14 \cdot 10^3$, $9.1 \cdot 10^3$ and $2.9 \cdot 10^3$ ng/mL per group, respectively.

PSA independent PFS

No. at risk

Q1:	16	7	4	2	1	1	1	1
Q2:	15	9	7	3	2	0	0	0
Q3:	15	8	5	0	0	0	0	0
Q4:	16	8	5	2	1	1	1	1

Time to PSA progression

No. at risk

Q1:	16	8	6	4	2	2	2	1
Q2:	15	10	7	1	0	0	0	0
Q3:	15	6	4	1	1	0	0	0
Q4:	16	9	6	2	1	0	0	0
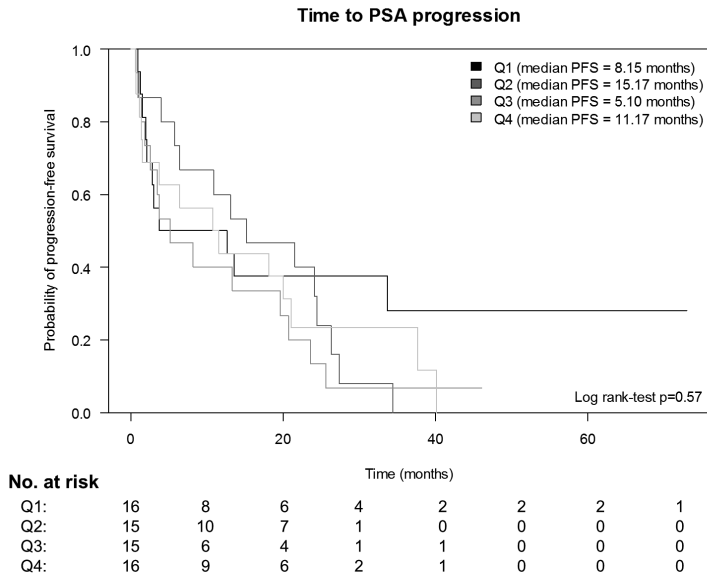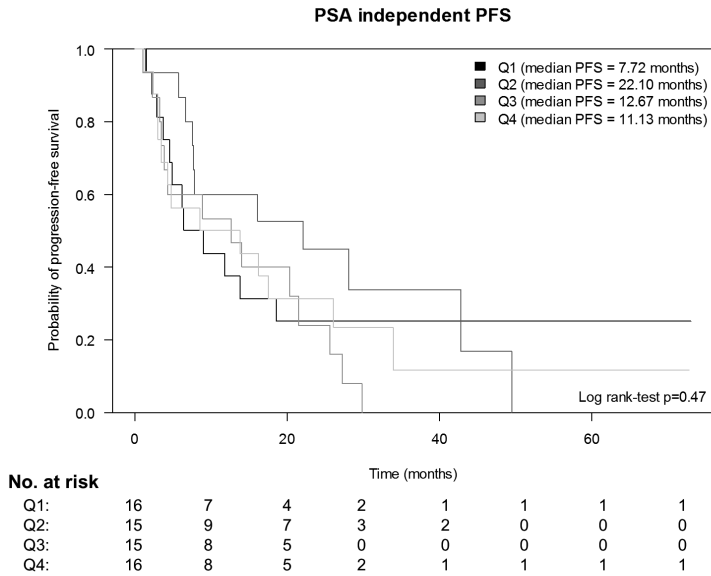
Supplementary Figure 3. Kaplan-meier plots of PSA independent progression-free survival (PFS) in metastatic castration-resistant prostate cancer (mCRPC) patients for each quartile of Δ(4)-abiraterone (D4A) concentrations. Prostate-specific antigen (PSA)-independent PFS is shown in the upper panel, and time to PSA progression is shown in the lower panel.

References

1. de Bono JS, Logothetis CJ, Molina A, Fizazi K, North S, Chu L, et al. Abiraterone and increased survival in metastatic prostate cancer. N Engl J Med. 2011;364:1995–2005.

2. Ryan CJ, Smith MR, de Bono JS, Molina A, Logothetis CJ, de Souza P, et al. Abiraterone in metastatic prostate cancer without previous chemotherapy. N Engl J Med. 2013;368:138–48.

3. US Food and Drug Administration (FDA). Clinical Pharmacology and Biopharmaceutics Review: Zytiga (abiraterone acetate). 2010 [cited 2019 May]. p. 1–86. Available from: https://www.accessdata.fda.gov/drugsatfda_docs/nda/2011/202379orig1s000clinpharmr.pdf

4. Li Z, Alyamani M, Li J, Rogacki K, Abazeed M, Upadhyay SK, et al. Redirecting abiraterone metabolism to fine-tune prostate cancer anti-androgen therapy. Nature. 2016;533:547–51.

5. Li Z, Bishop AC, Alyamani M, Garcia JA, Dreicer R, Bunch D, et al. Conversion of abiraterone to D4A drives anti-tumour activity in prostate cancer. Nature. 2015;523:347–51.

6. Emamekhoo H, Li Z, Sharifi N. Clinical significance of D4A in prostate cancer therapy with abiraterone. Cell cycle. 2015;14:3213–4.

7. Hettel D, Sharifi N. HSD3B1 status as a biomarker of androgen deprivation resistance and implications for prostate cancer. Nat Rev Urol. 2018;15:191–6.

8. Alyamani M, Emamekhoo H, Park S, Taylor J, Almassi N, Upadhyay S, et al. HSD3B1(1245A>C) variant regulates dueling abiraterone metabolite effects in prostate cancer. J Clin Invest. 2018;128:3333–40.

9. Blanchet B, Carton E, Alyamani M, Golmard L, Huillard O, Thomas-Scheomann A, et al. A PK/PD study of Delta-4 abiraterone metabolite in metastatic castration-resistant prostate cancer patients. Pharmacol Res. 2018;136:56–61.

10. Carton E, Noe G, Huillard O, Golmard L, Giroux J, Cessot A, et al. Relation between plasma trough concentration of abiraterone and prostate-specific antigen response in metastatic castration-resistant prostate cancer patients. Eur J Cancer. 2017;72:54–61.

11. Chi KN, Spratlin J, Kollmannsberger C, North S, Pankras C, Gonzalez M, et al. Food effects on abiraterone pharmacokinetics in healthy subjects and patients with metastatic castration-resistant prostate cancer. J Clin Pharmacol. 2015;55:1406–14.

12. Szmulewitz RZ, Peer CJ, Ibraheem A, Martinez E, Kozloff MF, Carthon B, et al. Prospective International Randomized Phase II Study of Low-Dose Abiraterone With Food Versus Standard Dose Abiraterone In Castration-Resistant Prostate Cancer. J Clin Oncol. 2018;36:1389–95.

13. Stover JT, Moore RA, Davis K, Harrison MR, Armstrong AJ. Reversal of PSA progression on abiraterone acetate through the administration with food in men with metastatic castration-resistant prostate cancer. Prostate Cancer Prostatic Dis. 2015;18:161–6.

14. van Nuland M, Venekamp N, Wouters WME, van Rossum HH, Rosing H, Beijnen JH. LC–MS/MS assay for the quantification of testosterone, dihydrotestosterone, androstenedione, cortisol and prednisone in plasma from castrated prostate cancer patients treated with abiraterone acetate or enzalutamide. J Pharm Biomed Anal. 2019;170:161–8.

15. van Nuland M, Hillebrand MJ., Rosing H, Schellens JHM, Beijnen JH. Development and validation of an LC-MS/MS method for the simultaneous quantification of abiraterone, enzalutamide, and their major metabolites in human plasma. Ther Drug Monit. 2017;39:243–51.

16. van Nuland M, Rosing H, de Vries J, Ovaa H, Schellens JHM, Beijnen JH. An LC–MS/MS method for quantification of the active abiraterone metabolite Δ(4)-abiraterone (D4A) in human plasma. J Chromatogr B. 2017;1068–1069:119–24.

17. Stuyckens K, Saad F, Xu XS, Ryan CJ, Smith MR, Griffin TW, et al. Population pharmacokinetic analysis of abiraterone in chemotherapy-naive and docetaxel-treated patients with metastatic castration-resistant prostate cancer. Clin Pharmacokinet. 2014;53:1149–60.

18. Scher HI, Morris MJ, Stadler WM, Higano CS, Halabi S, Smith MR, et al. The Prostate Cancer Working Group 3 (PCWG3) consensus for trials in castration-resistant prostate cancer (CRPC). J Clin Oncol. 2015;33:5000.

19. Scher HI, Halabi S, Tannock I, Morris M, Sternberg CN, Carducci MA, et al. Design and end points of clinical trials for patients with progressive prostate cancer and castrate levels of testosterone: recommendations of the Prostate Cancer Clinical Trials Working Group. J Clin Oncol. 2008;26:1148–59.

20. Therasse P, Arbuck SG, Eisenhauer EA, Wanders J, Kaplan RS, Rubinstein L, et al. New Guidelines to Evaluate the Response to Treatment in Solid Tumors. JNCI J Natl Cancer Inst. 2000;92:205–16.

21. Westgeest HM, Uyl-de Groot CA, van Moorselaar RJA, de Wit R, van den Bergh ACM, Coenen JLLM, et al. Differences in Trial and Real-world Populations in the Dutch Castration-resistant Prostate Cancer Registry. Eur Urol Focus. 2018;4:694–701.

22. Groenland SL, van Eerden RAG, Verheijen RB, Koolen SLW, Moes DJAR, Desar IME, et al. Therapeutic drug monitoring of oral anticancer drugs: the DPOG-TDM protocol for a prospective study. Ther Drug Monit. 2019;Epub ahead of print.

2.3

Concomitant intake of abiraterone acetate and food to increase pharmacokinetic exposure: real life data from a therapeutic drug monitoring program

Manuscript in preparation

Stefanie L. Groenland
Merel van Nuland
Andries M. Bergman
Jeantine M. de Feijter
Vincent O. Dezentje
Jos H. Beijnen
Alwin D.R. Huitema
Neeltje Steeghs

Abstract

Aim
Abiraterone acetate is approved for the treatment of metastatic prostate cancer. At the currently used fixed dose of 1,000 mg once daily (QD) in modified fasting state, approximately 40% of patients do not reach the efficacy threshold of a minimum plasma concentration (C_{min}) ≥ 8.4 ng/mL and are thereby at risk of decreased treatment efficacy. This study aims to evaluate whether pharmacokinetically guided abiraterone acetate dosing with a food-intervention is feasible and results in an increased proportion of patients with concentrations above the target.

Methods
Patients starting regular treatment with abiraterone acetate in modified fasting state were included. Pharmacokinetic analysis was performed 4, 8 and 12 weeks after start of treatment, and every 12 weeks thereafter. In case of C_{min} < 8.4 ng/mL and acceptable toxicity, a pharmacokinetically guided intervention was recommended. In case of low exposure, concomitant intake of abiraterone acetate and a light meal or a snack was recommended.

Results
In total, 32 patients have been included, of which 20 patients (63%) had a C_{min} < 8.4 ng/mL at a certain time point during treatment. These patients were recommended to take abiraterone acetate concomitantly with food, after which C_{min} increased significantly from 7 ng/mL to 22.5 ng/mL (p<0.001) without additional toxicities. This intervention led to adequate exposure in 28 patients (87.5%).

Conclusion
Therapeutic drug monitoring of abiraterone was applied in daily clinical practice and proved to be feasible. Concomitant intake with food resulted in a significant increase in C_{min} and offers a cost-neutral opportunity to optimize treatment in patients with low pharmacokinetic exposure.

Introduction

Abiraterone acetate (Zytiga®) is an anti-hormonal prodrug, which is rapidly converted to its active form abiraterone after oral ingestion. Abiraterone inhibits 17α-hydroxylase/C17,20-lyase (CYP17) and thereby blocks both the intra- and extragonadal (i.e. adrenal and intratumoural) androgen biosynthesis. Initially, abiraterone acetate was approved for the treatment of metastatic castration-resistant prostate cancer (mCRPC), but recently it has also been approved for the treatment of metastatic castration-sensitive prostate cancer (mHSPC) (1).

Exposure-response analyses have shown that plasma concentrations of abiraterone are related to efficacy (2–4). Carton *et al.* demonstrated that the minimum plasma concentration (C_{min}) was significantly higher in responders compared to non-responders (12.0 vs. 8.0 ng/mL, p=0.0015), in which response was defined as a PSA decline of ≥ 50% after three months. A C_{min} ≥ 8.4 ng/mL was identified as the optimal cut-off value, with progression-free survival (PFS) being significantly longer in patients with an exposure above this efficacy threshold compared with those below (12.2 vs. 7.4 months, respectively, p=0.044). PFS was defined as the time until either PSA or radiological progression (3). We have confirmed this exposure-efficacy threshold in a real-life patient cohort (4).

Abiraterone acetate is currently administered using a one-size-fits-all approach, in which all patients receive a dose of 1,000 mg once daily (QD) without food. This dosing strategy results in a high interindividual variability in pharmacokinetic exposure to abiraterone, with a coefficient of variation of 46-70% for C_{min} (3,4). At the currently used fixed dose, 35-42% of patients do not reach the efficacy threshold of C_{min} ≥ 8.4 ng/mL and are thus underdosed (3,4). This provides a strong rationale for therapeutic drug monitoring (TDM) to intervene and to increase the number of patients having an adequate abiraterone exposure.

As food intake impacts the absorption of abiraterone, concomitant intake of abiraterone acetate and food could be applied in case of low pharmacokinetic exposure. According to the drug label (5), abiraterone acetate should be administered in a modified fasting state, which means no food two hours before and one hour after intake of the drug. However, concomitant intake with food has been shown to result in a clinically relevant increase in pharmacokinetic exposure (five- to seven-fold with a low-fat meal and ten- to seventeen-fold with a high-fat meal, when compared to an overnight fasting state in healthy volunteers) in a food effect study (6). This effect was less pronounced when compared to a modified fasting state in mCRPC patients (similar exposure and two-fold increase with low- and high-fat meals, respectively) (6).

The aim of this study was to evaluate whether TDM of abiraterone with a food-intervention is feasible in clinical practice and results in an increased proportion of patients with efficacious exposure to abiraterone without additional toxicities.

2.4

Methods

Patients
Patients starting regular treatment with abiraterone acetate at the registered dose of 1,000 mg QD in a modified fasting state were included in an ongoing prospective study on TDM of oral anticancer drugs (www.trialregister.nl; NL6695) (7).

Objectives
The primary objective of this study was to halve the proportion of patients with an exposure below the target of 8.4 ng/mL after 12 weeks, compared to historical data. The study of Carton *et al.* was taken as a reference, in which 35% of patients had a mean C_{min} < 8.4 ng/mL (3). Secondary objectives were to evaluate the feasibility, tolerability and efficacy of TDM of abiraterone with a food-intervention in clinical practice and to achieve a physician adherence > 90% (i.e. whether TDM recommendations were followed by the treating physician). Feasibility was defined as the percentage of successful pharmacokinetically (PK)-guided interventions (i.e. target attainment without additional toxicities). Tolerability was evaluated by the incidence of clinically relevant toxicities, defined as toxicities leading to dose reduction, treatment interruption or treatment discontinuation, as evaluated by the treating physician. Preliminary efficacy was assessed by comparing time on abiraterone treatment between patients who needed a PK-guided intervention and those who did not (i.e. all C_{min} ≥ 8.4 ng/mL).

PK samples
PK samples were collected 4, 8 and 12 weeks after start of treatment; and every 12 weeks thereafter. Figure 1 provides a schematic overview of the study design. Abiraterone concentrations were measured using a validated liquid chromatography-tandem mass spectrometry (LC-MS/MS) assay (8). C_{min} was estimated using the following formula:

$$C_{min} = C_{measured} * 0.5^{\frac{dosing\ interval - TAD}{t_{1/2}}}$$

in which C_{min} is the calculated minimum plasma concentration, $C_{measured}$ is the measured plasma concentration, dosing interval is the time between two consecutive administrations of the drug (i.e. 24 hours for abiraterone acetate), TAD is the Time After Dose (i.e. the time between last intake of the drug and collection of the PK sample) and $t_{1/2}$ is the elimination half-life of the drug (i.e. 12 hours for abiraterone (9)).

PK-guided interventions
In case of C_{min} < 8.4 ng/mL and acceptable toxicity, a PK-guided intervention was recommended. After compliance and drug-drug interactions were checked, the first step was concomitant intake of abiraterone acetate with a light meal or a snack. No
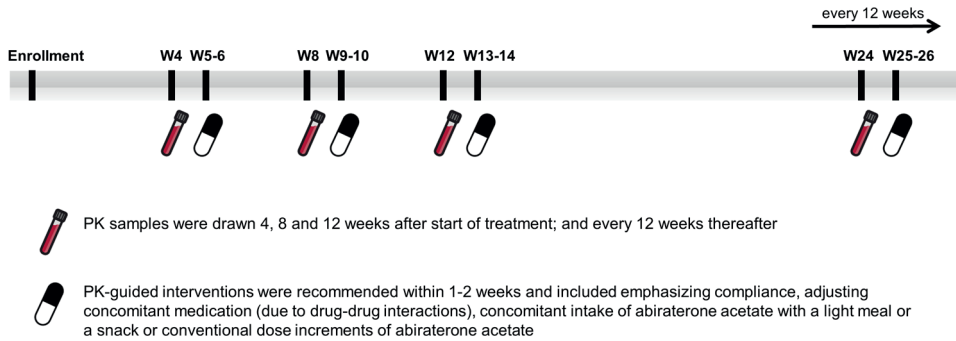
Figure 1. Schematic overview of study design.
Abbreviations: PK = pharmacokinetics, W = week.

prespecified meals were used. Patients were instructed that they could take abiraterone acetate for example with some bread, yoghurt or fruit but not with food high in fat. If exposure remained below the target, dose increments of abiraterone acetate were recommended (to 1,250 and 1,500 mg, respectively). Dose reductions were solely based on toxicities, not on pharmacokinetic exposure.

Statistical analyses

Patients were evaluable for the primary endpoint if they completed the first three PK measurements. The effect of concomitant intake of abiraterone acetate and food was evaluated by a Wilcoxon signed rank rest and a Mann Whitney U test. Other data were analysed using descriptive statistics. Statistical analyses were performed using R version 3.3.2 (R Project, Vienna, Austria) (10).

Ethical regulations

This study was assessed by the accredited Medical Ethics Committee of the Netherlands Cancer Institute – Antoni van Leeuwenhoek (NKI-AVL), Amsterdam, The Netherlands, on 3 May 2017 and it was reviewed not to fall under the Dutch Medical Research Involving Human Subjects Act, since TDM is performed as standard of care and no additional procedures were required for the participants. The institutional review board authorized the study on 7 August 2017. Patients did give written informed consent, since data were collected and shared. The study protocol followed the principles of the Declaration of Helsinki.

Results

Patient characteristics

In total, 32 evaluable patients were enrolled in the study between June 2017 and December 2018 (Figure 2). Baseline characteristics of these patients are provided in

Table 1. All patients had mCRPC, and the median age was 73 years. Twenty-nine patients completed the first three PK measurements and were eligible for the evaluation of the primary endpoint. Twenty patients (63%) had one or more C_{min} < 8.4 ng/mL at a certain time point during their treatment. In general, these patients tended to have a worse WHO performance status and received more prior lines of treatment compared to the patients with all C_{min} ≥ 8.4 ng/mL. At the time of data cut-off (30 August 2019), 13 patients (41%) were still on abiraterone acetate treatment with a median time of 11.4 months (range: 2.8 – 26.3 months).

Pharmacokinetic measurements
In total, 195 samples have been collected, with a median number of samples per patient of 6 (range: 1 – 13). An overview of the mean C_{min} and the proportion of patients with C_{min} below the efficacy threshold at each time point can be found in Table 2. After 4 weeks of abiraterone acetate treatment at 1,000 mg QD in modified fasting state, median abiraterone C_{min} was 12.5 ng/mL (range: 1 – 100 ng/mL) and 8 patients (25%) had a C_{min} < 8.4 ng/mL. After 12 weeks, median abiraterone C_{min} increased to 17 ng/mL (range: 7 – 126 ng/mL) after a food-intervention was implemented in patients with a low exposure, with 10% of patients not reaching the target.
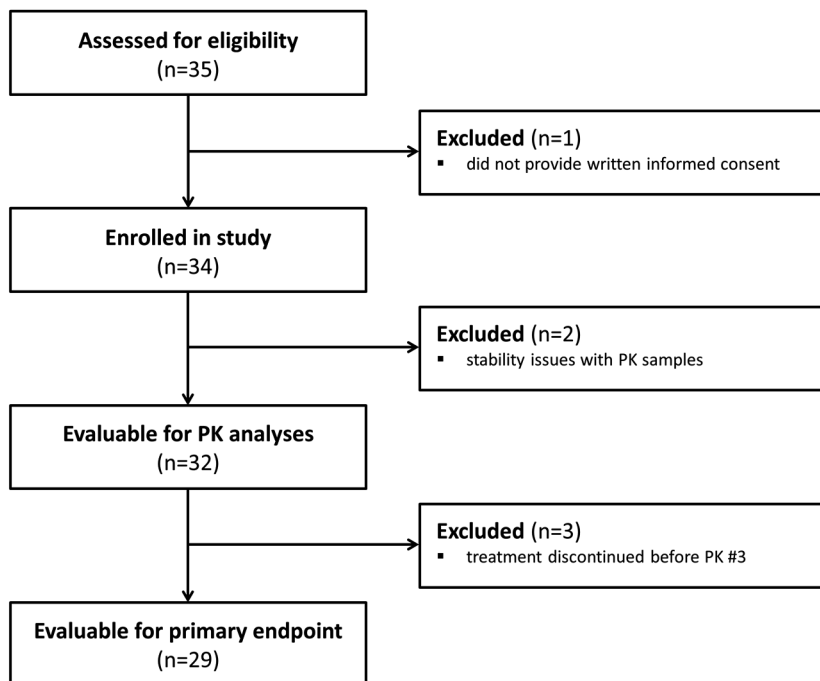
Figure 2. Patient flow chart.
Abbreviation: PK = pharmacokinetic.

Table 1. Baseline characteristics.

Characteristic	Patients with ≥ 1 measurement of abiraterone C_{min} < 8.4 ng/mL (n=20)	Patients with all measurements of abiraterone C_{min} ≥ 8.4 ng/mL (n=12)	All patients (n=32)
Age (years)	73 [52 – 87]	73 [63 – 83]	73 [52 – 87]
WHO performance status			
0	3 (15%)	5 (42%)	8 (25%)
1	11 (55%)	6 (50%)	17 (53%)
2	5 (25%)	1 (8%)	6 (19%)
3	1 (5%)	0	1 (3%)
Previous lines of systemic treatment			
0	11 (55%)	9 (75%)	20 (63%)
1	4 (20%)	2 (17%)	6 (19%)
≥ 2	5 (25%)	1 (8%)	6 (19%)
Previous systemic treatment			
Docetaxel	9 (45%)	2 (17%)	11 (34%)
Enzalutamide	3 (15%)	1 (8%)	4 (13%)
Radium-223	3 (15%)	1 (8%)	4 (13%)
Cabazitaxel	4 (20%)	0	4 (13%)
Gleason score			
≤ 7	10 (50%)	7 (58%)	17 (53%)
8 – 10	9 (45%)	5 (42%)	14 (44%)
missing	1 (5%)	0	1 (3%)
Baseline PSA (ng/mL)	83 [6 – 1036]	32 [6 – 282]	48 [6 – 1036]

Data are expressed as no. (%) or median [range], as appropriate.
Abbreviations: C_{min} = minimum plasma concentration, PSA = prostate specific antigen.

2.4

Pharmacokinetically guided dosing

Figure 3 provides a schematic overview of the PK-guided interventions and its results. The twenty patients (63%) with C_{min} < 8.4 ng/mL at a certain time point during treatment were recommended to take abiraterone acetate concomitantly with a light meal or a snack. In one patient, this PK-guided intervention could not be performed, since treatment was discontinued due to progressive disease. The interventions resulted in adequate pharmacokinetic exposure (i.e. C_{min} ≥ 8.4 ng/mL) in 16 patients (84%). In two patients, the effect could not be evaluated, as treatment was discontinued due to progressive disease before the next PK measurement. In one patient, C_{min} remained below the target level initially, and further dose escalation was not deemed feasible due to prior liver toxicity. Eventually, the target was reached with the recommended intake of food. Physician adherence to the recommendations was 100%.

Figure 4 shows box plots of abiraterone C_{min} in patients with adequate and low pharmacokinetic exposure, before and after concomitant intake with food. In the group of patients with adequate pharmacokinetic exposure (i.e. all C_{min} ≥ 8.4 ng/mL), in which no PK-guided intervention was needed, median abiraterone C_{min} was 22.5 ng/mL (range:

14.5 – 70 ng/mL). In the group with low pharmacokinetic exposure (i.e. C_{min} < 8.4 ng/mL), median abiraterone C_{min} before the PK-guided intervention was 7 ng/mL (range: 1 – 8 ng/mL). Concomitant intake of abiraterone acetate and food resulted in a significant increase in C_{min} to 26.5 ng/mL (range: 4 – 94 ng/mL, $p < 0.001$), which was comparable to the patients with all C_{min} above the target.

Table 2. Pharmacokinetic parameters.

Parameter	Result
Abiraterone C_{min}	in ng/mL [range]
PK #1 (week 4)	12.5 [1-100]
PK #2 (week 8)	17 [6-114]
PK #3 (week 12)	17 [7-126]
Patients with C_{min} below the target of 8.4 ng/mL	n (%)
PK #1 (week 4)	8 (25%)
PK #2 (week 8)	6 (19%)
PK #3 (week 12)	3 (10%)

Data are expressed as median [range] or number (%), as appropriate.
PK#1: 32 patients; PK#2: 31 patients; PK#3: 29 patients.
Abbreviations: C_{min} = minimum plasma concentration, PK = pharmacokinetic.
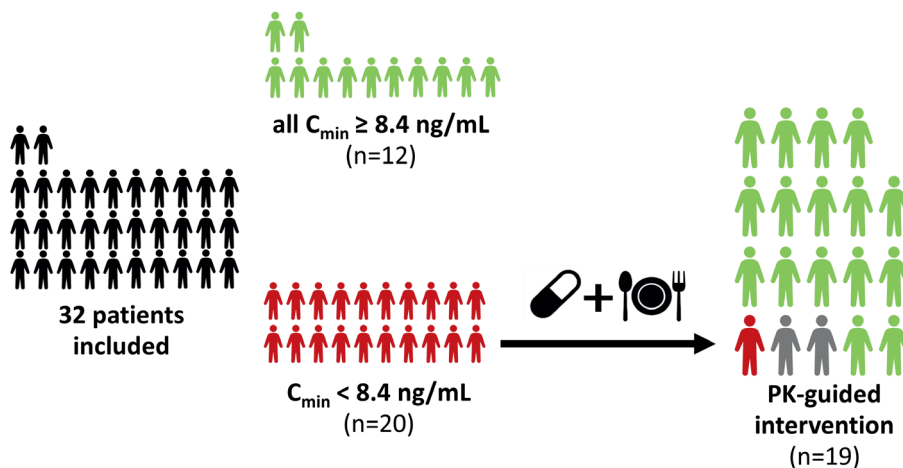
Figure 3. Schematic overview of study results.

Twenty patients (63%) had a C_{min} < 8.4 ng/mL at a certain time point during treatment. In one patient, a PK-guided intervention could not be performed, since treatment was discontinued due to progressive disease. In two patients, the effect of the PK-guided intervention could not be evaluated, since treatment was discontinued due to progressive disease before the next PK measurement. In one patient, the PK-guided intervention did not result in C_{min} ≥ 8.4 µg/L, further dose escalation was not deemed feasible due to prior liver toxicity.
Abbreviations: C_{min} = minimum plasma concentration, PK = pharmacokinetic.
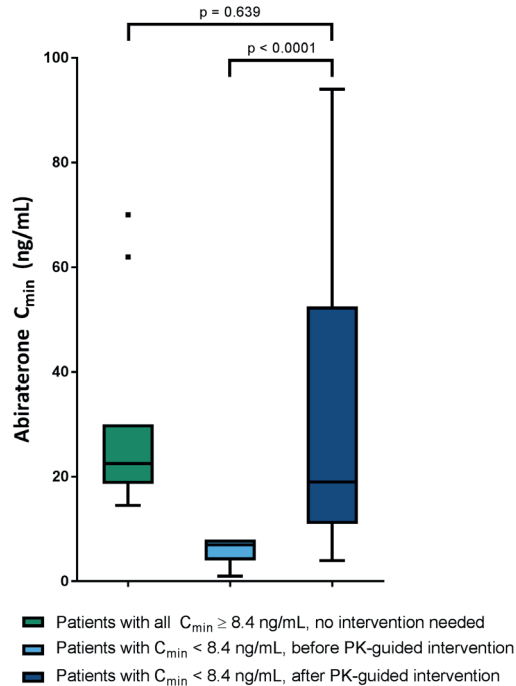
Figure 4. Box plots of abiraterone C_{min} in patients with adequate and low pharmacokinetic exposure, before and after concomitant intake with food.

Abbreviations: C_{min} = minimum plasma concentration, PK = pharmacokinetic.

2.4

Toxicity

None of the PK-guided interventions led to additional toxicities. In total, three patients needed a dose reduction to 500 mg QD due to toxicity (elevated liver enzymes (n=2) and fatigue (n=1)). Median C_{min} at presentation was 33 ng/mL (range: 11 – 48 ng/mL). After dose reduction, pharmacokinetic exposure remained adequate in two patients. In one patient, C_{min} dropped below the target, after which the dose was carefully increased to 1,000 mg QD concomitant with food and the target was reached eventually.

Efficacy

Median time on abiraterone acetate treatment was 9.5 months (95% CI: 6.8 – NA) in patients with one or more C_{min} < 8.4 ng/mL, compared to 17.4 months (95% CI: 16.0 – NA) in patients with all $C_{min} \geq 8.4$ ng/mL. In six patients, the last C_{min} before treatment discontinuation was < 8.4 ng/mL.

Discussion

In this prospective clinical study we evaluated the feasibility of pharmacokinetically guided abiraterone acetate dosing. At the authorized dose of 1,000 mg QD in modified fasting state, 63% of patients had a C_{min} < 8.4 ng/mL at a certain time point during treatment. Concomitant intake with a light meal or a snack in these patients resulted in a 3.8-fold increase in C_{min} without additional toxicities (Figures 3 and 4; Table 2). In this way, the proportion of patients with a low pharmacokinetic exposure was reduced from 25% after 4 weeks to 10% after 12 weeks. Hence, TDM of abiraterone is feasible and concomitant intake with food offers a cost-neutral strategy to optimize treatment in patients with a low pharmacokinetic exposure. For the small proportion of patients in whom the target is not attained with this food-intervention, a dose increase can be recommended.

In our study, 63% of patients had a low exposure at a certain time point during treatment, which is notably higher than the 35 – 42% reported in literature (3,4). However, these values refer to the mean and median exposure to abiraterone, respectively, while in our study it represents the proportion of patients with a single measurement below the target. It is remarkable that especially patients with more prior lines of treatment appear to be at risk of a low pharmacokinetic exposure, which was also seen in our previous exposure-response analysis for abiraterone (4). It would be of interest to further investigate the mechanism behind the lower exposure in this subgroup of patients (e.g. higher clearance, due to enzyme induction, or decreased absorption).

Concomitant intake with food not only resulted in an increased pharmacokinetic exposure, but also led to a considerably higher interindividual variability (Figure 4). This is illustrated by the fact that some patients attained very high C_{min} levels (up to 94 ng/mL). This may be attributed to the fact that meals were not prespecified and that the composition could thus differ between patients and time points. However, no additional toxicities were experienced by these patients, which is in line with previous literature where no exposure-toxicity relationship was found either (1,3,4). Therefore, the increased interindividual variability in pharmacokinetic exposure is considered acceptable, as long as C_{min} levels are above 8.4 ng/mL.

The magnitude of the food-effect on pharmacokinetic exposure in our study is not in line with the previous food-effect study by Chi *et al*. While they found a similar pharmacokinetic exposure (i.e. area under the concentration-time curve (AUC)) for a low-fat meal compared to modified fasting state, our study shows a 3.8-fold increase in C_{min} after concomitant intake with a light meal or a snack. A possible explanation for this could be the fact that many patients (65%) took abiraterone acetate early in the morning, which was probably after an overnight fast. In that case, the results would be more consistent with the study of Chi *et* al., who reported a five-fold increase in AUC for a low-fat meal compared to overnight fasting in healthy volunteers (6).

Compared to conventional dose increments, concomitant intake with food offers a cost-neutral opportunity to increase pharmacokinetic exposure. Although a longer treatment duration could result in higher total treatment costs, this was demonstrated to be cost-effective (11). Additional costs for a 250 mg or 500 mg increase in abiraterone acetate dose would be €862 or €1782, respectively, per patient per month in The Netherlands. Furthermore, concomitant intake with food provides a more patient-friendly alternative, since patients do not have to take into account the modified fasting conditions.

This prospective study provides real life data on a TDM program. Advantages of this study design include the fact that data are representative for the abiraterone population in clinical practice and that our findings can easily be implemented in routine care. On the other hand, this is simultaneously a limitation of our study, since compliance could not be guaranteed (i.e. no drug accountability has been performed and no patient diaries were used).

Although this study demonstrated that an adequate pharmacokinetic exposure could be attained in the majority of patients by the support of TDM, the ultimate goal of TDM is to improve treatment efficacy. Preliminary data on efficacy in this small group of patients indicate that patients who needed a PK-guided intervention still have a shorter time on abiraterone acetate treatment than patients with all adequate C_{min}. However, patients with a low C_{min} had a less favourable prognosis at baseline, as they received more prior lines of treatment and had a worse WHO performance status. To evaluate whether TDM actually improves treatment outcomes, a larger cohort of patients will be needed. Therefore, patient inclusion in this study will continue in order to investigate the effect on treatment efficacy as well.

The significant food effect of abiraterone raises two other interesting concepts. The first of which is a cost-saving approach: treating patients at a lower abiraterone acetate dose with food, as has been evaluated by Szmulewitz *et al*. (12). The other is a more pragmatic concept: to recommend concomitant intake with food to all patients, regardless of pharmacokinetic exposure.

In conclusion, we demonstrated that TDM of abiraterone is feasible in clinical practice. Furthermore, concomitant intake of abiraterone acetate and food resulted in a significant increase in C_{min} and thereby offers a safe and cost-neutral opportunity to optimize treatment in patients with a low pharmacokinetic exposure. Therefore, we recommend to implement TDM of abiraterone for all patients in routine care.

2.4

References

1. Committee for Medicinal Products for Human Use (CHMP) European Medicines Agency. Abiraterone European Public Assessment Report. 2011 [cited 2019 Sept]. Available from: http://www.ema.europa.eu/docs/en_GB/document_library/EPAR_-_Product_Information/human/002321/WC500112858.pdf

2. Steven X, Charles X, Kim JR, Matthew S, Saad F, Griffin TW, et al. Modeling the Relationship Between Exposure to Abiraterone and Prostate-Specific Antigen Dynamics in Patients with Metastatic Castration-Resistant Prostate Cancer. Clin Pharmacokinet. 2017;56:55–63.

3. Carton E, Noe G, Huillard O, Golmard L, Giroux J, Cessot A, et al. Relation between plasma trough concentration of abiraterone and prostate-specific antigen response in metastatic castration-resistant prostate cancer patients. Eur J Cancer. 2017;72:54–61.

4. van Nuland M, Groenland S, Bergman A, Steeghs N, Rosing H, Venekamp N, et al. Exposure-response analyses of abiraterone and its metabolites in real-world patients with metastatic castration-resistant prostate cancer. Prostate Cancer Prostatic Dis. 2019;Epub ahead of print.

5. Summary of Product Characteristics of abiraterone acetate. 2016 [cited 2019 Sept]. Available from: https://www.ema.europa.eu/en/documents/product-information/zytiga-epar-product-information_en.pdf

6. Chi KN, Spratlin J, Kollmannsberger C, North S, Pankras C, Gonzalez M, et al. Food effects on abiraterone pharmacokinetics in healthy subjects and patients with metastatic castration-resistant prostate cancer. J Clin Pharmacol. 2015;55:1406–14.

7. Groenland SL, van Eerden RAG, Verheijen RB, Koolen SLW, Moes DJAR, Desar IME, et al. Therapeutic drug monitoring of oral anticancer drugs: the DPOG-TDM protocol for a prospective study. Ther Drug Monit. 2019; Epub ahead of print.

8. Nuland M Van, Venekamp N, Vries N De, Jong KAM De, Rosing H, Beijnen JH. Development and validation of an UPLC-MS / MS method for the therapeutic drug monitoring of oral anti-hormonal drugs in oncology. J Chromatogr B. 2019;1106–1107:26–34.

9. Food and Drug Administration. Center for Drug Evaluation and Research. Abiraterone Clinical Pharmacology and Biopharmaceutics Review. 2010 [cited 2019 Sept]. Available from: https://www.accessdata.fda.gov/drugsatfda_docs/nda/2011/202379Orig1s000ClinPharmR.pdf

10. R Core Development Team. A language and environment for statistical computing. R Found Statistical Computing, Vienna. 2016 [cited 2019 Sept]. Available from: https://www.r-project.org/

11. ten Ham R, van Nuland M, Vreman R, de Graaf L, Rosing H, Bergman A, et al. Early health technology assessment: monitoring abiraterone levels in metastatic castration-resistant prostate cancer patients treated with abiraterone acetate. Chapter 2.9. Submitted.

12. Szmulewitz RZ, Peer C, Ibraheem A, Martinez E, Kozloff MF, Carthon B, et al. Prospective International Randomized Phase II Study of Low-Dose Abiraterone With Food Versus Standard Dose Abiraterone In Castration-Resistant Prostate Cancer. J Clin Oncol. 2018;36:1389–95.

2.4

Plasma levels of enzalutamide and its main metabolites in a metastatic castration-resistant prostate cancer patient undergoing hemodialysis

Merel van Nuland
Stefanie L. Groenland
Andries M. Bergman
Joris I. Rotmans
Hilde Rosing
Jos H. Beijnen
Alwin D.R. Huitema

Clinical practice points

- Enzalutamide is a well-established treatment option for patients with metastatic castration-resistant prostate cancer (mCRPC). However, for patients with end-stage renal disease, no pharmacokinetic data is available. Therefore, we present a case of a patient with end-stage renal disease undergoing hemodialysis treated with enzalutamide, including plasma levels of enzalutamide and its main metabolites.
- The pharmacokinetics of enzalutamide were explored in a 79-year old man diagnosed with mCRPC undergoing hemodialysis. The patient was initially treated with 160 mg enzalutamide daily, but received a dose reduction to 80 mg due to adverse events.
- Plasma levels of enzalutamide and *N*-desmethyl enzalutamide were in line with the average values cited in the literature in patients with normal renal function, however, enzalutamide carboxylic acid concentrations were significantly increased compared to literature (34 µg/mL versus 4.22 µg/mL; 80 mg QD).
- We are the first to show that the pharmacokinetics of enzalutamide and the active metabolite *N*-desmethyl enzalutamide are not affected by hemodialysis in a 79-year old man with end-stage renal disease. Enzalutamide seems a feasible treatment strategy for patients undergoing hemodialysis. However, further studies will be required to confirm these findings.

Introduction

Prostate cancer is the most common malignancy in men in the Western population (1–3). After initial response to androgen deprivation therapy, the disease will eventually progress into metastatic castration-resistant prostate cancer (mCRPC); a clinical state in which the androgen receptor axis is reactivated, despite testosterone suppression. Treatment options of patients with mCRPC currently consists of docetaxel, cabazitaxel, radium-223, and anti-hormonal treatment with enzalutamide or abiraterone acetate (4). Enzalutamide inhibits the androgen signaling pathway by androgen receptor blockage (5,6). After gastrointestinal uptake, enzalutamide is converted to the active metabolite *N*-desmethyl enzalutamide by cytochrome P450 2C8/3A4 and to the inactive metabolite enzalutamide carboxylic acid by carboxylesterase 1 (5). The potency of *N*-desmethyl enzalutamide is similar to that of enzalutamide itself. Median steady-state trough plasma concentrations of enzalutamide, *N*-desmethyl enzalutamide and enzalutamide carboxylic acid are 11.4 ± 3.0 µg/mL, 13.0 ± 3.8 µg/mL, and 8.44 ± 6.8 µg/mL, respectively (5,7). Due to the long half-life of enzalutamide (~6 days), steady-state concentrations are reached after approximately one month. Enzalutamide and *N*-desmethyl enzalutamide are cleared hepatically, while enzalutamide carboxylic acid clearance mainly depends on renal excretion. Furthermore, enzalutamide is highly protein-bound in plasma (>95%). Therefore, substantial clearance of enzalutamide by hemodialysis is unlikely.

There is limited evidence to support therapeutic drug monitoring (TDM) of enzalutamide. However, in a phase 1 trial higher androgen receptor binding has been shown with a median plasma trough concentration of 11.4 µg/mL compared to 5.0 µg/mL (8). Therefore, a minimum trough concentration of 5.0 µg/mL could be considered as a target for exposure to enzalutamide (9).

No dose adjustments of enzalutamide are needed for patients with mild or moderate renal impairment. However, no recommendations are available for patients with severe renal impairment or end-stage renal disease, since these patients have not been included in the registration studies (5). Two case-reports have been published describing safe use of enzalutamide in this vulnerable patient population, focusing solely on the safety of enzalutamide treatment without pharmacokinetic assessment (10,11). We present a case of enzalutamide treatment in a patient with end-stage renal disease undergoing hemodialysis, including plasma levels of enzalutamide, the active metabolite *N*-desmethyl enzalutamide and the inactive metabolite enzalutamide carboxylic acid.

Case report

A 79-year-old male presented with a history of mCRPC and end-stage renal disease secondary to chronic post renal obstruction, for which he started hemodialysis six months earlier. Hemodialysis was performed only 2 times per week during 3 hours (Kt/V 1.1 per session) as he had some residual kidney function (creatinine clearance 5 mL/min).

2.5

Table 1. Patient characteristics at baseline and during treatment. Abbreviations: eGFR = estimated glomerular filtration rate, MDRD-4 = modification on diet in renal disease, ASAT = aspartate aminotransferase, ALAT = alanine aminotransferase, γ-GT = gamma glutamyltransferase.

Parameter	Baseline	2 weeks	4 weeks	8 weeks
Dose (mg, QD)	-	160	80	80
Plasma concentrations (µg/mL):				
Enzalutamide	-	6.74	4.94	5.59
N-Desmethyl enzalutamide		3.71	5.95	3.83
Enzalutamide carboxylic acid		14.0	34.0	36.4
PSA (µg/L)	2.2	14.5	19.5	39.2
Kidney function:				
Creatinine (µmol/L)	460	654	515	588
eGFR (MDRD-4)	11	7	9	8
Liver function:				
Bilirubin (µmol/L)	5	5	6	7
ASAT (U/L)	14	47	19	19
ALAT (U/L)	7	11	17	12
γ-GT (U/L)	14	15	15	14
Testosterone (ng/mL) [a]	<0.5	0.02	0.03	0.02

[a] At baseline, testosterone was determined with an immunoassay (limit of quantification being 0.5 ng/mL), while at later time points testosterone was quantified using liquid-chromatography mass spectrometry (limit of quantification being 0.01 ng/mL)

This patient was initially diagnosed with a cT1cNxM0 prostate carcinoma in 2002, with a Gleason score of 4+4, and treated with External Beam Radiotherapy to the prostate. In 2015, multiple metastases in the bones and lymph nodes were found, after which systemic treatment with cyproterone acetate was started. In 2017, PSA progression was seen and triptorelin was added to the treatment. After 8 months, progression of the bone metastases was observed and enzalutamide treatment was initiated. Treatment was started at the regular dose of 160 mg once daily (QD). Three weeks after start of treatment, enzalutamide was temporarily withheld due to skeletal pain, anorexia and dysgeusia. A few days later enzalutamide was resumed after a dose reduction to 80 mg QD, which was well tolerated. After two months, further treatment with enzalutamide was ceased due to prostate specific antigen (PSA) progression. Patient characteristics at baseline and during treatment are given in Table 1. Concomitant medication during treatment consisted of alfuzosin (10 mg QD), alfacalcidol (0.25 mg QD), omeprazole (20 mg QD), sodium carbonate (500 mg QD) and triptorelin (11.25 mg once every 3 months).

During treatment, plasma concentrations of enzalutamide, *N*-desmethyl enzalutamide and enzalutamide carboxylic acid were measured using a validated LC-MS/MS assay as part of routine clinical care (12). Minimum plasma concentrations were not calculated for enzalutamide and its metabolites regarding the long elimination half-lives (~6 days).
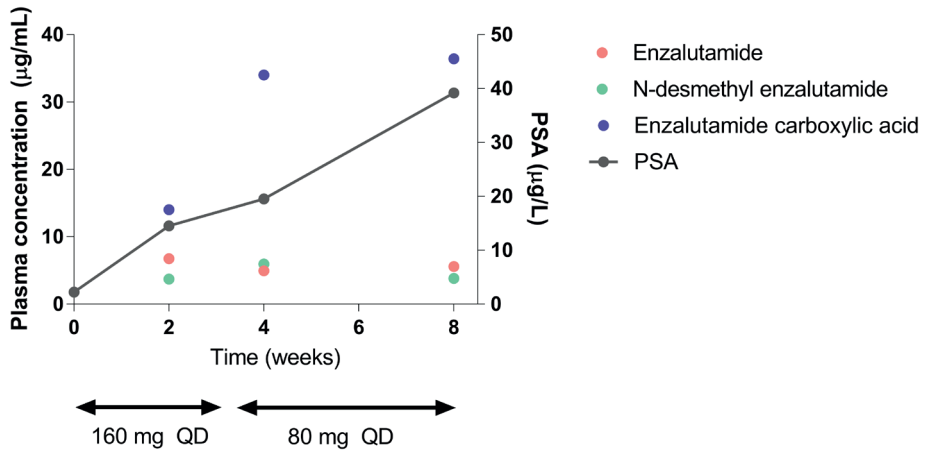
Figure 1. Plasma concentrations of enzalutamide and its main metabolites, PSA levels and corresponding enzalutamide dosages in a patient with end-stage renal disease undergoing hemodialysis. Three weeks after start of treatment, enzalutamide was temporarily withheld due to skeletal pain, anorexia and dysgeusia. A few days later enzalutamide was resumed after a dose reduction to 80 mg QD, which was well tolerated. After two months, further treatment with enzalutamide was ceased due to PSA progression. Abbreviations: PSA = prostate specific antigen, QD = once daily.

Table 1 shows the plasma concentrations of enzalutamide and both metabolites after 2, 4 and 8 weeks of treatment. Figure 1 visualizes concentrations, PSA levels and the corresponding enzalutamide dosages.

2.5

Discussion

In metastatic castration-resistant prostate cancer, anti-hormonal therapy is an important treatment modality. Enzalutamide was granted market access in 2011 (5). However, no data existed for plasma concentrations of enzalutamide and both major metabolites, in patients with end-stage renal disease undergoing chronic hemodialysis, which we described in this case report.

Overall, treatment with 160 mg of enzalutamide QD was not well tolerated by the patient. Therefore, the daily dose was reduced to 80 mg QD. In similar case reports, no significant toxicities were observed (10,11). Plasma levels were measured at two weeks, one month and two months after start of treatment. Although the first sample was taken while plasma concentrations were not yet at steady-state, the enzalutamide concentration was above the suggested target of 5.0 µg/mL. Thus far, no data on steady-state concentrations after administration of an 80 mg dose have been reported in previous studies. However, the phase 1 dose-escalation study showed linear pharmacokinetics over the studied dose range (30-600 mg) (8). Taken this data into account, estimated plasma concentrations would be half of those observed after administration of an 160 mg dose: 5.7 µg/mL, 6.5 µg/mL and 4.22 µg/mL for

enzalutamide, *N*-desmethyl enzalutamide and enzalutamide carboxylic acid, respectively. Enzalutamide and *N*-desmethyl enzalutamide concentrations after 4 and 8 weeks of therapy are in line with the average values in patients with adequate renal function, considering the 80 mg dose. However, plasma levels of the enzalutamide carboxylic acid metabolite rise far above reported concentrations (34.0 and 36.4 μg/mL versus 4.22 μg/mL). This can be attributed to the fact that carboxylic acid enzalutamide is excreted renally, while enzalutamide and *N*-desmethyl enzalutamide are not detected in urine (5,6). Although enzalutamide carboxylic acid is considered inactive at a median concentration of 8.44 μg/mL (160 mg QD), a safety profile of accumulation up to 36.4 μg/mL due to renal failure has not been evaluated. Therefore, this clinical significance of higher enzalutamide carboxylic acid plasma concentrations is unknown. Although we did not measure enzalutamide levels in the dialysate, our results indicate that hemodialysis does not affect the pharmacokinetics of enzalutamide and its active metabolite, while plasma concentrations of the inactive metabolite are increased.

Conclusion

In this case report we present a patient with metastatic castration-resistant prostate cancer undergoing hemodialysis. Plasma levels of enzalutamide and the active metabolite *N*-desmethyl enzalutamide were similar to those observed in patients with an adequate renal function, taking into account the 80 mg dose QD, while plasma concentrations of the inactive metabolite enzalutamide carboxylic acid were increased up to 8-fold. As the pharmacokinetics of enzalutamide and the active metabolite *N*-desmethyl enzalutamide are rarely affected by hemodialysis, enzalutamide seems to be a feasible treatment strategy for patients with end-stage renal disease undergoing hemodialysis. However, further studies will be required to confirm these findings.

References

1. Fitzmaurice C, Allen C, Barber RM, Barregard L, Bhutta ZA, Brenner H, et al. Global, regional, and national cancer incidence, mortality, years of life lost, years lived with disability, and disability-adjusted life-years for 32 cancer groups, 1990 to 2015: A Systematic Analysis for the Global Burden of Disease Study Global Burden . JAMA Oncol. 2017;3:524–48.

2. Siegel RL, Miller KD, Jemal A. Cancer statistics, 2016. CA Cancer J Clin. 2016;66:7–30.

3. American Cancer Society. Global Cancer Facts & Figures 3rd Edition. American Cancer Society. 2015.

4. Heidenreich A, Bastian PJ, Bellmunt J, Bolla M, Joniau S, van der Kwast T, et al. EAU guidelines on prostate cancer. Part II: Treatment of advanced, relapsing, and castration-resistant prostate cancer. Eur Urol. 2014;65:467–79.

5. US Food and Drug Administration. Clinical Pharmacology and Biopharmaceutics Review: Xtandi (Enzalutamide). Silver Spring (MD). 2012 [cited 2018 Jun]. p. 1–75. Available from: https://www.accessdata. fda.gov/drugsatfda_docs/nda/2012/203415Orig1s000ClinPharmR.pdf

6. US Food and Drug Administration. Prescribing information: Xtandi (enzalutamide). Silver Spring (MD). 2012 [cited 2018 Jun]. p. 1–16. Available from: https://www.accessdata.fda.gov/drugsatfda_docs/ label/2012/203415lbl.pdf

7. Gibbons JA, Ouatas T, Krauwinkel W, Ohtsu Y, van der Walt J-S, Beddo V, et al. Clinical Pharmacokinetic Studies of Enzalutamide. Clin Pharmacokinet. 2015;54:1043–55.

8. Scher HI, Beer TM, Higano CS, Anand A, Taplin M-E, Efstathiou E, et al. Antitumour activity of MDV3100 in castration-resistant prostate cancer: a phase 1-2 study. Lancet . 2010;375:1437–46.

9. Groenland SL, van Nuland M, Verheijen RB, Schellens JHM, Beijnen JH, Huitema ADR, et al. Therapeutic Drug Monitoring of Oral Anti-Hormonal Drugs in Oncology. Clin Pharmacokinet. 2018:Epub ahead of print.

10. Simoes J, Augusto I, Meireles S, Vendeira L, Silva C. Metastatic castration-resistant prostate cancer and the challenge of a patient with chronic kidney disease in hemodialysis. Autops case reports. 2018;8:e2018011.

11. Tsang ES, de Haan M, Eigl BJ. A case report of enzalutamide administration in a dialysis-dependent patient with castration-resistant prostate cancer. J Oncol Pharm Pract. 2018;24:143–5.

12. van Nuland M, Hillebrand MJ., Rosing H, Schellens JHM, Beijnen JH. Development and validation of an LC-MS/MS method for the simultaneous quantification of abiraterone, enzalutamide, and their major metabolites in human plasma. Ther Drug Monit. 2017;39:243–51.

2.5

Efficacy, tolerance and plasma levels of abiraterone and its main metabolites in a metastatic castration-resistant prostate cancer patient with a hepatic transplant

Merel van Nuland
Julie M. Janssen
Bart van Hoek
Hilde Rosing
Jos H. Beijnen
Andries M. Bergman

Clinical practice points

- Abiraterone acetate is a well-established treatment option for metastatic castration-resistant prostate cancer (mCRPC) patients, which is metabolized in the liver. The impact of hepatic impairment on exposure to abiraterone was well studied during registration studies and abiraterone acetate is contra-indicated for patients with severe hepatic impairment. Patients with a liver transplant are prone to impaired liver functions and use medication that may affect drug metabolism. However, no efficacy, tolerance and pharmacokinetic data have been published on abiraterone treatment in liver transplant patients.
- In this case report we established plasma concentrations of abiraterone and its major metabolites Δ(4)-abiraterone (D4A), abiraterone N-oxide sulfate and abiraterone sulfate in a mCRPC patient with a hepatic transplant who was treated with abiraterone in a reduced dose of 500 mg daily.
- Treatment was effective, well tolerated and plasma concentrations were above the suggested trough concentration (Cmin) threshold of 8.4 ng/mL. Moreover, the exposure to immunosuppressive drugs was within expected therapeutic ranges.
- From this case we conclude that abiraterone actetate seems to be a feasible and safe treatment strategy for patients with a hepatic transplant. However, further clinical studies should be performed in order to confirm these findings.

Introduction

Abiraterone acetate (Zytiga®) is a 17α-hydroxylase/C17,20-lyase (CYP17) inhibitor, thereby preventing the production of tumor-stimulating androgens such as testosterone. Abiraterone acetate was registered for treatment of metastatic castration-resistant prostate cancer (mCRPC) as it improves overall survival (OS) and progression free survival (PFS) in this patient population compared to placebo (1,2).

After oral ingestion, abiraterone acetate is rapidly deacetylated into the active substance abiraterone (3). Further hepatic metabolism of abiraterone is extensive and the inactive metabolites abiraterone N-oxide sulfate and abiraterone sulfate are formed (3,4). More recently, the active metabolite Δ(4)-abiraterone (D4A) was discovered, which is formed by conversion of abiraterone by the enzyme 3β-hydroxysteroid-dehydrogenase (3βHSD) (5,6). D4A not only blocks CYP17, but also inhibits multiple steroidic enzymes and blocks the androgen receptor (6,7), which makes it likely that D4A is even more potent than abiraterone.

Clinical studies have shown that approximately 2% of patients using abiraterone acetate show liver function test elevations. Therefore, dose modifications are recommended for patients who develop hepatotoxicity while on treatment (3). In a dedicated hepatic impairment study, exposure to abiraterone (1000 mg once daily, QD) was similar in subjects with mild hepatic impairment (Child-Pugh classification A, n=8) and in subjects with normal hepatic function. However, subjects with moderate hepatic impairment (Child-Pugh classification B, n=8) and severe hepatic impairment (Child-Pugh classification C, n=8) had higher exposure, a higher maximum concentration (C_{max}) and a longer elimination half-life ($t_{1/2}$) compared to subjects with a normal hepatic function. From this study it was concluded that a dose reduction to 250 mg is recommended in patients with moderate hepatic impairment, while abiraterone acetate is contra-indicated in patients with severe hepatic impairment. (8)

Although the impact of hepatic impairment on abiraterone exposure was studied during registration, no treatment adjustments are provided for cancer patients with a hepatic transplant. Patients with a functional liver transplant are at risk to develop impaired liver functions and use medication that may affect drug pharmacokinetics (9). We here present a case of a mCRPC patient with a hepatic transplant who was treated with abiraterone acetate. Plasma concentrations of abiraterone and its major metabolites were assessed and concomitant treatment with immunosuppressive agents cyclosporin and mycophenolic acid was evaluated.

Case report

A 76-year old male with a history of localized prostate cancer and a hepatic transplant presented with mCRPC. The liver transplant was placed in 2006 because of liver failure due to primary biliary cirrhosis with Child-Pugh classification B/C. After a first rejection of the liver allograft, a second liver transplant was placed in the same year. To date, the liver function of this second transplant is adequate.

2.6

The patient was first diagnosed with cT1cNxM0 prostate cancer and a Gleason score of 6 in 2000 and initially treated with External Beam Radiotherapy to the prostate. In 2017, bone metastases were found and androgen deprivation treatment (goserelin 10.8 mg subcutaneously every 3 months) was initiated. mCRPC was established in 2018 when serum prostate specitifc antigen (PSA) levels progressed under suppressed serum testosterone levels (<1.7 nmol/L). Patient characteristics are given in Table 1. Concomitant immunosuppressive medication consisted of cyclosporin (50 mg bi daily, BID), mycophenolic acid (1500 mg BID) and other medication of denosumab (70 mg every month), calcium carbonate / cholicalciferol (1.25g / 800 IE QD), ursodeoxycholic acid (250 mg BID) and pantoprazole (20 mg BID). In october 2018, progressive bone metastases were established and abiraterone acetate in combination with prednisone (5 mg BID) under fasting conditions was initiated. Since tolerance of abiraterone in a patient with a liver transplant could not be predicted, abiraterone treatment was initiated at a reduced dose of 500 mg QD. Abiraterone acetate treatment was well tolerated with an initial drop in serum PSA from 119 to 36.6 ng/mL. However, two months after therapy start, the PSA level slightly increased and prednisone was replaced by dexamethasone (0.5 mg QD) to re-induce abiraterone sensitivity (10). During abiraterone and dexamethasone treatment, the PSA further declined to 28.8 ng/mL. Furthermore, a decrease in serum alkaline phosphatase levels was observed, which may serve as a biomarker for the extent of bone metastasis (11).

During treatment, plasma concentrations of abiraterone and its main metabolites D4A, abiraterone N-oxide sulfate and abiraterone sulfate were measured using validated liquid chromatography- tandem mass spectrometry (LC-MS/MS) methods (12,13). Plasma trough concentrations (C_{trough}) of abiraterone and its metabolites were calculated using Equation 1, in order to compare the individual plasma levels with C_{trough} concentrations from literature. Plasma concentrations were above the suggested target concentration of 8.4 µg/L (14) sand thus abiraterone remained at 50% of the dose troughout treatment. Table 1 shows the exposure to cyclosporin and mycophenolic acid as well as plasma concentrations of abiraterone and its metabolites during treatment. Figure 1 visualizes active drug and metabolite concentrations along with PSA levels.

Equation 1 (15): $$C_{trough} = C_{TAD} * 0.5^{\frac{24-TAD}{t_{\frac{1}{2}}}}$$

Wherein C_{trough} is the calculated trough concentration in µg/L and C_{TAD} the measured concentration in µg/L at the recorded time after abiraterone acetate dosing (TAD), given in hours. Trough concentrations were calculated using the following $t_{1/2}$: 15 hours for abiraterone, abiraterone sulphate, and D4A, and 21.6 hours for abiraterone N-oxide sulphate, respectively (4). Furthermore, exposure to cyclosporin and mycophenolic acid was monitored using a limited sampling stategy: drug concentrations were determined at 0, 1, 2 and 3 hours after administration, and the area under the curve was estimated from 0 to 12 hours (AUC_{0-12}) (16).

Table 1. Patient characteristics at baseline and during treatment.

Parameter	Baseline	1 month	2 months	3 months	4 months
Dose (mg, QD)	-	500	500	500	500
Plasma concentrations (µg/L)*:					
Abiraterone	-	47.8 (131)	30.3 (70.1)	20.9 (45.8)	-
D4A	-	2.00 (5.42)	1.40 (3.31)	1.00 (2.15)	-
Abiraterone N-oxide sulfate	-	3619 (7,440)	5609 (10,200)	5991 (10,500)	-
Abiraterone sulfate	-	5907 (16,200)	3966 (9,160)	3123 (6,850)	-
AUC_{0-12} (mg/L•h)					
Ciclosporin	1.42	-	-	1.08	-
Mycophenolic acid	48	-	-	34	-
PSA (µg/L)	119.2	36.61	39.65	46.07	28.76
Kidney function:					
Creatinine (µmol/L)	100	100	87	99	90
eGFR (MDRD-4)	63	63	74	64	71
Hepatic markers:					
Bilirubin, total (µmol/L)	18	11	13	14	15
Bilirubin, direct (µmol/L)	-	-	-	-	7
ASAT (U/L)	33	21	24	19	26
ALAT (U/L)	20	21	18	15	13
γ-GT (U/L)	141	89	70	49	56
Alkaline phosphatase (U/L)	1153	2326	1045	419	359
(change from baseline, %)	-	202	91	36	31
Albumin (g/L)	41	41	45	43	45
Total protein (g/L)	73	69	71	71	69
LDH (U/L)	182	148	179	168	176
APTT (sec)	28	-	-	-	29
PT-INR	1.1	-	-	-	1.1
Haptoglobulin (g/L)	-	-	-	-	1.0
t-Amylase (U/L)	-	-	-	-	61
Cholesterol (mmol/L)	-	-	-	-	4.7
Tryglicerides (mmol/L)	-	-	-	-	1.0
Ammoniak (µmol/L)	-	-	-	-	32
Testosterone (nmol/L)	-	<0.025	<0.025	<0.025	<0.025

Abbreviations: D4A = Δ(4)-Abiraterone, AUC = area under the curve, PSA = prostate specific antigen, eGFR = estimated glomerular filtration rate, ASAT = aspartate aminotransferase, ALAT = alanine aminotransferase, γ-GT = gamma-glutamyltransferase, LDH = lactate dehydrogenase, APTT = activated partial thromboplastin time, PT-INR = prothrombin time-international normalized ratio. * Calculated trough concentrations and the originally measured plasma concentrations between brackets.

2.6

Discussion

Abiraterone acetate treatment is an effective treatment option for mCRPC patients. Although it is known that the exposure to abiraterone is higher in patients with moderate and severe hepatic impairment compared to subjects with a normal hepatic function (8), no data has been published on the exposure to abiraterone in hepatic transplant recipients. In this case report we describe the treatment of a liver transplant mCRPC patient with abiraterone.
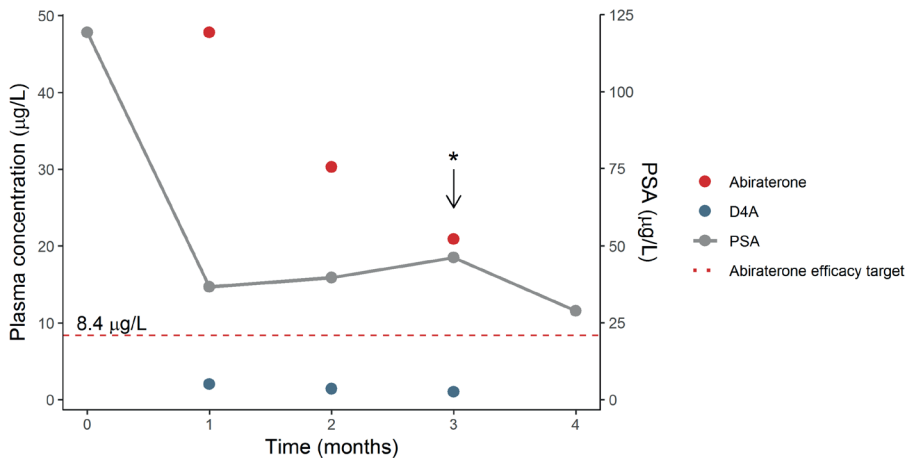
Figure 1. Plasma concentrations of abiraterone and Δ(4)-abiraterone (D4A), including PSA levels in a patient with a hepatic transplant treated with abiraterone acetate (500 mg QD). * Prednisone was replaced by dexamethasone, resulting in a PSA decline. Abbreviations: D4A = Δ(4)-abiraterone, PSA = prostate specific antigen, QD = once daily.

Treatment options for mCRPC, apart from abiraterone acetate, include enzalutamide and docetaxel. Enzalutamide is a strong cytochrome P450 3A4 (CYP3A4) inducer and was therefore not recommended in combination with cyclosporin, while docetaxel may elevate hepatic markers and is contra-indicated for patients with hepatic dysfunction (17,18). Therefore, this patient was treated with abiraterone acetate, which was tolerated well at the administered dose of 500 mg QD, and most importantly, no hepatotoxicity was observed. Plasma concentrations were determined at steady-state, with the mean trough concentration of abiraterone being 33 µg/L. In a prospective observational trial in patients with mCRPC, a relationship was found between abiraterone trough levels and PSA response. PSA-responders (n=38) had significantly higher plasma concentrations of abiraterone compared to non-responders (n=23) (12.0 versus 8.0 µg/L, p=0.0015). By receiver operating characteristics (ROC) analysis, a minimum C_{trough} of 8.4 µg/L was defined as a target for exposure to abiraterone (14). In our case, the calculated trough concentrations were above this threshold, indicating adequate exposure to abiraterone with 50% of the dose.

The mean trough concentration of the active metabolite D4A (1.5 µg/L) was in line with the mean C_{trough} in a previously reported study (1.6 µg/L, n=36) (19). Mean trough concentrations of abiraterone N-oxide sulfate and abiraterone sulfate were 5,073 and 4,332 µg/L, respectively. To our knowledge, no abiraterone N-oxide sulfate and abiraterone sulfate concentrations have been reported in mCRPC patients to compare these data with.

Abiraterone is a strong inhibitor of CYP2D6 and a mild inhibitor of CYP2C8, while being metabolized by SULT2A1, CYP3A4 and 3βHSD. Furthermore, the major metabolites

abiraterone sulfate and abiterone N-oxide sulate inhibit the uptake transporter *organic-anion*-transporting polypeptide 1B1 (OATP1B1) in vitro (20). Cyclosporin inhibits breast cancer resistant protein (BCRP) and OATP1B and is substrate for CYP3A4 and P-glycoprotein (P-gp), while mycophenolic acid is predominantly metabolized by uridine 5'-diphospho-*glucuronosyltransferase* 1A9 (UGT1A9) and is substrate for transporters OATP, BCRP and multi-drug resistant associated protein 2 (MRP2) (21,22). Based on this information, OATP inhibition by abiraterone metabolites and cyclosporin may affect mycopholic acid exposure. However, this putative interaction did not affect treatment of our patient, as exposure to mycophenolic acid was well tolerated and the AUC was within the therapeutic range (30-60 mg/L•h (16)). The combination of cyclosporin and mycophenolic acid was given to preserve renal function in this patient with one kidney and some renal insufficiency, as cyclosporin may induce nefrotoxicity. The cyclosporin dose was based on liver enzymes, resulting in an AUC of 1.08 mg/L•h.

Conclusion

In this case report a mCRPC patient with a hepatic transplant was treated with abiraterone acetate at a reduced dose of 500 mg QD. Plasma levels of abiraterone and its active metabolite D4A were similar to those observed in mCRPC patients without a hepatic transplant, no clinical relevant toxicity was observed and exposure to immunosuppressive drugs mycophenolic acid and cyclosprin were within expected therapeutic ranges. The patient responded well to the treatment, showing a PSA decrease of >50%. It can thus be concluded that treatment with abiraterone acetate at a 50% reduced dose seems feasible and safe for hepatic transplant recipients. It is, however, recommended to monitor liver functions and plasma concentrations of abiraterone during treatment. Further clinical studies should be performed in order to confirm these findings.

2.6

References

1. de Bono JS, Logothetis CJ, Molina A, Fizazi K, North S, Chu L, et al. Abiraterone and increased survival in metastatic prostate cancer. N Engl J Med. 2011;364:1995–2005.

2. Ryan CJ, Smith MR, de Bono JS, Molina A, Logothetis CJ, de Souza P, et al. Abiraterone in metastatic prostate cancer without previous chemotherapy. N Engl J Med. 2013;368:138–48.

3. US Food and Drug Administration (FDA). Clinical Pharmacology and Biopharmaceutics Review: Zytiga (abiraterone acetate). 2010 [cited 2019 May]. p. 1–86. Available from: https://www.accessdata.fda.gov/drugsatfda_docs/nda/2011/202379orig1s000clinpharmr.pdf

4. Acharya M, Gonzalez M, Mannens G, De Vries R, Lopez C, Griffin T, et al. A phase I, open-label, single-dose, mass balance study of 14C-labeled abiraterone acetate in healthy male subjects. Xenobiotica. 2013;43:379–89.

5. Li Z, Alyamani M, Li J, Rogacki K, Abazeed M, Upadhyay SK, et al. Redirecting abiraterone metabolism to fine-tune prostate cancer anti-androgen therapy. Nature. 2016;533:547–51.

6. Li Z, Bishop AC, Alyamani M, Garcia JA, Dreicer R, Bunch D, et al. Conversion of abiraterone to D4A drives anti-tumour activity in prostate cancer. Nature. 2015;523:347–51.

7. Emamekhoo H, Li Z, Sharifi N. Clinical significance of D4A in prostate cancer therapy with abiraterone. Cell cycle. 2015;14:3213–4.

8. Marbury T, Lawitz E, Stonerock R, Gonzalez M, Jiao J, Breeding J, et al. Single-dose pharmacokinetic studies of abiraterone acetate in men with hepatic or renal impairment. J Clin Pharmacol. 2014;54:732–41.

9. Parikh ND, Levitsky J. Hepatotoxicity and drug interactions in liver transplant candidates and recipients. Clin Liver Dis. 2013;17:737–47.

10. Lorente D, Omlin A, Ferraldeschi R, Pezaro C, Perez R, Mateo J, et al. Tumour responses following a steroid switch from prednisone to dexamethasone in castration-resistant prostate cancer patients progressing on abiraterone. Br J Cancer. 2014;111:2248–53.

11. Armstrong AJ, Febbo PG. Using surrogate biomarkers to predict clinical benefit in men with castration-resistant prostate cancer: an update and review of the literature. Oncologist. 2009;14:816–27.

12. van Nuland M, Hillebrand MJX, Rosing H, Schellens JHM, Beijnen JH. Development and Validation of an LC-MS/MS Method for the Simultaneous Quantification of Abiraterone, Enzalutamide, and Their Major Metabolites in Human Plasma. Ther Drug Monit. 2017;39:243–51.

13. van Nuland M, Rosing H, de Vries J, Ovaa H, Schellens JHM, Beijnen JH. An LC–MS/MS method for quantification of the active abiraterone metabolite Δ(4)-abiraterone (D4A) in human plasma. J Chromatogr B. 2017;1068–1069:119–24.

14. Carton E, Noe G, Huillard O, Golmard L, Giroux J, Cessot A, et al. Relation between plasma trough concentration of abiraterone and prostate-specific antigen response in metastatic castration-resistant prostate cancer patients. Eur J Cancer. 2017;72:54–61.

15. Wang Y, Chia YL, Nedelman J, Schran H, Mahon F-X, Molimard M. A therapeutic drug monitoring algorithm for refining the imatinib trough level obtained at different sampling times. Ther Drug Monit. 2009;31:579–84.

16. van Gelder T, Le Meur Y, Shaw LM, Oellerich M, DeNofrio D, Holt C, et al. Therapeutic drug monitoring of mycophenolate mofetil in transplantation. Ther Drug Monit. 2006;28:145–54.

17. US Food and Drug Administration. Clinical Pharmacology and Biopharmaceutics Review: Xtandi (Enzalutamide). Silver Spring (MD). 2012 [cited 2019 Jan]. p. 1–75. Available from: https://www.accessdata.fda.gov/drugsatfda_docs/nda/2012/203415Orig1s000ClinPharmR.pdf

18. Minami H, Kawada K, Sasaki Y, Tahara M, Igarashi T, Itoh K, et al. Population pharmacokinetics of docetaxel in patients with hepatic dysfunction treated in an oncology practice. Cancer Sci. 2009;100:144–9.

19. Blanchet B, Carton E, Alyamani M, Golmard L, Huillard O, Thomas-Scheomann A, et al. A PK/PD study of Delta-4 abiraterone metabolite in metastatic castration-resistant prostate cancer patients. Pharmacol Res. 2018;136:56–61.

20. European Medicines Agency (EMA). Zytiga-H-C-2321-PSUV-19. European public assessment report: scientific conclusions and grounds recommending the variation to the terms of the marketing authorisation. 2014 [cited 2019 May]. p. 1–11. Available from: https://www.ema.europa.eu/en/documents/scientific-conclusion/zytiga-h-c-2321-psuv-0017-epar-scientific-conclusions-grounds-recommending-variation-terms-marketing_en.pdf

21. Staatz CE, Tett SE. Clinical pharmacokinetics and pharmacodynamics of mycophenolate in solid organ transplant recipients. Clin Pharmacokinet. 2007;46:13–58.

22. Fahr A. Cyclosporin clinical pharmacokinetics. Clin Pharmacokinet. 1993;24:472–95.

2.6

Impact of age on exposure to oral anti-androgen therapies in clinical practice

Merel van Nuland *
Marie-Rose B.S. Crombag *
Andries M. Bergman
Hilde Rosing
Jan H.M. Schellens
Alwin D.R. Huitema
Jos H. Beijnen

*These authors have contributed equally and thus share first authorship

Abstract

Background

Oral anti-androgen therapies are predominantly used in older men, but real-life studies evaluating the impact of age on pharmacokinetic exposure are lacking. This study aims to evaluate the impact of age on the pharmacokinetic profiles of abiraterone acetate and enzalutamide in clinical practice.

Patients and method

Retrospective observational study to evaluate the impact of age on the first steady-state sample of patients treated with abiraterone acetate or enzalutamide in routine daily clinical practice. The effect of age on target attainment was assessed.

Results

For abiraterone acetate and enzalutamide, 71 and 64 patients were included, respectively. Baseline patient characteristics and administered doses were not age-dependent. No age-related differences were observed in exposure to the main metabolites of abiraterone acetate, except for active metabolite Δ(4)-Abiraterone (D4A) with a median plasma concentration of $2.5*10^{-3}$ mg/L in the oldest versus $1.3*10^{-3}$ mg/L in the youngest age quartile (coefficient of variation, CV, 72%, p=0.03). For enzalutamide, no significant differences in exposure were found, except for carboxylic acid enzalutamide, having a median plasma concentration of 5.8 mg/L versus 3.9 mg/L in the oldest versus the youngest age quartile (CV 66%, p=0.03). However, this was driven by one patient aged 99 years old. Age had no significant influence on target attainment of either compound.

Conclusions

This study showed no significant impact of age on the pharmacokinetic profiles of abiraterone acetate and enzalutamide, except for the active metabolite D4A and the inactive metabolite carboxylic acid enzalutamide, both having significantly higher exposure in older males. Target attainments of abiraterone and enzalutamide were not significantly affected by age, which suggests that age has no clinically relevant impact on exposure to these oral anti-androgen therapies. However, the clinical impact of higher exposure to D4A in older males remains undetermined.

Introduction

Prostate cancer is the most common malignancy in men in the Western world and especially older men are diagnosed with this disease(1–3). Prostate cancer can progress into metastatic castration-resistant prostate cancer (mCRPC); a clinical state in which the androgen receptor axis is reactivated, despite adequate testosterone suppression(4). The introduction of the novel oral anti-androgen drugs, abiraterone acetate and enzalutamide, had a large impact on the treatment options of mCRPC patients as both drugs increase the time to tumor progression and prolong survival (5–9).

The prodrug abiraterone acetate is rapidly converted into abiraterone in the intestine by deacetylation. Abiraterone inhibits cytochrome P450 17 (CYP17), thereby preventing the production of tumor-growth stimulating testosterone(4). The bioavailability of abiraterone is only 10-20% when taken on an empty stomach, while the area under the plasma concentration-time curve (AUC) increases up to 10-fold when administered with food (4). Hence, use of lowered doses of abiraterone acetate in combination with food is interesting from a pharmacoeconomic perspective (10), although this may also introduce larger inter- and intrapatient variability. Hepatic metabolism of abiraterone is extensive and the main circulating metabolites are abiraterone sulphate and N-oxide abiraterone sulphate (11). Abiraterone and both metabolites are primarily excreted in feces, while only 5% of abiraterone metabolites are recovered in urine (11). Recent studies have shown that abiraterone can also be converted into Δ(4)-Abiraterone (D4A) by the enzyme 3β-hydroxysteroid-dehydrogenase (3βHSD) (12). Limited data is available on pharmacokinetic properties as this metabolite was discovered after market approval. However, its pharmacodynamic effects have been established and D4A is able to inhibit multiple steroidic enzymes and directly blocks androgen receptor signaling (12). These combined mechanisms of action makes D4A even more potent than abiraterone itself. The conversion ratio of abiraterone to D4A is about 5% and the clinical significance of this metabolite needs to be established in future studies (12,13). In a prospective observational trial, abiraterone showed a clear exposure-response relationship in patients with mCRPC (14). Higher abiraterone trough concentrations (C_{trough}) were found in PSA responders (n=38) compared to non-responders (n=23), with an optimal threshold to serve as a target of 8.4 ng/mL, as determined in multivariate analysis (14).

Enzalutamide is a competitive inhibitor of the androgen receptor (15). The bioavailability of enzalutamide is 84% and food intake has no clinically relevant influence on absorption. Enzalutamide is metabolized by CYP2C8 and CYP3A4 to *N*-desmethyl enzalutamide and carboxylic acid enzalutamide. *N*-Desmethyl enzalutamide is known to have a clinically relevant anti-androgen activity similar to enzalutamide. The major route of elimination is via the urine as inactive metabolite carboxylic acid enzalutamide (62.7%) (16). There is limited evidence to support an exposure-efficacy relationship for enzalutamide. However, in a phase 1 trial a higher androgen receptor binding with median plasma C_{trough} of 11.4 mg/L compared to 5.0 mg/L has been shown (17). Therefore, a minimum trough concentration of 5.0 mg/L could be considered as a target for exposure to enzalutamide (18).

2.7

Abiraterone acetate and enzalutamide are mainly administered to elderly patients as prostate cancer predominantly occurs in older men. This patient population was well represented in the pivotal trials of abiraterone acetate and enzalutamide with a median age of 69 years for both agents (6,9). These studies showed no effect of age on pharmacokinetic drug exposure, as reported by the regulatory agencies. Post hoc analyses of pivotal trials showed similar safety and efficacy in elderly and younger patients (19–23). Although clinical trials suggest that age does not influence abiraterone acetate or enzalutamide treatment, there is a lack of real-life data from daily clinical practice that underscores these findings. With increasing age body composition and organ functions may alter (24,25), which may affect distribution and elimination of these oral anti-androgen therapies. Furthermore, pivotal trials did not investigate the relationship between age and target attainment. As far as we know, this study is the first to investigate the impact of age on exposure to the new anti-androgens abiraterone acetate and enzalutamide and their main active and inactive metabolites in clinical practice. Furthermore, this study examined whether target attainment is related to older age.

Patients and Methods

A retrospective observational study was performed in the outpatient clinic of the Netherlands Cancer Institute – Antoni van Leeuwenhoek hospital, Amsterdam, The Netherlands. As part of routine clinical care, blood samples (4 mL) were collected for therapeutic drug monitoring (TDM) from patients who were treated with abiraterone acetate or enzalutamide at each hospital visit. The date and time of the last drug intake and the time of blood collection were recorded. All samples were measured using a previously validated liquid chromatography-mass spectrometry assay (LC-MS/MS) (26). Data were collected from May 2015 to January 2018. Patients were included in the dataset if at least one sample was withdrawn at steady-state. Steady-state was considered to be reached after at least 1 week of treatment with abiraterone acetate or 1 month of enzalutamide treatment, as their half-lives are 15 hours and 5.8 days, respectively (15,27,28). The first eligible sample per patient was included in the analysis. Samples were excluded if the time of drug intake was unknown, if the timing of sampling was during the absorption phase (i.e. within two hours after administration), if timing of sampling was >0.5 hour after the next scheduled administration, or if the measurement was below the validated limit of quantitation, to preclude non-compliant patients from the analysis (26). Trough concentrations (C_{trough}) were calculated as measure for exposure to abiraterone, abiraterone sulphate, N-oxide abiraterone sulphate, and D4A using the following equation (29):

$$C_{trough} = C_{TAD} * 0.5^{\frac{24-TAD}{t_{1/2}}}$$

Wherein C_{TAD} is the measured concentration in mg/L at the recorded time after the last dose administration (TAD), depicted in hours. In this equation, the following elimination half-lifes ($t_{1/2}$) were used, 15 hours for abiraterone, abiraterone sulphate, and D4A, and 21.6 hours for N-oxide abiraterone sulphate, respectively (28). For enzalutamide and its main metabolites *N*-desmethyl enzalutamide and carboxylic acid enzalutamide, no trough concentrations were calculated because of their long elimination half-lives of 5.8 days, 8.6 days, and 9.3 days, respectively (15,16). For these compounds, the actual measured concentrations were evaluated. Clinical characteristics including demographic data, drug dose and kidney and liver function were retrospectively collected from the patients' medical records. Conduct of this study was approved by the Medical Research Ethics Committee of the Antoni van Leeuwenhoek.

Statistical analysis

Descriptive analyses were used to depict baseline characteristics. The impact of age on pharmacokinetics of abiraterone, abiraterone sulphate, abiraterone N-oxide sulphate, D4A, enzalutamide, *N*-desmethyl enzalutamide, and carboxylic acid enzalutamide was evaluated using ANOVA. Regression analysis was used to evaluate the influence of other covariates on exposure, including dose, Body Mass Index (BMI), alanine transaminase (ALT), aspartate transaminase (AST), and estimated glomerular filtration rate (eGFR). The eGFR was calculated using the Modification of Diet in Renal Disease (MDRD) equation (30). Age was tested both as an ordinal variable, divided into quartiles conform analyses reported by the U.S. Food and Drug Administration (FDA) (4), and as a continuous variable. A statistical significance threshold of 0.05 was used.

Results

Abiraterone acetate

The dataset contained 79 patients treated with abiraterone acetate in clinical practice of whom 71 could be included in this study. Three patients were excluded because plasma concentrations of abiraterone were below the limit of quantification, two patients were excluded as the time of drug intake was unknown, and three more patients were excluded because sampling was during the absorption phase. The median age of included patients was 71 years, ranging from 53 to 86 years, with 62% of patients aged 70 years or older, as depicted in Table 1. Baseline patient characteristics, administered dose, and timing of blood withdrawal were not age-related. The majority of patients received 1,000 mg abiraterone acetate once daily. Five patients received a lower dose (250, 500, or 750 mg) based on tolerance. The median estimated trough concentration was $15 *10^{-3}$ mg/L with a coefficient of variation (CV) of 94% for abiraterone, 4.0 mg/L (CV 59%) for abiraterone *N*-oxide sulphate, and 4.1 mg/L (CV 87%) for abiraterone sulphate. For the recently discovered active metabolite D4A, median estimated plasma concentration was $1.7*10^{-3}$ mg/L (CV 72%).

2.7

Table 1. Patient characteristics.

Parameter	Age quartile 1	Age quartile 2	Age quartile 3	Age quartile 4	p-value (quartiles)	p-value (continuous)
Abiraterone acetate						
Number of patients	18	17	18	18		
Age (y), med. [range]	64 [53-67]	70 [67-71]	73 [71-75]	79 [75-86]		
Dose (mg), med. [range]	1,000 [500-1,000]	1,000 [250-1,000]	1,000 [500-1,000]	1,000	0.33	0.55
TAD (h), med. [range]	6.3 [2.1-22.1]	6.3 [2.4-23.3]	7.7 [2.1-23.7]	5.9 [2.3-24.0]	0.98	0.66
BMI (kg/m²), med. [IQR]	26 [24-29]	28 [26-30]	28 [25-31]	26 [24-28]	0.57	0.55
ALT (IU/L), med. [IQR]	20 [16-24]	22 [16-27]	19 [13-23]	20 [18-27]	0.62	0.53
<45 (%)	100	100	89	94		
≥45 (%)	0	0	11	6		
AST (IU/L), med. [IQR]	22 [21-27]	22 [20-29]	20 [17-23]	25 [20-31]	0.66	0.98
<35 (%)	88	82	94	75		
≥35 (%)	12	18	6	25		
eGFR (ml/min/1.73m²), med. [IQR]	85 [69-97]	85 [69-100]	87 [64-100]	82 [63-90]	0.19	0.13
>60 (%)	94	94	83	82		
≤60 (%)	6	6	17	18		
Enzalutamide						
Number of patients	16	16	16	16		
Age (y), med. [range]	58 [48-65]	68 [65-70]	72 [70-75]	79 [75-99]		
Dose (mg), med. [range]	160	160 [120-160]	160	160 [80-160]	0.32	0.48
TAD (h), med. [range]	6.0 [2.2-18.7]	13.6 [3.3-23.0]	5.4 [2.1-22.0]	13.6 [2.5-23.1]	0.55	0.63
BMI (kg/m²), med. [IQR]	27 [25-33]	26 [25-31]	29 [25-32]	25 [23-27]	0.13	0.04*

Table 1. Continued

Parameter	Age quartile 1	Age quartile 2	Age quartile 3	Age quartile 4	p-value (quartiles)	p-value (continuous)
ALT (IU/L), med. [IQR]	17 [11-22]	13 [9-18]	15 [12-18]	14 [10-19]	0.75	0.62
<45 (%)	100	100	100	100		
≥45 (%)	0	0	0	0		
AST (IU/L), med. [IQR]	25 [18-29]	23 [19-32]	24 [20-29]	23 [17-30]	0.90	0.95
<35 (%)	93	80	100	88		
≥35 (%)	7	20	0	12		
eGFR (ml/min/1.73m²), med. [IQR]	89 [79-95]	102 [81-109]	94 [78-110]	81 [66-97]	0.35	0.15
>60 (%)	94	100	93	81		
≤60 (%)	6	0	7	19		

Age quartile 1-4 = patients divided by age into four equally sized groups; ALT = alanine aminotransferase; AST = aspartate aminotransferase; BMI = body mass index; eGFR = estimated glomerular filtration rate, calculated using the Modification of Diet in Renal Disease (MDRD) equation; IQR=interquartile range 25%-75%; med.=median; p-value (quartiles) = p-value with age treated as an ordinal variable, divided into age quartiles; p-value (continuous) = p-value with age handled as a continuous variable; TAD = time after dose in hours; y = years.
* Significance threshold of 0.05 reached.

2.7

Exposure to abiraterone, abiraterone sulphate, and abiraterone N-oxide sulphate were comparable between the different age quartiles, as depicted in Table 2. Additionally, age handled as a continuous variable also did not significantly impact estimated trough concentrations of these metabolites. However, age significantly influenced exposure to D4A (p=0.03 for age either treated as an ordinal or continuous variable), with a median trough concentration of 2.5×10^{-3} mg/L in the oldest age quartile compared to

Table 2. Estimated trough concentrations of abiraterone, enzalutamide, and metabolites abiraterone sulphate, abiraterone N-oxide sulphate, *N*-desmethyl enzalutamide and carboxylic acid metabolite.

Parameter	Age quartile 1	Age quartile 2	Age quartile 3	Age quartile 4	p-value (quartiles)	p-value (continuous)
Abiraterone						
Trough concentration ($\times 10^{-3}$ mg/L), med. [IQR]	16 [14-21]	16 [10-25]	8.0 [4.9-16]	18.5 [9.0-42]	0.86	0.69
Target attainment[#] (%)	94	76	44	78	0.08	0.08
Abiraterone N-oxide sulphate						
Trough concentration (mg/L), med. [IQR]	3.7 [3.2-5.2]	3.1 [2.8-4.7]	4.1 [3.3-6.3]	4.8 [3.4-6.5]	0.07	0.06
Abiraterone sulphate						
Trough concentration (mg/L), med. [IQR]	3.9 [3.2-6.7]	3.8 [1.0-6.1]	3.1 [1.8-5.9]	6.0 [3.6-9.6]	0.25	0.19
Δ(4)-Abiraterone						
Trough concentration ($\times 10^{-3}$ mg/L), med. [IQR]	1.3 [1.0-2.1]	1.8 [1.1-2.9]	1.5 [0.7-1.8]	2.5 [1.8-3.0]	0.03[*]	0.03[*]
Enzalutamide						
Concentration (mg/L), med. [IQR]	9.9 [8.8-11.4]	10.1 [9.1-11.7]	11.9 [10.7-12.9]	12.0 [8.5-12.6]	0.21	0.07
Target attainment[§] (%)	94	100	100	88	0.44	0.75
_N_-desmethyl enzalutamide						
Concentration (mg/L), med. [IQR]	8.4 [7.0-10.5]	10.1 [7.3-12.3]	8.3 [7.6-10.1]	10.3 [7.6-13.4]	0.21	0.06
Carboxylic acid metabolite						
Concentration (mg/L), med. [IQR]	3.9 [2.9-6.1]	3.8 [3.1-5.0]	4.0 [3.3-5.6]	5.8 [4.8-8.3]	0.03[*]	0.002[*]

Age quartile 1-4 = patients divided by age into four equally sized groups; IQR=interquartile range 25%-75%; med.=median; p-value (quartiles) = p-value with age treated as an ordinal variable, divided into age quartiles; p-value (continuous) = p-value with age handled as a continuous variable.
[*] Significance threshold of 0.05 reached.
[#] Percentage of patients reaching the proposed abiraterone target concentration of 8.4×10^{-3} mg/L.
[§] Percentage of patients reaching the proposed enzalutamide target concentration of 5 mg/L.
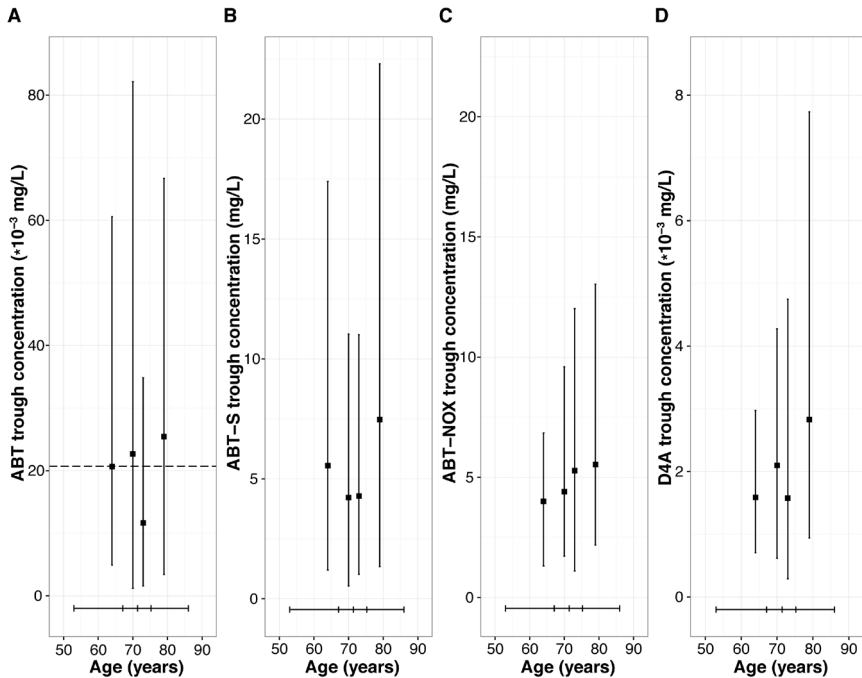
Figure 1. Exposure to the main metabolites of abiraterone acetate versus age quartiles.
Abbreviations: ABT = abiraterone, ABT-S = abiraterone sulphate, ABT-NOX = N-oxide abiraterone sulphate, D4A = Δ(4)-Abiraterone. Dotted line represents the mean abiraterone trough concentration (mg/L), as reported by the FDA.

$1.3*10^{-3}$ mg/L in the youngest age quartile. For comparison with FDA reported data, the mean estimated trough concentrations of abiraterone, abiraterone sulphate, abiraterone N-oxide sulphate, and D4A are depicted in Figure 1. The proposed abiraterone target concentration of $8.4*10^{-3}$ mg/L(14,18) was reached by 73% of patients, and target attainment was not significantly related to older age, as shown in Table 2. Of the five patients who received a reduced dose, three patients did not reach the proposed target concentration.

Univariate regression analyses showed that the covariates dose, BMI, ALT, AST, and eGFR did not significantly influence exposure to abiraterone or abiraterone sulphate. For abiraterone N-oxide sulphate and D4A, only eGFR significantly influenced exposure (p=0.008, and p=0.002, respectively).
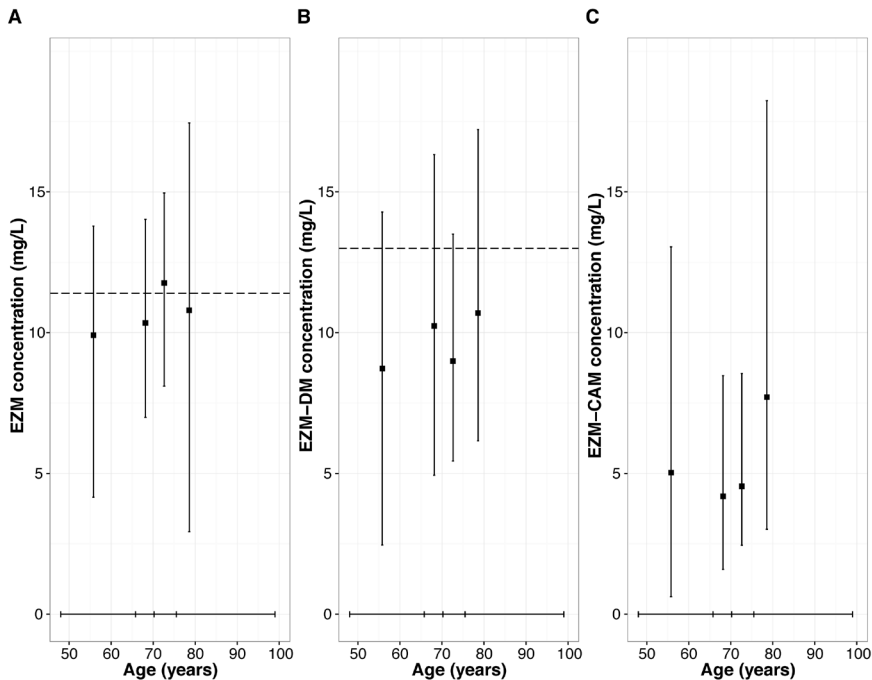
Enzalutamide
The dataset contained 74 patients who received enzalutamide of whom 64 were included in this study. One patient was excluded because the plasma concentration of enzalutamide was below the limit of quantification nine more patients were excluded because the timing of sampling was during the absorption phase. Median age of the

2.7

64 included patients was 70 years (range 48-99 years), as depicted in Table 1. Fifty-two percent of patients were aged 70 years or older. Baseline patient characteristics, administered dose, and timing of blood withdrawal were not age-related, except for BMI which was significantly influenced by age if handled as a continuous variable (p=0.04). Patients generally received 160 mg enzalutamide once daily, except for two patients who received 80 mg and 120 mg enzalutamide once daily. These dose reductions were based on tolerance. In the total enzalutamide cohort, median plasma concentration of enzalutamide was 11 mg/L (CV 27%), as shown in Table 2. Median concentrations of the major metabolites were 9.1 mg/L (CV 35%) for *N*-desmethyl enzalutamide and 4.6 mg/L (CV 66%) for carboxylic acid enzalutamide. Age, either treated as an ordinal or continuous variable, did not significantly influence exposure to the active compounds enzalutamide and *N*-desmethyl enzalutamide. Exposure to the inactive metabolite carboxylic acid enzalutamide was significantly higher in older patients (p=0.03 and p=0.002 for age either treated as an ordinal or continuous variable). In Figure 2 the mean concentrations of enzalutamide, *N*-desmethyl enzalutamide, and carboxylic acid enzalutamide per age quartile are depicted. The significant age-related difference in carboxylic acid enzalutamide exposure was driven by one patient aged 99 years old. This patient had comparable exposure to enzalutamide and *N*-desmethyl enzalutamide, but high exposure to carboxylic acid enzalutamide (19.4 mg/L versus the median carboxylic acid enzalutamide concentration of 4.6 mg/L). This oldest patient also had the lowest eGFR recorded in the cohort, which was 46 ml/min/1.73m^2. In the total cohort, 95% of patients reached the proposed enzalutamide target concentration of 5 mg/L[17,18] which was regardless of patients' age, as depicted in Table 2. Additionally, the two patients who took a reduced dose both reached the proposed target concentration.

Univariate regression showed that eGFR only significantly influenced exposure to carboxylic acid enzalutamide (p<0.001). The covariates dose, BMI, ALT, and AST did not significantly impact exposure to enzalutamide or its main metabolites.

Discussion

To our knowledge this study is the first to evaluate the pharmacokinetic profiles of abiraterone acetate, enzalutamide, and their main active and inactive metabolites in patients treated in daily clinical practice. Exposure to abiraterone, abiraterone sulphate, abiraterone N-oxide sulphate, enzalutamide, and *N*-desmethyl enzalutamide was not significantly influenced by age. However, exposure to the recently discovered active metabolite D4A was almost doubled in the oldest compared to the youngest age group. D4A was reported to be the more potent analogue of abiraterone, but its exposure was about a thousand-fold lower than estimated trough concentrations of abiraterone sulphate and abiraterone N-oxide sulphate, which is in line with previous findings (12,13). Nevertheless, whereas abiraterone sulphate and abiraterone N-oxide sulphate are formed hepatically, conversion of abiraterone by 3β-hydroxysteroid hydrogenase

Figure 2. Exposure to enzalutamide and its main metabolites versus age quartiles.
Abbreviations: EZM = enzalutamide, EZM-DM = *N*-desmethyl enzalutamide, EZM-CAM = carboxylic acid enzalutamide. Dotted lines represent the mean enzalutamide and *N*-desmethyl enzalutamide trough concentrations (mg/L), as reported by the FDA.

into D4A may take place in peripheral tissues. This may result in higher on-target concentrations in spite of relatively low plasma concentrations. The clinical relevance of the observed higher exposure to D4A in older males remains unclear. Furthermore, older males treated with enzalutamide had significantly higher exposure to the inactive metabolite carboxylic acid enzalutamide. This difference was driven by one patient aged 99 years, who had a relatively high carboxylic acid enzalutamide plasma concentration. Therefore, it remains disputable whether this concerns an outlier or an actual age-related difference. Nonetheless, this difference may be due to the fact that carboxylic acid enzalutamide is excreted renally, while enzalutamide and *N*-desmethyl enzalutamide are not detected in urine (15,16). The absence of an age-related difference in exposure to abiraterone, abiraterone sulphate, abiraterone N-oxide sulphate, enzalutamide and *N*-desmethyl enzalutamide was anticipated as these are mainly eliminated hepatically and may therefore be less prone to age-related effects.

Regardless of age, the majority of patients treated with abiraterone acetate and enzalutamide reached their proposed target concentration. As a result, most patients were treated adequately according to current knowledge on exposure-response relationships, while other patients may be treated suboptimally. Evaluation of treatment

2.7

outcome and incidence of side effects were not within the scope of this study. However, based on comparable target attainment, our data suggests that older age has no clinically relevant impact on treatment with either abiraterone acetate or enzalutamide, which is in line with post hoc analyses of pivotal trials showing no effect of age on exposure, safety and efficacy of abiraterone acetate and enzalutamide (4,16,19–23). However, these clinical trials did not report exposure to D4A. The current study is the first to observe higher exposure to D4A in older males. Although D4A is a potent active compound, it represents only a small percentage of the total abiraterone exposure. Furthermore, it should be kept in mind that patient data in post hoc analyses was derived from clinical trials in which drug intake was closely monitored, thus may not be representative for clinical practice (4,16,19–23).

In the current analysis, age was evaluated both as an ordinal variable, with age divided into quartiles, and as a continuous variable. Evaluating age as an ordinal variable is a fitting approach when sparse data is available, if the data distribution is skewed or when the relationship with another variable is nonlinear. As the data in this study is sparse, we analyzed the data using age both as a continuous and as an ordinal variable. The FDA used a similar strategy in their analysis on the influence of age on abiraterone exposure (4). Furthermore, the impact of age on exposure to oral anti-androgen therapies may be thwarted by other covariates that were not assessed in this study. Due to the retrospective study design, data regarding e.g. concomitant use of potentially interacting medication could not be adequately obtained from electronic patients' records. This is a limitation of the current study. Nonetheless, both treating physicians and hospital pharmacists performed robust medication reconciliation at each hospital visit. As part of routine clinical practice, all patients were also strictly instructed to take abiraterone acetate on an empty stomach to minimize inter- and intrapatient variability. Besides exposure to abiraterone and enzalutamide, plasma concentrations of their main metabolites were also assessed in this study. The mass-balance study of abiraterone acetate reported elimination half-lives of 2.5 hours and 21.6 hours for abiraterone sulphate and abiraterone N-oxide sulphate, respectively, based on limited sampling up to 8 hours post-dose (28). We believe that the $t_{1/2}$ of 2.5 hours for abiraterone sulphate was based on insufficient data points and may actually be longer. In case of formation rate limited elimination, the $t_{1/2}$ of metabolites equals the $t_{1/2}$ of the parent drug. For D4A was detected with a novel analysis method that was published after market approval, it was not reported in the mass-balance study or regulatory agency analyses. The $t_{1/2}$ of D4A has not been established yet. To approximate the $t_{1/2}$ of abiraterone sulphate and D4A, we performed visual inspection and non-compartmental analyses using naïve pooling of data. Because $t_{1/2}$ of abiraterone sulphate and D4A were in the same range as the $t_{1/2}$ of abiraterone, we decided to also use a $t_{1/2}$ of 15 hours for these compounds. The interindividual variability of abiraterone was relatively high, which is in line with findings reported by the regulatory agencies. This may be due to the poor and highly variable bioavailability of abiraterone acetate (4). For enzalutamide, much lower CVs were determined, which was also in line with previously published data (16).

Conclusions

In this observational study in a "real-world" patient population we found that there is no significant impact of age on the pharmacokinetic profiles of abiraterone acetate and enzalutamide, except for the active metabolite D4A and the inactive metabolite carboxylic acid enzalutamide, of which exposure was significantly higher in older males. Target attainment was not significantly affected by age, which suggests that age has no clinically relevant impact on exposure to these oral anti-androgen therapies. However, in this study higher exposure to the recently detected active metabolite D4A in older males was found. It is of interest to assess potential implications of this observation further by evaluating pharmacokinetics and pharmacodynamics of D4A in the heterogeneous group of older males treated in daily practice.

2.7

References

1. Fitzmaurice C, Allen C, Barber RM, Barregard L, Bhutta ZA, Brenner H, et al. Global, regional, and national cancer incidence, mortality, years of life lost, years lived with disability, and disability-adjusted life-years for 32 cancer groups, 1990 to 2015: A Systematic Analysis for the Global Burden of Disease Study Global Burden . JAMA Oncol. 2017;3:524–48.

2. Siegel RL, Miller KD, Jemal A. Cancer statistics, 2016. CA Cancer J Clin. 2016;66:7–30.

3. American Cancer Society. Global Cancer Facts & Figures 3rd Edition. American Cancer Society. 2015.

4. US Food and Drug Administration (FDA). Clinical Pharmacology and Biopharmaceutics Review: Zytiga (abiraterone acetate). 2010 [cited 2019 May]. p. 1–86. Available from: https://www.accessdata.fda.gov/drugsatfda_docs/nda/2011/202379orig1s000clinpharmr.pdf

5. Scher HI, Fizazi K, Saad F, Taplin M-E, Sternberg CN, Miller K, et al. Increased survival with enzalutamide in prostate cancer after chemotherapy. N Engl J Med. 2012;367:1187–97.

6. Beer TM, Armstrong AJ, Rathkopf DE, Loriot Y, Sternberg CN, Higano CS, et al. Enzalutamide in metastatic prostate cancer before chemotherapy. N Engl J Med. 2014;371:424–33.

7. de Bono JS, Logothetis CJ, Molina A, Fizazi K, North S, Chu L, et al. Abiraterone and increased survival in metastatic prostate cancer. N Engl J Med. 2011;364:1995–2005.

8. Ryan CJ, Smith MR, de Bono JS, Molina A, Logothetis CJ, de Souza P, et al. Abiraterone in metastatic prostate cancer without previous chemotherapy. N Engl J Med. 2013;368:138–48.

9. Fizazi K, Scher HI, Molina A, Logothetis CJ, Chi KN, Jones RJ, et al. Abiraterone acetate for treatment of metastatic castration-resistant prostate cancer: final overall survival analysis of the COU-AA-301 randomised, double-blind, placebo-controlled phase 3 study. Lancet Oncol. 2012;13:983–92.

10. Szmulewitz RZ, Peer CJ, Ibraheem A, Martinez E, Kozloff MF, Carthon B, et al. Prospective International Randomized Phase II Study of Low-Dose Abiraterone With Food Versus Standard Dose Abiraterone In Castration-Resistant Prostate Cancer. J Clin Oncol. 2018;36:1389–95.

11. Acharya M, Gonzalez M, Mannens G, De Vries R, Lopez C, Griffin T, et al. A phase I, open-label, single-dose, mass balance study of 14C-labeled abiraterone acetate in healthy male subjects. Xenobiotica. 2013;43:379–89.

12. Li Z, Bishop AC, Alyamani M, Garcia JA, Dreicer R, Bunch D, et al. Conversion of abiraterone to D4A drives anti-tumour activity in prostate cancer. Nature. 2015;523:347–51.

13. Emamekhoo H, Li Z, Sharifi N. Clinical significance of D4A in prostate cancer therapy with abiraterone. Cell cycle. 2015;14:3213–4.

14. Carton E, Noe G, Huillard O, Golmard L, Giroux J, Cessot A, et al. Relation between plasma trough concentration of abiraterone and prostate-specific antigen response in metastatic castration-resistant prostate cancer patients. Eur J Cancer. 2017;72:54–61.

15. US Food and Drug Administration. Prescribing information: Xtandi (enzalutamide). Silver Spring (MD). 2012 [cited 2018 Jun]. p. 1–16. Available from: https://www.accessdata.fda.gov/drugsatfda_docs/label/2012/203415lbl.pdf

16. US Food and Drug Administration. Clinical Pharmacology and Biopharmaceutics Review: Xtandi (Enzalutamide). Silver Spring (MD). 2012 [cited 2019 Jan]. p. 1–75. Available from: https://www.accessdata.fda.gov/drugsatfda_docs/nda/2012/203415Orig1s000ClinPharmR.pdf

17. Scher HI, Beer TM, Higano CS, Anand A, Taplin M-E, Efstathiou E, et al. Antitumour activity of MDV3100 in castration-resistant prostate cancer: a phase 1-2 study. Lancet. 2010;375:1437–46.

18. Groenland SL, van Nuland M, Verheijen RB, Schellens JHM, Beijnen JH, Huitema ADR, et al. Therapeutic Drug Monitoring of Oral Anti-Hormonal Drugs in Oncology. Clin Pharmacokinet. 2019;58:299–308.

19. Smith MR, Rathkopf DE, Mulders PFA, Carles J, Van Poppel H, Li J, et al. Efficacy and Safety of Abiraterone Acetate in Elderly (75 Years or Older) Chemotherapy Naive Patients with Metastatic Castration Resistant Prostate Cancer. J Urol. 2015;194:1277–84.

20. Mulders PFA, Molina A, Marberger M, Saad F, Higano CS, Chi KN, et al. Efficacy and safety of abiraterone acetate in an elderly patient subgroup (aged 75 and older) with metastatic castration-resistant prostate cancer after docetaxel-based chemotherapy. Eur Urol. 2014;65:875–83.

21. Siemens DR, Klotz L, Heidenreich A, Chowdhury S, Villers A, Baron B, et al. Efficacy and Safety of Enzalutamide vs Bicalutamide in Younger and Older Patients with Metastatic Castration Resistant Prostate Cancer in the TERRAIN Trial. J Urol. 2018;199:147–54.

22. Graff JN, Baciarello G, Armstrong AJ, Higano CS, Iversen P, Flaig TW, et al. Efficacy and safety of enzalutamide in patients 75 years or older with chemotherapy-naive metastatic castration-resistant prostate cancer: results from PREVAIL. Ann Oncol Off J Eur Soc Med Oncol. 2016;27:286–94.

23. Sternberg CN, de Bono JS, Chi KN, Fizazi K, Mulders P, Cerbone L, et al. Improved outcomes in elderly patients with metastatic castration-resistant prostate cancer treated with the androgen receptor inhibitor enzalutamide: results from the phase III AFFIRM trial. Ann Oncol Off J Eur Soc Med Oncol. 2014;25:429–34.

24. Dawson A, Dennison E. Measuring the musculoskeletal aging phenotype. Maturitas. 2016;93:13–7.

25. Seripa D, Panza F, Daragjati J, Paroni G, Pilotto A. Measuring pharmacogenetics in special groups: geriatrics. Expert Opin Drug Metab Toxicol. 2015;11:1073–88.

26. van Nuland M, Hillebrand MJX, Rosing H, Schellens JHM, Beijnen JH. Development and Validation of an LC-MS/MS Method for the Simultaneous Quantification of Abiraterone, Enzalutamide, and Their Major Metabolites in Human Plasma. Ther Drug Monit. 2017;39:243–51.

27. European Medicines Agency. European Public Assessment Report (EPAR): Zytiga (Abiraterone Acetate). London. 2016 [cited 2018 May]. Available from: https://www.ema.europa.eu/en/documents/variation-report/zytiga-h-c-2321-ii-0004-g-epar-assessment-report-variation_en.pdf

28. Acharya M, Gonzalez M, Mannens G, De Vries R, Lopez C, Griffin T, et al. A phase I, open-label, single-dose, mass balance study of 14C-labeled abiraterone acetate in healthy male subjects. Xenobiotica. 2012;43:1–11.

29. Wang Y, Chia YL, Nedelman J, Schran H, Mahon F-X, Molimard M. A therapeutic drug monitoring algorithm for refining the imatinib trough level obtained at different sampling times. Ther Drug Monit. 2009;31:579–84.

30. Jones GRD, Lim. E-M. The National Kidney Foundation Guideline on Estimation of the Glomerular Filtration Rate. Clin Biochem Rev. 2003;24:95–8.

2.7

Cost-effectiveness of monitoring endoxifen levels in breast cancer patients adjuvantly treated with tamoxifen

Merel van Nuland *
Rick A. Vreman *
Renske M.T. ten Ham
Aurelia H.M. de Vries Schultink
Hilde Rosing
Jan H.M. Schellens
Jos H. Beijnen
Anke M. Hövels

*These authors have contributed equally and thus share first authorship

Abstract

Purpose
Breast cancer is the most common malignancy in women worldwide. Recurrence rates in breast cancer are considered to be dependent on the serum concentration of endoxifen, the active metabolite of tamoxifen. The goal of this study is to investigate the cost-effectiveness of periodically monitoring serum concentrations of endoxifen in adjuvant estrogen receptor alfa (ERα) positive breast cancer patients treated with tamoxifen in the Netherlands.

Methods
A Markov model with disease free survival (DFS), recurrent disease (RD) and death states was constructed. The benefit of drug monitoring was modeled via a difference in the fraction of patients achieving adequate serum concentrations. Robustness of results to changes in model assumptions were tested through deterministic and probabilistic sensitivity analyses.

Results
Monitoring of endoxifen added 0.0115 quality-adjusted life years (QALYs) and saved € 1,564 per patient in the base case scenario. Deterministic sensitivity analysis demonstrated a large effect on the incremental cost-effectiveness ratio (ICER) of the differences in costs and utilities between the DFS and RD states. Probabilistic sensitivity analysis showed that the probability of cost-effectiveness at a willingness to pay of € 0 per quality-adjusted life year (QALY) was 89.8%.

Conclusions
Based on this model, monitoring of endoxifen in adjuvant ERα+ breast cancer patients treated with tamoxifen is likely to add QALYs and save costs from a healthcare payer perspective. We advise clinicians to consider integrating serum endoxifen concentration monitoring into standard adjuvant tamoxifen treatment of ERα+ breast cancer patients.

Introduction

Breast cancer is the most common malignancy in women worldwide (1). The heterogeneity of breast cancer manifests in a broad differentiation of phenotypes and morphological profiles. Breast cancer can be categorized, based on immunohistochemical features, in three main types: hormone receptor positive, human epidermal growth factor receptor 2 positive, and triple negative tumors (2). Hormone receptor positive types are characterized by a positive status of the estrogen and/or progesterone hormone receptor. Women with estrogen receptor alfa (ERα) positive breast cancer can be treated with tamoxifen; an anti-hormonal drug that blocks estrogen signaling by antagonizing the estrogen receptor (3). Adjuvant tamoxifen treatment in ERα positive breast cancer reduces recurrence and mortality rates (4). The reduction in breast cancer recurrence and in breast cancer associated death is shown after one to two years of adjuvant therapy with tamoxifen. These benefits increase after five years of tamoxifen intake (5). Prolongation of tamoxifen treatment up to 10 years further decreases recurrence and mortality rates in a subgroup of patients (6,7). Tamoxifen can be prescribed for both premenopausal and postmenopausal women with breast cancer. In the postmenopausal setting, tamoxifen can be administered for 2-3 years in sequence before or after aromatase inhibitors (8), while only tamoxifen is given to premenopausal women (9).

Although tamoxifen reduces recurrence and mortality rates in a large group of patients, variable efficacy of tamoxifen therapy remains a major clinical challenge (5). The anti-estrogenic activity of tamoxifen is limited. However, tamoxifen is rapidly converted into metabolites by CYP enzymes. Z-Endoxifen and (Z)-4-hydroxytamoxifen are the most active metabolites, of which endoxifen is most abundant and therefore most relevant for the anti-tumor effect. Endoxifen is formed through conversion by CYP2D6. Madlensky et al. were the first to describe a relationship between endoxifen serum concentrations and breast cancer survival in a retrospective study (10). Patients with endoxifen levels above the reported threshold of 5.97 ng/mL had a better disease prognosis with a 26% lower recurrence rate than women with endoxifen concentrations below 5.97 ng/mL (HR 0.74; 95% CI 0.55-1.00). Integration of tamoxifen concentrations and concentrations of metabolites (Z)-4-hydroxytamoxifen and N-desmethyltamoxifen in an anti-estrogenic activity score demonstrated that endoxifen can serve as a proxy for the total anti-estrogenic effect of tamoxifen and metabolites (11). Approximately 80% percent of patients treated with standard dose tamoxifen reaches these target concentrations of 5.97 ng/mL (10,12). Therefore, treatment optimization may improve outcomes for the remaining 20% of patients. To identify patients with an exposure below 5.97 ng/mL, endoxifen concentrations can be monitored after therapy initiation. Consequently, dose increase can be recommended to women with endoxifen levels below the threshold. The clinical practice of measuring drug concentrations to individualize drug dosing is called therapeutic drug monitoring (TDM). The pharmacokinetics of endoxifen are suitable

2.8

for TDM, considering stable steady-state concentrations, low inter-occasional variability and easy measurement in serum (13,14).

The goal of this study is to assess the cost-effectiveness of monitoring endoxifen serum concentrations and subsequent personalized dosing of tamoxifen in patients with ERα positive breast cancer treated with tamoxifen in the adjuvant setting in the Netherlands.

Methods

In order to model the costs and benefits of endoxifen monitoring in patients with ERα positive breast cancer treated with tamoxifen in the adjuvant setting in the Netherlands, a Markov state transition model was constructed in Excel (Microsoft, Redmond, WA). In the Markov model, time spent by patients in disease states was modeled. A difference in time spent in certain disease states between two populations is modeled due to the effect of an intervention. The intervention, endoxifen monitoring is compared with no TDM. Incremental costs and effects are thus attributed to the intervention, leading to an incremental cost-effectiveness ratio (ICER), which represents the added costs divided by the added QALYs due to the intervention. The ICER indicates how much should be invested to gain one QALY.

The model included three disease states: disease-free survival (DFS), recurrent disease (RD) and death (Figure 1). Approximately 7-8% of patients who transit from DFS to RD get a locoregional recurrence (15,16). This type of recurrence can again be treated with tamoxifen (17). No information is available on the probabilities of recurrence or death in this patient population. As we expect a higher probability of recurrent disease and death compared to patients with first-line tamoxifen treatment, we modeled these patients as staying in the RD state. Cycle duration was 28 days with an effectively lifetime horizon. Total quality adjusted life-years and costs were calculated for adjuvant tamoxifen treatment with and without concomitant therapeutic drug monitoring of endoxifen serum concentrations. The analysis is performed from a healthcare payer perspective in The Netherlands. All input parameters and their ranges for sensitivity analyses are specified in Table 1. This method section is constructed according to the CHEERS reporting guideline (18).

Modeled patients and intervention

The starting average age of patients was assumed equal to those found in the Women's Healthy Eating and Living randomized trial (53 years), which was the source for the data on differences between recurrence rates for high and low endoxifen serum concentrations (10,19).

The intervention consists of testing the serum concentration of endoxifen three months after starting treatment with tamoxifen, to ensure steady-state concentrations based on tamoxifen 7-day half-life (13). Serum levels of endoxifen are defined as low when they are below 5.97 ng/mL and as high when they are equal to or above 5.97 ng/mL,

Table 1. Input parameters and the ranges used in deterministic and probabilistic sensitivity analysis.

| Parameter		Base	Low	High	Distribution	Mean	SE	Source
Patient characteristics								
Age		53			Fixed	N/A	N/A	(18)
Discount rates								
Costs		0.045			Fixed	N/A	N/A	(28)
Effects		0.015			Fixed	N/A	N/A	(28)
Survival								
DFS (low endoxifen levels)								
	Intercept	3.28	3.20	3.37	Lognormal (correlated)	N/A	N/A	(5, 10)
	log(scale)	0.61	0.57	0.64	Lognormal (correlated)	N/A	N/A	(5, 10)
DFS (high endoxifen levels)								
Hazard ratio high versus low endoxifen		0.74	0.55	1,00	Lognormal	-0.301	0.153	(10)
Breast cancer mortality (RD survival)								
	Intercept	3.71	3.66	3.76	Lognormal (correlated)	N/A	N/A	(5, 20)
	log(scale)	0.40	0.37	0.42	Lognormal (correlated)	N/A	N/A	(5, 20)
Endoxifen levels						Alfa	Beta	
% of patients high endoxifen at start		0.76	0.57	0.94	Beta	14.8	4.7	(19)
% of patients high endoxifen after dose increase		0.94	0.76	1.00	Beta	13.2	0.8	(19)
Annual costs								
	DFS state	2872	1769	3975	Gamma	26.0	110.4	(M-C16)
	RD state	16125	9980	22270	Gamma	26.5	609.5	(M-C16)
	Death	8296	6222	10370	Gamma	61.5	135.0	(M-C16)
Endoxifen blood level testing		113	85	141	Gamma	61.5	1.8	(22)
Utilities								
	DFS state	0.80	0.73	0.87	Beta	99.55	24.89	(M-C16)
	RD state	0.73	0.66	0.80	Beta	112.07	41.45	(M-C16)

2.8

according to the target defined by Madlensky et al. (10). For all patients showing low serum concentrations, dosage of tamoxifen is doubled and their endoxifen serum concentration is evaluated after another three months. The percentage of patients that do not reach high serum concentrations of endoxifen was extracted from literature and found to be 24% after the first test and 6% after dose increase to 30 or 40 mg per day, as decided by the treating physician (20). Decreasing endoxifen concentration after tamoxifen dose escalation was modeled as impossible.

Quality of life before and after dose increase of tamoxifen was assumed equal. This is based on the fact that no correlation has been found between adverse events, such as hot flashes, and serum concentrations of tamoxifen and its metabolites (21). Furthermore, dose increase of tamoxifen in patients with reduced or absent CYP2D6 activity did not increase adverse events (22). This suggests that tamoxifen dose can be increased while preserving quality of life.

Survival estimates

Disease free survival and breast cancer mortality were included from a meta-analysis on tamoxifen efficacy from the Early Breast Cancer Trialists' Collaborative Group (EBCTCG) (5). These estimates are based on 10.645 women with ERα positive breast cancer treated with adjuvant tamoxifen for about five years.

Disease free survival as estimated in the meta-analysis was first corrected for the hazard ratio provided by Madlensky et al. for patients with low versus high serum concentrations of endoxifen, namely 0.74 (95% CI: 0.55 to 1.00) (10). To extrapolate survival curves beyond the duration of the EBCTCG trial, multiple parametric survival curves (exponential, Weibull, lognormal, loglogistic) were fitted on the published survival data for patients with a low serum concentration, according to the method provided by Hoyle and Henley (23). This method appropriately reconstructs individual patient data from published curves. The best fit according to the Akaike Information Criterion (AIC) and Bayesian Information Criterion (BIC) was the lognormal curve. The lognormal curve is a function of an intercept and log(scale). The hazard ratio was applied to estimate disease free survival for patients with high serum concentrations of endoxifen. The maximum hazard ratio that was possible in probabilistic analysis was 1.00. A lognormal curve also provided the best fit for breast cancer related mortality. Overall survival (OS), assumed the same for both groups, was acquired by adding the Dutch national background mortality according to data from Statistics Netherlands (CBS), specified per age, to the breast cancer related mortality provided by the meta-analysis (24). Patients with recurrent disease represent the difference between overall survival and disease free survival (RD = OS – DFS). Table 1 shows the used hazard ratio, and the intercept and log(scale) for the lognormal curves for disease free survival and breast cancer survival. Survival rates for probabilistic sensitivity analysis are provided by a Cholesky correlation matrix according to the method provided by Hoyle and Henley (25).
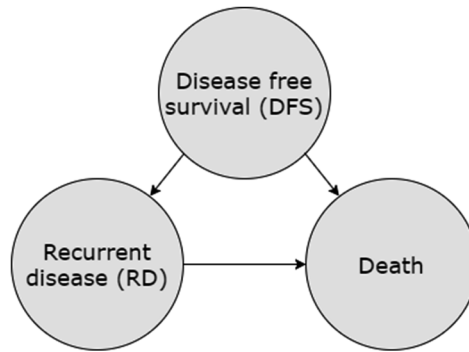
Figure 1. Markov model structure.

Cost and utilities

Costs are included from a Dutch health care perspective. Costs are discounted by 4.0% annually and presented in 2017 euros, as recommended by the Dutch National Health Care Institute (Zorginstituut Nederland, ZIN) (26,27). When disease costs were based on data from before 2017, cost inflation was performed with the Dutch national inflation calculator. Included costs are disease state costs and TDM costs. Costs for DFS and RD were included from a recent study on breast cancer costs for women with ERα positive/HER2-negative breast cancer in The Netherlands (28,29). Mortality costs occurring at end-of-life are inflicted once in the cycle wherein death occurs. Drug monitoring costs are based on the tariff list of the Dutch Healthcare Authority (30). All costs and ranges are specified in Table 1.

Utility values are implemented from the same study as disease state costs and are discounted by 1.5% annually, as recommended by ZIN (28,31). It was modeled as impossible for RD utility to be higher than utility in DFS. Utilities and used ranges are specified in Table 1.

Sensitivity analysis

Deterministic and probabilistic sensitivity analyses were performed (32). Deterministic sensitivity analysis showed the impact of varying each parameter individually according to its minimum and maximum value as specified in Table 1. This shows the importance of each individual parameter on incremental costs and QALY's. Probabilistic sensitivity analysis included 10,000 trials with random values for all model parameters according to their individual distributions. Through randomly sampling all input parameters of the model simultaneously, a comprehensive estimate of the uncertainty around the model outcomes is provided. The model outcomes incremental costs, quality-adjusted life years (QALYs) and the incremental cost-effectiveness ratio were calculated with a 95% confidence interval. Furthermore, a cost-effectiveness acceptability curve was calculated. This shows the likelihood that TDM is cost-effective (taking into account the

2.8

uncertainty of the outcomes) in relation to different willingness-to-pay (WTP) thresholds; e.g. the probability that TDM is cost-effective if a decision-maker is willing to pay 20,000 euros for gaining one QALY.

Clinical validation

As a clinical validation, we analyzed data from patients with ERα positive breast cancer with tailored tamoxifen therapy in the adjuvant setting from the Antoni van Leeuwenhoek/ Netherlands Cancer Institute (AvL-NKI). Patients with endoxifen levels below 5.97 ng/mL and a dose increment were included. Serum samples were obtained as routine clinical care in the period between March 2013 and March 2017. Patients received tamoxifen at a dose of 20 mg. Dose escalation to 30 or 40 mg, as decided by the treating physician, was advised to patients with a serum concentration below 5.97 ng/mL and a second serum level was determined at least three months after dose adjustment. Endoxifen levels were measured with a validated liquid-chromatography mass spectrometry (LC-MS/MS) method (14).

We found that of 813 patients for whom at least one serum test was available, 277 (34%) patients had a low serum concentration of endoxifen. From this cohort, we included 113 patients with a serum endoxifen level below 5.97 ng/mL to whom a dose increase was recommended. The remaining 164 patients were not evaluable because the tamoxifen dose was not increased after finding low endoxifen levels. Of 113 patients with low serum levels, a dose increment to 40 mg was advised to 90 patients and a dose increment to 30 mg was advised to 23 patients. In total, 66.4% of these patients reached the endoxifen target concentration of 5.97 ng/mL after dose increase (Figure 2). This percentage is lower than previously reported. Jager et al. showed that
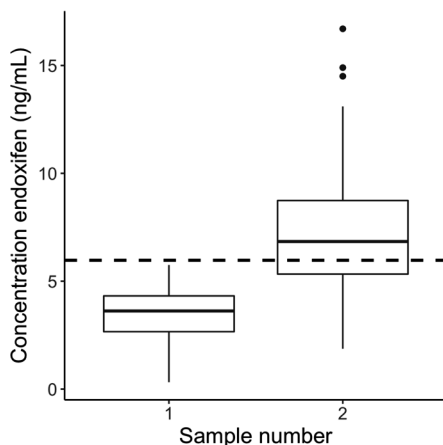
Figure 2. Boxplot showing endoxifen serum concentrations of 113 patients before (sampling point 1) and after (sampling point 2) dose increase. The dashed line represents the 5.97 ng/mL endoxifen threshold. After dose increase, 66.4% of patients have adequate serum levels.

96% of patients reach the target concentration of 5.97 ng/mL after dose increase to 30 or 40 mg (33). However, this was based on a small population of only 27 patients. A low percentage of patients with adequate serum levels before dose increase leads to a potentially higher effect of monitoring. We therefore implemented the more conservative estimate from literature (76% in literature vs 66% from the clinical data (20)). For consistency, we have also included the previously reported percentage of patients that receive a dose increase that achieve adequate serum levels (75% in literature vs 66.4% from the clinical data). Furthermore, dose increase to 30 and 40 mg have been described. We chose to model dose increase to 40 mg to get a more conservative estimate of cost-effectiveness.

Results

Base case results showed an overall reduction in costs of € 1,564 and an increase in QALYs of 0.0115 per patient due to therapeutic drug monitoring. Total average discounted costs for patients without TDM were € 48,809 and with TDM € 47,245. Total average QALYs without TDM were 15.32 and with TDM 15.33. This led to an ICER of € -136,000.

The results from the one-way sensitivity analysis are shown in Figure 3. Note that the ICER is negative due to the cost-saving effect of monitoring. No scenarios led to a positive ICER. However, five situations gave zero QALY benefit (ICER cannot be calculated). These situations represent extreme scenarios where there is no effect of drug monitoring: either there are no differences in utility between DFS and RD states, there is no effect of serum levels on recurrence (HR=1.00), everyone already has a high serum concentration at the first test or no one shows an increase in serum concentration after dose escalation.
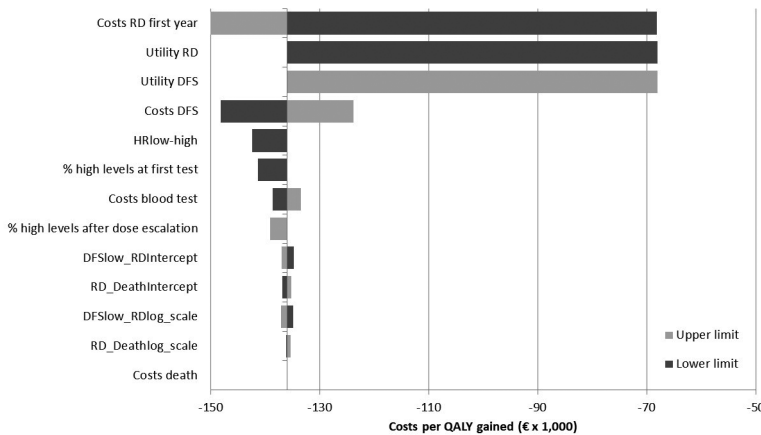
Figure 3. Deterministic sensitivity analysis. TP: transition probability, DFS: disease free survival, RD: recurrent disease, low/high levels: low or high serum levels (cut-off 5.97 ng/mL) of endoxifen.

The cost-effectiveness plane resulting from the probabilistic sensitivity analysis is shown in Figure 4. Because the distribution of ICERs include two quadrants (upper and lower right), we cannot calculate a valid confidence interval around the mean ICER. A valid method to adequately show the uncertainty around the ICER is the calculation of incremental net monetary benefits by multiplying the incremental QALYs with the willingness to pay threshold and subtracting the incremental costs. We assumed a WTP threshold of € 20,000 per QALY as a conservative base case provided by the Dutch National Health Care Institute, with € 80,000 per QALY as an upper bound (27). Mean net monetary benefits of serum monitoring were € 1,687 (95% CI: € -133 to € 5,089) for this base case WTP. The cost-effectiveness acceptability curve indicated that with a WTP of € 0 the probability of endoxifen serum concentration monitoring being cost-effective was 89.8%. This increased gradually to 90.6% with a WTP of € 80,000. It does not converge to 100% because of the inclusion of scenarios where no TDM benefit is demonstrated.

Discussion

Our analysis shows that monitoring serum concentrations of endoxifen after three months and accordingly escalating the dose of adjuvant tamoxifen in women with breast cancer who have serum concentrations lower than 5.97 ng/mL will likely be cost-effective. Indeed, in most cases this will be a cost-saving intervention. Just a minor intervention of one to two blood drawings will save an estimated € 1,564 per patient. Though the individual QALY benefit is relatively small, the affected population is large which could lead to significant QALY's gained on a macro level.

The difference between our intervention and our control arm is the number of people that will have a good serum concentration during DFS, which leads to a different distribution over DFS and RD states. Thus, the deterministic sensitivity analysis shows that inputs associated with these states, such as utilities and costs, have the biggest impact on the ICER. This is explained by the fact that if the utilities and costs in both living states converge, a big part of the effect is lost.

Strengths and limitations

A strength of our approach is that it provides a straightforward and clinically supported way to estimate the cost-effectiveness of endoxifen serum concentration monitoring in breast cancer patients. Although the relationship between tamoxifen efficacy and endoxifen serum concentrations has been shown in a retrospective study, we are the first to show cost-effectiveness of monitoring during therapy optimization. Our conclusion of cost-effectiveness can guide best practices.

However, our analysis does have some limitations. First, the number of patients that acquire a serum concentration >5.97 ng/mL after three months of treatment without dose escalation was extracted from a study with only 122 participants. We have validated these percentages by retrospectively assessing patient records in our hospital. Although the retrospective character of the clinical validation might cause selection
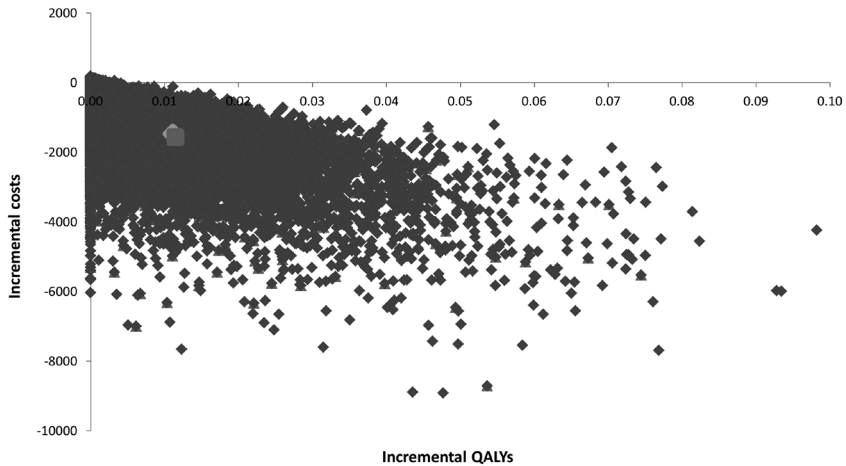
Figure 4. Results of the probabilistic sensitivity analysis in a cost-effectiveness plane. The larger light grey dot indicates the probabilistic mean and the larger darker grey dot indicates the base case scenario.

bias of included patients, this is not a problem in our analysis as all patients with tamoxifen therapy were monitored. However, the Antoni van Leeuwenhoek hospital is a tertiary referral center and patients visiting this hospital are referred for specialized healthcare. Despite the potential difference in study population, similar percentages were previously reported, and we believe that the clinical validation adequately describes the clinical setting. Additionally, we assumed that all patients with a low plasma concentration received a dose increase. In practice, this might not always be possible.

Additionally, our model is based on the underlying concept that a serum concentration lower than 5.97 ng/mL induces a higher risk for recurrence. Though this cut-off value is also used in clinical practice, it is based on a single retrospective analysis and thus might be subject to change when additional research is performed. Similarly, this study provided the hazard ratio (0.74) associated with these different recurrence risks. It would be best if the relationship between endoxifen serum concentrations and recurrence rates in the adjuvant setting was studied prospectively. Recent prospective trials studying the effect of endoxifen concentrations on clinical outcome were unable to confirm the 5.97 ng/mL threshold. However, in these studies endoxifen was monitored in neo-adjuvant and metastatic setting with a follow-up time of five years, which makes it difficult to properly interpret the relevance of the results for our study (34,35). Furthermore, power calculations were based on a rather large effect size, which might be less in real life. A threshold of endoxifen concentrations was not evaluated. To study the impact of varying the hazard ratio and the target threshold, we executed sensitivity analyses with the confidence interval of the described hazard ratio and the percentage of patients below or above the threshold. The deterministic sensitivity

2.8

analysis shows that reducing these effects would still lead to a conclusion of cost-effectiveness (unless the effect is completely diminished). The probabilistic sensitivity analysis furthermore shows a high likelihood of cost-effectiveness. On the basis of these results, we would expect endoxifen monitoring to be cost-effective, even when differences between recurrence rates would be smaller.

Conclusion

Based on this model, monitoring of endoxifen in adjuvant ER+ breast cancer patients is likely to add QALYs and save costs from a healthcare payer perspective. We advise clinicians to consider integrating serum endoxifen concentration monitoring into standard adjuvant tamoxifen treatment of ERα+ breast cancer patients.

References

1.   Torre LA, Bray F, Siegel RL, Ferlay J, Lortet-Tieulent J, Jemal A. Global cancer statistics, 2012. CA Cancer J Clin. 2015;65:87–108.

2.   Tang Y, Wang Y, Kiani MF, Wang B. Classification, Treatment Strategy, and Associated Drug Resistance in Breast Cancer. Clin Breast Cancer. 2016;16:335–43.

3.   European Medicines Agency. Tamoxifen summary of product characteristics. 2016 [cited 2017 Oct). Available at: https://www.medicines.org.uk/emc/medicine/30769

4.   Early Breast Cancer Trialists' Collaborative Group (EBCTCG). Effects of chemotherapy and hormonal therapy for early breast cancer on recurrence and 15-year survival: an overview of the randomised trials. Lancet (London, England). 2005;365:1687–717.

5.   Early Breast Cancer Trialists' Collaborative Group (EBCTCG) EBCTCG, Davies C, Godwin J, Gray R, Clarke M, Cutter D, et al. Relevance of breast cancer hormone receptors and other factors to the efficacy of adjuvant tamoxifen: patient-level meta-analysis of randomised trials. Lancet. 2011;378:771–84.

6.   Gray RG, Rea D, Handley K, Bowden SJ, Perry P, H.M. E, et al. ATTom: Long-term effects of continuing adjuvant tamoxifen to 10 years versus stopping at 5 years in 6,953 women with early breast cancer. J Clin Oncol. 2013;31:5.

7.   Davies C, Pan H, Godwin J, Gray R, Arriagada R, Raina V, et al. Long-term effects of continuing adjuvant tamoxifen to 10 years versus stopping at 5 years after diagnosis of oestrogen receptor-positive breast cancer: ATLAS, a randomised trial. Lancet. 2013;381:805–16.

8.   Regan MM, Neven P, Giobbie-Hurder A, Goldhirsch A, Ejlertsen B, Mauriac L, et al. Assessment of letrozole and tamoxifen alone and in sequence for postmenopausal women with steroid hormone receptor-positive breast cancer: the BIG 1-98 randomised clinical trial at 8.1 years median follow-up. Lancet Oncol. 2011;12:1101–8.

9.   Francis PA, Regan MM, Fleming GF, Lang I, Ciruelos E, Bellet M, et al. Adjuvant ovarian suppression in premenopausal breast cancer. N Engl J Med. 2015;372:436–46.

10.   Madlensky L, Natarajan L, Tchu S, Pu M, Mortimer J, Flatt SW, et al. Tamoxifen metabolite concentrations, CYP2D6 genotype, and breast cancer outcomes. Clin Pharmacol Ther. 2011;89:718–25.

11.   de Vries Schultink AHM, Alexi X, van Werkhoven E, Madlensky L, Natarajan L, Flatt SW, et al. An Antiestrogenic Activity Score for tamoxifen and its metabolites is associated with breast cancer outcome. Breast Cancer Res Treat. 2017;161:567–74.

12.   Jager NGL, Rosing H, Schellens JHM, Beijnen JH, Linn SC. Use of dried blood spots for the determination of serum concentrations of tamoxifen and endoxifen. Breast Cancer Res Treat. 2014;146:137–44.

13.   US Food and Drug Administration (FDA). Prescribing information: nolvadex. 2004 [cited 2017 Oct]. Available from: https://www.accessdata.fda.gov/drugsatfda_docs/label/2005/17970s053lbl.pdf

14.   Teunissen SF, Jager NGL, Rosing H, Schinkel AH, Schellens JHM, Beijnen JH. Development and validation of a quantitative assay for the determination of tamoxifen and its five main phase I metabolites in human serum using liquid chromatography coupled with tandem mass spectrometry. J Chromatogr B, Anal Technol Biomed life Sci. 2011;879:1677–85.

15.   Khoshnoud MR, Fornander T, Johansson H, Rutqvist L-E. Long-term pattern of disease recurrence among patients with early-stage breast cancer according to estrogen receptor status and use of adjuvant tamoxifen. Breast Cancer Res Treat. 2008;107:71–8.

16.   Goldhirsch A, Gelber RD, Price KN, Castiglione M, Coates AS, Rudenstam CM, et al. Effect of systemic adjuvant treatment on first sites of breast cancer relapse. Lancet. 1994;343:377–81.

2.8

17. Borner M, Bacchi M, Goldhirsch A, Greiner R, Harder F, Castiglione M, et al. First isolated locoregional recurrence following mastectomy for breast cancer: results of a phase III multicenter study comparing systemic treatment with observation after excision and radiation. Swiss Group for Clinical Cancer Research. J Clin Oncol. 1994;12:2071–7.

18. Husereau D, Drummond M, Petrou S, Carswell C, Moher D, Greenberg D, et al. Consolidated health economic evaluation reporting standards (CHEERS)-explanation and elaboration: A report of the ISPOR health economic evaluation publication guidelines good reporting practices task force. Value Heal. 2013;16:231–50.

19. Pierce JP, Faerber S, Wright FA, Rock CL, Newman V, Flatt SW, et al. A randomized trial of the effect of a plant-based dietary pattern on additional breast cancer events and survival: the Women's Healthy Eating and Living (WHEL) Study. Control Clin Trials. 2002;23:728–56.

20. Fox P, Balleine RL, Lee C, Gao B, Balakrishnar B, Menzies AM, et al. Dose Escalation of Tamoxifen in Patients with Low Endoxifen Level: Evidence for Therapeutic Drug Monitoring-The TADE Study. Clin Cancer Res. 2016;22:3164–71.

21. Jager NGL, Koornstra RHT, Vincent AD, van Schaik RHN, Huitema ADR, Korse TM, et al. Hot flashes are not predictive for serum concentrations of tamoxifen and its metabolites. BMC Cancer. 2013;13:612.

22. Dezentjé VO, Opdam FL, Gelderblom H, Hartigh den J, Van der Straaten T, Vree R, et al. CYP2D6 genotype- and endoxifen-guided tamoxifen dose escalation increases endoxifen serum concentrations without increasing side effects. Breast Cancer Res Treat. 2015;153:583–90.

23. Hoyle MW, Henley W. Improved curve fits to summary survival data: application to economic evaluation of health technologies. BMC Med Res Methodol. 2011;11:139.

24. Statistics Netherlands (CBS). Sterfte; geslacht, leeftijd (op 31 december) en burgerlijke staat 1950-2014 [mortality by age and sex 1950-2014]. 2015.

25. Hoyle MW, Henley W. Improved curve fits to summary survival data: application to economic evaluation of health technologies. BMC Med Res Methodol. 2011;11:139.

26. Institute for Medical Technology Assessment. Kostenhandleiding: Methodologie van kostenonderzoek en referentieprijzen voor economische evaluaties in de gezondheidszorg [methodology of cost research and reference prices for economic evaluation in health care. p. 120. Available from: https://www.zorginstituutnederland.nl/binaries/zinl/documenten/publicatie/2016/02/29/richtlijn-voor-het-uitvoeren-van-economische-evaluaties-in-de-gezondheidszorg/Richtlijn+voor+het+uitvoeren+van+economische+evaluaties+in+de+gezondheidszorg+(verdiepingsmo

27. Dutch National Health Institute (Zorginstituut Nederland). Richtlijn voor het uitvoeren van economische evaluaties in de gezondheidszorg [guideline for economic evaluation in health care]. 2016. p. 38.

28. Essers BAB, Seferina SC, Tjan-Heijnen VCG, Severens JL, Novák A, Pompen M, et al. Transferability of model-based economic evaluations: The case of trastuzumab for the adjuvant treatment of her2-positive early breast cancer in the netherlands. Value Heal. 2010;13:375–80.

29. Miquel-Cases A, Retèl VP, Lederer B, von Minckwitz G, Steuten LMG, van Harten WH. Exploratory Cost-Effectiveness Analysis of Response-Guided Neoadjuvant Chemotherapy for Hormone Positive Breast Cancer Patients. PLoS One. 2016;11:e0154386.

30. Dutch Healthcare Authority (NZa). DBC product-finder for tariffs 2017. 2017. Available from: http://www.nza.nl/organisatie/

31. Dutch National Health Institute (Zorginstituut Nederland). Richtlijn voor het uitvoeren van economische evaluaties in de gezondheidszorg [guideline for economic evaluation in health care. 2016. p. 38. Available from: https://www.zorginstituutnederland.nl/binaries/zinl/documenten/publicatie/2016/02/29/richtlijn-voor-het-uitvoeren-van-economische-evaluaties-in-de-gezondheidszorg/richtlijn-voor-het-uitvoeren-van-economische-evaluaties-in-de-gezondheidszorg.pdf

32. Briggs AH, Weinstein MC, Fenwick EAL, Karnon J, Sculpher MJ, Paltiel AD. Model parameter estimation and uncertainty analysis: a report of the ISPOR-SMDM Modeling Good Research Practices Task Force Working Group-6. Med Decis Making. 2012;32:722–32.

33. Jager NGL, Rosing H, Schellens JHM, Linn SC, Beijnen JH. Tamoxifen dose and serum concentrations of tamoxifen and six of its metabolites in routine clinical outpatient care. Breast Cancer Res Treat. 2014;143:477–83.

34. Neven P, Jongen L, Lintermans A, Van Asten K, Blomme C, Lambrechts D, et al. Tamoxifen Metabolism and Efficacy in Breast Cancer: A Prospective Multicenter Trial. Clin Cancer Res. 2018;24:2312–8.

35. Lintermans A, Van Asten K, Jongen L, Blomme C, Lambrechts D, Van Calster B, et al. Prospective study evaluating the effect of impaired tamoxifen metabolisation on efficacy in breast cancer patients receiving tamoxifen in the neo-adjuvant or metastatic setting. J Clin Oncol. 2016 20;34:523.

2.8

Cost-effectiveness assessment of monitoring abiraterone levels in metastatic castration-resistant prostate cancer patients

Submitted

Merel van Nuland *
Renske M.T. ten Ham *
Rick A. Vreman
Laurens G. de Graaf
Hilde Rosing
Andries M. Bergman
Alwin D.R. Huitema
Jos H. Beijnen
Anke M. Hövels

*These authors have contributed equally and thus share first authorship

Abstract

Background/objectives
Abiraterone acetate is registered for the treatment of metastatic castration- sensitive and resistant prostate cancer (mCRPC). Treatment outcome is associated with plasma trough concentrations (C_{min}) of abiraterone. Patients with a plasma C_{min} below the target of 8.4 ng/mL may benefit from treatment optimization by dose increase or concomitant intake with food. This study aims to investigate the cost-effectiveness of monitoring abiraterone C_{min} in patients with mCRPC.

Methods
A Markov model was built with health states of progression-free survival, progressed disease and death. The benefits of monitoring abiraterone C_{min} followed by a dose increase or food-intervention were modeled via a difference in the percentage of patients achieving adequate C_{min}, from a healthcare payer perspective. Deterministic and probabilistic sensitivity analyses were performed to assess uncertainties in the calculated incremental cost-effectiveness ratio (ICER).

Results
Monitoring abiraterone followed by a dose increase resulted in 0.089 incremental quality-adjusted life years (QALYs) with €13,524 incremental costs and an ICER of €154,393/QALY. The food-intervention assumed equal effects and estimated incremental costs of €5,319, resulting in an ICER of €60,717/QALY. The likelihoods of therapeutic drug monitoring (TDM) with a dose increase or food-intervention being cost-effective were 20.4%and 81.4%, respectively.

Conclusions
Monitoring abiraterone followed by a dose increase is not cost-effective in patients with mCRPC from a healthcare payer perspective. However, monitoring in combination with a food intervention is likely to be cost-effective. Therefore, we advise clinicians to apply TDM and advise patients who do not reach adequate C_{min} to take abiraterone acetate together with food.

Introduction

Abiraterone acetate (Zytiga®) is approved for the treatment of metastatic castration-sensitive and resistant prostate cancer (mCRPC), as it improves overall survival (OS) and progression-free survival (PFS) in these patient populations (1), (2,3). Since the launch of abiraterone in 2012, a few cost-effectiveness analyses (CEA's) have been performed, quantifying the costs of abiraterone treatment versus its benefits (4–8). Although these CEA's use different comparators - such as androgen deprivation therapy, docetaxel, or radium-223 - and are performed in different countries applying local treatment guidelines, the available CEA's unanimously conclude that treatment of mCRPC with abiraterone is not cost-effective, mainly driven by high drug costs.

A prospective observational study in patients with mCRPC showed a correlation between abiraterone trough concentrations (C_{min}) - the lowest plasma concentration reached before next dose administration - and prostate specific antigen (PSA) response - an accepted prostate cancer specific biomarker (9). An optimal abiraterone plasma C_{min} threshold of 8.4 ng/mL was defined, above which patients have longer PFS compared to patients with lower C_{min} (12.2 vs 7.4 months, HR: 0.55) (10). However, approximately 65% of patients treated with a fixed dose of abiraterone acetate (1,000 mg once daily) reach the target concentration of 8.4 ng/mL (10), which means treatment optimization may improve clinical outcomes for the remaining 35%. Measuring concentrations of a drug to personalize treatment is known as therapeutic drug monitoring (TDM) and can be applied in clinical practice for agents with known high interpatient variability (11). There is potential to optimize treatment for the 35% of mCRPC patients with an abiraterone C_{min} <8.4 ng/mL by implementation of TDM. However, TDM of this drug is not yet common in clinical practice.

It is known that food has a clinically significant effect on the bioavailability and pharmacokinetics of abiraterone [12], [13]. According to the label, abiraterone should be administered in modified fasting state (1). In a dedicated food-effect study, exposure (area under the plasma concentration-time curve; AUC) increased 5-fold with a low-fat meal and 10-fold with a high-fat meal compared to overnight fasting. Furthermore, the maximum plasma concentration (C_{max}) increased 7-fold and 17-fold when taken with a low-fat and high-fat meal, respectively (13,14). A milder food-effect was seen in mCRPC patients when compared to modified fasting, with a similar exposure when taken with a low-fat meal and a 2-fold increase with a high-fat meal. Based on this information, concomitant intake of abiraterone with food may increase C_{min} for patients with a low C_{min} (<8.4 ng/mL) (13,14).

The goal of this study is to assess the cost-effectiveness of monitoring abiraterone C_{min} and subsequently dose increase to 1,500 mg once daily in patients with mCRPC in the Netherlands. In an additional scenario, the cost-effectiveness of monitoring abiraterone C_{min} and subsequently advising intake of abiraterone acetate with a low-fat meal is explored.

2.9

Methods

To model benefits and costs in patients with mCRPC treated with abiraterone in the Netherlands, a partitioned survival model was constructed using Microsoft Excel (Microsoft, Redmond, WA). We compared a hypothetical group of patients receiving a fixed dose of abiraterone acetate 1,000 mg once daily without TDM as current standard of care with a hypothetical intervention group. The intervention consisted of TDM, after which patients with a plasma C_{min} <8.4 ng/mL received a dose increase to 1,500 mg once daily. Given the evidence of a food-effect relationship for abiraterone, we investigated an alternative scenario in which patients were advised to combine the fixed dose of abiraterone acetate of 1,000 mg once daily with a low-fat meal (hereafter called the food-intervention). Benefits were expressed as incremental life-years (LYs) and incremental quality-adjusted life years (QALYs) gained due to TDM as compared to no TDM, and costs were expressed as incremental costs in 2018 euros.

Model overview

The Markov model included three health states: progression free survival (PFS), progressed disease (PD) and death (see Figure 1). PFS was defined as time from treatment initiation to first progression event (measured as PSA or radiologic progression) or death (any cause). PSA progression was defined as 25% increase from nadir with an increase in absolute PSA of at least 2 ng/mL. Radiographic progression was defined according to Response Evaluation Criteria in Solid Tumours or when bone scans showedg two or more new lesions (10).

In accordance with Dutch treatment guidelines, after progression, patients received second-line treatment with docetaxel, enzalutamide, cabazitaxel, radium-223 or no treatment. Upon entering the PD-state patients were proportionally distributed amongst the second line treatment options. Based on a trial by Carton et al. we assumed 35% of patients starting abiraterone treatment do not reach the 8.4 ng/mL threshold (10). Cycle length was one month (30.5 days) with a five-year time horizon.
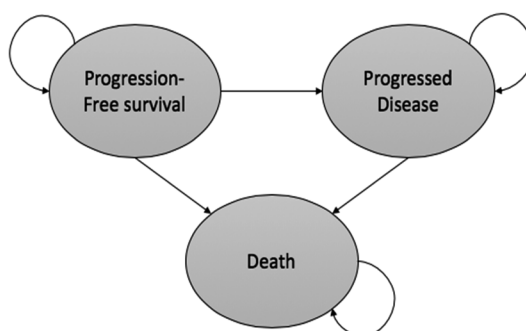
Figure 1. Structure of the Markov model.

This time cut-off reflects overall survival in mCRPC patients. A healthcare payer perspective was used. Input parameters and their ranges for sensitivity analyses are specified in Table 1. Reporting of this economic evaluation was done according to the CHEERS reporting guideline (15).

Table 1. Patient characteristics and input parameters calculated for a cycle length of one month. Abbreviations: PFS = progression-free survival, PD = progressed disease, PSA = prostate-specific antigen.

Parameter	Base	Low	High	Distribution	Source
Patient characteristics					
Age	77,0	-	-	Fixed	(10)
Fraction patients low plasma level (<8.4ng/mL)	0.35	0.235	0.466	Beta	(10)
Body Weight (kg)	75	70	95	Beta	(10)
Body Surface (m^2)	1.9	1.6	2.0	Beta	(41)
Treatment naïve fraction	0.79	0.738	0.843	Beta	(10)
PFS (low abiraterone plasma levels)					
Intercept	2.16	1.65	2.67	Exponential	(10)
Log(scale)	1	1	1	Exponential	(10)
PFS (high abiraterone plasma levels)					
Intercept	2.34	2.03	2.65	Loglogistic	(10)
Log(scale)	-0.71	-1.04	-0.39	Loglogistic	(10)
RD (enzalutamide)					
Intercept	2.42	2.23	2.60	Weibull	(23)
Log(scale)	-0.56	-0.81	-0.31	Weibull	(23)
RD (docetaxel)					
Intercept	2.33	2.09	2.57	Loglogistic	(24)
Log(scale)	-1.07	-1.41	-0.02	Loglogistic	(24)
RD (cabazitaxel)					
Intercept	2.62	2.44	2.79	Weibull	(25)
Log(scale)	-0.043	-0.27	0.19	Weibull	(25)
RD (RA-223)					
Intercept	2.67	2.42	2.74	Loglogistic	(26)
Log(scale)	-0.66	-0.56	-0.53	Loglogistic	(26)
Prostate cancer mortality (treatment naïve)					
Intercept	3.42	3.36	3.49	Loglogistic	(20)
Log(scale)	-0.86	-0.94	-0.77	Loglogistic	(20)
Prostate cancer mortality (post docetaxel)					
Intercept	2.47	2.36	2.57	Loglogistic	(21)
Log(scale)	-0.52	0.62	-0.42	Loglogistic	(21)
Utility					
PFS abiraterone	0.84	0.63	1	Beta	(42)

2.9

Table 1. Continued

Parameter	Base	Low	High	Distribution	Source
Disutility PD abiraterone First Cycle PD	0.052	0.039	0.065	Beta	(2,28,29)
Disutility PD abiraterone > First Cycle PD	0.047	0.036	0.059	Beta	(2,28,29)
Costs					
TDM	€ 111	€ 84	€ 139	Gamma	(30)
Cost abiraterone (montly)	€ 3,353	€ 2,514	€ 4,191	Gamma	(2,16,28,29,43)
Care Used PFS (monthly)	€ 794	€ 447	€ 1,241	Gamma	(22,31,44,45)
Care Used PD (monthly)	€ 2,570	€ 1,446	€ 4,016	Gamma	(22,31,44,45)
Adverse Events Abiraterone First Cycle	€ 51	€ 38	€ 64	Gamma	(2,22,28,29)
Adverse Event Abiraterone >First Cycle	€ 11	€ 8	€ 14	Gamma	(2,28,29)

Modeled population and intervention

Mean age of patients in our model was 77 years old, based on Carton et al. which was the main source for survival and progression data between intervention groups (10). After diagnosis of mCRPC, several treatment options are available according to treatment guidelines, being either abiraterone, docetaxel, enzalutamide, cabazitaxel, radium-223 or palliative treatment (16). Based on previous studies, 21% of the modeled population was treated with docetaxel prior to starting abiraterone treatment (10), and this was included in the model accordingly. Abiraterone is registered for mCRPC in combination with prednisone or prednisolone 10 mg/day, which is reflected in our model. Plasma samples for TDM were collected during routine visits to the outpatient clinic at steady-state, which is considered to be reached after 1 week of treatment (1). Trough levels were considered low when <8.4 ng/mL, and adequate when ≥8.4 ng/mL. Patients with low C_{min} received a dose increase from 1,000 mg abiraterone aceteate once daily to 1,500 mg abiraterone acetate once daily to be taken in a fasting state. Fasting state was defined as an overnight fast of at least 8 hours and at least 2 hours before any food intake. The fraction of patients with low abiraterone plasma levels was extracted from literature and assumed to be 35% (10). We assumed that patients reached adequate high plasma levels after dose increase, based on the expected increase in AUC and C_{max} (1). The adherence to abiraterone is 92.7% (17) and, with the assumption that the TDM intervention did not affect adherence rate, the percentage of patients with adequate C_{min} when applying TDM was set at 92.7%.

In the alternative scenario we modelled the effect and cost of TDM followed by intake of 1,000 mg once daily abiraterone acetate with a low-fat continental meal. A low-fat continental meal is defined as 160-320 kilocalories with 25-50% of fat (12). We assumed all patients receiving the food-intervention reached adequate high plasma levels, based

on the high food-effect described by Chi et al. (13). Consequently, effects were assumed identical as in the dose increase base case.

Patient survival

PFS and OS were based on Kaplan-Meier curves of a clinical trial directly comparing survival difference between patients with low and high abiraterone C_{min} (10). The fraction of patients with progressed disease (PD) was calculated using the OS and PFS (PD=OS-PFS). To extrapolate patient survival beyond the duration of the clinical trial, different parametric survival curves (exponential, Weibull, log-normal, log-logistic) were fitted on the published survival data of patients with mCRPC following methods provided by Hoyle, Henley and Tierney (18,19). Best fit was determined through the Akaike Information Criterion (AIC) and the Bayesian Information Criterion (BIC) and plausibility of the estimated long-term survival (18).

Background mortality (BM) was assumed equal for patients with low and high abiraterone plasma levels and represents the transition probability from PFS directly to the Death state. BM was calculated using a weighted average of placebo arm data from trials with mCRPC patients, adjusting for chemotherapy-naïve (79%) and docetaxel pretreated patients (21%) (20,21).

After disease progression, patients were modelled to receive one of five treatment options in line with Dutch treatment guidelines: docetaxel, enzalutamide, cabazitaxel, radium-223 or no treatment (16). Patients were distributed over the five treatment options according to Restelli et al., which was found to be generalizable to the Dutch setting based on the clinical validation (22). Survival curves were modeled separately for each treatment option in the PD state based on clinical studies from literature (23–26). Again, survival was extrapolated beyond trial duration by fitting different parametric survival curves (exponential, Weibull, log-normal, log-logistic) (18,19). The model did not allow patients pretreated with docetaxel to receive this drug after disease progression.

Cost and utility inputs

Costs were included according to the healthcare payer perspective and are expressed in 2018 euros. Cost based on pre-2018 data were corrected for inflation using the national inflation calculator (27). Discounting of 4% annually was applied in line with guidelines from the Dutch National Healthcare Institute (Zorginstituut Nederland; ZIN) (28). Treatment specific cost and frequency of adverse events were extracted from recent clinical studies and available ZIN reports (2,28,29). We assume that dose increase does not cause additional adverse events, as there is no literature to suggest an exposure-toxicity relationship for abiraterone. Reference prices published by the Dutch Healthcare Authority (Nederlandse Zorgautoriteit, NZa) and ZIN were used to establish the costs for drugs and care (30,31). In the food intervention scenario we did not include costs of the low-fat meal as this falls outside the healthcare payer perspective. A detailed list of all costs is included in supplemental Tables S1 and S2, and a summary is shown in Table 1.

2.9

Utility values were used from the abiraterone acetate assessment report by ZIN (28). Utilities were proportionally corrected in each cycle depending on frequency and occurrence of adverse events, distinguishing one-time and chronic adverse events. QALY's were discounted by 1.5% annually, per the guidelines of ZIN (31). Utilities and disutilities of health states and adverse events are listed in Table 1. A detailed list of included utilities, disutilities and adverse event frequency adjustments as applied to each treatment option can be found in supplemental Table S2.*Sensitivity analyses* Deterministic and probabilistic sensitivity analyses were performed to determine the impact of the uncertainty in input parameters on the end result. The deterministic analysis shows the influence of each individual parameter on the incremental cost-effectiveness ratio (ICER) by varying parameters between their minimum and maximum values (Table 1 and the supplementary Tables S1 and S2). For survival parameters, the 95%-confidence intervals were used from the probabilistic sensitivity analysis. The probabilistic sensitivity analysis consisted of 10,000 iterations with random values according to their individual distributions for all parameters included in the model (32). The simultaneous random sampling of all input parameters gives a comprehensive estimate of the uncertainty around the model estimations.

To show the correlation of the likelihood of the intervention being cost-effective to different willingness-to-pay (WTP) thresholds, a cost-effectiveness acceptability curve (CEAC) was constructed. A WTP threshold of €80,000.- per QALY was used as the relevant threshold for the Dutch situation (33). Last, we calculated the incremental net monetary benefit (34). A positive Incremental Net Monetary Benefit (INMB) implies an intervention is cost-effective and guidelines advise adoption of such an intervention.

Clinical validation
Data from a real-life mCRPC patient cohort treated with abiraterone acetate at the Antoni van Leeuwenhoek/Netherlands Cancer Institute were used retrospectively to validate key model assumptions. Plasma samples of mCRPC patients using abiraterone were obtained as routine clinical care in the period between June 2016 and June 2018. Abiraterone plasma concentrations were measured with a validated liquid-chromatography mass spectrometry (LC-MS/MS) method (35). Samples were taken at random time points during the dosing interval and C_{min} was calculated using the pharmacokinetic model by Stuyckens et al. (36). Of 62 included patients, 42% had a low abiraterone C_{min}. The mean age of patients in the clinical population was 72 years. After progression on abiraterone acetate, 18% of patients received docetaxel, 2% received enzalutamide, 8% received cabazitaxel and 22% received radium-treatment, which is similar to data reported by Restelli et al. (22). Furthermore, 41% of patients were treated with abiraterone acetate post docetaxel compared to 21% in literature. This may be due to the fact that the Antoni van Leeuwenhoek hospital is a tertiary referral center and patients visiting this hospital are referred for specialized healthcare. In general, the clinical data support the data from literature. We chose to implement the slightly more conservative estimates from literature in our model, such as the 35% of patients with low C_{min} compared to 42% from the real-life cohort.
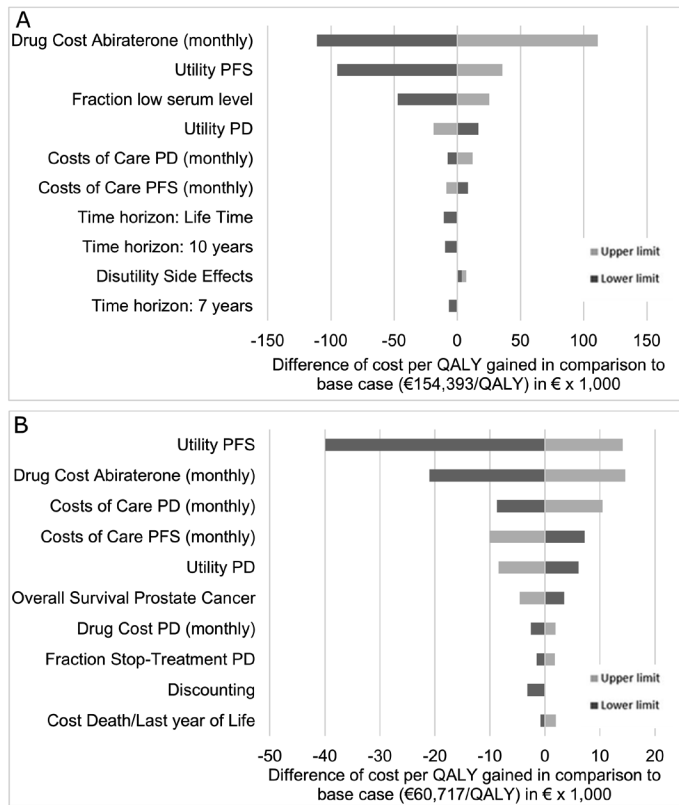
Figure 2. A: Deterministic sensitivity analysis of TDM with dose increase scenario compred to base case. B: Deterministic sensitivity analysis of TDM with food intervention compared to base case. PFS = progression-free survival, PD = progressed disease, TDM = therapeutic drug monitoring. Low C_{min} = the fraction of patients with abiraterone C_{min} <8.4ng/mL. The ten most sensitive parameters are displayed in each figure.

Results

Regular abiraterone acetetate treatment, not including TDM, resulted in 1.698 LYs and 1.283 QALYs per treated patient, with a cost of €98,873. The TDM intervention group followed by dose increase resulted in 0.107 incremental LYs and 0.089 incremental QALYs (1.802 LYs and 1.370 QALYs) against incremental costs of €13,524 (total: €112,398) resulting in an ICER of €154,353 per QALY. The scenario exploring TDM followed by the food-intervention resulted in equal incremental QALYs (assumption) and incremental costs of €5,319 (total: €104,192), resulting in an ICER of €60,717 per QALY.

Results of the deterministic sensitivity analysis (DSA) for the base case are given in Figure 2A, showing the ten most sensitive input parameters. The parameter which influenced the ICER most was montly abiraterone drug cost. The ICER varied from

2.9

€43,371 and €265,413 per QALY when varied to extremes (+/-25%). Monthly abiraterone drug cost was followed by PFS utility and fraction of patients with a low plasma level. The costs of TDM and change in time horizon from 5 to 7 or 10 years had little influence on the ICER. Figure 2B displays the DSA result for the food-intervention scenario, which shows similar results. Here, PFS utility is the most sensitivity parameter, followed by monthly abiraterone cost and monthly cost of care in PD. The fraction of patients with low plasma C_{min} was not amongst the ten most influential parameters. Results of the probabilistic sensitivity analysis are depicted in Figure 3.

Figure 4 presents the cost-effectiveness acceptability curves (CEAC). The likelihood of TDM with a dose increase being cost-effective given a WTP of €80,000.- was 20.4%. The food-intervention scenario increases the likelihood of cost-effectiveness to 81.4%. We could not calculate a 95% CI for the ICER because the probabilistic ICER results included negative values.

The INMB of the dose increase scenario was €-7,228 (95% CI € -26,238 to 10,209), indicating net losses for this intervention and the INMB of the low-fat meal scenario was €1,367 (95% CI € -2,477 to 6,019), indicating non-significant benefits for this intervention.
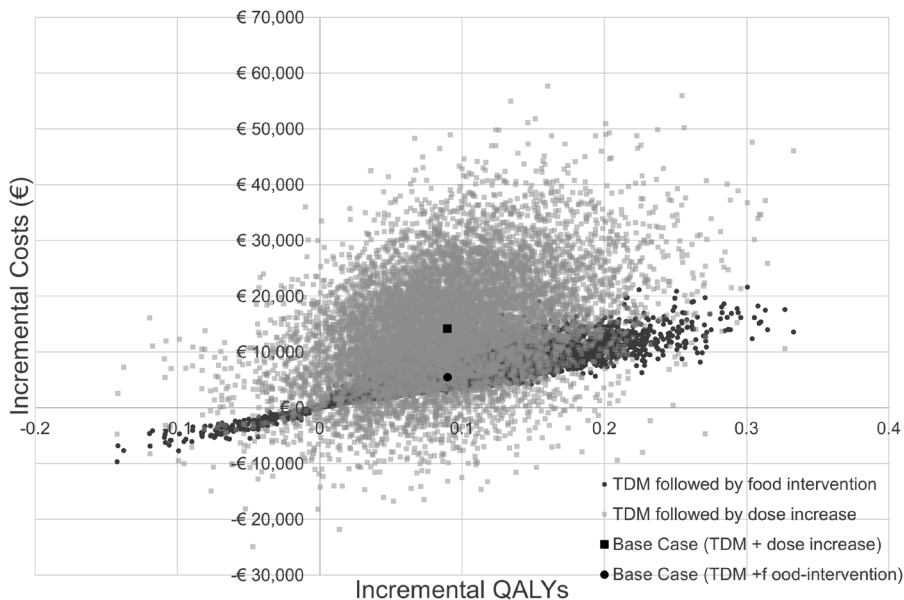
Figure 3. Cost-effectiveness plane of the results of the probabilistic sensitivity analysis. The scenario in which standard of care (1,000 mg abiraterone acetate once daily) is compared to the intervention of TDM followed by a dose increase (1,500 mg abiraterone acetate once daily) for patient with low plasma C_{min} (<8.4ng/mL) is shown in orange, with the base case shown in yellow. An alternative treatment scenario of TDM with a food intervention is displayed in blue, with the base case shown in red. Abbreviations: QALY = quality-adjusted life year, TDM = therapeutic drug monitoring.
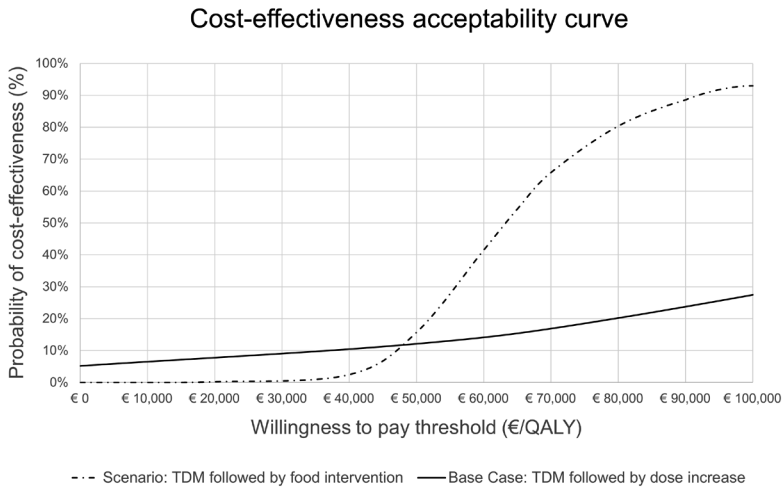
Figure 4. Cost-effectiveness acceptability curve (CEAC) for the base case and alternative treatment scenario. Abbreviations: ICER = incremental cost effectiveness ratio, TDM = therapeutic drug monitoring.

Discussion

Therapeutic drug monitoring of abiraterone followed by a dose increase to 1,500 mg daily for patients with low C_{min} (<8.4ng/mL) gives an ICER of €154,393 per QALY and is therefore not cost-effective when using the relevant Dutch WTP of €80.000 per QALY. The scenario in which patients with low plasma concentrations were advised to combine drug intake with a low-fat meal resulted in an ICER of €60,717. Based on our model, TDM for all patients followed by a food-intervention to increase clinical effectiveness in 35% of mCRPC patients could be a cost-effective option for clinical practice. Costs are driven solely by prolonged abiraterone acetate treatment, which is favorable from a clinical perspective.

The ICER was sensitive to some of the assumptions of the model, as shown in the deterministic sensitivity analyses. TDM of abiraterone followed by dose increase will result in an ICER below the relevant Dutch WTP threshold if a 16% abiraterone cost reduction is applied. A decrease in costs for abiraterone would substantially reduce the ICER in both scenarios. In our model, we used a range of +/- 25% to test the sensitivity of the ICER to the costs of abiraterone. If a generic competitor would enter the market, the cost reduction might be more substantial, potentially changing our conclusions. However, the patent of abiraterone acetate (Zytiga©) is set to expire in 2027, therefore we do not expect a lower drug list price soon (37), indicating that the finding of cost-ineffectiveness is robust. The robustness of the conclusions is confirmed in the probabilistic analysis and the cost-effectiveness acceptability curve, which show a very small likelihood of cost-effectiveness at the WTP threshold of €80,000 per QALY when combining TDM with a dose increase. These findings are also in line with general

2.9

findings of previous cost-effectiveness analyses that showed that the benefits of abiraterone do not outweigh its costs, although direct comparisons are difficult because settings differ between studies (4–8).

Food-drug interactions are often considered undesirable, but examples are available in which drug intake with a specific food can be used to a therapeutic advantage (38,39). For example, increased bioavailability of the antimycotic agent itraconazole is seen when ingested with an acidic beverage in patients pretreated with an H_2-blocker (40). As an alternative to conventional TDM, we show that TDM of abiraterone in mCRPC patients in combination with a low-fat meal is likely to be cost-effective.

Limitations

Our study has some limitations. First, the relationship between abiraterone C_{min} and response has been established in a prospective trial with only 61 participants (10). Additionally, an assumption in the model is that all patients with C_{min} <8.4 ng/mL will have adequate C_{min} after dose increase or the food-intervention. Based on current data we believe that the majority of patients will have an adequate C_{min} after both TDM interventions as the food-effect on AUC and C_{max} of abiraterone is proven to be strong when compared with fasting state (13). Due to the large variability in bioavailability, the percentage of patients reaching adequate C_{min} after dose increase may be slightly lower than after the food-intervention, resulting in conservative cost-effectiveness estimates.

Multiple sources were used for input parameters to approximate the cost-effectiveness of monitoring abiraterone C_{min} in mCRPC patients. There are some discrepancies in patient populations, causing an uncertainty in survival curves. Futhermore, the clinical validation was done at the Antoni van Leeuwenhoek hospital, which is a tertiary referral center. Patients visiting this hospital are referred for specialized treatment and may therefore have a different life expectancy. Although this might introduce bias, data from the real-life cohort are in line with data from literature. Therefore, we believe that our clinical validation adequately represents the clinical setting.

Conclusion

Based on this model, monitoring of abiraterone in mCRPC patients followed by a dose increase is not cost-effective from a healthcare payer perspective given a WTP of €80,000.-. However, TDM combined with a food-intervention is likely to be cost-effective. We advise clinicians to integrate TDM of abiraterone followed by a food intervention into standard abiraterone acetate treatment practices of mCRPC patients.

Table S1. List of utility and cost input parameters used in the Markov model. Abbreviations: PFS = Progression-Free Survival, PD = Progressed Disease, TDM = Therapeutic Drug Monitoring.

Parameter	Base	Low	High	Distribution	Source
Utility					
PFS	0.84	0.63	1.00	Beta	(42)
PD	0.715	0.536	0.894	Beta	(42)
Disutility					
Abiraterone					
First Cycle	0.052	0.039	0.065	Beta	(2,28,29)
>First Cycle	0.047	0.036	0.060	Beta	(2,28,29)
Docetaxel					
First Cycle	0.043	0.0322	0.054	Beta	(28,29,46)
>First Cycle	0.016	0.012	0.020	Beta	(28,29,46)
Cabazitaxel					
First Cycle	0.185	0.138	0.231	Beta	(28,29,47)
>First Cycle	0.031	0.023	0.039	Beta	(28,29,47)
Enzalutamide					
First Cycle	0.016	0.012	0.020	Beta	(28,29,48)
>First Cycle	0.015	0.012	0.020	Beta	(28,29,48)
Radium-223					
First Cycle	0.052	0.039	0.064	Beta	(26,28,29)
>First Cycle	0.037	0.028	0.047	Beta	(26,28,29)
Costs					
Intervention: TDM	€ 111.41	€ 83.55	€ 139.26	Gamma	(30)
Drug costs					
Abiraterone	€ 3,352.83	€ 2,514.62	€ 4,191.04	Gamma	(2,16,28,29,43)
Docetaxel	€ 1,736.38	€ 1,302.29	€ 2,170.48	Gamma	(16,41,43)
Cabazitaxel	€ 5,494.31	€ 4,120.73	€ 6,867.88	Gamma	(2,5,11,29,39)
Enzalutamide	€ 3,548.89	€ 2,661.67	€ 4,436.12	Gamma	(5,39)
Radium-223	€ 3,416.67	€ 2,562.50	€ 4,270.84	Gamma	(5,29,39)
Adverse Events: First cycle					
Abiraterone	€ 51.10	€ 38.32	€ 63.87	Gamma	(2,22,28,29)
Docetaxel	€ 193.87	€ 145.41	€ 242.34	Gamma	(22,28,29,46)
Cabazitaxel	€ 670.30	€ 502.72	€ 837.87	Gamma	(22,28,29,47)
Enzalutamide	€ 4.66	€ 3.49	€ 5.82	Gamma	(28,29,48)
Radium-223	€ 122.42	€ 91.82	€ 153.03	Gamma	(22,26,28,29)
Adverse Events: >First cycle					
Abiraterone	€ 10.94	€ 8.20	€ 13.67	Gamma	(2,28,29)
Docetaxel	€ 3.03	€ 2.28	€ 3.79	Gamma	(28,29,46)
Cabazitaxel	€ 4.99	€ 3.74	€ 6.24	Gamma	(28,29,47)

2.9

Table S1. Continued

Parameter	Base	Low	High	Distribution	Source
Enzalutamide	€ 6.32	€ 4.74	€ 7.90	Gamma	(28,29,48)
Radium-223	€ 5.53	€ 4.15	€ 6.92	Gamma	(26,28,29)
Home Care					
PFS	€ 793.93	€ 446.58	€ 1,240.51	Gamma	(31,44,45,49)
PD	€ 2,569.89	€ 1,445.56	€ 4,015.45	Gamma	(31,44,45,49)
Other					
Death	€ 18.287,10	€ 13,715.32	€ 41,098.41	Gamma	(50)

Table S2. Detailed disutility, costs, and frequency of adverse events per treatment option.*Average of pulmonary embolism and deep vein thrombosis.

Adverse event	Disutility	Costs		Frequency				
		Single time	Chronic	Abiraterone Acetate	Docetaxel	Cabazitaxel	Ra-223	Enzaluta-mide
Anemia	0.125	€ 67.32	€ 19.58	0.074	0.049	0.105	0.127	-
Cardiovascular event*	0.197*	€ 34.05	€ 8.74	0.054	-	-	-	0.028
Asthenia	0.094	€ 129.98	€ 20.28	0.023	-	0.046	0.008	0.013
Diarrhea	0.047	€ 197.13	€ 0.00	0.006	0.012	0.062	0.015	0.002
Dyspnea	0.067	€ 302.16	€ 0.00	0.013	0.006	0.013	0.02	-
Edema	0.085	€ 91.45	€ 1.14	-	0.006	-	0.002	0.002
Fatigue	0.094	€ 0.00	€ 0.00	0.083	0.03	0.049	0.04	0.018
Febrile neutropenia	0.12	€ 3,442.69	€ 0.00	-	0.02	0.075	-	-
Fracture	0.067	€ 2,323.69	€ 0.00	-	-	-	0.022	-
Hematuria	0.067	€ 0.00	€ 0.00	0.014	-	0.019	0.012	-
Hypertension	0.067	€ 0.00	€ 80.57	0.013	-	-	-	0.068
Hypokalemia	0.067	€ 0.00	€ 131.48	0.038	-	-	-	-
Infections and Infestations	0.067	€ 34.05	€ 0.00	0.021	0.08	0.011	0.033	-
Leukopenia	0.09	€ 0.00	€ 0.00	-	-	0.682	-	-
Nausea/vomiting	0.076	€ 797.75	€ 31.88	0.034	0.036	0.038	0.033	-
Neuropathy	0.116	€ 0.00	€ 54.82	-	0.012	-	-	-
Neutropenia	0.09	€ 418.18	€ 0.00	0.001	0.2	0.817	0.022	-
Pain	0.069	€ 34.05	€ 8.74	0.166	0.03	0.092	0.208	0.042
Thrombocyto-penia	0.09	€ 148.94	€ 0.00	0.014	0.006	0.040	0.063	-
Source	(28,29)	(22,28,29)		(2)	(51)	(52)	(26)	(53)

2.9

References

1. US Food and Drug Administration (FDA). Clinical Pharmacology and Biopharmaceutics Review: Zytiga (abiraterone acetate). 2010 [cited 2019 June]. Available from: https://www.accessdata.fda.gov/drugsatfda_docs/nda/2012/202379Orig1s005.pdf.

2. de Bono JS, Logothetis CJ, Molina A, Fizazi K, North S, Chu L, et al. Abiraterone and increased survival in metastatic prostate cancer. N Engl J Med. 2011;364:1995–2005.

3. Ryan CJ, Smith MR, de Bono JS, Molina A, Logothetis CJ, de Souza P, et al. Abiraterone in metastatic prostate cancer without previous chemotherapy. N Engl J Med. 2013;368:138–48.

4. Koninckx M, Marco JL, Pérez I, Faus MT, Alcolea V, Gómez F. Effectiveness, safety and cost of abiraterone acetate in patients with metastatic castration-resistant prostate cancer: a real-world data analysis. Clin Transl Oncol. 2019;21:314–23.

5. Pollard ME, Moskowitz AJ, Diefenbach MA, Hall SJ. Cost-effectiveness analysis of treatments for metastatic castration resistant prostate cancer. Asian J Urol. 2017;4:37–43.

6. Chiang CL, So TH, Lam TC, Choi HCW. Cost-effectiveness analysis of Abiraterone Acetate versus Docetaxel in the management of metastatic castration-sensitive prostate cancer: Hong Kong's perspective. Prostate Cancer Prostatic Dis. 2019;Epub ahead of print.

7. Peters ML, de Meijer C, Wyndaele D, Noordzij W, Leliveld-Kors AM, van den Bosch J, et al. Dutch Economic Value of Radium-223 in Metastatic Castration-Resistant Prostate Cancer. Appl Health Econ Health Policy. 2018;16:133–43.

8. Aguiar PN, Tan PS, Simko S, Barreto CMN, Gutierres B de S, Giglio A del, et al. Cost-effectiveness analysis of abiraterone, docetaxel or placebo plus androgen deprivation therapy for hormone-sensitive advanced prostate cancer. Heal Econ Manag. 2018;16:1–10.

9. Lojanapiwat B, Anutrakulchai W, Chongruksut W, Udomphot C. Correlation and diagnostic performance of the prostate-specific antigen level with the diagnosis, aggressiveness, and bone metastasis of prostate cancer in clinical practice. Prostate Int. 2014;2:133–9.

10. Carton E, Noe G, Huillard O, Golmard L, Giroux J, Cessot A, et al. Relation between plasma trough concentration of abiraterone and prostate-specific antigen response in metastatic castration-resistant prostate cancer patients. Eur J Cancer. 2017;72:54–61.

11. Groenland SL, van Nuland M, Verheijen RB, Schellens JHM, Beijnen JH, Huitema ADR, et al. Therapeutic Drug Monitoring of Oral Anti-Hormonal Drugs in Oncology. Clin Pharmacokinet. 2018;58:299-308.

12. Szmulewitz RZ, Peer CJ, Ibraheem A, Martinez E, Kozloff MF, Carthon B, et al. Prospective International Randomized Phase II Study of Low-Dose Abiraterone With Food Versus Standard Dose Abiraterone In Castration-Resistant Prostate Cancer. J Clin Oncol. 2018;36:1389–95.

13. Chi KN, Spratlin J, Kollmannsberger C, North S, Pankras C, Gonzalez M, et al. Food effects on abiraterone pharmacokinetics in healthy subjects and patients with metastatic castration-resistant prostate cancer. J Clin Pharmacol. 2015;55:1406–14.

14. Groenland SL, Bergman AM, Huitema A, Steeghs N. Concomitant intake of abiraterone and food to increase pharmacokinetic exposure: Real-life data from a therapeutic drug monitoring program. J Clin Oncol. 2019;37:3117.

15. Husereau D, Drummond M, Petrou S, Carswell C, Moher D, Greenberg D, et al. Consolidated health economic evaluation reporting standards (CHEERS)-explanation and elaboration: A report of the ISPOR health economic evaluation publication guidelines good reporting practices task force. Value Heal. 2013;16:231–50.

16. Nederlandse Vereniging voor Urologie. Landelijke Richtlijn: Prostaatcarcinoom [National guideline for prostate cancer treatment]. 2016 [cited 2019 Apr]. Available from: https://www.oncoline.nl/prostaatcarcinoom

17. Behl AS, Ellis LA, Pilon D, Xiao Y, Lefebvre P. Medication adherence, treatment patterns, and dose reduction in patients with metastatic castration-resistant prostate cancer receiving abiraterone acetate or enzalutamide. Am Heal Drug Benefits. 2017;10:296–302.

18. Hoyle M, Henley W. Improved curve fits to summary survival data: application to economic evaluation of health technologies. BMC Med Res Methodo. 2011;11:1139.

19. Tierney JF, Stewart LA, Ghersi D, Burdett S, Sydes MR. Practical methods for incorporating summary time-to-event data into meta-analysis. Trials. 2007;8:1–16.

20. Ryan CJ, Smith MR, Fizazi K, Saad F, Mulders PFA, Sternberg CN, et al. Abiraterone acetate plus prednisone versus placebo plus prednisone in chemotherapy-naive men with metastatic castration-resistant prostate cancer (COU-AA-302): Final overall survival analysis of a randomised, double-blind, placebo-controlled phase 3 study. Lancet Oncol. 2015;16:152–60.

21. Fizazi K, Scher HI, Molina A, Logothetis CJ, Chi KN, Jones RJ, et al. Abiraterone acetate for treatment of metastatic castration-resistant prostate cancer: Final overall survival analysis of the COU-AA-301 randomised, double-blind, placebo-controlled phase 3 study. Lancet Oncol. 2012;13:983–92.

22. Restelli U, Ceresoli GL, Croce D, Evangelista L, Maffioli LS, Gianoncelli L, et al. Economic burden of the management of metastatic castrate-resistant prostate cancer in Italy: A cost of illness study. Cancer Manag Res. 2017;9:789–800.

23. Azad AA, Eigl BJ, Murray RN, Kollmannsberger C, Chi KN. Efficacy of enzalutamide following abiraterone acetate in chemotherapy-naive metastatic castration-resistant prostate cancer patients. Eur Urol. 2015;67:23–9.

24. Mezynski J, Pezaro C, Bianchini D, Zivi A, Sandhu S, Thompson E, et al. Antitumour activity of docetaxel following treatment with the CYP17A1 inhibitor abiraterone: Clinical evidence for cross-resistance? Ann Oncol. 2012;23:2943–7.

25. Al Nakouzi N, Le Moulec S, Albigès L, Wang C, Beuzeboc P, Gross-Goupil M, et al. Cabazitaxel Remains Active in Patients Progressing after Docetaxel Followed by Novel Androgen Receptor Pathway Targeted Therapies. Eur Urol. 2015;68:228–35.

26. Parker C, Nilsson S, Heinrich D, Helle SI, O'Sullivan JM, Fosså SD, et al. Alpha emitter radium-223 and survival in metastatic prostate cancer. N Engl J Med. 2013;369:213–23.

27. Centraal burea voor Statistiek. Statistics Netherlands [Centraal bureau voor Statistiek. 2018 [cited 2019 Jan]. Available from: https://www.cbs.nl/nl-nl

28. de graaff M. Farmacotherapeutic report abirateron (Zytiga®) in metastatic castration-resistant prostate cancer mCRPC [Dutch]. 2011 [cited 2019 August]. Available from: file:///C:/Users/3260909/AppData/Local/Google/Chrome/Downloads/Abirateron+(Zytiga)+bij+gemetastaseerd+castratieresistent+prostaat carcinoom+mCRPC (1).pdf

29. Boer A. Farmacotherapeutic report cabazitaxel (Jevtana®) indicated for castrate resistant metastatic prostate cancer [Dutch]. 2011.

30. Dutch Healthcare Authority (NZa). DBC product-finder for tariffs. 2018.

31. Kanters TA, Bouwmans CAM, Linden N van der, Tan SS, Hakkaart-Van Roijen L. Update of the Dutch Manual for Costing in Economic Evaluations. PLoS One. 2017;12:11.

32. Drummond MF, Sculpher MJ, Torrance GW, O'Brien, Stoddart BJ and GL. Methods for the economic evaluation of health care programmes. Oxford University Press; 2005. 379 p.

2.9

33. Dutch National Health Institute (Zorginstituut Nederland). Richtlijn voor het uitvoeren van economische evaluaties in de gezondheidszorg [guideline for economic evaluation in health care]. 2016. p. 38.

34. Trippoli S. Incremental cost-effectiveness ratio and net monetary benefit: Current use in pharmacoeconomics and future perspectives. Eur J Intern Med. 2017;43:e36.

35. van Nuland M, Hillebrand MJX, Rosing H, Schellens JHM, Beijnen JH. Development and validation of an LC-MS/MS method for the simultaneous quantification of abiraterone, enzalutamide, and their major metabolites in human plasma. Ther Drug Monit. 2017;39:243–51.

36. Stuyckens K, Saad F, Xu XS, Ryan CJ, Smith MR, Griffin TW, et al. Population pharmacokinetic analysis of abiraterone in chemotherapy-naive and docetaxel-treated patients with metastatic castration-resistant prostate cancer. Clin Pharmacokinet. Dec;53:1149–60.

37. Janssen Biotech Inc. Abiraterone acetate (Zytiga) Tablet 250mg. 2011 [cited 2019 August]. Available from: https://www.accessdata.fda.gov/scripts/cder/ob/results_product.cfm?Appl_Type=N&Appl_No=202379

38. Bushra R, Aslam N, Khan AY. Food-drug interactions. Oman Med J. 2011;26:77–83.

39. Segal EM, Flood MR, Mancini RS, Whiteman RT, Friedt GA, Kramer AR, et al. Oral Chemotherapy Food and Drug Interactions: A Comprehensive Review of the Literature. J Oncol Pract. 2014;10:e255–68.

40. Lange D, Pavao JH, Wu J, Klausner M. Effect of a cola beverage on the bioavailability of itraconazole in the presence of H2 blockers. J Clin Pharmacol. 1997;37:535–40.

41. Haycock GB, GJ S, DH I. Geometric method for measuring body surface area: A height weight formula validated in infants, children and adults. J Pediatr. 1978;93:62–6.

42. Committee for Medicinal Product for Human Use (CHMP). Assessment report Zytiga (abiraterone acetate). Eur Med Agency. 2017;44:1–81.

43. Dutch National Health Institute (Zorginstituut Nederland). Drug costs in the Netherlands [Dutch]. 2018 [cited 2019 Jul]. Available from: https://www.medicijnkosten.nl/

44. Mehra M, Wu Y, Dhawan R. Healthcare resource use in advanced prostate cancer patients treated with docetaxel. J Med Econ. 2012;15:836–43.

45. Heine R Ter, Frederix GW, Geenen JW, Hövels AM, Vulpen M van, Kooistra A, et al. Cost of illness of metastatic prostate cancer: a perspective of costs for new treatment options in The Netherlands. J Comp Eff Res. 2017;6:575-81.

46. European Medicines Agency (EMA). Annex I: Summary of Product Characteristics. Taxotere (docetaxel). 2012 [cited 2019 August]. Available from: https://www.ema.europa.eu/en/documents/product-information/taxotere-epar-product-information_en.pdf

47. De Bono JS, Oudard S, Ozguroglu M, Hansen S, MacHiels JP, Kocak I, et al. Prednisone plus cabazitaxel or mitoxantrone for metastatic castration-resistant prostate cancer progressing after docetaxel treatment: A randomised open-label trial. Lancet. 2010;376:1147–54.

48. Beer TM, Armstrong AJ, Rathkopf DE, Loriot Y, Sternberg CN, Higano CS, et al. Enzalutamide in metastatic prostate cancer before chemotherapy. N Engl J Med. 2014;371:424–33.

49. Krahn MD, Bremner KE, Zagorski B, Alibhai SMH, Chen W, Tomlinson G, et al. Health care costs for state transition models in prostate cancer. Med Decis Mak. 2014;34:366–78.

50. Carter HE, Martin A, Schofield D, Duchesne G, Haworth A, Hornby C, et al. A decision model to estimate the cost-effectiveness of intensity modulated radiation therapy (IMRT) compared to three dimensional conformal radiation therapy (3DCRT) in patients receiving radiotherapy to the prostate bed. Radiother Oncol. 2014;112:187–93.

51. European Medicines Agency (EMA). Zytiga : Annex I - Summary of product characteristics. 2017 [cited 2019 August]. Available from: https://www.ema.europa.eu/en/documents/product-information/zytiga-epar-product-information_en.pdf

52. De Bono JS, Oudard S, Ozguroglu M, Hansen S, MacHiels JP, Kocak I, et al. Prednisone plus cabazitaxel or mitoxantrone for metastatic castration-resistant prostate cancer progressing after docetaxel treatment: A randomised open-label trial. Lancet. 2010;376:1147–54.

53. Beer TM, Armstrong AJ, Rathkopf DE, Loriot Y, Sternberg CN, Higano CS, et al. Enzalutamide in metastatic prostate cancer before chemotherapy. N Engl J Med. 2014;371:424–33.

2.9

Pharmacokinetic predictions using microdosing

Predictive value of microdose pharmacokinetics

Merel van Nuland
Hilde Rosing
Alwin D.R. Huitema
Jos H. Beijnen

Abstract

Phase 0 microdose trials are exploratory studies to early assess human pharmacokinetics of new chemical entities, while limiting drug exposure and risks for participants. The microdose concept is based on the assumption that microdose pharmacokinetics can be extrapolated to pharmacokinetics of a therapeutic dose. It is, however, unknown whether microdose pharmacokinetics are actually indicative of the pharmacokinetics at therapeutic dose. The aim of this review is to investigate the predictive value of microdose pharmacokinetics and to identify drug characteristics that may influence the scalability of these parameters. The predictive value of microdose pharmacokinetics was determined for 46 compounds and showed adequate predictability for 28 out of 41 orally administered drugs (68%) and for 15 out of 16 intravenously administered drugs (94%). Microdose pharmacokinetics were considered predictive if the mean observed values of the microdose and the therapeutic dose were within a two-fold. Nonlinearity may be caused by saturation of enzyme and transporter systems, such as intestinal and hepatic efflux and uptake transporters. The high degree of success regarding linear pharmacokinetics shows that phase 0 microdose trials can be used as an early human model for determination of drug pharmacokinetics.

Introduction

Drug development is an extensive endeavor in which only 10% of newly developed compounds eventually gain market authorization (1–3). Although clinical failure is mainly attributed to lack of efficacy or poor drug tolerability, 10% of failure is caused by undesirable pharmacokinetics such as poor absorption or a short half-life (4). Early determination of drug pharmacokinetics could increase success rates in further development and thereby reduce costs. In recent times, drug pharmacokinetics in human are estimated by extrapolation of pharmacokinetics from *in vitro* and preclinical studies to a clinical setting. The predictability of human pharmacokinetics from preclinical data is based on assumptions about the behavior of the drug across species (5–7). Although interspecies scaling may be used to predict pharmacokinetic parameters, extrapolation from animals to humans is complex. Therefore, a more accurate predictive model of pharmacokinetic parameters could improve selection of drugs and increase clinical approval.

The European Medicines Agency (EMA) introduced the concept of microdose studies as a human model, in which a small portion of a drug is administered to participants with the aim of investigating pharmacokinetics. Currently, the EMA M3 (R2) guideline is widely accepted as guidance for microdose studies. A microdose is defined as 1% of the anticipated therapeutic dose, with a maximum of 100 µg for chemical entities and 30 nmol for protein drugs (8). Because these trials are conducted prior to traditional phase 1, they are denoted phase 0 microdose trials.

The main feature of phase 0 microdose trials is early assessment of human pharmacokinetics of new chemical entities, with limited drug exposure, including mass balance and metabolite profiling. Hereby, phase 0 microdose trials have the potential to make drug development more efficient by earlier selection of promising candidates. Microdoses are considered harmless because of the limited drug exposure, therefore, less extensive preclinical toxicology studies are required. Due to this nontoxic nature of a microdose, neither a therapeutic effect nor adverse events are to be expected (8). The microdose concept is based on the assumption that microdose pharmacokinetics can be extrapolated to pharmacokinetics of a therapeutic dose. It is, however, unknown whether microdose pharmacokinetics are really indicative of the pharmacokinetics at therapeutic dose. A previous review assessed microdose predictability in human for 25 orally administered and 12 intravenously administered drugs. It was shown that 62% of orally administered and 100% of intravenously administered drugs tested between microdose and therapeutic dose demonstrated scalable pharmacokinetics within a two-fold (9). Many new microdose trials have been published since. Furthermore, the last review did not discuss the influence of enzymes or transporter systems on the linearity of microdose pharmacokinetics. In this review we collect drug characteristics, including relevant metabolizing enzymes and transporters, to identify similarities between drugs with nonlinear pharmacokinetics in terms of saturation mechanisms. The aim of this review is to update previous data by investigating whether

3.1

279

the pharmacokinetics in a clinically relevant therapeutic dose can be predicted from the pharmacokinetics of a microdose and to identify drug characteristics that may influence the scalability of these parameters.

Methods

Literature search

Pubmed and Embase databases were searched to identify pharmacokinetic microdose trials, using the following terms: microdose OR microdosing OR "phase 0". The search was performed on November 19th 2018 and results were restricted to the English language and to studies in humans. Additional papers were selected from review articles. Initial screening was based on title and abstract, while inclusion was performed manually by full-text assessment of eligibility. Furthermore, publications were only included if pharmacokinetic outcome measures were available for both the microdose and a clinically relevant therapeutic dose. Microtracer studies, in which a radio-labeled microdose is co-administered with a non-radiolabeled therapeutic dose, were excluded as the total administered dose exceeds the criteria to be regarded a microdose (>1/100th of the therapeutic dose with a maximum of 100 μg) (9).

For each oral drug investigated in included microdose trials, the following drug characteristics were gathered: solubility, lipophilicity (logP) and biopharmaceutical drug disposition and classification system (BDDCS) class (Figure 1). Furthermore, metabolizing enzymes and relevant drug transporters were collected. Information on registered drugs were obtained from a review article on BDDCS class (10) and FDA documents (prescribing data, clinical pharmacology and biopharmaceutics review, label text). Drug characteristics of non-registered drugs were collected from literature and the BDDCS classification was based on solubility and permeability: good solubility was defined as being soluble in 250 mL water or less at the highest marketed dose strength and good permeability was defined as the logP being greater than the logP of metoprolol (1.88) as proposed by Benet et al. (10).

Pharmacokinetic scalability

The predictive value of microdose pharmacokinetics was determined by comparing pharmacokinetic parameters of the microdose with those of the therapeutic dose. For the area under the curve (AUC), the   value to infinity in ng·h/ml was used, unless otherwise denoted, and presented dose-adjusted to 100 μg. Furthermore, half-life (t½) was reported in hours, clearance (CL) in L/h and volume of distribution (Vd) in L. Pharmacokinetic data from trials in which only microdose pharmacokinetics were determined were complemented with literature data on therapeutic pharmacokinetics. Microdose pharmacokinetics were considered predictive if the mean observed values of the microdose and the therapeutic dose were within a two-fold as described previously (11,12). The predictive value was determined for all pharmacokinetic parameters that were available for both the microdose and therapeutic dose. Drugs
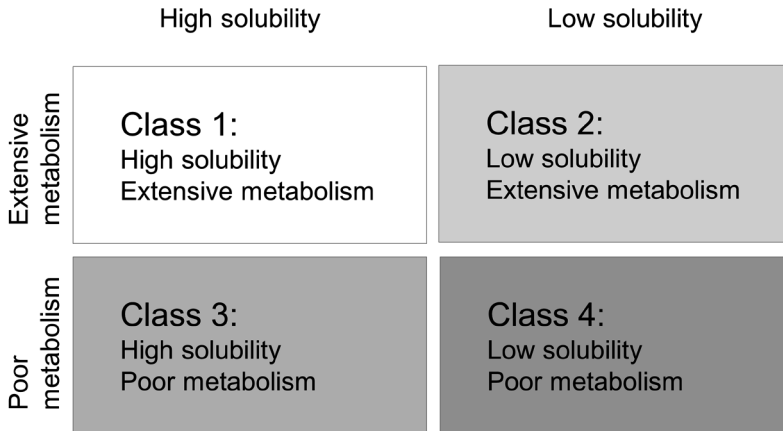
Figure 1. Biopharmaceutics Drug Disposition Classification System (BDDCS) as described by Benet et al. (44).

with at least one poorly scalable parameter (i.e. outside the two-fold threshold) were denoted as having non-linear pharmacokinetics

Results

Studies
The literature search identified 2107 publications of which 35 articles were found eligible for inclusion. Four more papers were selected from the references cited in other review articles. Microdose pharmacokinetics were available for 46 different drugs; eight drugs were investigated in more than one trial. Table 1 shows the characteristics of drugs investigated in cross-over trials (n=25) in which a microdose and a therapeutic dose were administered, thereby facilitating a direct comparison of pharmacokinetic parameters. Furthermore, Table 2 contains pharmacokinetic parameters of drugs from trials in which only a microdose was administered. Results from these studies were compared with pharmacokinetics of the therapeutic dose as described in literature. In general, three types of study designs could be distinguished; single drug microdose trials (n=24), multiple drug microdose trials (n=9) and cassette microdose trials (n=6). In multiple drug microdose trials, >1 drug was administered separately to participants, while a combination of drugs was administered simultaneously in cassette microdose trials.

Pharmacokinetics
Microdose pharmacokinetics were reported for 30 drugs investigated in cross-over trials and for 20 drugs studied in single microdose trials. In total, the predictive value could be determined for 45 drugs, of which 41 were given orally and 16 were given intravenously. Twelve drugs were administered both orally and intravenously.

3.1

Table 1. Pharmacokinetic parameters of drugs from cross-over trials in which a microdose and a therapeutic dose were administered.

Drug	Microdose (µg)	Therapeutic dose (mg)	Route of administration	Pharmacokinetics microdose ‡	Pharmacokinetics therapeutic dose ‡	Linear pharmacokinetics?	Ref.
Atenolol	100	50	po	t½ = 7.11 AUC = 8.88	t½ = 7.23 AUC = 7.27	Yes	(45)
Atorvastatin	100	10	po	AUC = 0.20	AUC = 0.45	No	(15)
Celiprolol	37.5	100	po	t½ = 13.35 AUC_{0-24} = 0.232 CL/F = 488	t½ = 6.14 AUC_{0-24} = 1.29 CL/F = 109	No	(14)
Clarithromycin	100	250	iv	t½ = 4.10 AUC = 4.78	t½ = 4.50 AUC = 5.44	Yes	(17)
	100	250	po	t½ = 4.00 AUC = 0.99 F = 22%	t½ = 3.40 AUC = 1.96 F = 39%	Yes	(17)
Diltiazem	30	30	po	AUC = 0.138	AUC = 0.264	Yes	(20)
Docetaxel	100	100	iv	$t_{1/2}$ = 5.10 AUC = 3.64 V = 3.91	$t_{1/2}$ = 3.41 AUC = 2.23 V = 13.7	No	(46)
Enalapril	100	10	po	t½ = 12.1 AUC = 13.0	t½ = 11.8 AUC = 12.0	Yes	(45)
Fexofenadine	100	120	iv	t½ = 8.10 AUC = 8.06 CL = 13	t½ = 10 AUC = 7.47 CL = 16	Yes	(47)
	100	120	po	t½ = 16 AUC = 2.77	t½ = 12 AUC = 1.84	Yes	(47)
	100	60	po	t½ = 3.2 AUC = 3.19	t½ = 2.90 AUC = 2.39	Yes	(48)
hRESCAP	53	5.3	iv	$t_{1/2}$ = 108 AUC = 531	$t_{1/2}$ = 104 AUC = 716	Yes	(38)
Losartan	100	50	po	t½ = 3.31 AUC = 3.62	t½ = 3.41 AUC = 3.41	Yes	(45)

Table 1. Continued

Drug	Microdose (µg)	Therapeutic dose (mg)	Route of administration	Pharmacokinetics microdose ‡	Pharmacokinetics therapeutic dose ‡	Linear pharmacokinetics?	Ref.
Metformin	100	250	po	$AUC_{0-12} = 2.13$ $CL_R = 623$	$AUC_{0-12} = 2.24$ $CL_R = 395$	Yes	(28)
Midazolam	100	7,5	iv	$t_{1/2} = 4.87$ $AUC = 4.53$ $CL = 21.2$	$t_{1/2} = 2.55$ $AUC = 4.68$ $CL = 20.4$	Yes	(24)
	1	1	iv	$t_{1/2} = 3.55$ $AUC = 3.79$	$t_{1/2} = 4.02$ $AUC = 3.90$	Yes	(49,50)
	100	7,5	po	$t_{1/2} = 3.95$ $F = 22.8\%$	$t_{1/2} = 3.31$ $F = 22.1\%$	Yes	(24)
	3	3	po	$t_{1/2} = 3.26$ $AUC = 0.89$ $F = 23.4\%$	$t_{1/2} = 3.96$ $AUC = 0.81$ $F = 20.9\%$	Yes	(49,50)
	0.3	3	po	$t_{1/2} = 3.54$ $AUC = 3.67$ $V/F = 376$	$t_{1/2} = 4.11$ $AUC = 3.53$ $V/F = 353$	Yes	(51)
Mirodenafil	100	100	po	$t_{1/2} = 1.80$ $AUC = 0.27$ $CL/F = 538$	$t_{1/2} = 1.32$ $AUC = 0.89$ $CL/F = 131$	No	(18)
NBI-1	100	10	po	$t½ = 6.70$ $AUC = 2.86$	$t½ = 8.40$ $AUC = 3.28$	Yes	(52)
Mirodenafil	100	100	po	$t½ = 1.80$ $AUC = 0.27$ $CL/F = 538$	$t_{1/2} = 1.32$ $AUC = 0.89$ $CL/F = 131$	No	(18)
NBI-1	100	10	po	$t½ = 6.70$ $AUC = 2.86$	$t½ = 8.40$ $AUC = 3.28$	Yes	(52)
Nicardipine	100	20	po	Comparable concentration-time curves for the metabolites	$AUC = 0.22$	Yes	(23)
	30	30	po	$AUC = 0.098$		No	(20)

3.1

Table 1. Continued

Drug	Microdose (µg)	Therapeutic dose (mg)	Route of administration	Pharmacokinetics microdose ‡	Pharmacokinetics therapeutic dose ‡	Linear pharmacokinetics?	Ref.
Nifedipine	40	20	po	AUC = 2.13	AUC = 2.76	Yes	(20)
Omeprazol	100	20	po	t½ = 1.21 AUC = 2.59	t½ = 2.40 AUC = 8.24	No	(22)
Paracetamol	0.024*	15	iv	t½ = 3.78 AUC$_{0-6}$ = 8.4 CL = 2.72	t½ = 2.62 AUC$_{0-6}$ = 5.4 CL = 2.93	Yes	(53)
	0.024*	15	po	t½ = 1.6 AUC$_{0-8}$ = 9.0 CL = 1.5	t½ = 2.6 AUC$_{0-8}$ = 7.0 CL = 2.9	Yes	
PF-05089771	100	2400	iv	t$_{1/2}$ = 6.50 AUC= 33	t$_{1/2}$ = 8.20 – 11.4 AUC= 33	Yes	(54)
Propafenone	100	150	iv	t½ = 5.40 AUC = 1.90 V = 273	t½ = 4.70 AUC =2.20 V = 214	Yes	(17)
	100	150	po	t½ = 3.80 AUC = 0.12 F = 5.8%	t½ = 2.60 AUC = 0.27 F = 13.0%	No	
Quinidine	100	100	po	t½ = 5.07 AUC = 0.813	t½ = 5.59 AUC = 2.08	No	(13)
RDEA806	80	200	iv	-	-	Yes	(55)
Sumatriptan	100	50	iv	t½ = 6.50 AUC = 2.20 V = 426	t½ = 5.60 AUC = 2.10 V = 397	Yes	(17)
	100	50	po	t½ = 1.90 AUC = 0.44 F = 20%	t½ = 1.40 AUC = 0.15 F = 7.6%	No	

Table 1. Continued

Drug	Microdose (µg)	Therapeutic dose (mg)	Route of administration	Pharmacokinetics microdose‡	Pharmacokinetics therapeutic dose‡	Linear pharmacokinetics?	Ref.
Telmisartan	100	80	po	UGT1A1*1/*1: AUC_{0-24} = 1.76 CL/F = 64.0 UGT1A1*1/*28: $AUC_{(0-24)}$ = 0.771 CL/F = 126	UGT1A1*1/*1: AUC_{0-24} = 3.97 CL/F = 23.6 UGT1A1*1/*28: $AUC_{(0-24)}$ = 1.57 CL/F = 50.8	No	(19)
Tenofovir[†]	100	300	po	$t_{1/2}$ = 14.1 AUC = 9658 CL/F = 31.3 Intracellular metabolites; C_{max} = 13.1 AUC = 2334 Intracellular metabolites CD4+: C_{max} = 13.2 AUC = 1925	$t_{1/2}$ = 21.4 AUC = 6653 CL/F = 45.6 Intracellular metabolites: C_{max} = 10.4 AUC = 1526 Intracellular metabolites CD4+: C_{max} = 5.1 AUC = 1500	Yes Yes	(27)
Unknown integrase inhibitors A	50	?	iv po	$t_{1/2}$ = 3.30 AUC = 4.37 $t_{1/2}$ = 3.02 AUC = 2.69 F = 57%	-	Yes[†]	(56)
Unknown integrase inhibitors B	50	?	iv po	$t_{1/2}$ = 2.75 AUC = 5.20 $t_{1/2}$ = 2.28 AUC = 2.62 F = 54%	-	Yes[†]	(56)
Unknown integrase inhibitors C	50	?	iv po	$t_{1/2}$ = 4.08 AUC = 4.12 $t_{1/2}$ = 3.31 AUC = 1.60 F = 43%	-	Yes[†]	(56)

Table 1. Continued

Drug	Microdose (µg)	Therapeutic dose (mg)	Route of administration	Pharmacokinetics microdose ‡	Pharmacokinetics therapeutic dose ‡	Linear pharmacokinetics?	Ref.
Unknown integrase inhibitors D	50	?	iv	$t_{1/2}$ = 2.22 AUC = 3.96	-	Yes[†]	(56)
			po	$t_{1/2}$ = 1.69 AUC = 1.75 F = 53%			
Verapamil	50	80	iv	K_1 = 0.030 V = 0.66	K_1 = 0.031 V = 0.56	Yes	(57)
	100	80	po	$t_{1/2}$ = 2.48 AUC = 0.139	$t_{1/2}$ = 3.21 AUC = 0.320	No	(13)
Zidovudine[¥]	100	300	po	Intracellular metabolites in PBMCs: AUC = 1837 Intracellular metabolites CD4+: AUC = 1266	Intracellular metabolites in PBMCs: AUC = 578 Intracellular metabolites CD4+: AUC = 151	No	(27)
ZK253	100	50	iv	$t_{1/2}$ = 61.4 AUC = 7.42 CL = 9.29 F = 0.16%	$t_{1/2}$ = 56.2 AUC = 7.15 CL = 14.8 F <1%	Yes	(24)
	100	50	po			Yes	

Abbreviations: Route of ad.=Route of administration, ref.=references, iv=intravenously, po=orally.
‡Pharmacokinetic parameters: AUC=AUC$_{(0-inf)}$ in ng·h/ml unless otherwise denoted and is shown dose-normalized to 100 µg. t½ is reported in hours, CL in L/h and Vd in L.
* Study in children with a dose of 6 ng/kg and mean weight of 4 kg
† Therapeutic dose pharmacokinetics were not given in the literature, however, linearity was determined based on unpublished data
¥Intracellular pharmacokinetics in peripheral blood mononuclear cells and CD4+ cells. C_{max} of intracellular metabolites in fmol/10^6 cells and AUC of intracellular metabolites in fmol*h/10^6 cells

Microdose pharmacokinetics were predictive within the two-fold criteria for 28 out of 41 (68%) oral formulations and for 15 out of 16 (94%) intravenous formulations. Conflicting data were found for atorvastatin, verapamil and fexofenadine (13–17). Pharmacokinetic linearity was determined in cross-over trials, in which both a microdose and therapeutic dose were administered (Table 1), or comparing microdose data to literature (Table 2). As a cross-over design reduces inter-individual variability, the results of the cross-over trials were regarded more accurate. Therefore, verapamil and fexofenadine were considered as having predictive microdose pharmacokinetics, while atorvastatin was regarded as having poor predictability.

Pharmacokinetic nonlinearity of oral drugs was predominantly reflected in the exposure (AUC), with 11 out of 13 (85%) drugs showing poorly scalable AUC. A nonlinear increase in AUC after dose escalation was seen for atorvastatin (2.3-fold), celiprolol (2.2-fold), mirodenafil (3.3-fold), nicardipine (2.2-fold), omeprazole (3.2-fold), propafenone (2.3-fold), quinidine (2.6-fold), telmisartan (5.6-fold) and verapamil (2.3-fold), while a decrease in AUC was shown for sumatriptan (2.9-fold) and rosuvastatin (2.2-fold) (13–15,17–23). Bioavailability (F) was determined for two of these drugs, with a nonlinear increase at therapeutic dose for propafenone (2.3-fold) and a decrease for sumatriptan (2.6-fold) (17).

Nonlinearity in V_d was described for iv administration of docetaxel and oral administration of warfarin (24,25). V_d decreased 3.5-fold for docetaxel and 3.8-fold for warfarin following dose escalation.

Five microdose trials specifically focused on the metabolism of a drug and metabolite pharmacokinetics. Linear metabolite pharmacokinetics were described for nicardipine and verapamil (1.0-fold) (13,23), while quinidine exhibited nonlinear pharmacokinetics for both the parent compound and three major metabolites (2.6-fold) (13). The pharmacokinetics of celiprolol, telmisartan and tolbutamide were assessed for various CYP-enzyme genotypes, responsible for metabolic conversion (14,19,26). The predictive value was similar for poor, extensive and ultra-rapid metabolizers. Moreover, the pharmacokinetics of intracellular metabolites were described for the drugs zidovudine and tenofovir. These anti-retroviral drugs are phosphorylated intracellularly to pharmacologically active triphosphate metabolites. The pharmacokinetics of the intracellular metabolites of tenofovir (measured in PBMCs and CD4+ cells) and of the parent compound in plasma were found to be linear (1.3-1.5-fold) (27), while pharmacokinetics of zidovudine triphosphates were nonlinear with a 3.9-fold higher dose-adjusted AUC at therapeutic dose compared to microdose (27).

Kusuhara et al. specifically focused on the pharmacokinetics of metformin after inhibition of the multidrug and toxin extrusion (MATE) protein that is responsible for renal elimination of this drug and reported linear pharmacokinetics (28). Celiprolol, warfarin and pitavastatin showed a nonlinear decrease in half-life ($t_{1/2}$) at therapeutic dose compared to microdose of 2.2-fold, 5.8-fold and 3.1-fold, respectively (14,21,24).

3.1

Table 2. Pharmacokinetic parameters of drugs from trials in which only a microdose was administered; microdose pharmacokinetics were compared to pharmacokinetics of the therapeutic dose as described in literature.

Drug	Microdose (μg)	Therapeutic dose (mg)	Route of administration	Pharmacokinetics microdose‡	Pharmacokinetics therapeutic dose‡	Linear pharmacokinetics?	Ref.
AFN-1252	100	400	po	$t\frac{1}{2}$ = 7.40 AUC = 16.8	$t\frac{1}{2}$ = 7.74 AUC = 13.5	Yes	(58,59)
Anastrozole	1.98	1	po	$t\frac{1}{2}$ = 37.2 AUC = 65.2	$t\frac{1}{2}$ = 56.3 AUC = 104	Yes	(60,61)
Atenolol	30	50	po	$t\frac{1}{2}$ = 6.47 AUC_{0-24} = 10.2 T_{max} = 3.13	$t\frac{1}{2}$ = 7.23 AUC^{*} = 7.27 T_{max} = 4.14	Yes	(14,45)
Atorvastatin	33	40	po	AUC_{0-10} = 0.19	$AUC_{0-24}{}^{*}$ = 0.22	Yes	(16,62)
	50	40	po	$t\frac{1}{2}$ = 9.00 AUC = 0.24	$t\frac{1}{2}$ = 8.05 AUC = 0.25	Yes	(21,62)
Caffeine	25	250	po	$t\frac{1}{2}$ = 4.13 AUC = 10.8	$t\frac{1}{2}$ = 5.20 AUC = 13.0	Yes	(63–66)
Diazepam	100	10	iv	$t_{1/2}$ = 45.1 AUC = 65.5 CL = 1.38	$t_{1/2}$ = 35.7 AUC = 55.8 CL = 1.30	Yes	(24,67)
Diphenhydramine	100	50	po	$t\frac{1}{2}$ = 12.0 F = 34.0% AUC = 1.35	$t\frac{1}{2}$ = 6.32 F = 66.3% AUC = 1.01	Yes	(52,68–72)
	100	50	iv	$t\frac{1}{2}$ = 9.30	$t\frac{1}{2}$ = 7.30	Yes	
Fexofenadine	25	120	po	$t\frac{1}{2}$ = 5.75 AUC = 2.00	$t\frac{1}{2}$ = 2.90 AUC = 2.12	Yes	(14,47,48,63)
	30	120	po	$t\frac{1}{2}$ = 7.05		No	
IDX899 (Fosdevirine)	100	800	po	$t_{1/2}$ = 4.40 AUC = 7.60	$t_{1/2}$ = 8.30 AUC = 8.90	Yes	(73,74)
Midazolam	25	7.5	po	$t\frac{1}{2}$ = 4.01 AUC = 1.76	$t\frac{1}{2}$ = 3.31 AUC = 1.16	Yes	(24,63)
	10	7.5	po	$t\frac{1}{2}$ = 5.80 AUC = 1.97	$t\frac{1}{2}$ = 3.31 AUC = 1.16	Yes	(21,24,63)
NS-304 (Selexipag)	33	7.5	po	AUC_{0-10} = 1.41	$AUC_{0-12}{}^{*}$ = 2.14	Yes	(16,75)
	100	0.8	po	$t_{1/2}$ = 1.7 AUC = 5.8	$t_{1/2}$ = 2.3 AUC = 3.12	Yes	(76,77)
Paracetamol	100	1000	po	$t\frac{1}{2}$ = 2.41 AUC = 4.11	$t\frac{1}{2}$ = 3.61 AUC = 5.46	Yes	(17,78–82)
	100	1000	po	$t\frac{1}{2}$ = 5.80 AUC = 4.80 F = 88%	F = 89%	Yes	

Table 2. Continued

Drug	Microdose (µg)	Therapeutic dose	Route of ad.	Microdose PK	Therapeutic dose PK	Linear	Ref.
	100	1000-1500	iv	$t_{1/2}$ = 4.60 CL = 19.0 V = 123	$t_{1/2}$ = 2.50 CL = 19.7 V = 66.5	Yes	(17,82,83)
Phenobarbital	100	240	po	$t_{1/2}$ = 180	$t_{1/2}$ = 98.0	Yes	(17,84)
Pitavastatin	10	1	po	$t_{1/2}$ = 12.3 AUC = 4.61	$t_{1/2}$ = 4.0 AUC = 2.90	No	(21,85)
Pravastatin	33	600	po	AUC_{0-8} = 0.60	AUC_{0-8} = 0.36	Yes	(16,86-89)
Raltegravir	50	400	po	AUC = 3.86 T_{max} = 0.50	AUC = 2.64 T_{max} = 1.00	Yes	(56,90)
Rosuvastatin	25	5	po	$t_{1/2}$ = 7.70 AUC = 1.03	$t_{1/2}$ = 12.8 AUC = 0.47	No	(21,85)
Tolbutamide	100	125	po	CYP2C9*1/*1: $t_{1/2}$ = 7.90 CL = 0.82 AUC = 123 CYP2C9*1/*3: $t_{1/2}$ = 13.9 CL = 0.50 AUC = 206	CYP2C9*1/*1: $t_{1/2}$ = 7.30 (7.10-7.50) CL = 0.91 (0.85-0.97) AUC = 119 CYP2C9*1/*3: $t_{1/2}$ = 13.1 (12.2-13.9) CL = 0.91 (0.56-0.60) AUC = 166	Yes	(26,91-93)
	25	125	po	$t_{1/2}$ = 8.13 AUC = 167	$t_{1/2}$ = 7.70 AUC = 143	Yes	(63,94)
Warfarin	100	5	po	$t_{1/2}$ = 274 AUC = 571 V = 67.3	$t_{1/2}$ = 48.6 AUC = 416 V = 17.9	No	(24,95)
Zidovudine	100	300	po	$t_{1/2}$ = 4.5 AUC = 4269 CL/F = 70.5	$t_{1/2}$ = 6.6 AUC = 4458 CL/F = 68.2	Yes	(27,96,97)

Abbreviations: Route of ad.=Route of administration, ref.=references, iv=intravenously, po=orally.

‡ Pharmacokinetic parameters: AUC=$AUC_{(0-inf)}$ in ng·h/ml unless otherwise denoted and is shown dose-normalized to 100 µg. $t_{1/2}$ is reported in hours, CL in L/h and Vd in L.

* The $AUC_{(0-t)}$ calculated for microdose exposure was not found in literature for therapeutic dose exposure, therefore the closest $AUC_{(0-t)}$ time point was chosen.

† Therapeutic dose pharmacokinetics were not given in the literature, however, linearity was determined based on unpublished data.

3.1

Drug characteristics

Drug characteristics were collected for orally administered drugs of included microdose trials (n=41). Table 3 shows the solubility, lipophilicity (logP), BDDCS class, metabolizing enzymes and relevant drug transporters of these compounds. The majority of drugs with linear pharmacokinetics are in BDDCS class 1 and 3, while the majority of drugs with nonlinear pharmacokinetics are class 1 and 2. Drugs were metabolized or transported by a great variety of proteins, such as organic anion-transporting polypeptides (OATP), P-glycoprotein (P-gp), multidrug resistance-associated protein (MRP), breast cancer resistance protein (BCRP) and organic cation transporting proteins (OCT), with the majority of BDDCS class 2 drugs being transported by OATPs.

Discussion

The predictive value of microdose pharmacokinetics was determined for 46 compounds and showed adequate predictability for 68% of orally administered drugs (n=41) and for 94% of intravenously administered drugs (n=16). These results are in line with previously reported data (9). Importantly, these numbers may underestimate the predictive value as included studies examined compounds known or suspected to have nonlinearity issues. This overview is different to the last literature survey because more drugs are included and drug characteristics are identified that may influence the pharmacokinetic scalability. Furthermore, the relevance of metabolizing enzymes and transporters was discussed with regard to saturation mechanisms. With this increased number of microdose data, our review provides new information on microdose predictability, while confirming findings from previous literature.

Microdose pharmacokinetics were considered predictive if all given pharmacokinetic parameters of the microdose and the therapeutic dose were within a two-fold (11,12). This two-fold criterion is commonly used in allometry, however, limitations should be acknowledged. For example, the AUC increased nonlinear with an average of 2.4-fold for 12 drugs, being just outside the two-fold threshold. Although these drugs are denoted as having nonlinear pharmacokinetics, the question arises if the predictive value would be significantly different with an AUC increase of 1.9-fold, indicating linear pharmacokinetics within two-fold. With this in mind, microdose data should be regarded as exploratory, providing early pharmacokinetic information for newly developed compounds.

Data gathered in this review clearly show that the absorption phase is pivotal for predictability of microdose pharmacokinetics. Nonlinearity may arise in the gastrointestinal dissolution process or when enzymes or transporter systems saturate at therapeutic dose (29–31). Dissolution, solubility and intestinal uptake are reflected in the BDDCS class. Saturation of enzyme and transporter systems may occur at different sites; intestinal and hepatic efflux transporters, uptake transporters and metabolizing enzymes. The most important intestinal and hepatic efflux transporters in drug pharmacokinetics are P-gp, MRP2 and BCRP, and the most relevant uptake

Table 3. Drug characteristics of orally administered drugs (n=41), with linear pharmacokinetics (n=28) and nonlinear pharmacokinetics (n=13).

Linear PK drugs (n=28)	Solubility* (mg/mL)	Lipophilicity (logP)	BDDCS class	Metabolizing enzymes	Transporter proteins	References
AFN-1252‡	0.003-0.01	3.21	3	NR	Passive transport	(58)(98)
Anastrozole	0.5	1.29	1	CYP3A4/5 CYP2C8 UGT1A4	P-gp	(44)(99)(100)(101)
Atenolol	24.8	0.16	3	Minimal metabolism	OATP2B1 OATP1A2	(44)(102)(103)
Caffeine	21.5	-0.07	1	CYP1A2	Passive transport	(44)(104)(105)
Clarithromycin	2	3.16	3	CYP3A4	P-gp	(44)(106)(107)(108)
Diltiazem (hydrochloride)	30-100	2.70	1	CYP3A4/5	P-gp	(44)(109)(110)
Diphenhydramine	1000	3.27	1	CYP2D6 CYP1A2 CYP2C9 CYP2C19	NR	(44)(111)
Enalapril	25	0.67	1	Carboxylesterase	OATP1B1 MRP2	(44)(112)(113)
Fexofenadine	1-10	1.96	3	Minimal metabolism	P-gp OATP2B1/3 OATP1A2	(44)(114)(103)(115)
Fosdevirine‡	0.0094	3.50	3	NR	NR	(116)
Losartan (potassium)	0.048	4.10	2	CYP3A4 CYP2C9	P-gp	(44)(117)(118)(119)
Metformin	30-100	-1.63	3	Minimal metabolism	OCT1/2	(44)(120)(121)(122)(123)(124)
Midazolam (hydrochloride)	30-100	3.27	1	CYP3A4/5/7	P-gp	(44)(125)(126)
NBI-1‡	Highly soluble	Highly permeable	1	NR	NR	(52)
Nifedipine	0.006	2.20	2	CYP3A4	P-gp	(44)(127)
Selexipag	<0.1	4.40	3	CYP2C8	P-gP OATP1B1 OATP1B3 BCRP	(128)

3.1

Table 3. Continued

Linear PK drugs (n=28)	Solubility* (mg/mL)	Lipophilicity (logP)	BDDCS class	Metabolizing enzymes	Transporter proteins	References
Paracetamol	23.7	0.20	1	UGT1A1/6/9 SULT1A1/3/4 CYP1A2 CYP2E1	P-gp MRP1/5	(44)(129)
Phenobarbital	1	1.47	1	NR	P-gp	(44)(130)
Pravastatin	300	2.18	3	CYP3A4	P-gp OATP2	(44)(131)(132)
Raltegravir (potassium)	71	1.16	2	UGT1A1	P-gp BCRP	(44)(133)(134)
Tenofovir (disoproxil)	13.4	0.80	3	Carboxylesterase	OATP1/3 MRP4	(44)(135)
Tolbutamide	0.109	2.34	2	CYP2C9	OATP2	(44)(136)(137)
Unknown integrase inhibitors A‡	NR	NR	NR	NR	NR	(56)
Unknown integrase inhibitors B‡	NR	NR	NR	NR	NR	(56)
Unknown integrase inhibitors C‡	NR	NR	NR	NR	NR	(56)
Unknown integrase inhibitors D‡	NR	NR	NR	NR	NR	(56)
Zidovudine	25	0.08	1	UGT2B7	SLC28A1/3 SLC 22A6/7/8/11	(44)(138) (139,140)
ZK253‡	NR	Poor permeability	NR	NR	NR	(24)

Nonlinear PK drugs (n=13)	Nonlinear PK parameters	Solubility* (mg/mL)	Lipophilicity (logP)	BDDCS class	Metabolizing enzymes	Transporter proteins	References
Atorvastatin (calcium)	AUC	0.0000204	4.46	2	CYP3A4	OATP1B1 P-gP	(44)(141)
Celiprolol	AUC, t½	151	1.92	3	Minimal metabolism	OATP2B1 OATP1A2	(44) (103)(142)
Mirodenafil‡	AUC, CL/F	0.181	2.85	3	CYP3A4 CYP2C19 CYP2D6	NR	(143)(144)(145)
Nicardipine	AUC	7.9	3.82	1	CYP3A4	NR	(44)(146)

Table 3. Continued

Nonlinear PK drugs (n=13)	Nonlinear PK parameters	Solubility* (mg/mL)	Lipophilicity (logP)	BDDCS class	Metabolizing enzymes	Transporter proteins	References
Omeprazol	AUC	0.5	2.23	1	CYP2C19 CYP3A4	NR	(44)(147)
Pitavastatin	t½	0.1-1	3.59	2	UGT1A3 UGT2B7 CYP2C9	OATP1B1/3 BCRP	(44)(148)(149)
Propafenone (hydrochloride)	AUC, F	0.093	3.64	2	CYP2D6 CYP1A2 CYP3A4	NR	(44)(150)(151)
Quinidine (sulfate)	AUC	11.1	3.77	1	CYP3A4	P-gp	(44)(152)
Rosuvastatin (calcium)	AUC	10-33	1.90	3	CYP2C9 CYP2C19 CYP3A4 CYP2D6	OATP1B1/3 BCRP P-gp	(44)(153)(154)(155)
Sumatriptan (succinate)	AUC, F	21.4	0.93	1	Monoamine oxidase-A	OCT1	(44)(156)
Telmisartan	AUC, CL/F	<0.1	7.54	2	UGT	OATP1B3 P-gp MRP2 BCRP	(44)(157)(158)(159)
Verapamil (hydrochloride)	AUC	0.75	4.47	1	CYP3A4 CYP1A2	P-gp OCT	(44)(160)(108)
Warfarin	V, t½	0.018	2.60	2	CYP2C9	BCRP	(44)(136)(161)

Abbreviations: AUC = area under the curve, BDDCS = biopharmaceutical drug disposition classification system, BCRP = breast cancer resistant protein, CL = clearance, CYP = cytochroom p450, F = biological availability, NR = not reported, OATP = organic-anion-transporting polypeptide, OCT = organic cation transporting proteins, P-gP = p-glycoprotein, PK = pharmacokinetics, t½ = half-life, SLC = solute carrier family, UGT = uridine diphosphate (UDP)-glucuronosyltransferase, V = volume of distribution.
* Experimental solubility in 250 ml or less of aqueous media over a pH range of 1-7.5 at 37°C. When experimental solubility was not reported, quanlitative evaluation such as 'highly soluble in water' were used and a range is given in the table.
‡ Drug characteristics of non-registered drugs were collected from literature other than FDA documents or Benet et al. (44) and the BDDCS class was based on these literature values.

3.1

293

transporters are the OATP 1B1/3 and 2B1 (32). In attempt to identify drug characteristics responsible for non-linearity, the scalability was examined in relation to BDDCS class, metabolizing enzymes and drug transporters. Drugs in BDDCS class 2 and 4 might be prone to nonlinearity regarding low solubility, where class 2 will be even more challenging due to potential extensive metabolism. The majority of drugs with linear pharmacokinetics are class 1 and 3, while the majority of drugs with nonlinear pharmacokinetics are class 1 and 2. Extensive metabolism seems to complicate the scalability of pharmacokinetics, while solubility is less of a problem.

When further zooming into specific metabolizing enzymes and transporters, a great variety is shown among linear and nonlinear compounds. Although nonlinearity could be caused by saturated metabolism (13,18,22), in most cases it may be attributed to saturation of transporters in the gut wall (13–15,17,21). Among these transporters are OATP, P-gp, MRP2, BCRP and organic cation transporting proteins (OCT), with the majority of BDDCS class 2 drugs being transported by OATPs. OATPs mostly transport large, hydrophobic organic anions from the portal blood into hepatocytes and may therefore influence the rate of elimination (33). Although saturation of OATPs may be a cause of nonlinearity, due to great inter-patient variability in transporter abundance and difference in transporter affinity for each drug, it is difficult to predict nonlinearity beforehand. This is reflected in the group of seven drugs with linear pharmacokinetics that are also transported by OATPs. Based on current data it is hard to draw conclusions, however, drugs in BDDCS class 2 and drugs with affinity for drug transporters may be prone to having nonlinear pharmacokinetics.

The percentage of predictable pharmacokinetics, especially for intravenous administration, is much higher in microdose studies than for extrapolation from preclinical models. When predicting human pharmacokinetics with physiologically based pharmacokinetic modelling (PB-PK) or in vitro to in vivo extrapolation (IVIVE), the degree of success for predicting V_d, CL and oral AUC is only 78% (n=18), 78% (n=19) and 51% (n=108) of cases, respectively (6,34–37). This may be due to physiological differences between animal and human, but also due to poor animal models of human illness and conflicting data from in vivo and/or in vitro experiments. Results from this review clearly show an added value of microdose data to predict pharmacokinetics at therapeutic dose.

Microdose trials have been performed for small molecule drugs, while there is only one trial in which a protein drug, human recombinant alkaline phosphatase (hRESCAP), has been administered to healthy volunteers (38). A major concern regarding microdosing with targeted therapies is the expectation of nonlinear pharmacokinetics as is seen for monoclonal antibodies (39,40). Target-mediated drug disposition (TMDD) of these drugs causes poor linearity in the low dose range by saturated target binding and clearance pathways (41). However, TMDD could also occur for small molecules when the target is expressed at relatively high concentrations and the compound has a high affinity for this target (42). An example of such a drug is warfarin; a small molecule with high affinity to vitamin-K epoxide reductase. Nonlinearity due to TMDD

is reflected in nonlinear volume of distribution and half-life, while the exposure is well predicted from the microdose (24). Although very few small molecules show this type of nonlinearity, one should be aware of the possible implications of TMDD for microdose trials.

Based on all data available, it is difficult to describe specific drug characteristics that influence the predictability of microdose pharmacokinetics. When performing a microdose study, guidance on the predictive value may be derived from preclinical data. Bosgra et al. showed how to integrate available preclinical data in a decision tree by combining information on dissolution, active transport or metabolism, and protein binding (43). Of ten previously published cases, this decision tree was able to identify drugs with non-linear pharmacokinetics. Combining microdose trials with preclinical data, and modeling and simulation methods may improve the reliability of decision making in the future.

Conclusion

In this review we questioned whether the pharmacokinetics in a clinically relevant therapeutic dose could be predicted from a microdose. Additionally, we incorporated drug characteristics in order to explain causes of nonlinearity. 94% of intravenously and 68% orally administered drugs displayed linear pharmacokinetics within the two-fold criterion. Nonlinearity was caused by saturation of enzyme and transporter systems, especially intestinal and hepatic efflux and uptake transporters. The high degree of success regarding linear pharmacokinetics confirms the strength of phase 0 microdose trials in gaining early pharmacokinetic data, thereby providing safety and reducing developmental costs.

3.1

References

1. Dickson M, Gagnon JP. The cost of new drug discovery and development. Discov Med. 2004;4:172–9.

2. Tonkens R. An overview of the drug development process. Physician Exec. 2005;31(3):48–52.

3. Kola I, Landis J. Can the pharmaceutical industry reduce attrition rates? Nat Rev Drug Discov. 2004;3:711–5.

4. Kola I. The State of Innovation in Drug Development. Clin Pharmacol Ther. 2008;83:227–30.

5. Rowland M, Benet LZ. Lead PK commentary: predicting human pharmacokinetics. Vol. 100, Journal of pharmaceutical sciences. 2011. p. 4047–9.

6. Poulin P, Jones HM, Jones R Do, Yates JWT, Gibson CR, Chien JY, et al. PhRMA CPCDC initiative on predictive models of human pharmacokinetics, part 1: goals, properties of the PhRMA dataset, and comparison with literature datasets. J Pharm Sci. 2011;100:4050–73.

7. Nair A, Morsy MA, Jacob S. Dose translation between laboratory animals and human in preclinical and clinical phases of drug development. Drug Dev Res. 2018;

8. FDA/CDER. Guidance for Industry, Investigators, and Reviewers: Exploratory IND Studies. Biotechnol Law Rep. 2006;25:167–74.

9. Lappin G, Noveck R, Burt T. Microdosing and drug development: past, present and future. Expert Opin Drug Metab Toxicol. 2013;9:817–34.

10. Benet LZ, Broccatelli F, Oprea TI. BDDCS applied to over 900 drugs. AAPS J. 2011;13:519–47.

11. Lappin G, Garner RC. The utility of microdosing over the past 5 years. Expert Opin Drug Metab Toxicol. 2008;4:1499–506.

12. M. R, Rowland M. Commentary on ACCP position statement on the use of microdosing in the drug development process. J Clin Pharmacol. 2007;47:1595–6.

13. Maeda K, Takano J, Ikeda Y, Fujita T, Oyama Y, Nozawa K, et al. Nonlinear pharmacokinetics of oral quinidine and verapamil in healthy subjects: A clinical microdosing study. Clin Pharmacol Ther. 2011;90:263–70.

14. Ieiri I, Doi Y, Maeda K, Sasaki T, Kimura M, Hirota T, et al. Microdosing clinical study: Pharmacokinetic, pharmacogenomic (SLCO2B1), and interaction (grapefruit juice) profiles of celiprolol following the oral microdose and therapeutic dose. J Clin Pharmacol. 2012;52:1078–89.

15. Kajinami K, Takeda K, Maeda K, Sugiyama Y, Ieir I, Masaugi T, et al. SLCO1B1 polymorphisms affect atorvastatin pharmacokinetics and cholesterol-lowering effects in patients with hypercholesterolemia in a microdosing approach. Eur Hear. 2013;34:1.

16. Maeda K, Ikeda Y, Fujita T, Yoshida K, Azuma Y, Haruyama Y, et al. Identification of the rate-determining process in the hepatic clearance of atorvastatin in a clinical cassette microdosing study. Clin Pharmacol Ther. 2011;90:575–81.

17. Lappin G, Shishikura Y, Jochemsen R, Weaver RJ, Gesson C, Brian Houston J, et al. Comparative pharmacokinetics between a microdose and therapeutic dose for clarithromycin, sumatriptan, propafenone, paracetamol (acetaminophen), and phenobarbital in human volunteers. Vol. 43, European Journal of Pharmaceutical Sciences. 2011. 141-150 p.

18. Cho D-Y, Bae SHK, Shon J-H, Bae SHK. High-sensitive LC-MS/MS method for the simultaneous determination of mirodenafil and its major metabolite, SK-3541, in human plasma: Application to microdose clinical trials of mirodenafil. J Sep Sci. 362:840–8.

19. Ieiri I, Nishimura C, Maeda K, Sasaki T, Kimura M, Chiyoda T, et al. Pharmacokinetic and pharmacogenomic profiles of telmisartan after the oral microdose and therapeutic dose. Pharmacogenet Genomics. 2011;21:495–505.

20. Yamashita S, Kataoka M, Suzaki Y, Imai H, Morimoto T, Ohashi K, et al. An Assessment of the Oral Bioavailability of Three Ca-Channel Blockers Using a Cassette-Microdose Study: A New Strategy for Streamlining Oral Drug Development. J Pharm Sci. 2015;104:3154–61.

21. Prueksaritanont T, Tatosian DA, Chu X, Railkar R, Evers R, Chavez-Eng C, et al. Validation of a microdose probe drug cocktail for clinical drug interaction assessments for drug transporters and CYP3A. Clin Pharmacol Ther. 2017;101:519–30.

22. Park G-J, Bae SH, Park W-S, Han S, Park M-H, Shin S-H, et al. Drug-drug interaction of microdose and regular-dose omeprazole with a CYP2C19 inhibitor and inducer. Drug Des Devel Ther. 2017;11:1043–53.

23. Yamane N, Tozuka Z, Sugiyama Y, Tanimoto T, Yamazaki A, Kumagai Y. Microdose clinical trial: Quantitative determination of nicardipine and prediction of metabolites in human plasma. Drug Metab Pharmacokinet. 2009;24:389–403.

24. Lappin G, Kuhnz W, Jochemsen R, Kneer J, Chaudhary A, Oosterhuis B, et al. Use of microdosing to predict pharmacokinetics at the therapeutic dose: Experience with 5 drugs. Clin Pharmacol Ther. 2006;80:203–15.

25. Fujita K-I, Yoshino E, Kawara K, Maeda K, Kusuhara H, Sugiyama Y, et al. A clinical pharmacokinetic microdosing study of docetaxel with Japanese patients with cancer. Cancer Chemother Pharmacol. 2015;76:793–801.

26. Ikeda T, Aoyama S, Tozuka Z, Nozawa K, Hamabe Y, Matsui T, et al. Microdose pharmacogenetic study of (14)C-tolbutamide in healthy subjects with accelerator mass spectrometry to examine the effects of CYP2C9 *3 on its pharmacokinetics and metabolism. Eur J Pharm Sci. 2013;49:642–8.

27. Chen J, Flexner C, Liberman RG, Skipper PL, Louissaint NA, Tannenbaum SR, et al. Biphasic elimination of tenofovir diphosphate and nonlinear pharmacokinetics of zidovudine triphosphate in a microdosing study. J Acquir Immune Defic Syndr. 2012;61:593–9.

28. Kusuhara H, Ito S, Kumagai Y, Jiang M, Shiroshita T, Moriyama Y, et al. Effects of a MATE protein inhibitor, pyrimethamine, on the renal elimination of metformin at oral microdose and at therapeutic dose in healthy subjects. Clin Pharmacol Ther. 2011;89:837–44.

29. Lappin G, Noveck R, Burt T. Microdosing and drug development: Past, present and future. Expert Opin Drug Metab Toxicol. 2013;9:817–34.

30. Harrison A, Gardner I, Hay T, Dickins M, Beaumont K, Phipps A, et al. Case studies addressing human pharmacokinetic uncertainty using a combination of pharmacokinetic simulation and alternative first in human paradigms. Xenobiotica. 2012;42:57–74.

31. Seto C, Sakuma T, Ni J, Ouyang F, Lo L, Welty D, et al. Assessment of pharmacokinetic linearity of metabolites from a microdose to a normal dose. Drug Metab Rev. 2009;41:148–9.

32. Zhang L, Strong JM, Qiu W, Lesko LJ, Huang S-M. Scientific perspectives on drug transporters and their role in drug interactions. Mol Pharm. 2006;3:62–9.

33. Kalliokoski A, Niemi M. Impact of OATP transporters on pharmacokinetics. Br J Pharmacol. 2009;158:693–705.

34. Jones R Do, Jones HM, Rowland M, Gibson CR, Yates JWT, Chien JY, et al. PhRMA CPCDC initiative on predictive models of human pharmacokinetics, part 2: comparative assessment of prediction methods of human volume of distribution. J Pharm Sci. 2011;100:4074–89.

3.1

35. Ring BJ, Chien JY, Adkison KK, Jones HM, Rowland M, Jones R Do, et al. PhRMA CPCDC initiative on predictive models of human pharmacokinetics, part 3: comparative assessement of prediction methods of human clearance. J Pharm Sci. 2011;100:4090–110.

36. Vuppugalla R, Marathe P, He H, Jones RDO, Yates JWT, Jones HM, et al. PhRMA CPCDC initiative on predictive models of human pharmacokinetics, part 4: prediction of plasma concentration-time profiles in human from in vivo preclinical data by using the Wajima approach. J Pharm Sci. 2011;100:4111–26.

37. Poulin P, Jones RDO, Jones HM, Gibson CR, Rowland M, Chien JY, et al. PHRMA CPCDC initiative on predictive models of human pharmacokinetics, part 5: prediction of plasma concentration-time profiles in human by using the physiologically-based pharmacokinetic modeling approach. J Pharm Sci. 2011;100:4127–57.

38. Vlaming MLH, van Duijn E, Dillingh MR, Brands R, Windhorst AD, Hendrikse NH, et al. Microdosing of a Carbon-14 Labeled Protein in Healthy Volunteers Accurately Predicts Its Pharmacokinetics at Therapeutic Dosages. Clin Pharmacol Ther. 2015;98:196–204.

39. Glassman PM, Balthasar JP. Mechanistic considerations for the use of monoclonal antibodies for cancer therapy. Cancer Biol Med. 2014;11:20–33.

40. Rowland M. Microdosing of Protein Drugs. Clin Pharmacol Ther. 2016;99:150–2.

41. Dirks NL, Meibohm B. Population pharmacokinetics of therapeutic monoclonal antibodies. Clin Pharmacokinet. 2010;49:633–59.

42. Smith DA, van Waterschoot RAB, Parrott NJ, Olivares-Morales A, Lave T, Rowland M. Importance of target-mediated drug disposition for small molecules. Drug Discov Today. 2018;23:2023-30.

43. Bosgra S, Vlaming MLH, Vaes WHJ. To Apply Microdosing or Not? Recommendations to Single Out Compounds with Non-Linear Pharmacokinetics. Clin Pharmacdokinet. 2015;55:1–15.

44. Benet LZ, Broccatelli F, Oprea TI. BDDCS Applied to Over 900 Drugs. AAPS J. 2011;13:519–47.

45. Mahajan R, Parvez A, Gupta K. Microdosing vs. Therapeutic dosing for evaluation of pharmacokinetic data: A comparative study. J Young Pharm. 2009;1:290.

46. Fujita K-I, Yoshino E, Kawara K, Maeda K, Kusuhara H, Sugiyama Y, et al. A clinical pharmacokinetic microdosing study of docetaxel with Japanese cancer patients. Eur J Cancer. 2015;51:S62.

47. Lappin G, Shishikura Y, Jochemsen R, Weaver RJ, Gesson C, Houston B, et al. Pharmacokinetics of fexofenadine: evaluation of a microdose and assessment of absolute oral bioavailability. Eur J Pharm Sci. 2010;40:125–31.

48. Yamazaki A, Kumagai Y, Yamane N, Tozuka Z, Sugiyama Y, Fujita T, et al. Microdose study of a P-glycoprotein substrate, fexofenadine, using a non-radioisotope-labelled drug and LC/MS/MS. J Clin Pharm Ther. 2010;35:169–75.

49. Hohmann N, Kocheise F, Carls A, Burhenne J, Haefeli W, Gerd M. Pharmacokinetics of an intravenous microgram dose of midazolam. Clin Pharmacol Ther. 2014;95:S45.

50. Hohmann N, Kocheise F, Carls A, Burhenne J, Haefeli WE, Mikus G. Midazolam microdose to determine systemic and pre-systemic metabolic CYP3A activity in humans. Br J Clin Pharmacol. 2015;79:278–85.

51. Halama B, Hohmann N, Burhenne J, Weiss J, Mikus G, Haefeli WE. A Nanogram Dose of the CYP3A Probe Substrate Midazolam to Evaluate Drug Interactions. Clin Pharmacol Ther. 2013;93:564–71.

52. Madan A, O'Brien Z, Wen J, O'Brien C, Farber RH, Beaton G, et al. A pharmacokinetic evaluation of five H1 antagonists after an oral and intravenous microdose to human subjects. Br J Clin Pharmacol. 2009;67:288–98.

53. Garner CR, Park KB, French NS, Earnshaw C, Schipani A, Selby AM, et al. Observational infant exploratory [(14)C]-paracetamol pharmacokinetic microdose/therapeutic dose study with accelerator mass spectrometry bioanadlysis. Br J Clin Pharmacol. 2015;80:157–67.

54. Jones HM, Butt RP, Webster RW, Gurrell I, Dzygiel P, Flanagan N, et al. Clinical Micro-Dose Studies to Explore the Human Pharmacokinetics of Four Selective Inhibitors of Human Nav1.7 Voltage-Dependent Sodium Channels. Clin Pharmacokinet. 2016;55:875–87.

55. Stevens L, Evans P, Dueker S, Lostroh P, Giacomo J, Yeh L, et al. Microdose and microtracer intravenous pharmacokinetics of RDEA806 in healthy subjects. Clin Pharmacol Ther. 2009;85:S24-5.

56. Sun L, Li H, Willson K, Breidinger S, Rizk ML, Wenning L, et al. Ultrasensitive Liquid Chromatography − Tandem Mass Spectrometric Methodologies for Quanti fi cation of Five HIV - 1 Integrase Inhibitors in Plasma for a Microdose Clinical Trial. Anal Chem. 2012;84:8614–21.

57. Wagner CC, Simpson M, Zeitlinger M, Bauer M, Karch R, Abrahim A, et al. A Combined Accelerator Mass Spectrometry-Positron Emission Tomography Human Microdose Study with 14C- and 11C-Labelled Verapamil. Clin Pharmacokinet. 2011;50:111–20.

58. Kaplan N, Garner C, Hafkin B. AFN-1252 in vitro absorption studies and pharmacokinetics following microdosing in healthy subjects. Eur J Pharm Sci. 2013;50:440–6.

59. Hafkin B, Kaplan N, Hunt TL. Safety, tolerability and pharmacokinetics of AFN-1252 administered as immediate release tablets in healthy subjects. Future Microbiol. 2015;10:1805–13.

60. Kusuhara H, Takashima T, Fujii H, Takashima T, Tanaka M, Ishii A, et al. Comparison of pharmacokinetics of newly discovered aromatase inhibitors by a cassette microdosing approach in healthy Japanese subjects. Drug Metab Pharmacokinet. 2017;32:293–300.

61. Nomura Y, Koyama H, Ohashi Y, Watanabe H. Clinical Dosage Determination of a New Aromatase Inhibitor, Anastrozole, in Postmenopausal Japanese Women with Advanced Breast Cancer. Clin Drug Investig. 2000;20:357–69.

62. Lau YY, Huang Y, Frassetto L, Benet LZ. effect of OATP1B transporter inhibition on the pharmacokinetics of atorvastatin in healthy volunteers. Clin Pharmacol Ther. 2007;81:194–204.

63. Croft M, Keely B, Morris I, Tann L, Lappin G, M. C, et al. Predicting drug candidate victims of drug-drug interactions, using microdosing. Clin Pharmacokinet. 2012;51:237–46.

64. Culm-Merdek KE, von Moltke LL, Harmatz JS, Greenblatt DJ. Fluvoxamine impairs single-dose caffeine clearance without altering caffeine pharmacodynamics. Br J Clin Pharmacol. 2005;60:486–93.

65. Perera V, Gross AS, Xu H, McLachlan AJ. Pharmacokinetics of caffeine in plasma and saliva, and the influence of caffeine abstinence on CYP1A2 metrics. J Pharm Pharmacol. 2011;63:1161–8.

66. Amchin J, Zarycranski W, Taylor KP, Albano D, Klockowski PM. Effect of venlafaxine on CYP1A2-dependent pharmacokinetics and metabolism of caffeine. J Clin Pharmacol. 1999;39:252–9.

67. Friedman H, Greenblatt DJ, Peters GR, Metzler CM, Charlton MD, Harmatz JS, et al. Pharmacokinetics and pharmacodynamics of oral diazepam: effect of dose, plasma concentration, and time. Clin Pharmacol Ther. 1992;52:139–50.

68. Spector R, Choudhury AK, Chiang CK, Goldberg MJ, Ghoneim MM. Diphenhydramine in Orientals and Caucasians. Clin Pharmacol Ther. 1980;28:229–34.

69. Blyden GT, Greenblatt DJ, Scavone JM, Shader RI. Pharmacokinetics of diphenhydramine and a demethylated metabolite following intravenous and oral administration. J Clin Pharmacol. 1986;26:529–33.

3.1

70. Scavone JM, Luna BG, Harmatz JS, von Moltke L, Greenblatt DJ. Diphenhydramine kinetics following intravenous, oral, and sublingual dimenhydrinate administration. Biopharm Drug Dispos. 1990;11:185–9.

71. Simons KJ, Watson WT, Martin TJ, Chen XY, Simons FE. Diphenhydramine: pharmacokinetics and pharmacodynamics in elderly adults, young adults, and children. J Clin Pharmacol. 1990;30:665–71.

72. Meredith CG, Christian CDJ, Johnson RF, Madhavan S V, Schenker S. Diphenhydramine disposition in chronic liver disease. Clin Pharmacol Ther. 1984;35:474–9.

73. Zhou X-J, Garner RC, Nicholson S, Kissling CJ, Mayers D. Microdose pharmacokinetics of IDX899 and IDX989, candidate HIV-1 non-nucleoside reverse transcriptase inhibitors, following oral and intravenous administration in healthy male subjects. J Clin Pharmacol. 2009;49:1408–16.

74. Zhou X-J, Pietropaolo K, Damphousse D, Belanger B, Chen J, Sullivan-Bolyai J, et al. Single-dose escalation and multiple-dose safety, tolerability, and pharmacokinetics of IDX899, a candidate human immunodeficiency virus type 1 nonnucleoside reverse transcriptase inhibitor, in healthy subjects. Antimicrob Agents Chemother. 2009;53:1739–46.

75. Nguyen MA, Staubach P, Wolffram S, Langguth P. The Influence of Single-Dose and Short-Term Administration of Quercetin on the Pharmacokinetics of Midazolam in Humans. J Pharm Sci. 2015;104:3199–207.

76. Kuwano K, Hashino A, Asaki T, Hamamoto T, Yamada T, Okubo K, et al. 2-{4-[(5,6-Diphenylpyrazin-2-yl)(isopropyl)amino]butoxy}-N-(methylsulfonyl) acetamide (NS-304), an orally available and long-acting prostacyclin receptor agonist prodrug. J Pharmacol Exp Ther. 2007;322:1181–8.

77. Kaufmann P, Okubo K, Bruderer S, Mant T, Yamada T, Dingemanse J, et al. Pharmacokinetics and Tolerability of the Novel Oral Prostacyclin IP Receptor Agonist Selexipag. Am J Cardiovasc Drugs. 2015;15:195–203.

78. Tozuka Z, Kusuhara H, Nozawa K, Hamabe Y, Ikushima I, Ikeda T, et al. Microdose study of 14c-acetaminophen with accelerator mass spectrometry to examine pharmacokinetics of parent drug and metabolites in healthy subjects. Clin Pharmacol Ther. 2010;88:824–30.

79. Kapitza C, Zdravkovic M, Hindsberger C, Flint A. The effect of the once-daily human glucagon-like peptide 1 analog liraglutide on the pharmacokinetics of acetaminophen. Adv Ther. 2011;28:650–60.

80. Shinoda S, Aoyama T, Aoyama Y, Tomioka S, Matsumoto Y, Ohe Y. Pharmacokinetics/pharmacodynamics of acetaminophen analgesia in Japanese patients with chronic pain. Biol Pharm Bull. 2007;30:157–61.

81. Stangier J, Su CA, Fraunhofer A, Tetzloff W. Pharmacokinetics of acetaminophen and ibuprofen when coadministered with telmisartan in healthy volunteers. J Clin Pharmacol. 2000;40:1338–46.

82. Rawlins MD, Henderson DB, Hijab AR. Pharmacokinetics of paracetamol (acetaminophen) after intravenous and oral administration. Eur J Clin Pharmacol. 1977;11:283–6.

83. Albert KS, Sedman AJ, Wilkinson P, Stoll RG, Murray WJ, Wagner JG. Bioavailability studies of acetaminophen and nitrofurantoin. J Clin Pharmacol. 1974;14:264–70.

84. Viswanathan CT, Booker HE, Welling PG. Pharmacokinetics of phenobarbital following single and repeated doses. J Clin Pharmacol. 1979;19:282–9.

85. Prueksaritanont T, Chu X, Evers R, Klopfer SO, Caro L, Kothare PA, et al. Pitavastatin is a more sensitive and selective organic anion-transporting polypeptide 1B clinical probe than rosuvastatin. Br J Clin Pharmacol. 2014;78:587–98.

86. Deng S, Chen X-P, Cao D, Yin T, Dai Z-Y, Luo J, et al. Effects of a concomitant single oral dose of rifampicin on the pharmacokinetics of pravastatin in a two-phase, randomized, single-blind, placebo-controlled, crossover study in healthy Chinese male subjects. Clin Ther. 2009;31:1256–63.

87. Fukazawa I, Uchida N, Uchida E, Yasuhara H. Effects of grapefruit juice on pharmacokinetics of atorvastatin and pravastatin in Japanese. Br J Clin Pharmacol. 2004;57:448–55.

88. Ogawa K, Hasegawa S, Udaka Y, Nara K, Iwai S, Oguchi K. Individual difference in the pharmacokinetics of a drug, pravastatin, in healthy subjects. J Clin Pharmacol. 2003;43:1268–73.

89. Sugimoto K, Ohmori M, Tsuruoka S, Nishiki K, Kawaguchi A, Harada K, et al. Different effects of St John's wort on the pharmacokinetics of simvastatin and pravastatin. Clin Pharmacol Ther. 2001;70:518–24.

90. Iwamoto M, Wenning LA, Petry AS, Laethem M, De Smet M, Kost JT, et al. Safety, tolerability, and pharmacokinetics of raltegravir after single and multiple doses in healthy subjects. Clin Pharmacol Ther. 2008;83:293–9.

91. Kirchheiner J, Bauer S, Meineke I, Rohde W, Prang V, Meisel C, et al. Impact of CYP2C9 and CYP2C19 polymorphisms on tolbutamide kinetics and the insulin and glucose response in healthy volunteers. Pharmacogenetics. 2002;12:101–9.

92. Chen K, Wang R, Wen S-Y, Li J, Wang S-Q. Relationship of P450 2C9 genetic polymorphisms in Chinese and the pharmacokinetics of tolbutamide. J Clin Pharm Ther. 2005;30:241–9.

93. Jetter A, Kinzig-Schippers M, Skott A, Lazar A, Tomalik-Scharte D, Kirchheiner J, et al. Cytochrome P450 2C9 phenotyping using low-dose tolbutamide. Eur J Clin Pharmacol. 2004;60:165–71.

94. Uchida S, Yamada H, Li XD, Maruyama S, Ohmori Y, Oki T, et al. Effects of Ginkgo biloba extract on pharmacokinetics and pharmacodynamics of tolbutamide and midazolam in healthy volunteers. J Clin Pharmacol. 2006;46:1290–8.

95. Chan E, McLachlan AJ, Pegg M, MacKay AD, Cole RB, Rowland M. Disposition of warfarin enantiomers and metabolites in patients during multiple dosing with rac-warfarin. Br J Clin Pharmacol. 1994;37:563–9.

96. Chen J, Garner RC, Lee LS, Seymour M, Fuchs EJ, Hubbard WC, et al. Accelerator mass spectrometry measurement of intracellular concentrations of active drug metabolites in human target cells in vivo. Clin Pharmacol Ther. 2010;88:796–800.

97. Vuong LT, Ruckle JL, Blood AB, Reid MJ, Wasnich RD, Synal H-A, et al. Use of accelerator mass spectrometry to measure the pharmacokinetics and peripheral blood mononuclear cell concentrations of zidovudine. J Pharm Sci. 2008;97:2833–43.

98. Drugbank: AFN-1252. 2018 [cited 2019 Jan]. Available from: https://www.drugbank.ca/drugs/DB12658

99. Kamdem LK, Liu Y, Stearns V, Kadlubar SA, Ramirez J, Jeter S, et al. In vitro and in vivo oxidative metabolism and glucuronidation of anastrozole. Br J Clin Pharmacol. 2010;70:854–69.

100. Lazarus P, Sun D. Potential role of UGT pharmacogenetics in cancer treatment and prevention: focus on tamoxifen and aromatase inhibitors. Drug Metab Rev. 2010;42:182–94.

101. Miyajima M, Kusuhara H, Takahashi K, Takashima T, Hosoya T, Watanabe Y, et al. Investigation of the effect of active efflux at the blood-brain barrier on the distribution of nonsteroidal aromatase inhibitors in the central nervous system. J Pharm Sci. 2013;102:3309–19.

102. Reeves PR, McAinsh J, McIntosh DA, Winrow MJ. Metabolism of atenolol in man. Xenobiotica. 1978;8:313–20.

103. Yu J, Zhou Z, Tay-Sontheimer J, Levy RH, Ragueneau-Majlessi I. Intestinal Drug Interactions Mediated by OATPs: A Systematic Review of Preclinical and Clinical Findings. J Pharm Sci. 2017;106:2312–25.

104. Arnaud MJ. Pharmacokinetics and metabolism of natural methylxanthines in animal and man. Handb Exp Pharmacol. 2011;:33–91.

3.1

105. Nehlig A. Interindividual Differences in Caffeine Metabolism and Factors Driving Caffeine Consumption. Pharmacol Rev. 2018;70:384–411.

106. Rodrigues AD, Roberts EM, Mulford DJ, Yao Y, Ouellet D. Oxidative metabolism of clarithromycin in the presence of human liver microsomes. Major role for the cytochrome P4503A (CYP3A) subfamily. Drug Metab Dispos. 1997;25:623–30.

107. Togami K, Chono S, Morimoto K. Transport characteristics of clarithromycin, azithromycin and telithromycin, antibiotics applied for treatment of respiratory infections, in Calu-3 cell monolayers as model lung epithelial cells. Pharmazie. 2012;67:389–93.

108. Wessler JD, Grip LT, Mendell J, Giugliano RP. The P-Glycoprotein Transport System and Cardiovascular Drugs. J Am Coll Cardiol. 2013;61:2495–502.

109. US Food and Drug Administration (FDA). FDA Label: Cardizem (diltiazem). 2010 [cited 2019 Jan]. p. 9. Available from: https://www.accessdata.fda.gov/drugsatfda_docs/label/2010/018602s063lbl.pdf

110. Yamamoto T, Kubota T, Ozeki T, Sawada M, Yokota S, Yamada Y, et al. Effects of the CYP3A5 genetic polymorphism on the pharmacokinetics of diltiazem. Clin Chim Acta. 2005;362:147–54.

111. Akutsu T, Kobayashi K, Sakurada K, Ikegaya H, Furihata T, Chiba K. Identification of human cytochrome p450 isozymes involved in diphenhydramine N-demethylation. Drug Metab Dispos. 2007;35:72–8.

112. MacFadyen RJ, Meredith PA, Elliott HL. Enalapril clinical pharmacokinetics and pharmacokinetic-pharmacodynamic relationships. An overview. Clin Pharmacokinet. 1993;25:274–82.

113. Liu L, Cui Y, Chung AY, Shitara Y, Sugiyama Y, Keppler D, et al. Vectorial transport of enalapril by Oatp1a1/Mrp2 and OATP1B1 and OATP1B3/MRP2 in rat and human livers. J Pharmacol Exp Ther. 2006;318:395–402.

114. US Food and Drug Administration (FDA). Prescribing information: Allegra (fexofenadine). 1996 [cited 2019 Jan]. p. 7. Available from: https://www.accessdata.fda.gov/drugsatfda_docs/label/2001/20625lbl.pdf

115. Shimizu M, Fuse K, Okudaira K, Nishigaki R, Maeda K, Kusuhara H, et al. Contribution of OATP (organic anion-transporting polypeptide) family transporters to the hepatic uptake of fexofenadine in humans. Drug Metab Dispos. 2005;33:1477–81.

116. Drugbank: Fosdevirine (IDX-899). 2018 [cited 2019 Jan]. Available from: https://www.drugbank.ca/drugs/DB06166

117. Sica DA, Gehr TWB, Ghosh S. Clinical pharmacokinetics of losartan. Clin Pharmacokinet. 2005;44:797–814.

118. Stearns RA, Chakravarty PK, Chen R, Chiu SH. Biotransformation of losartan to its active carboxylic acid metabolite in human liver microsomes. Role of cytochrome P4502C and 3A subfamily members. Drug Metab Dispos. 1995;23:207–15.

119. Soldner A, Benet LZ, Mutschler E, Christians U. Active transport of the angiotensin-II antagonist losartan and its main metabolite EXP 3174 across MDCK-MDR1 and caco-2 cell monolayers. Br J Pharmacol. 2000;129:1235–43.

120. US Food and Drug Administration (FDA). FDA Label: Glucophage (metformin). 1997 [cited 2019 Jan]. p. 23. Available from: https://www.accessdata.fda.gov/drugsatfda_docs/nda/97/020357a_s006.pdf

121. Graham GG, Punt J, Arora M, Day RO, Doogue MP, Duong JK, et al. Clinical pharmacokinetics of metformin. Clin Pharmacokinet. 2011;50:81–98.

122. Pentikainen PJ, Neuvonen PJ, Penttila A. Pharmacokinetics of metformin after intravenous and oral administration to man. Eur J Clin Pharmacol. 1979;16:195–202.

123. Liang X, Giacomini KM. Transporters Involved in Metformin Pharmacokinetics and Treatment Response. J Pharm Sci. 2017;106:2245–50.

124. Kimura N, Masuda S, Tanihara Y, Ueo H, Okuda M, Katsura T, et al. Metformin is a superior substrate for renal organic cation transporter OCT2 rather than hepatic OCT1. Drug Metab Pharmacokinet. 2005;20:379–86.

125. US Food and Drug Administration (FDA). FDA Label: Versed (midazolam). 1996 [cited 2019 Jan]. p. 79. Available from: https://www.accessdata.fda.gov/drugsatfda_docs/nda/97/018654ap.pdf

126. Heizmann P, Ziegler WH. Excretion and metabolism of 14C-midazolam in humans following oral dosing. Arzneimittelforschung. 1981;31:2220–3.

127. Wrighton SA, Stevens JC. The human hepatic cytochromes P450 involved in drug metabolism. Crit Rev Toxicol. 1992;22:1–21.

128. US Food and Drug Administration (FDA). Clinical pharmacology and biopharmaceutics review: Uptravi (selexipag) . 2014 [cited 2019 Jan]. p. 31. Available from: https://www.accessdata.fda.gov/drugsatfda_docs/nda/2015/207947Orig1s000ClinPharmR.pdf

129. Mazaleuskaya LL, Sangkuhl K, Thorn CF, FitzGerald GA, Altman RB, Klein TE. PharmGKB summary: pathways of acetaminophen metabolism at the therapeutic versus toxic doses. Pharmacogenet Genomics. 2015;25:416–26.

130. Zhang C, Kwan P, Zuo Z, Baum L. In vitro concentration dependent transport of phenytoin and phenobarbital, but not ethosuximide, by human P-glycoprotein. Life Sci. 2010;86:899–905.

131. US Food and Drug Administration (FDA). FDA label: Pravachol (pravastatin). 2012 [cited 2019 Jan]. p. 111. Available from: https://www.accessdata.fda.gov/drugsatfda_docs/nda/2012/019898s062.pdf

132. Nishizato Y, Ieiri I, Suzuki H, Kimura M, Kawabata K, Hirota T, et al. Polymorphisms of OATP-C (SLC21A6) and OAT3 (SLC22A8) genes: consequences for pravastatin pharmacokinetics. Clin Pharmacol Ther. 2003;73:554–65.

133. US Food and Drug Administration (FDA). Clinical pharmacology and biopharmaceutics review: Isentress (raltegravir) . 2011 [cited 2019 Jan]. p. 58. Available from: https://www.accessdata.fda.gov/drugsatfda_docs/nda/2011/203045Orig1s000ClinPharmR.pdf

134. Hashiguchi Y, Hamada A, Shinohara T, Tsuchiya K, Jono H, Saito H. Role of P-glycoprotein in the efflux of raltegravir from human intestinal cells and CD4+ T-cells as an interaction target for anti-HIV agents. Biochem Biophys Res Commun. 2013;439:221–7.

135. US Food and Drug Administration (FDA). Clinical pharmacology and biopharmaceutics review: Viread (tenofovir) . 2001 [cited 2018 Jan]. p. 53. Available from: https://www.accessdata.fda.gov/drugsatfda_docs/nda/2001/21-356_Viread_biopharmr.pdf

136. Miners JO, Birkett DJ. Cytochrome P4502C9: an enzyme of major importance in human drug metabolism. Br J Clin Pharmacol. 1998;45:525–38.

137. Bi Y-A, Mathialagan S, Tylaska L, Fu M, Keefer J, Vildhede A, et al. Organic Anion Transporter 2 Mediates Hepatic Uptake of Tolbutamide, a CYP2C9 Probe Drug. J Pharmacol Exp Ther. 2018;364:390–8.

138. Cload PA. A review of the pharmacokinetics of zidovudine in man. J Infect. 1989;18:15–21.

139. Errasti-Murugarren E, Pastor-Anglada M. Drug transporter pharmacogenetics in nucleoside-based therapies. Pharmacogenomics. 2010;11:809–41.

140. VanWert AL, Gionfriddo MR, Sweet DH. Organic anion transporters: discovery, pharmacology, regulation and roles in pathophysiology. Biopharm Drug Dispos. 2010;31:1–71.

3.1

141. US Food and Drug Administration (FDA). FDA label: Lipitor (atorvastatin). 2009 [cited 2019 Oct]. p. 48. Available from: https://www.accessdata.fda.gov/drugsatfda_docs/nda/2009/020702Orig1s056.pdf

142. Caruso FS, Doshan HD, Hernandez PH, Costello R, Applin W, Neiss ES. Celiprolol: pharmacokinetics and duration of pharmacodynamic activity. Br J Clin Pract Suppl. 1985;40:12–6.

143. Drugbank: Mirodenafil. 2018 [cited 2019 Jan]. Available from: https://www.drugbank.ca/drugs/DB11792

144. Lee HS, Park EJ, Ji HY, Kim SY, Im G-J, Lee SM, et al. Identification of cytochrome P450 enzymes responsible for N -dealkylation of a new oral erectogenic, mirodenafil. Xenobiotica. 2008;38:21–33.

145. Shin K-H, Kim B-H, Kim T-E, Kim JW, Yi S, Yoon S-H, et al. The effects of ketoconazole and rifampicin on the pharmacokinetics of mirodenafil in healthy Korean male volunteers: an open-label, one-sequence, three-period, three-treatment crossover study. Clin Ther. 2009;31:3009–20.

146. Guengerich FP, Brian WR, Iwasaki M, Sari MA, Baarnhielm C, Berntsson P. Oxidation of dihydropyridine calcium channel blockers and analogues by human liver cytochrome P-450 IIIA4. J Med Chem. 1991;34:1838–44.

147. Andersson T. Pharmacokinetics, metabolism and interactions of acid pump inhibitors. Focus on omeprazole, lansoprazole and pantoprazole. Clin Pharmacokinet. 1996;31:9–28.

148. US Food and Drug Administration (FDA). Prescribing information: Livalo (pitavastatin). 2009 [cited 2019 Jan]. p. 15. Available from: https://www.accessdata.fda.gov/drugsatfda_docs/label/2009/022363s000lbl.pdf

149. US Food and Drug Administration (FDA). Clinical pharmacology and biopharmaceutics review: Zypitamag (pitavastatin). 2015 [cited 2019 Jan]. p. 35. Available from: https://www.accessdata.fda.gov/drugsatfda_docs/nda/2017/208379Orig1s000ClinPharmR.pdf

150. Clinical pharmacology and biopharmaceutics review: Rytmonorm (propafenone). 2003 [cited 2019 Jan]. p. 91. Available from: https://www.accessdata.fda.gov/drugsatfda_docs/nda/2003/21-416_Rythmol SR_BioPharmr.pdf

151. Botsch S, Gautier JC, Beaune P, Eichelbaum M, Kroemer HK. Identification and characterization of the cytochrome P450 enzymes involved in N-dealkylation of propafenone: molecular base for interaction potential and variable disposition of active metabolites. Mol Pharmacol. 1993;43:120–6.

152. Guengerich FP, Muller-Enoch D, Blair IA. Oxidation of quinidine by human liver cytochrome P-450. Mol Pharmacol. 1986;30:287–95.

153. US Food and Drug Administration (FDA). Prescribing information: Crestor (rosuvastatin). 2003 [cited 2019 Jan]. p. 43. Available from: https://www.accessdata.fda.gov/drugsatfda_docs/label/2010/021366s016lbl.pdf

154. US Food and Drug Administration (FDA). Clinical pharmacology and biopharmaceutics review: Crestor (rosuvastatin). 2003 [cited 2019 Jan]. p. 86. Available from: https://www.accessdata.fda.gov/drugsatfda_docs/nda/2003/21-366_Crestor_BioPharmr.pdf

155. Wu H-F, Hristeva N, Chang J, Liang X, Li R, Frassetto L, et al. Rosuvastatin Pharmacokinetics in Asian and White Subjects Wild Type for Both OATP1B1 and BCRP Under Control and Inhibited Conditions. J Pharm Sci. 2017;106:2751–7.

156. Matthaei J, Kuron D, Faltraco F, Knoch T, Dos Santos Pereira JN, Abu Abed M, et al. OCT1 mediates hepatic uptake of sumatriptan and loss-of-function OCT1 polymorphisms affect sumatriptan pharmacokinetics. Clin Pharmacol Ther. 2016;99:633–41.

157. US Food and Drug Administration (FDA). Prescribing information: Micardis (telmisartan). 1998 [cited 2019 Jan]. p. 13. Available from: https://www.accessdata.fda.gov/drugsatfda_docs/label/2011/020850s032lbl.pdf

158. Ishiguro N, Maeda K, Kishimoto W, Saito A, Harada A, Ebner T, et al. Predominant contribution of OATP1B3 to the hepatic uptake of telmisartan, an angiotensin II receptor antagonist, in humans. Drug Metab Dispos. 2006;34:1109–15.

159. Ishiguro N, Maeda K, Saito A, Kishimoto W, Matsushima S, Ebner T, et al. Establishment of a set of double transfectants coexpressing organic anion transporting polypeptide 1B3 and hepatic efflux transporters for the characterization of the hepatobiliary transport of telmisartan acylglucuronide. Drug Metab Dispos. 2008;36:796–805.

160. Kroemer HK, Gautier JC, Beaune P, Henderson C, Wolf CR, Eichelbaum M. Identification of P450 enzymes involved in metabolism of verapamil in humans. Naunyn Schmiedebergs Arch Pharmacol. 1993;348:332–7.

161. Yang M-S, Yu C-P, Chao P-DL, Lin S-P, Hou Y-C. R- and S-Warfarin Were Transported by Breast Cancer Resistance Protein: From In Vitro to Pharmacokinetic-Pharmacodynamic Studies. J Pharm Sci. 2017;106:1419–25.

3.1

A phase 0 study to predict the pharmacokinetics of a therapeutic gemcitabine dose from a microdose

Merel van Nuland
Hilde Rosing
Bas Thijssen
Sjaak A. Burgers
Alwin D.R. Huitema
Serena Marchetti
Jan H.M. Schellens
Jos H. Beijnen

Abstract

Aims
Microdose studies are exploratory trials to determine early drug pharmacokinetics in humans. In this trial, we examined whether the pharmacokinetics of gemcitabine at a therapeutic dose could be predicted from the pharmacokinetics of a microdose. Methods: In this prospective, open-label microdosing study, a gemcitabine microdose (100 µg) was given intravenously to participants on day 1, followed by a therapeutic dose (1,250 mg/m^2) on day 2. Gemcitabine and its metabolite 2'-2'-difluorodeoxyuracil (dFdU) were quantified in plasma and intracellularly by using liquid chromatography-mass spectrometry (LC-MS/MS). Non-compartmental pharmacokinetic analysis was performed.

Results
Ten patients participated in this study. The mean area under the plasma concentration-time curve (AUC_{0-8}) of gemcitabine after microdosing was 0.00074 h·mg/L and after therapeutic dosing was 16 h·mg/L. The mean AUC_{0-8} of dFdU following the microdose and therapeutic dose were 0.022 h·mg/L and 169 h·mg/L, respectively. Exposure to gemcitabine after the therapeutic dose was within two-fold of the exposure following a microdose, when linearly extrapolated to 1,250 mg/m^2. However, the shape of the concentration-time curve was different, as reflected by poor scalability in volume of distribution (939 L vs 222 L). Furthermore, intracellularly phosphorylated gemcitabine and phosphorylated dFdU levels could not be predicted from the microdose.

Conclusions
The AUC_{0-8} of gemcitabine at therapeutic dose was accurately predicted by the pharmacokinetics of a microdose, when linearly extrapolated to 1,250 mg/m^2. Volume of distribution, elimination rate constant and intracellular pharmacokinetics of the therapeutic dose could not be predicted from the microdose, which demonstrates limitations of the microdose approach in this case.

Introduction

Microdose trials are studies in which up to 1/100th of the therapeutic dosage is administered, with a maximum of 100 µg per day, to preliminary study drug pharmacokinetics. In pursuit of optimizing drug development, phase 0 microdose trials may be conducted prior to traditional phase 1 to gather information on the pharmacokinetic behaviour of new drugs. Early establishment of such parameters might shorten overall development time and increase success rates, for instance by helping to select the candidate drug best performing in terms of pharmacokinetics for further clinical development and shortening the preclinical package (1). The concept of phase 0 microdosing was first addressed by the European Medicines Agency (EMA) and US Food and Drug Administration (FDA) in 2004 and 2006 (2,3), respectively, and resulted in the currently accepted international ICH M3[R2] guideline on experimental investigational new drug (eIND) studies by the EMA (4).

The limited drug exposure in phase 0 microdose trials requires the use of ultra-sensitive techniques to quantify very low drug concentrations. The three most commonly used instruments for this are liquid chromatography-mass spectrometry (LC-MS/MS), accelerator mass spectrometry (AMS) and positron emission tomography (PET) (5). AMS is the most sensitive technique while PET provides the opportunity to visualize drug distribution throughout the body. However, both techniques require radioactive labelling of the drug of interest. LC-MS/MS does not require radiolabelling and has additional advantages such as its high availability and the ability to identify drug metabolites. The combination of these features makes LC-MS/MS the optimal option for quantification of drugs in microdose trials.

The principle of a microdose trial is that the pharmacokinetics of a microdose are thought to be indicative of the pharmacokinetics following a therapeutic dose. In a literature survey, the microdose predictability of 46 drugs was assessed and demonstrated scalable pharmacokinetics for 68% of orally administered drugs (n=41) and for 94% of intravenously administered (n=16) drugs (6). Predictability may be defined as the mean of observed values of the microdose, after linear extrapolation to correct for the dose difference, and the therapeutic dose being within a two-fold, as described previously (7,8). While conducting a phase 0 trial it is unknown whether pharmacokinetics are predictive or not. The ultimate approach to prove microdose predictability is by comparing the pharmacokinetics of a microdose with the pharmacokinetics at a relevant therapeutic dose as we investigated in this study.

In this phase 0 trial, we studied the pharmacokinetics of 2'-2'-difluorodeoxycytidine (dFdC, gemcitabine) and its main metabolite 2'-2'-difluorodeoxyuracil (dFdU) following a microdose and a therapeutic dose. Gemcitabine is a cytotoxic pyrimidine nucleoside analogue, widely used for the treatment of a variety of cancers such as non-small cell lung cancer (NSCLC), bladder, breast and ovarian cancer (9). Gemcitabine is rapidly metabolized in the blood by cytidine deaminase (CDA) to its main circulating metabolite dFdU (9) and after cellular uptake, gemcitabine is metabolized into mono-, di- and

3.2

triphosphates (gemcitabine-MP, gemcitabine-DP, gemcitabine -TP). Gemcitabine-DP blocks ribonucleotide reductase while gemcitabine-TP competes with deoxycytidine triphosphate for incorporation into the DNA and RNA, thereby inhibiting DNA synthesis and initiating apoptotic cell death (10). Gemcitabine is known to have linear pharmacokinetics over a dose range of 10 to 1,000 mg/m^2 (11,12). In the present microdose study, drug concentrations of gemcitabine and its metabolite dFdU, including intracellular metabolites, were quantified using an ultra-sensitive LC-MS/MS method to investigate whether the pharmacokinetics of gemcitabine at a therapeutic dose could be predicted from the pharmacokinetics of a microdose. The predictability of intravenously administered microdoses is high, therefore we hypothesise that all pharmacokinetic parameters (not only area under the plasma concentration-time curve (AUC), but also of maximum concentration (C_{max}), elimination rate constant (K_e), half-life ($t_{1/2}$), volume of distribution (Vd) and clearance (CL)) should be predicted adequately. The secondary aim of the study was to show the feasibility of LC-MS/MS analysis in these types of trials.

Methods

Study design
This was a prospective, open-label, single arm, microdose study. The trial was conducted in accordance with the principles of the Declaration of Helsinki and the protocol was approved by the local ethical committee. The study was registered in the Netherlands Trial Register (NTR6183). All patients provided written informed consent prior to participating.
The pharmacokinetics of a gemcitabine microdose and therapeutic dose were assessed in a cross-over design. Patients received a microdose (100 µg) and a therapeutic dose (1,250 mg/m^2) within a 1-day interval. Both the microdose and therapeutic dose were administered as a 30-minute intravenous infusion. If patients were eligible for a gemcitabine combination therapy (with either cisplatin or paclitaxel), the second chemotherapeutic compound was administered separately on the following day to avoid interference with gemcitabine pharmacokinetics. Patients were monitored throughout the study for clinical adverse events: all adverse events were documented on the day the microdose was administered, and unexpected adverse events were documented during the first treatment cycle. Non-compartmental analysis (NCA) was performed to determine pharmacokinetic parameters.

Patients
Patients aged >18 years old, with solid tumors with an indication for treatment with gemcitabine according to standard of care were included. Adequate bone marrow, liver and renal function were required for enrolment.

Blood sampling

Blood samples were collected for pharmacokinetic evaluation via venipuncture, after administration of the microdose and the therapeutic dose, at the following time points: 0, 0.25, 0.5, 0.75, 1, 1.25, 1.5, 1.75, 2, 4 and 8 hours after start of the 30-minute infusion. Whole venous blood was obtained in K_2EDTA tubes spiked with tetrahydrouridine (THU) and centrifuged for 10 minutes at 4 °C at 1,800 g. The plasma fraction was isolated and stored at -70 ºC until further analysis. Two hours after start of infusion peripheral blood mononuclear cells (PBMCs) were isolated and processed as described previously (13,14).

Safety assessments

Adverse events were graded according to National Cancer Institute Common Terminology Criteria for adverse events (NCI-CTCAE) version 4.03. Adverse events were documented if reported after administration of the microdose or when not described in the summary of product characteristics (SmPC).

Swab sampling

Swabs were taken to check the patients' surroundings for potential interferences with sensitive LC-MS/MS measurements. These swabs were taken from the patient's bedside and from a closet next to the bed by swabing 10 cm^2 surface with a sterile cotton gauze wetted with water for injection. Each gauze was stored in 50 mL PP tubes at 4 °C until analysis. Swabs were pretreated by adding 25 mL of methanol and shaking the tubes on an automatic shaker for 30 minutes at 1,275 rpm. The samples were dried using a rotary evaporator at 40 °C. The residues were reconstituted in 1 mL of 10 mM ammonium acetate in water-acetonitrile (93:7, v/v) and analyzed with an ultra-sensitive gemcitabine LC-MS/MS method with a lower limit of quantification (LLOQ) of 5 pg/mL, which was specifically developed for this study (15).

Bioanalysis

Gemcitabine and dFdU concentrations after administration of the microdose were quantified using a validated LC-MS/MS method with a LLOQ of 5 pg/mL and 500 pg/mL, respectively (15). Furthermore, gemcitabine and dFdU concentrations after administration of the therapeutic dose were assessed using a validated LC-MS/MS method with a LLOQ of 0.5 ng/mL for gemcitabine and 50 ng/mL for dFdU (16). Figure 1 shows the chemical structures of gemcitabine and dFdU.

The sample preparation was similar for both methods. In short, 200 µL of plasma was prepared with solid phase extraction (SPE) using OASIS HLB 1cc vac cartridges (Waters, Milford, MA, USA). After equilibration, samples were transferred to the cartridges, washed with water, and eluted with methanol. Afterwards, the samples were dried under a gentle stream of nitrogen at 40 °C and reconstituted in a mixture of ammonium acetate in water and acetonitrile.

3.2
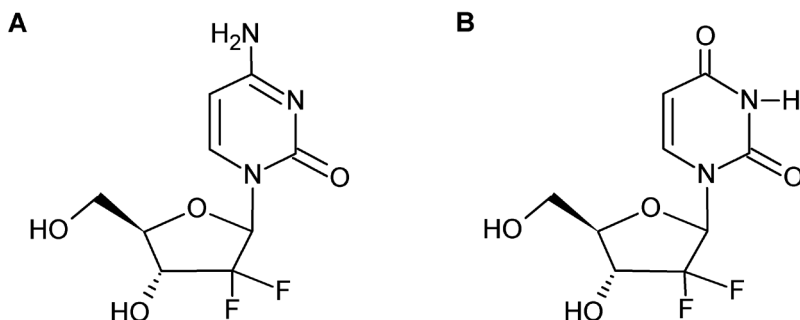
Figure 1. Chemical structures of gemcitabine (A) and its metabolite 2′,2′-difluorodeoxyuridine (dFdU; B).

Intracellular gemcitabine and dFdU were quantified in PBMC lysate by injecting the lysate into the analytical system without prior sample preparation. Furthermore, intracellular gemcitabine and dFdU phosphate concentrations were determined as the total concentration of mono-, di- and triphosphates, after dephosphorylation. This procedure was followed to increase the sensitivity of the quantification of these compounds since nucleosides are better MS responders than their corresponding phosphorylated forms. Gemcitabine and dFdU were expressed as a concentration in pmol per million PBMCs. PBMC lysate samples (50 µL) were incubated for 1 hour at 37 ˚C with 10 µL tris(hydroxymethyl)aminomethane (Trizma® base) and 2 units of alkaline phosphatase (both Sigma-Aldrich, St. Louis, MO). Afterwards, samples were dried under a gentle stream of nitrogen at 40 °C and reconstituted in 50 µL water. Quality control (QC) samples were prepared including gemcitabine-MP, gemcitabine-DP and gemcitabine-TP at a concentration of 0.5 ng/mL of each compound to measure the dephosphorylation efficiency. These samples showed a complete conversion from gemcitabine-XP to gemcitabine by alkaline phosphatase under the described conditions. The total concentration of gemcitabine-XP and dFdU-XP were calculated by subtracting the intracellular concentration prior to phosphorylation from the intracellular concentration post phosphorylation.

Statistical analysis

All calculations were done with the R statistical software package version 3.4.3 (R Project, Vienna, Austria). Non-compartmental analysis of data was performed. Calculated parameters were AUC_{0-8}, AUC_{0-inf}, C_{max}, K_e, $t_{1/2}$, Vd and CL, using the following equations:

$$CL = \frac{Dose}{AUC_{0-inf}} \quad \text{and} \quad Vd = \frac{CL}{K_e} \quad \text{and} \quad t_{1/2} = \frac{\ln(2)}{K_e}$$

Statistical analyses were performed using a Wilcoxon signed-rank test to compare pharmacokinetic parameters after administration of the microdose and the therapeutic

Table 1. Patient demographic and baseline characteristics.

Patient characteristics	
Total number of patients	9
Gender	
Male	5
Female	4
Age, median (range), years	66 (48-73)
Tumor type	
NSCLC	4
Mesothelioma	3
Thymoma	2
Renal function, median (range)	
Creatinine (µmol/l)	73 (53-122)
eGFR (Cockroft-Gault, mL/minute)	81 (59-121)
Liver function, median (range)	
Total bilirubin (µmol/l)	4 (3-11)
ASAT (U/l)	22 (15-28)
ALAT(U/l)	16 (9-39)

Abbreviations: ALAT = alanine aminotransferase, ASAT = aspartate aminotransferase, NSCLC = non-small cell lung cancer

dose. Interpatient variability was calculated as the percentage coefficient of variation (CV%) by dividing the standard deviation (sd) by the mean and multiplying this value by 100.

Results

Patients
Ten patients were enrolled in this study between May 2017 and January 2019. One patient was excluded from further analysis because this patient received 1 mg instead of 100 µg due to a production error. Patients' characteristics are shown in Table 1. The median age of the patients was 66 years (range 48 to 73 years). Gemcitabine was prescribed for treatment of three different tumor types: NSCLC (n=4), mesothelioma (n=3) and thymoma (n=2).

Safety assessment
No adverse events were reported after administration of gemcitabine as a microdose and no unexpected adverse events were seen after administration of gemcitabine at therapeutic dose.

3.2

Pharmacokinetics

Plasma concentrations of the microdose and therapeutic dose are shown in Figure 2. Measured microdose concentrations were presented (A-series) as well as microdose concentrations linearly extrapolated to 1,250 mg/m^2 (B-series), to show the shape of the predicted therapeutic curve. An overview of the pharmacokinetic parameters, the ratio between microdose and therapeutic parameters and the predictability within two-fold are reported in Table 2. Interpatient variability (CV%) for AUC_{0-8}, Vd and CL after administration of the microdose was 44%, 28% and 31%, respectively, while the CV% for AUC_{0-8}, Vd and CL after administration of the therapeutic dose was 16%, 24% and 17%, respectively.

The mean AUC_{0-8} was 0.00074 h·mg/L following the microdose and 16 h·mg/L following the therapeutic dose. The predicted therapeutic AUC of gemcitabine after linear extrapolation to 1,250 mg/m^2 of the microdose was 11 h·mg/L. Vd was 939 L after administration of the microdose and 222 L after administration of the therapeutic dose and CL was 222 L/h following a microdose and 147 L/h following a therapeutic dose.
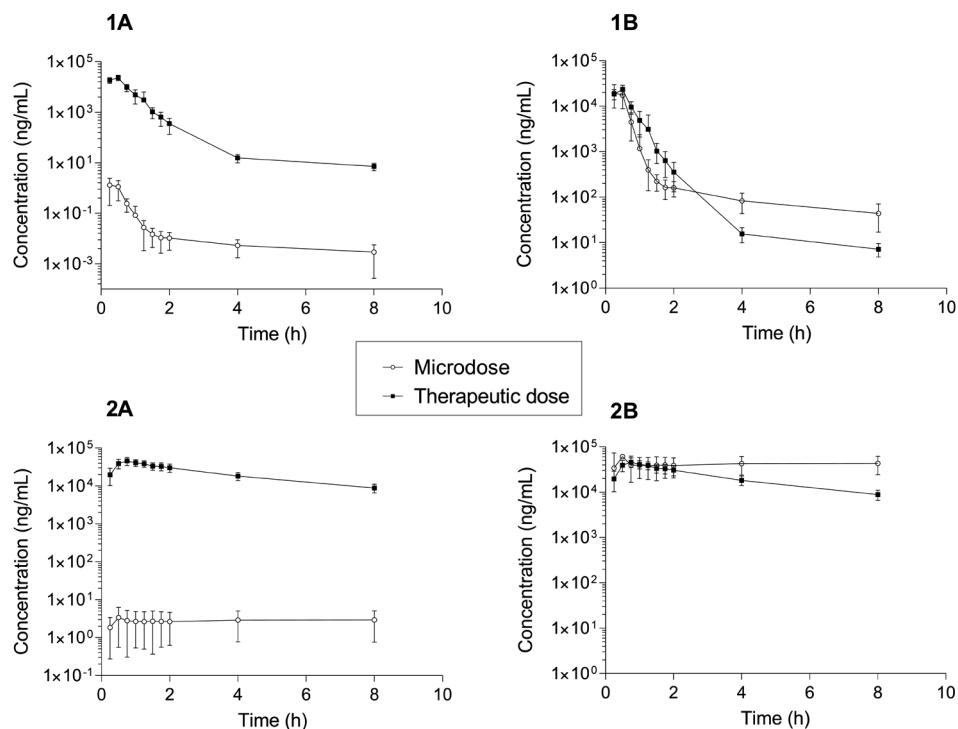
Figure 2. Concentration-times curves of gemcitabine (1) and its metabolite 2′,2′-difluorodeoxyuridine (dFdU; 2) after administration of a microdose (white dots) and a therapeutic dose (black squares) (n=9). Measured concentrations (A-series) and microdose concentrations linearly extrapolated to 1,250 mg/m^2 (B-series) are presented to show the predicted therapeutic profile.

Table 2. Mean (SD) pharmacokinetic parameters of gemcitabine administered as a microdose (100 µg) and as a therapeutic dose (1,250 mg/m²) (n=9). Microdose data are presented as the observed values and linearly extrapolated to 1,250 mg/m².

PK parameter	Microdose	Microdose, extrapolated	Therapeutic dose	Ratio (microdose/ therapeutic dose)	Predicta- bility	p-value [τ]
AUC_{0-8} (h·mg/L)	0.00074 (0.00053)	11 (4.9)	16 (2.5)	0.62	Yes	0.10
AUC_{inf} (h·mg/L)	0.00076 (0.00055)	12 (5.1)	16 (2.5)	0.63	Yes	0.10
Cmax (mg/L)	0.0013 (0.0011)	20 (10)	24 (5.2)	0.83	Yes	0.50
Ke (h⁻¹)	0.24 (0.064)	-	0.68 (0.072)	0.35	No	0.0039
$t_{1/2}$ (h)	3.1 (0.69)	-	1.0 (0.12)	3.1	No	0.0039
Vd (L)	939 (262)	-	222 (54)	4.2	No	0.0039
CL (L/h)	222 (69)	-	147 (25)	1.5	Yes	0.0039

Abbreviations: AUC = area under the curve, AUC_{inf} = area under the curve to infinity, CL = clearance, Ke = elimination constant, $t_{1/2}$ = half-life, Vd = volume of distribution.
[τ] Wilcoxon signed-rank test

AUC and CL of gemcitabine at a clinically relevant therapeutic dose could be predicted from the pharmacokinetics of a microdose in fulfilling the two-fold criterion. Vd and K_e at therapeutic dose were not predictable from the microdose within two-fold. This is reflected in the plasma-concentration time curves, as the elimination phases from end of infusion at t=0.5h to t=3h are different, with higher concentrations at therapeutic dose compared to the extrapolated microdose concentrations.

Plasma concentrations of the metabolite dFdU after administration of the microdose and therapeutic dose are shown in Figure 2. Interpatient variability (CV%) for AUC_{0-8} after administration of the microdose was 40% and after administration of the therapeutic dose 23%. The mean AUC_{0-8} of dFdU following the microdose was 0.022 h·mg/L and 169 h·mg/L following the therapeutic dose. The predicted therapeutic AUC of dFdU after linear extrapolation to 1,250 mg/m² of the microdose was 330 h·mg/L. The ratio between these two AUCs was exactly two-fold.

Gemcitabine, dFdU, gemcitabine-XP and dFdU-XP concentrations in PBMCs are reported in Table 3. Intracellular gemcitabine levels were below the quantification limit after administration of the microdose, while a mean gemcitabine concentration of 0.14 pmol/million PBMCs was determined after administration of the therapeutic dose. Intracellular gemcitabine-XP levels were detectable in all patients, with concentrations ranging from 0.0010 to 0.042 pmol/million PBMCs after administration of the microdose and from 0.23 to 11 pmol/million PBMCs after administration of the therapeutic dose (Table 2). In line with gemcitabine data, intracellular dFdU concentrations were below the LLOQ after administration of the microdose, and a mean dFdU concentration of 6.9 pmol/million PBMCs was observed after therapeutic dose administration. dFdU-XP concentrations ranged from 0.00086 to 0.025 pmol/million PBMCs and from 0.83 to

3.2

Table 3. Mean (SD) intracellular concentrations of gemcitabine and 2',2'-difluorodeoxyuridine (dFdU) in peripheral blood mononuclear cells (PBMCs) after administration of a microdose (100 µg) and a therapeutic dose (1,250 mg/m^2) (n=9). Microdose data are presented as the observed values and linearly extrapolated to 1,250 mg/m^2.

Analyte	Microdose (pmol/million PBMCs)	Microdose, extrapolated (pmol/million PBMCs)	Therapeutic dose (pmol/million PBMCs)	Ratio (microdose/ therapeutic dose)	Predicta-bility	p-value[T]
Gemcitabine	< 0.0050[‡]	-	0.14 (0.076)	-		
dFdU	< 0.0050[‡]	-	6.9 (4.3)			
Gemcitabine -XP	0.012 (0.014)	170 (140)	5.3 (3.9)	32	No	0.0039
dFdU-XP	0.0071 (0.0096)	90 (95)	7.0 (4.4)	13	No	0.0039

Abbreviations: gemcitabine-XP = gemcitabine phosphates, LLOQ = lower limit of quantification dFdU = 2',2'-difluorodeoxyuridine, dFdU-XP = 2',2'-difluorodeoxyuridine phosphates, PBMC = peripheral blood mononuclear cells.
[T] Wilcoxon signed-rank test
[‡] Measured values below the lower limit of quantification (LLOQ)

14 pmol/million PBMCs following a microdose and therapeutic dose, respectively. Microdose data were linearly extrapolated to 1,250 mg/m^2 and the ratio between these dose-adjusted microdose concentrations and therapeutic concentrations was 13 for dFdU-XP and 32 for gemcitabine-XP (Table 2). The large ratio clearly shows that intracellular gemcitabine, gemcitabine-XP, dFdU and dFdU-XP concentrations could not be predicted from the microdose.

Background swabs
The background swabs did not show any potential interferences in the surroundings of patients that could have influenced quantification of gemcitabine in plasma. Analytes were not detectable in the swabs as concentrations were below the LLOQ of the assay.

Discussion

Microdose studies provide the opportunity to early assess human pharmacokinetics of newly developed drugs with limited drug exposure. As expected, in this phase 0 study the exposure to gemcitabine could be adequately predicted from a microdose over a >10.000-fold dose range. These data are in line with clinical results from phase 1 trials, in which gemcitabine pharmacokinetics were linear over a dose range of 10 to 1,000 mg/m^2 (11,12). Although AUC was adequately predicted from the microdose, the shape of the concentration-time curve, as depicted in Figures 1B and 2B, is clearly different for both dosages and this was reflected by poor scalability in Vd and K_e. Moreover, intracellular concentrations of both gemcitabine and dFdU could not be predicted from measured concentrations after administration of a microdose. Nonlinearity may be caused by saturation of enzymes and transporter systems, which

can occur at different pharmacokinetic processes such as distribution, metabolism and elimination. Gemcitabine is transported across cell membranes via multiple active nucleoside transporters (NTs) (10,17). Both equilibrative nucleoside transporters (ENT or solute carrier 28, SLC28) and concentrative nucleoside transporters (CNT or solute carrier 29, SLC29) are involved in uptake of gemcitabine via facilitated diffusion or sodium-dependent uptake, respectively (17,18). Most of its uptake is mediated via hENT1, although gemcitabine has affinity also for hENT2, hCNT1, hCNT2 and hCNT3 (17). Furthermore, gemcitabine and its phosphorylated metabolites may be transported into extracellular space by ATP binding cassette (ABC) transporter 5, also called multidrug resistance protein 5 (MRP5) (19). Saturation of the ENT transporters has been reported previously for gemcitabine in rat hepatocytes at a concentration of 2.6 mg/mL (20), which is above clinically relevant therapeutic concentrations. No literature could be found on saturation of MRP5.

After intravenous administration, about 90% of gemcitabine is rapidly converted by CDA to its main metabolite dFdU in plasma, liver, kidneys and other tissues (9). Saturation of CDA has not been described in human or human cell lines, however, degradation of gemcitabine to dFdU by feline CDA was shown to be a saturable process at a fixed-dose rate of 2.5 mg/m^2 (21). Intracellularly, deoxycytidine kinase (dCK) is responsible for the metabolism of gemcitabine by phosphorylation to gemcitabine-MP, which can be further phosphorylated by nucleotide kinases to its active metabolites gemcitabine-DP and gemcitabine-TP. The formation of gemcitabine-TP by dCK is rate-limiting and saturable, as was observed in human mononuclear cells at gemcitabine plasma concentrations of 2.6-5.2 µg/mL (21,22). These concentrations are within the therapeutic window of gemcitabine.

Gemcitabine and its metabolite dFdU are eliminated renally. Up to 92 - 98% of the gemcitabine dose is recovered as dFdU in the urine whereas <10% is recovered as gemcitabine. The elimination of gemcitabine is biphasic and after a rapid initial elimination with a half-life of 40-90 minutes, the terminal elimination phase is around 14 hours (11,23). There are no transporters involved in the renal elimination of gemcitabine and its metabolite, and therefore, it is unlikely that nonlinearity is caused by this process. In our study, the terminal half-life was calculated using NCA and assumes linear elimination. A two-compartment model would better reflect gemcitabine elimination, therefore, calculated half-lives in this study will underestimate the terminal elimination phase.

Taken all data into account, saturation at hENT1 and CDA may contribute to the poor predictability of Vd and Ke. Saturation of hENT1 is supported by the intracellular data from this study, in which intracellular gemcitabine and dFdU concentrations were lower after administration of the therapeutic dose compared to the extrapolated microdose concentrations. Furthermore, intracellular data suggest that gemcitabine is completely phosphorylated by dCK after administration of the microdose, while gemcitabine could be measured intracellularly following a therapeutic dose. The poor predictability of Vd and intracellular gemcitabine and dFdU concentrations may be due to a combined

3.2

saturation at hENT and dCK.

In this study we use the two-fold criterion to define predictability. This threshold is common in the field of microdosing and is used in many microdose trials. However, the applicability of this threshold for drugs with a small therapeutic index, such as cytotoxic agents, has been poorly described. Although exposure to gemcitabine was found to be linear within two-fold, it should of note that extra caution is justified for drugs with a small therapeutic index used in the microdose setting.

In this study we demonstrate that gemcitabine and dFdU could be quantified after administration of a 100 µg microdose using LC-MS/MS. Increased sensitivity of LC-triple quadrupole mass spectrometers have led to an extended application of microdosing with better accessibility, while reducing costs. In this phase 0 study we showed that pharmacokinetic concentration-time curves may be obtained using these ultra-sensitive detectors. However, we were unable to quantify intracellular metabolites individually, which might be possible using AMS. Based on our data, we believe that LC-MS/MS, for LC-MSMS quantifiable compounds, is the method of choice in microdose studies since no radiolabeled drugs are required, instruments are readily available and furthermore drug metabolites can be measured at the same time.

In conclusion, the exposure to gemcitabine at therapeutic dose was accurately predicted from the pharmacokinetics of a microdose, which was 10,000-fold lower than the therapeutic dose. Although we expected adequate predictability for all pharmacokinetic parameters, Vd and Ke were not scalable within two-fold from the microdose to the therapeutic dose. This might be attributed to saturation of hENT1 and CDA. Our findings suggest that phase 0 microdose trials may prove valuable to early predict drug exposure of intravenously administered drugs, but in our case do not predict all relevant pharmacokinetic parameters.

References

1. Marchetti S, Schellens JHM, S. M, J.H.M. S. The impact of FDA and EMEA guidelines on drug development in relation to Phase 0 trials. Br J Cancer. 2007;97:577–81.

2. European Medicines Agency (EMA). Position paper on non-clinical safety studies to support clinical trials with a single microdose. 2004 [cited 2019 May]. Available from: http://www.iaa-ams.co.jp/img_bsnss/MD1.pdf

3. US Food and Drug Administration (FDA). Guidance for industry investigators and reviewers: Exploratory IND studies. 2006 [cited 2019 May]. Available from: https://www.fda.gov/media/72325/download

4. European Medicines Agency (EMA). ICH M3 (R2): Note for Guidance on Non-Clinical Safety Studies for the Conduct of Human Clinical Trials and Marketing Authorization for Pharmaceuticals. 2009 [cited 2019 May]. Available from: https://www.ema.europa.eu/en/documents/scientific-guideline/ich-m-3-r2-non-clinical-safety-studies-conduct-human-clinical-trials-marketing-authorization_en.pdf

5. Burt T, John CS, Ruckle JL, Vuong LT. Phase-0/microdosing studies using PET, AMS, and LC-MS/MS: a range of study methodologies and conduct considerations. Accelerating development of novel pharmaceuticals through safe testing in humans - a practical guide. Expert Opin Drug Deliv. 2016;14:1–16.

6. van Nuland M, Rosing H, Huitema ADR, Beijnen JH. Predictive Value of Microdose Pharmacokinetics. Clin Pharmacokinet. 2019;58:1221-36.

7. Lappin G, Garner RC. The utility of microdosing over the past 5 years. Expert Opin Drug Metab Toxicol. 2008;4:1499–506.

8. M. R, Rowland M. Commentary on ACCP position statement on the use of microdosing in the drug development process. J Clin Pharmacol. 2007;47:1595–6.

9. US Food and Drug Administration (FDA). Prescribing information: Gemzar. 1996 [cited 2019 May]. p. 24. Available from: https://pi.lilly.com/us/gemzar.pdf

10. Mini E, Nobili S, Caciagli B, Landini I, Mazzei T. Cellular pharmacology of gemcitabine. Ann Oncol. 2006;17:7–12.

11. Abbruzzese JL, Grunewald R, Weeks EA, Gravel D, Adams T, Nowak B, et al. A phase I clinical, plasma, and cellular pharmacology study of gemcitabine. J Clin Oncol. 1991;9:491–8.

12. Abbruzzese JL. Phase I studies with the novel nucleoside analog gemcitabine. Semin Oncol. 1996;23:25–31.

13. Veltkamp SA, Hillebrand MJX, Rosing H, Jansen RS, Wickremsinhe ER, Perkins EJ, et al. Quantitative analysis of gemcitabine triphosphate in human peripheral blood mononuclear cells using weak anion-exchange liquid chromatography coupled with tandem mass spectrometry. Journal of mass spectrometry. 2006;41:1633–42.

14. Jansen RS, Rosing H, Schellens JHM, Beijnen JH. Mass spectrometry in the quantitative analysis of therapeutic intracellular nucleotide analogs. Mass Spectrom Rev. 2011;30:321–43.

15. van Nuland M, Hillebrand MJX, Rosing H, Burgers JA, Schellens JHM, Beijnen JH. Ultra-sensitive LC–MS/MS method for the quantification of gemcitabine and its metabolite 2',2'-difluorodeoxyuridine in human plasma for a microdose clinical trial. J Pharm Biomed Anal. 2018;151:25–31.

16. Vainchtein LD, Rosing H, Thijssen B, Schellens JHM, Beijnen JH. Validated assay for the simultaneous determination of the anti-cancer agent gemcitabine and its metabolite 2',2'-difluorodeoxyuridine in human plasma by high-performance liquid chromatography with tandem mass spectrometry. Rapid Commun Mass Spectrom. 2007;21:2312–22.

3.2

17. Mackey JR, Mani RS, Selner M, Mowles D, Young JD, Belt JA, et al. Functional nucleoside transporters are required for gemcitabine influx and manifestation of toxicity in cancer cell lines. Cancer Res. 1998;58:4349–57.

18. Belt JA, Marina NM, Phelps DA, Crawford CR. Nucleoside transport in normal and neoplastic cells. Adv Enzyme Regul. 1993;33:235–52.

19. Hagmann WR, Jesnowski R, Löhr JM. Interdependence of gemcitabine treatment, transporter expression, and resistance in human pancreatic carcinoma cells. Neoplasia. 2010;12:740–7.

20. Shimada T, Nakanishi T, Tajima H, Yamazaki M, Yokono R, Takabayashi M, et al. Saturable Hepatic Extraction of Gemcitabine Involves Biphasic Uptake Mediated by Nucleoside Transporters Equilibrative Nucleoside Transporter 1 and 2. J Pharm Sci. 2015;104:3162–9.

21. Grunewald R, Abbruzzese JL, Tarassoff P, Plunkett W. Saturation of 2′, 2′-difluorodeoxycytidine 5′-triphosphate accumulation by mononuclear cells during a phase I trial of gemcitabine. Cancer Chemother Pharmacol. 1991;27:258–62.

22. Plunkett W, Huang P, Xu YZ, Heinemann V, Grunewald R, Gandhi V. Gemcitabine: metabolism, mechanisms of action, and self-potentiation. Semin Oncol. 1995;22:3–10.

23. Wong A, Soo RA, Yong W-P, Innocenti F. Clinical pharmacology and pharmacogenetics of gemcitabine. Drug Metab Rev. 2009;41:77–88.

3.2

Summarizing discussion and perspectives

Summarizing discussion and perspectives

The studies and results described in this thesis provide further insight into the clinical pharmacology of anti-hormonal drugs and gemcitabine in oncology. In particular, attention has been paid to bioanalysis, therapeutic drug monitoring (TDM) and microdosing. In this chapter, relevant aspects and conclusions as addressed in previous chapters are put in a wider perspective.

Development and validation of bioanalytical methods

Sensitive bioanalytical methods are pivotal for accurate quantification of drugs in biological samples from clinical studies. Liquid chromatography-mass spectrometry (LC-MS/MS) is frequently used for this purpose. Advantages of LC-MS/MS compared to other bioanalytical techniques are high sensitivity, specificity and selectivity. Validations of bioanalytical methods are performed to check if the method is suitable for its intended use. Validated methods are than applied in routine analysis allowing decision making on drug dosing and patient safety. The Food and Drug Administration (FDA) and European Medicines Agency (EMA) provide guidelines for bioanalytical method validation (1,2). Validation parameters are described and guidance is provided on how to validate these parameters and which criteria might be applied. Two LC-MS/MS methods described in this thesis were validated according to these FDA and EMA guidelines. The development and validation of an LC-MS/MS assay for the quantification of endogenous compounds testosterone, dihydrotestosterone, androstenedione, cortisol and the drug prednisone are presented in **Chapter 1.5**. The primary goal of this assay was to achieve high sensitivity to enable quantification of low plasma levels of these androgens in castrated prostate cancer patients. The other fully validated assay was intended to support a microdose trial with gemcitabine. An ultra-sensitive LC-MS/MS assay was developed and validated to quantify this drug and its major metabolite in human plasma (**Chapter 1.6**).

Although FDA and EMA guidelines provide valuable assistance for the validation of methods to support clinical pharmacokinetic and toxicokinetic studies, no guidance is provided on how to perform TDM assay validation. Therefore we suggested an adapted validation approach for assays specifically developed for TDM purpose based on the intended use of these methods. **Chapter 1.1** provides recommendations that could serve as a guide for bioanalytical validations and analysis of study samples for TDM. In short, we propose a maximum of four calibration standards over a condensed calibration range, a maximum of three concentration levels analyzed in a minimum of three analytical batches for determining inter- and intra-assay accuracy and precision. Furthermore, we recommend to exclude dilution integrity and matrix effect/recovery experiments if a stable labeled internal standard is available. The applicability of this limited validation protocol was demonstrated in three TDM assays. In **Chapter 1.2**, the development and validation of an LC-MS/MS method for TDM of seven anti-hormonal

4

compounds is presented. Chromatographic separation was challenging for Z-endoxifen and abiraterone, as both analytes show extensive metabolism, including the formation of isomers. Baseline separation of these isomers was required for unbiased quantification of the analytes. Furthermore, a plasma batch-dependent instability for abiraterone was observed at room temperature. This required abiraterone samples to be shipped on dry-ice. **Chapter 1.3** describes an LC-MS/MS assay for simultaneous quantification of abiraterone, enzalutamide and their major metabolites. Abiraterone N-oxide and enzalutamide carboxylic acid are unstable in stock solution prepared in DMSO. To minimize degradation of these metabolites, freshly prepared stocks were used for the preparation of working solutions in plasma. More recently, an active metabolite of abiraterone was discovered named metabolite Δ(4)-abiraterone (D4A). We developed an LC-MS/MS assay for this newly identified metabolite (**Chapter 1.4**). The validation of presented assays demonstrate that a minimal validation protocol for assays with TDM purpose is indeed feasible, justified, and cost-saving in clinical practice, yielding reliable results. Provided recommendations could serve as a standard for future validations of TDM assays and these recommendations may be applicable to other fields.

Therapeutic drug monitoring of anti-hormonal drugs in oncology

Therapeutic drug monitoring is the clinical practice of measuring drug concentrations in biological matrix to be used for individualization of drug dosing, in other words patient-tailored dosing. It is known that many oral anticancer agents, including anti-hormonal drugs, show large interpatient variability in pharmacokinetic exposure. Nevertheless, these drugs are administered at fixed doses, resulting in a risk of under – or overdosing. Treatment with these agents may be optimized by implementing TDM. Drugs that are to be considered as TDM candidates should be given as long-term therapy, with a high inter-patient variability, a narrow therapeutic window, an established concentration-response and/or concentration-toxicity relationship, a dose-concentration correlation and a feasible strategy for individualized dosing (3). To execute TDM, robust, selective, specific and validated methods should be available. The use of TDM in oncology has been evaluated extensively and exposure targets for targeted therapies have been advocated previously (4–9). **Chapter 2.1** gives an overview of relevant clinical pharmacokinetic and pharmacodynamic characteristics of oral anti-hormonal drugs in oncology which translates into practical guidelines for TDM. The trough concentration (C_{min}) target for abiraterone has been set at 8.4 ng/mL, based on a clear exposure-response relationship (10). This concentration target was validated in a "real-world" patient cohort with 62 patients in **Chapter 2.2**, showing a better prognosis for patients with a C_{min} >8.4 ng/mL compared to patients with a plasma C_{min} below this target. Monitoring C_{min} of abiraterone can help to identify those patients at risk of suboptimal treatment and these patients may be advised to take abiraterone concomitantly with a low-fat meal. It is known from previous studies that this could

increase plasma concentrations up to 5-fold (11). In **Chapter 2.4**, implementation of this food-intervention has led to adequate abiraterone exposure for 86% of the patients with an initial C_{min} below the target, and a 2.6-fold increase in median C_{min}. Although TDM may improve treatment outcome for patients using abiraterone acetate, there was no evidence found to support TDM of enzalutamide. As described in **Chapter 2.3**, enzalutamide plasma concentrations show no relationship with progression-free survival in metastasized castration-resistant prostate cancer patients. From this perspective, there is no binding role for TDM of enzalutamide in daily clinical practice for this patient population. However, exceptions can be made in specific situations, such as in patients with end-stage renal disease undergoing hemodialysis (**Chapter 2.5**) or in patients with a hepatic transplant (**Chapter 2.6**). Our case-reports show that plasma concentrations of enzalutamide and abiraterone were not affected by organ failure or concomitant medication and, therefore, treatment with these drugs seems feasible in patients undergoing hemodialysis or in patients with a hepatic transplant, respectively. Data gathered with TDM were used to study the effect of age on the exposure to abiraterone and enzalutamide. **Chapter 2.7** showed no significant age-related effects on exposure to oral anti-androgen therapies abiraterone and enzalutamide, except for the active metabolite D4A and the inactive metabolite enzalutamide carboxylic acid, both having significantly higher exposure in older males. The clinical relevance of the observed higher metabolite concentrations remains unclear. Abiraterone acetate and enzalutamide are primarily administered to elderly patients, and our data suggest there is no need for an age-based dose regimen.

Due to increasing expenditure on healthcare in the Netherlands, there is a rising need for studies in which health care costs are assessed critically. **Chapters 2.8** and **2.9** describe the cost-effectiveness of monitoring Z-endoxifen and abiraterone in a TDM setting. Implementation of Z-endoxifen TDM was found to be cost saving, while TDM of abiraterone is costly as patients will be treated with abiraterone acetate for a longer treatment period, but effective in terms of quality of life gain. These data show that cost-effectiveness analyses may be performed for simple interventions, as done with TDM, to substantiate its use in clinical practice. Based on our results, we advise clinicians to consider integrating monitoring Z-endoxifen and abiraterone into standard clinical care of estrogen receptor positive (ERα+) breast cancer patients and metastatic castration-resistant prostate cancer patients, respectively.

Predictive value of microdose pharmacokinetics

Microdose trials are exploratory investigational drug trials in which 1/100th of the therapeutic dose, with a maximum of 100 µg, is administered to human subjects (12). The goal of such trials is to obtain pharmacokinetic data with a minimal drug exposure. The question raised is if microdose pharmacokinetics are indicative for pharmacokinetics at therapeutic dose. Therefore, the predictive value of microdose pharmacokinetics was investigated for 46 compounds in **Chapter 3.1**. Pharmacokinetics at therapeutic

4

dose were adequately predicted for 68% of orally administered drugs and for 94% of intravenously administered drugs. Microdose pharmacokinetics were considered predictive if the mean observed pharmacokinetic values of the microdose and the therapeutic dose were within a two-fold (13,14). Nonlinear distribution may be caused by saturation of enzyme and transporter systems, such as intestinal and hepatic efflux and uptake transporters. In **Chapter 3.2**, a phase 0 study is described in which we examined whether the pharmacokinetics of gemcitabine at a therapeutic dose (1250 mg/m^2) could be predicted from the pharmacokinetics of a microdose (100 µg). The area under the concentration-time curve (AUC) at therapeutic dose was well predicted from the AUC at microdose, however, the elimination phase of the plasma concentration-time curves were different as reflected in poor scalability of elimination constant (K_e) and volume of distribution (V). Poor scalability may be attributed to saturation of hepatic equilibrative nucleoside transporter 1 (hENT1) or cyticine deaminase (CDA). Our findings suggest that phase 0 microdose trials may prove valuable to early predict exposure to intravenously administered drugs. Performing microdose trials such as the one described in this thesis broadens the insight into the usefulness of the microdose concept in clinical development.

Perspectives

Currently, many, particularly oral drugs are marketed for a specific cancer type at a fixed dose, while it is known that pharmacokinetic alterations justify tailored treatment. Therefore, precision, tailored medicine may help to improve patient care. A relatively simple intervention such as TDM can optimize treatment dramatically with a reduced risk of underdosing or toxic overdosing. In daily oncology practice, however, TDM has not been fully implemented yet. This may be due to difficulties in establishing appropriate exposure targets and a lack of sound exposure-response data from clinical trials. During clinical drug development, information is gathered about drug exposure and how it relates to efficacy or toxicity as part of the registration package and, therefore, exposure-response data is available for many novel anticancer agents. The increasing demand for precision medicine may give this type of research a boost and thereby help to identify exposure targets for newly developed compounds. For drugs that are already marketed, studies such as presented in this thesis can contribute towards the advancement of knowledge by exposure-response analyses in "real-world" patient cohorts. We have shown that TDM makes sense for abiraterone, while enzalutamide is not a suitable candidate for TDM because of the lack of an exposure-response relationship at the current dosing regimen. TDM of abiraterone has now been implemented in our Institute to personalize treatment of every patient with metastasized castration-resistant prostate cancer treated with this drug.

We have developed an alternative validation approach particularly suitable for bioanalytical methods used in a TDM setting. The growing demand for individualized treatment for many newly introduced drugs requires the development and validation

of new TDM assays. Our TDM validation approach provides guidance to efficiently execute method validation while still offering sufficient confidence in the fit-for-purpose of the method. Recommendations on a limited validation protocol for TDM assays as addressed in this thesis can probably be applied to other fields than oncology..

The concept or microdosing was first addressed in the late 1990s and the first data on microdose trials appeared in the literature in 2003. Many trials have been published since and the outcomes are ambiguous. The predictive value of microdose trials in human patients is much higher compared to extrapolation of preclinical data using physiologically based pharmacokinetic modeling or in vitro in vivo extrapolation. Although microdose trials in humans perform better in terms of predictability, pharmacokinetics at therapeutic dose were poorly predicted for 32% of orally administered drugs. During a phase 0 trial, it is unknown whether the pharmacokinetics may be linearly extrapolated, and, therefore the applicability of microdose trials for oral compounds is not fully established. On the contrary, pharmacokinetics at therapeutic dose were accurately predicted for 94% of intravenously administered drugs. This high degree of success confirms the strength of phase 0 microdose trials in gaining early pharmacokinetic data of intravenously administered compounds. Taken together, the uncertain predictability of microdose trials for orally administered compounds makes implementation of phase 0 microdose trials complicated for this route of administration, while it may help improve clinical development of intravenously administered drugs. Furthermore, other applications for microdose trials are emerging that show potential, such as oral bioavailability trials, drug-drug interaction studies and trials to investigate drug distribution by visualization in tissue that is difficult to sample, such as the brain.

4

References

1. US Food and Drug Administration (FDA). FDA Guidance for Industry: Bioanalytical Method Validation. Silver Spring, Maryland: US Food and Drug Administration. 2018 [cited 2018 Jun]. Available from: https://www.fda.gov/downloads/drugs/guidances/ucm070107.Pdf

2. European Medicines Agency (EMA). Guideline on Bioanalytical Method Validation. Committe for Medicinal Produts for Human Use and European Medicines Agency. 2011 [cited 2019 May]. Available from: http://www.ema.europa.eu/docs/en_GB/document_library/Scientific_guideline/2011/08/WC500109686.pdf

3. de Jonge ME, Huitema ADR, Schellens JHM, Rodenhuis S, Beijnen JH. Individualised cancer chemotherapy: strategies and performance of prospective studies on therapeutic drug monitoring with dose adaptation: a review. Clin Pharmacokinet. 2005;44:147–73.

4. Verheijen R, Yu H, Schellens J, Beijnen J, Steeghs N, Huitema A. Practical Recommendations for Therapeutic Drug Monitoring of Kinase Inhibitors in Oncology. Clin Pharmacol Ther. 2017;102:765–76.

5. Yu H, Steeghs N, Nijenhuis C, Schellens J, Beijnen J, Huitema A. Practical guidelines for therapeutic drug monitoring of anticancer tyrosine kinase inhibitors: Focus on the pharmacokinetic targets. Clin Pharmacokinet. 2014;53:305–25.

6. Paci A, Veal G, Bardin C, Levêque D, Widmer N, Beijnen J, et al. Review of therapeutic drug monitoring of anticancer drugs part 1 - Cytotoxics. Eur J Cancer. 2014;50:2010–9.

7. Widmer N, Bardin C, Chatelut E, Paci A, Beijnen J, Levêque D, et al. Review of therapeutic drug monitoring of anticancer drugs part two - Targeted therapies. Eur J Cancer. 2014;50:2020–36.

8. De Wit D, Guchelaar HJ, Den Hartigh J, Gelderblom H, Van Erp NP. Individualized dosing of tyrosine kinase inhibitors: Are we there yet? Drug Discov Today. 2015;20:18–36.

9. Bardin C, Veal G, Paci A, Chatelut E, Astier A, Levêque D, et al. Therapeutic drug monitoring in cancer - Are we missing a trick? Eur J Cancer. 2014;50:2005–9.

10. Carton E, Noe G, Huillard O, Golmard L, Giroux J, Cessot A, et al. Relation between plasma trough concentration of abiraterone and prostate-specific antigen response in metastatic castration-resistant prostate cancer patients. Eur J Cancer. 2017;72:54–61.

11. Chi KN, Spratlin J, Kollmannsberger C, North S, Pankras C, Gonzalez M, et al. Food effects on abiraterone pharmacokinetics in healthy subjects and patients with metastatic castration-resistant prostate cancer. J Clin Pharmacol. 2015;55:1406–14.

12. Lappin G, Noveck R, Burt T. Microdosing and drug development: past, present and future. Expert Opin Drug Metab Toxicol. 2013;9:817–34.

13. Lappin G, Garner RC. The utility of microdosing over the past 5 years. Expert Opin Drug Metab Toxicol. 2008;4:1499–506.

14. M. R, Rowland M. Commentary on ACCP position statement on the use of microdosing in the drug development process. J Clin Pharmacol. 2007;47:1595–6.

APPENDICES

Nederlandse samenvatting
Author affiliations
List of publications
Dankwoord
Curriculum vitae

Appendices

Nederlandse samenvatting

De ontwikkeling van nieuwe geneesmiddelen in de oncologie heeft de afgelopen jaren een grote vlucht genomen. Met de komst van doelgerichte geneesmiddelen kunnen patiënten met specifieke kankertypen en tumoreigenschappen beter behandeld worden. Een bijkomend voordeel van veel nieuwe geneesmiddelen is de orale toediening; de oudere cytostatica worden veelal intraveneus toegediend. Echter, orale toediening vergroot variabiliteit in blootstelling door de vele barrières die doorlopen moeten worden alvorens het geneesmiddel de bloedbaan bereikt. Deze variabiliteit vergroot het risico op onder- en overdosering en daarmee de kans op verminderde effectiviteit en verhoogde toxiciteit. Met kennis van de farmacokinetiek – "wat het lichaam doet met het geneesmiddel" - hopen we de medicamenteuze therapie te verbeteren en de veiligheid te vergroten.

In dit proefschrift wordt de klinische farmacologie van verschillende anti-hormonale oncolytica en gemcitabine beschreven met aandacht voor bioanalyse, 'therapeutic drug monitoring' (TDM) en microdoseren.

Ontwikkeling en validatie van bioanalytische methoden

Gevoelige bioanalytische methoden zijn onmisbaar voor de kwantificering van geneesmiddelen in biologische vloeistoffen en weefsels verkregen in klinische studies. Vloeistofchromatografie in combinatie met massaspectrometrie (LC-MS/MS) wordt vaak toegepast als bioanalytische techniek. Voordelen van deze combinatietechniek zijn hoge sensitiviteit, specificiteit en de mogelijkheid om meerdere geneesmiddelen, inclusief metabolieten, tegelijkertijd te kwantificeren. Om te bevestigen dat bioanalytische methoden geschikt zijn voor het beoogde doel dienen deze grondig te worden gevalideerd. De 'Food and Drug Administration' (FDA) en 'European Medicines Agency' (EMA) zijn overheidsinstituten die richtlijnen hebben opgesteld voor de validatie van bioanalytische methoden. Dit proefschrift bevat twee methoden die volgens deze richtlijnen zijn gevalideerd. **Hoofdstuk 1.5** beschrijft een gevoelige LC-MS/MS methode om de androgenen testosteron, androstenedion en dihydrotestosteron te bepalen in plasma van patiënten met gemetastaseerde castratieresistente prostaatkanker. Tevens kunnen met deze techniek cortisol – een hormoon dat via een vergelijkbare weg als testosteron gevormd wordt – en prednison – een hormonaal geneesmiddel dat tezamen met abirateronacetaat wordt toegediend – worden gekwantificeerd. Gecastreerde prostaatkankerpatiënten gebruiken hormoontherapie om de werking van androgenen op de tumor te onderdrukken. De androgeenconcentraties zijn doorgaans laag. Daarom is een hoge sensitiviteit van de analytische bepaling vereist. Hoge sensitiviteit staat ook centraal in **hoofdstuk 1.6**, waarin een methode wordt beschreven ter kwantificatie van gemcitabine en de metaboliet 2′,2′-difluorodeoxyuridine (dFdU) in plasma van patiënten die deelnemen aan een microdosis studie.

A

De richtlijnen van de FDA en EMA zijn waardevol ter ondersteuning van bioanalytische validaties voor farmacokinetische en toxicokinetische studies. Echter, men heeft de vrijheid om af te wijken van deze richtlijnen met de juiste onderbouwing. In dit proefschrift presenteren we een vereenvoudigd protocol voor de validatie van methoden die worden toegepast voor TDM doeleinden. In **Hoofdstuk 1.1** worden onze aanbevelingen beschreven. Kort samengevat adviseren we om het aantal kalibratiestandaarden en 'quality control' (QC) monsters te verminderen en om integriteit van verdunningen, matrix effect en 'recovery' experimenten achterwege te laten. De toepassing en juistheid van dit vereenvoudigde validatieprotocol zijn aangetoond in **hoofdstukken 1.2 t/m 1.4**. In deze hoofdstukken worden de ontwikkeling en validatie van drie analytische methoden besproken waarmee anti-hormonale geneesmiddelen in plasma van kankerpatiënten kunnen worden gekwantificeerd. In **Hoofdstuk 1.2** staat beschreven hoe zeven anti-hormonale geneesmiddelen tegelijkertijd bepaald kunnen worden in humaan plasma, namelijk abirateron, anastrozol, bicalutamide, enzalutamide, letrozol, Z-endoxifen en exemestaan. Abirateron en Z-endoxifen laten een uitgebreid metabolietprofiel zien, inclusief massa-identieke isomeervorming, waardoor chromatografische scheiding essentieel is. Het chromatografische systeem in **hoofdstuk 1.2** en **1.5** is vergelijkbaar en door beide methoden te combineren kunnen zowel geneesmiddelconcentraties als het effect op de hormoonspiegels nauwkeurig worden gekwantificeerd. **Hoofdstuk 1.3** beschrijft de ontwikkeling en validatie van een LC-MS/MS methode om abirateron, enzalutamide en de meest voorkomende metabolieten te analyseren in humaan plasma. In **hoofdstuk 1.4** is een recent ontdekte metaboliet van abirateron, namelijk Δ(4)-abirateron (D4A), toegevoegd aan de methode die is beschreven in het voorgaande hoofdstuk. D4A heeft anti-adrenerge eigenschappen en kan daarom bijdragen aan het antitumor effect van abirateron. De validatie van gepresenteerde methoden laat zien dat een minimaal validatieprotocol voor TDM methoden haalbaar en tijdbesparend is, met behoud van hoge reproduceerbaarheid, juistheid en precisie. Onze aanbevelingen kunnen een aanzet zijn om toekomstige methoden voor TDM toepassingen efficiënter te valideren.

Therapeutic drug monitoring van anti-hormonale geneesmiddelen in de oncologie

De komst van nieuwe orale oncolytica introduceert een grotere variabiliteit in blootstelling. Ondanks deze grote variabiliteit worden geneesmiddelen in een vastgestelde dosering geregistreerd en voorgeschreven, met het risico op onder- en overdosering. De behandeling van deze patiënten kan worden verbeterd door implementatie van TDM: de klinische praktijk waarbij geneesmiddelconcentraties worden bepaald in bloed, plasma of serum en op basis van deze concentratie een dosisadvies wordt verstrekt. Geneesmiddelen die in aanmerking komen voor TDM worden gekenmerkt door: lange-termijn behandeling, beschikbaarheid van gevoelige bioanalytische methoden, hoge interpatiënt variabiliteit, smalle therapeutische breedte,

vastgestelde concentratie-effect en/of concentratie-toxiciteit relaties, een dosis-concentratie correlatie en een klinisch haalbare strategie voor dosisindividualisatie. Het gebruik van TDM is nog altijd beperkt in de oncologie, al zijn er voldoende geneesmiddelen met genoemde kenmerken. **Hoofdstuk 2.1** geeft een overzicht van farmacokinetische en farmacodynamische – "wat het geneesmiddel doet met het lichaam" - eigenschappen van anti-hormonale geneesmiddelen in de oncologie die vertalen in praktische handvatten voor TDM in de kliniek. In een eerdere studie is aangetoond dat patiënten met gemetastaseerde castratieresistente prostaatkanker met een dalspiegel van abirateron ≥8,4 ng/mL een betere prognose hebben dan patiënten met een dalspiegel <8,4 ng/mL. In **hoofdstuk 2.2** blijkt dat deze resultaten reproduceerbaar zijn in een populatie van 62 patiënten met castratieresistente prostaatkanker die volgens de richtlijnen behandeld zijn in ons Instituut. Op basis van deze informatie kan TDM voor abirateron worden ingezet met een beoogde dalspiegel van 8,4 ng/mL. Patiënten met een dalspiegel <8,4 ng/mL kunnen worden aanbevolen om abirateron in te nemen met een lichte maaltijd, omdat inname met voedsel de dalspiegel tot factor 5 kan verhogen. De studie zoals beschreven in **hoofdstuk 2.4** laat zien dat een lage dalspiegel <8,4 ng/mL op eenvoudige wijze verhoogd kan worden door patiënten te adviseren om abirateron in te nemen met een lichte maaltijd. Bij 19 van de 22 patiënten met een lage dalspiegel bij start van de behandeling, heeft TDM geleid tot een beoogde dalspiegel van ≥8,4 ng/mL. In tegenstelling tot TDM voor abirateron, is er onvoldoende bewijs voor een rol van TDM voor het geneesmiddel enzalutamide. Zoals beschreven in **hoofdstuk 2.3** is er geen relatie gevonden tussen plasmaconcentraties van enzalutamide en progressievrije overleving. Met de huidige kennis wordt TDM van enzalutamide afgeraden omdat het geen behandelvoordeel oplevert voor de patiënt. Echter, er kan een uitzondering worden gemaakt voor specifieke populaties, zoals patiënten die hemodialyse ondergaan ten gevolge van ernstig nierfalen (**hoofdstuk 2.5**) of patiënten met een levertransplantatie (**hoofdstuk 2.6**). Deze casus laten zien dat plasmaconcentraties van enzalutamide en abirateron niet worden beïnvloed door orgaanfalen. **Hoofdstuk 2.7** onderzoekt de relatie tussen leeftijd en blootstelling aan abirateron en enzalutamide. Er is geen correlatie gevonden tussen leeftijd en plasmaconcentraties van beide geneesmiddelen, behalve voor de metabolieten D4A en enzalutamide carboxylzuur. Patiënten met een hogere leeftijd hebben hogere plasmaconcentraties van deze metabolieten. Dit wordt waarschijnlijk veroorzaakt door een afname van de nierfunctie. Het klinische effect van verhoogde metabolietconcentraties is niet verder onderzocht. Abirateronacetaat en enzalutamide worden voornamelijk toegediend aan oudere patiënten en de resultaten zoals beschreven in dit proefschrift geven geen aanwijzingen voor leeftijdgerelateerde dosisaanpassingen.

De kosten in de Nederlandse gezondheidszorg zijn de afgelopen jaren sterk gegroeid, waardoor onderzoek naar de kosteneffectiviteit van nieuwe interventies en therapieën steeds belangrijker wordt. In **hoofdstuk 2.8** laten we zien dat het op gezette tijden meten van Z-endoxifen in plasma van borstkankerpatiënten die tamoxifen gebruiken

A

leidt tot een kostenbesparing. Het monitoren van abirateron blijkt eveneens kosteneffectief (**hoofdstuk 2.9**), met een toename van levensjaren van goede kwaliteit. In tegenstelling tot TDM van Z-endoxifen zorgen hoge medicijnkosten van abirateron ervoor dat TDM van dit geneesmiddel niet kostenbesparend is. Dit kan in de toekomst veranderen met de komst van generieke varianten.

Voorspellende waarde van de farmacokinetiek van een microdosis

Microdosis studies zijn geneesmiddelonderzoeken waarin slechts 1/100[e] van de therapeutische dosis wordt toegediend aan patiënten of gezonde vrijwilligers, met een maximum van 100 μg per dag. In dit type studies wordt farmacokinetische informatie verzameld met een minimale blootstelling aan het geneesmiddel. Voorafgaand aan een microdosis studie is het onduidelijk of de farmacokinetiek zoals bepaald na toediening van een microdosis voorspellend is voor de farmacokinetiek van een therapeutische dosis. De voorspellende waarde van de farmacokinetiek van een microdosis is onderzocht voor 46 geneesmiddelen in **hoofdstuk 3.1**. Goede voorspellende waarde is als volgt gedefinieerd: farmacokinetische parameters van de microdosis en de therapeutische dosis verschillen met maximaal factor twee. De farmacokinetiek na toediening van een therapeutische dosis was goed voorspeld voor 68% van de oraal toegediende geneesmiddelen en voor 94% van de intraveneus toegediende geneesmiddelen. Non-lineaire distributie kan worden veroorzaakt door saturatie van enzymsystemen of geneesmiddeltransporters. **Hoofdstuk 3.2** beschrijft een fase 0 studie waarin de voorspellende waarde van de farmacokinetiek van een gemcitabine microdosis is onderzocht. De oppervlakte onder de concentratie-tijdcurve (AUC) was goed te voorspellen met toediening van een microdosis. Echter, de vorm van de concentratie-tijdcurve was verschillend voor de microdosis en de therapeutische dosis, wat zich uitte in een slecht voorspelbaar verdelingsvolume (V) en een slecht voorspelbare eliminatieconstante (K_e). Deze non-lineariteit wordt waarschijnlijk veroorzaakt door saturatie van de hepatische equilibrative nucleoside transporter (hENT) en door cytidine deaminase (CDA). Deze studie laat zien dat niet alle farmacokinetische parameters van gemcitabine goed voorspeld konden worden met de microdosis. Door het uitvoeren van dergelijke studies wordt meer informatie verzameld over het concept en het nut van microdosis studies.

In dit proefschrift worden verschillende aspecten beschreven van de klinische farmacologie van anti-hormonale geneesmiddelen en gemcitabine in de oncologie. Ten eerste worden de ontwikkeling en validatie van verschillende LC-MS/MS methoden uitgelicht die aan de basis staan van dit proefschrift. Vervolgens wordt het nut van TDM bij abirateron en enzalutamide geëvalueerd. Tot slot onderzoeken we de voorspellende waarde van de farmacokinetiek van een microdosis, met als voorbeeld een microdosis studie waarin gemcitabine is toegediend aan patiënten. Met deze nieuwe kennis hopen we bij te kunnen dragen aan het verbeteren van de behandeling van patiënten met kanker.

Author affiliations

Jos H. Beijnen | Department of Pharmacy & Pharmacology and Division of Pharmacology, The Netherlands Cancer Institute, Amsterdam, The Netherlands; Division of Pharmacoepidemiology and Clinical Pharmacology, Utrecht Institute for Pharmaceutical Sciences, Utrecht University, Utrecht, The Netherlands

Andries M. Bergman | Division of Medical Oncology, The Netherlands Cancer Institute, Amsterdam, The Netherlands

Jacobus A. Burgers | Department of Thoracic Oncology, The Netherlands Cancer Institute, Amsterdam, The Netherlands

Marie-Rose B.S. Crombag | Department of Pharmacy & Pharmacology, The Netherlands Cancer Institute, Amsterdam, The Netherlands

Vincent O. Dezentje | Division of Medical Oncology, The Netherlands Cancer Institute, Amsterdam, The Netherlands

Jeantine M. de Feijter | Division of Medical Oncology, The Netherlands Cancer Institute, Amsterdam, The Netherlands

Laurens G. de Graaf | Division of Pharmacoepidemiology and Clinical Pharmacology, Utrecht Institute for Pharmaceutical Sciences, Utrecht University, Utrecht, The Netherlands

Stefanie. Groenland | Department of Pharmacy & Pharmacology, The Netherlands Cancer Institute, Amsterdam, The Netherlands

Renske M.T. ten Ham | Division of Pharmacoepidemiology and Clinical Pharmacology, Utrecht Institute for Pharmaceutical Sciences, Utrecht University, Utrecht, The Netherlands

Michel J.X. Hillebrand | Department of Pharmacy & Pharmacology, The Netherlands Cancer Institute, Amsterdam, The Netherlands

A

Bart van Hoek	Department of Gastroenterology and Hepatology, Leiden University Medical Center, Leiden, The Netherlands
Anke M. Hövels	Division of Pharmacoepidemiology and Clinical Pharmacology, Utrecht Institute for Pharmaceutical Sciences, Utrecht University, Utrecht, The Netherlands
Alwin D.R. Huitema	Department of Pharmacy & Pharmacology and Division of Pharmacology, The Netherlands Cancer Institute, Amsterdam, The Netherlands; Department of Clinical Pharmacy, University Medical Center Utrecht, Utrecht University, Utrecht, The Netherlands
Julie M. Janssen	Department of Pharmacy & Pharmacology, The Netherlands Cancer Institute, Amsterdam, The Netherlands
Karen A.M. de Jong	Department of Pharmacy & Pharmacology, The Netherlands Cancer Institute, Amsterdam, The Netherlands
Serena Marchetti	Division of Medical Oncology, Department of Clinical Pharmacology, The Netherlands Cancer Institute, Amsterdam, The Netherlands
Huib Ovaa	Division of Cell Biology, The Netherlands Cancer Institute, Amsterdam and Department of Chemical Immunology, Leiden University Medical Center, Leiden, The Netherlands
Hilde Rosing	Department of Pharmacy & Pharmacology, The Netherlands Cancer Institute, Amsterdam, The Netherlands
Huub H. van Rossum	Department of Laboratory Medicine, The Netherlands Cancer Institute, Amsterdam, the Netherlands
Joris I. Rotmans	Department of Internal Medicine, Leiden University Medical Center, Leiden, The Netherlands

Jan H.M. Schellens — Division of Pharmacology and Division of Medical Oncology, Department of Clinical Pharmacology, The Netherlands Cancer Institute, Amsterdam ,The Netherlands;
Division of Pharmacoepidemiology and Clinical Pharmacology, Utrecht Institute for Pharmaceutical Sciences, Utrecht University, Utrecht, The Netherlands

Neeltje Steeghs — Division of Medical Oncology, Department of Clinical Pharmacology, The Netherlands Cancer Institute, Amsterdam, The Netherlands

Nikkie Venekamp — Department of Pharmacy & Pharmacology, The Netherlands Cancer Institute, Amsterdam, The Netherlands

Remy B. Verheijen — Department of Pharmacy & Pharmacology, The Netherlands Cancer Institute, Amsterdam, The Netherlands

Rick A. Vreman — Division of Pharmacoepidemiology and Clinical Pharmacology, Utrecht Institute for Pharmaceutical Sciences, Utrecht University, Utrecht, The Netherlands

Jelle de Vries — Division of Cell Biology, The Netherlands Cancer Institute, Amsterdam and
Department of Chemical Immunology, Leiden University Medical Center, Leiden, The Netherlands

Niels de Vries — Department of Pharmacy & Pharmacology, The Netherlands Cancer Institute, Amsterdam, The Netherlands

Aurelia H.M. de Vries Schultink — Department of Pharmacy & Pharmacology, The Netherlands Cancer Institute, Amsterdam, The Netherlands

Willemijn M.E. Wouters — Department of Pharmacy & Pharmacology, The Netherlands Cancer Institute, Amsterdam, The Netherlands

A

Appendices

List of publications

Van Nuland M, Groenland SL,Bergman AM, Steeghs N, Rosing H, Venekamp N, Huitema ADR, Beijnen JH. Exposure-response analyses of abiraterone and its metabolites in real-world patients with metastatic castration-resistant prostate cancer. Prostatic Dis. 2019;Epub ahead of print.

Van Nuland M, Bergman AM, Rosing H, de Vries N, Huitema ADR, Beijnen JH. Exposure-response assessments of enzalutamide and its major metabolites in real-world metastatic castration-resistant prostate cancer patients. Pharmacotherapy. 2019;Epub ahead of print.

Van Nuland M, Janssen JM, van Hoek B, Rosing H, Beijnen JH, Bergman AH. Efficacy, tolerance, and plasma levels of abiraterone and its main metabolites in a patient with metastatic castration-resistant prostate cancer with a hepatic transplant. Clin Genitourin Cancer. 2019;17:e893-6.

Van Nuland M, Rosing H, Schellens JHM, Beijnen JH. Bioanalytical LC-MS/MS validation of therapeutic drug monitoring assays in oncology. Biomed Chromatogr. 2019;Epub ahead of print.

Van Nuland M, Rosing H, Huitema ADR, Beijnen JH. Predictive value of microdose pharmacokinetics. Clin Pharmacokinet. 2019;58:1221-36.

Van Nuland M, Venekamp N, Wouters WME, van Rossum HH, Rosing H, Beijnen JH. LC–MS/MS assay for the quantification of testosterone, dihydrotestosterone, androstenedione, cortisol and prednisone in plasma from castrated prostate cancer patients treated with abiraterone acetate or enzalutamide. J Pharm Biomed Anal. 2019;170:161–8.

Van Nuland M, Crombag M-RBS, Bergman AM, Rosing H, Schellens JHM, Huitema ADR, Beijnen JH. Impact of age on exposure to oral antiandrogen therapies in clinical practice. Prostatic Dis. 2019;22:168–75**.**

Van Nuland M, Venekamp N, de Vries N, de Jong KAM, Rosing H, Beijnen JH. Development and validation of an UPLC-MS/MS method for the therapeutic drug monitoring of oral anti-hormonal drugs in oncology. J Chromatogr B. 2019;1106–1107:26–34.

van Nuland M, Groenland S, Bergman AM, Rotmans Jl, Rosing H, Beijnen JH, Huitema ADR. Plasma Levels of Enzalutamide and its main metabolites in a patient with metastatic castration-resistant prostate cancer undergoing hemodialysis. Clin Genitourin Cancer. 2019;17:e383–6.

A

Groenland SL, van Nuland M, Verheijen RB, Schellens JHM, Beijnen JH, Huitema ADR, Steeghs N. Therapeutic drug monitoring of oral anti-hormonal drugs in oncology. Clin Pharmacokinet .2019;58:299–308**.**

Van Nuland M, Vreman RA, ten Ham RMT, de Vries Schultink AHM, Rosing H, Schellens JHM, Beijnen JH, Hövels A. Cost-effectiveness of monitoring endoxifen levels in breast cancer patients adjuvantly treated with tamoxifen. Breast Cancer Res Treat. 2018;172:143–50.

Van Nuland M, Hillebrand MJX, Rosing H, Burgers JA, Schellens JHM, Beijnen JH. Ultra-sensitive LC–MS/MS method for the quantification of gemcitabine and its metabolite 2',2'-difluorodeoxyuridine in human plasma for a microdose clinical trial. J Pharm Biomed Anal. 2018;151:25-31.

Van Nuland M, Rosing H, de Vries J, Ovaa H, Schellens JHM, Beijnen JH. An LC–MS/MS method for quantification of the active abiraterone metabolite Δ(4)-abiraterone (D4A) in human plasma. J Chromatogr B. 2017;1068–1069:119–24.

Van Nuland M, Hillebrand MJX, Rosing H, Schellens JHM, Beijnen JH. Development and validation of an LC-MS/MS method for the simultaneous quantification of abiraterone, enzalutamide, and their major metabolites in human plasma. Ther Drug Monit. 2017;39:243-51.

Dankwoord

"Het enige wat jij moet doen is vier jaar keihard werken, de rest daar zorgen wij voor"

Met dit in mijn achterhoofd heb ik de afgelopen vier jaar met veel plezier gewerkt aan mijn promotieonderzoek. En nu is het dan eindelijk klaar. Dit proefschrift is tot stand gekomen met de hulp van een grote groep mensen. Graag wil ik iedereen bedanken die hier een bijdrage aan heeft geleverd.

Ten eerste wil ik alle patiënten die hebben deelgenomen hartelijk bedanken. De studies die beschreven staan in dit proefschrift leveren geen direct voordeel op voor de patiënt, dus ben ik hen, veelal in de laatste fase van hun leven, uiterst dankbaar voor deelname.

Ten tweede wil ik graag mijn promotor Jos Beijnen en copromotoren Hilde Rosing en André Bergman bedanken. Jos, bedankt voor de mogelijkheid om mijn promotieonderzoek in dit gerenommeerde instituut te mogen doen en voor de kritische helikopterblik. Hilde, bedankt voor alle tijd die je voor me hebt gehad de afgelopen jaren, waarin we samen sparden over het onderzoek en de labexperimenten. André, bedankt voor de fijne samenwerking en de klinische input die de hoofdstukken in dit proefschrift meer toepasbaar hebben gemaakt voor de praktijk. Verder wil ik graag de leden van de commissie bedanken voor het doorlezen en beoordelen van dit proefschrift.

Tijdens mij onderzoek heb ik samengewerkt met verschillende afdelingen binnen het Nederlands Kanker Instituut. Graag wil ik alle medewerkers van de CRU bedanken die ervoor gezorgd hebben dat de studies voorspoedig zijn verlopen. Tevens wil ik de CRA, het trialbureau, de klinische chemie en de statistiekafdeling bedanken voor de prettige samenwerking.

Voor mijn onderzoek heb ik vele uren in het bioanalytisch laboratorium doorgebracht. Altijd met veel plezier, soms met de nodige frustraties omdat experimenten niet verliepen zoals ik hoopte. De fijne sfeer in het lab maakt dat ik goede herinneringen heb aan de vele uren van pipetteren en meten. Bedankt allemaal!

Tijdens mijn onderzoek heb ik van verschillende afdelingen binnen de apotheek hulp gekregen. Daarom wil ik alle apotheekmedewerkers die een bijdrage hebben geleverd aan dit proefschrift bedanken voor hun inzet.

"Gedeelde smart is halve smart"

Mijn onderzoek had ik nooit met zoveel plezier kunnen doorlopen zonder de aanwezigheid van alle OIOs. Eerst in onze geliefde keet, later op H3. Bedankt voor de

A

gezelligheid, de OIO weekenden, kerst– en paasbrunches en natuurlijk voor de gedeelde smart. In het bijzonder wil ik mijn kamergenoten bedanken voor alle hulp, de pinballs, kameretentjes en koffie.

Lieve Commadoortjes, dank voor jullie luisterend oor en mentale support. Ik kan altijd op jullie rekenen en weet inmiddels dat HP grappen nooit gaan vervelen.

Tot slot wil ik mijn ouders en broers bedanken voor de onvoorwaardelijke steun en het vertrouwen. Lieve papa en mama, ik kan altijd op jullie bouwen. Lieve Victor en Hugo, bedankt dat jullie mijn paranimfen willen zijn.

Lieve Arthur, jij wordt natuurlijk niet vergeten. Jouw steun, liefde en humor heb ik de afgelopen jaren hard nodig gehad. Niet alleen persoonlijk, maar ook inhoudelijk heb je me bij dit proefschrift geholpen. Heel erg bedankt voor alles!

Curriculum vitae

Merel van Nuland was born on the 25th of October in Oss and grew up in Eindhoven, the Netherlands. After graduating from secondary school Eckartcollege, she chose to study Pharmacy at Utrecht University. As part of her master's program, she studied for six months at the Ludwig Maximilian University of Munich to investigate the use of protein structures as a carrier for phosphorodiamidate morpholino oligos (PMOs). Furthermore, she participated in the honours programme at the department of Pharmaceutical Sciences, for which several research projects were completed. In July 2015 she received her master's degree in Pharmacy (PharmD) cum laude, and in October 2015 she started her PhD program at the Netherlands Cancer Institute/Antoni van Leeuwenhoek, Department of Pharmacy & Pharmacology, Amsterdam, the Netherlands, under supervision of prof. dr. J.H. Beijnen, dr. H. Rosing and dr. A.M. Bergman. During her PhD she started her training in clinical pharmacology and in December 2018, Merel became a board certified pharmacologist of the Dutch Society for Clinical Pharmacology & Biopharmacy. Her PhD research resulted in this thesis, which she will defend at the Utrecht University on the 22nd of January 2020.

A